ECOLOGICAL AND BIOLOGICAL ASSESSMENT OF FRESHWATER PRAWNS IN THE UBEJI AXIS OF THE WARRI RIVER, DELTA STATE, NIGERIA

By

Success Ogheneruona, UWHUSEBA

UNIVERSITY OF BENIN

BENIN CITY

NOVEMBER, 2025

ECOLOGICAL AND BIOLOGICAL ASSESSMENT OF FRESHWATER PRAWNS IN THE UBEJI AXIS OF THE WARRI RIVER, DELTA STATE, NIGERIA

By

Success Ogheneruona, UWHUSEBA

B.Sc. (DELSU)

(PG/LSC2215702)

A THESIS WRITTEN IN THE DEPARTMENT OF ANIMAL AND ENVIRONMENTAL BIOLOGY, AND SUBMITTED TO THE COLLEGE OF POSTGRADUATE STUDIES IN PARTIAL FULFILMENT OF THE REQUIREMENTS FOR THE AWARD OF MASTER OF SCIENCE DEGREE IN ANIMAL AND ENVIRONMENTAL BIOLOGY, OF THE UNIVERSITY OF BENIN, BENIN CITY.

NOVEMBER, 2025

CERTIFICATION

We certify that this work was carried out by Success Ogheneruona UWHUSEBA in the Department of Animal and Environmental Biology, University of Benin, Benin City

_____ _____

Prof. A. E. Ogbeibu **Date**
(Supervisor)

_____ _____

Prof. (Mrs.) I. Tongo **Date**
(Head of Department)

CERTIFICATION OF THESIS

We the undersigned attest and declare that the thesis of Success Ogheneruona UWHUSEBA, titled Ecological and Biological Assessment of Freshwater Prawns in The Ubeji Axis of the Warri River, Delta State, Nigeria has successfully passed the anti-plagiarism test and does not violate any copyright regulations.

_____ _____

Prof. A. E. Ogbeibu **Date**
(Supervisor)

_____ _____

Prof. (Mrs.) I. Tongo **Date**
(Head of Department)

DEDICATION

This work is dedicated to my Father, Mr. Felix Uwhuseba and my Mother, Late. (Mrs) Roseline Uwhuseba.

ACKNOWLEDGEMENTS

This degree and thesis would not have been possible without the invaluable support, guidance, and encouragement I received from many remarkable individuals and institutions. First and foremost, I am profoundly grateful to my supervisor, Prof. A. E. Ogbeibu, for your unwavering mentorship, steadfast encouragement, and insightful guidance throughout every phase of this journey, from coursework and seminar presentations to fieldwork, laboratory analysis, and thesis writing. Your constructive feedback, patience, and support went far beyond expectations. You have not only been a mentor but a father figure and advisor, and for that, I remain deeply appreciative.

My sincere appreciation also goes to Prof. (Mrs.) I. Tongo, Head of Department, Former Departmental and later Faculty Postgraduate Coordinator. Your tireless efforts to ensure the smooth processing of my laboratory analyses, recommendations and referrals, paperwork, and your calm, sound advice were truly invaluable.

I extend my heartfelt thanks to Prof. M. O. Omoigberale, Immediate Past Head of Department, whose dedication and commitment ensured the seamless progression of my coursework and research. Your timely interventions, insightful feedback, and practical suggestions, especially your recommendation on pooled water sampling, greatly enriched this work. I am especially grateful for your support in facilitating my presentation at the 2024 FBAN Conference, and granting me access to the HOD's office. Your contributions are too numerous to list, but they will never be forgotten.

I sincerely appreciate Prof. (Mrs.) S. Ogoanah, the Postgraduate coordinator for her kind advise, recommendation and organization of the academic session, ensuring my graduation and Dr. (Mrs.) O. Edo-Taiwo for facilitating my synopsis at the College of Postgraduate studies.

To the professors and lecturers who enriched my academic journey during coursework, Prof. (Mrs.) I. Oboh, Prof. T. O. T. Imoobe, and Prof. J. O. Olomukoro, thank you for setting high standards and contributing meaningfully to my academic and professional development.

I am equally thankful to all academic and non-academic staff of the Department of Animal and Environmental Biology. Special thanks to Prof. (Mrs.) Awharitoma, Prof. (Mrs.) E. Edosomwan, Prof. M. S. O. Aisien, Dr. Kingsley Egun, Dr. Osaro Asemota, Dr. E. Nosakhare, Dr. A. Opute, Dr. Omoregie, Dr. Ikhuoriah Suleman, Mr. Alari Eghosa, Mr. Cyril Olowo, Mr. Peter Oseiti, and Dr. Ekene Biose. Your support made my MSc experience both meaningful and memorable.

I am deeply indebted to my BSc supervisor, Prof. R. B. Ikomi, for sowing the initial seed of interest in Hydrobiology and Fisheries. I also appreciate Dr. K. E. Adewumi, Mr. Israel Ayedokun, Mr. Nelson Akawo, Dr. Wumi, Dr. A. Obaihie, Mrs. Joyce, and Dr. Bernard Okolugbo for their selfless support and for introducing me to laboratory techniques, data analysis, geospatial methods, and academic research.

My gratitude extends to the institutions and networks that supported my learning and research development, including the Laboratory of Ecotoxicology and Environmental Forensics, Owena River Basin Lab, Environmental Systems Research Institute (ESRI), NASA ARSET, Intergovernmental Oceanographic Commission of UNESCO (UNESCO–IOC), Coalition Wild, Tropical Journal of Natural Product Research (TJNPR), Natural Product Research Lab, EarthEcho International, GenSea Community, FAO e-Learning Academy, African Regional Aquaculture Centre (ARAC), and the TETFund Centre of Excellence in Aquaculture and Food Technology, University of Benin.

To my research team, Oshodin Osagioduwa, Mary Shokunbi, Divine Osaigbovo, Adewale Omoshowafa, Omoshowafa Blessing, Abana Excel, and Kenegbe Jennifer, thank you for your

dedication and collaborative spirit. A journey that began in 2021 has taken a step towards its conclusion because of your commitment.

I am also grateful to my colleagues, Mr. Clinton Enabulele, Mr. David Aisosa, Mrs. Kevwe, Ms. Blessing Enudi, Mr. Aideyan George, Mr.Mahammed Aliyu, Ms. Godsgift Emmanuel, Mrs. Dorcas Onomor, and many others, for your friendship, encouragement, and shared experiences.

My deep appreciation goes to Prof. E. Atakpo, Dr. Onose Jude, Mr. and Mrs. Okpako, Mr. Evroro, Mr. and Mrs. Esume, Mr. and Mrs. Okotie, Mr. and Mrs. Ochonogor, Mr. Madu, Prof. E. Eromafuru and Dr. (Mrs.) Eromafuru, Prof. Abiodun Falodun and Prof. Osayenwenre Erhauyi for their generosity, mentorship, and financial or moral support.

To my friends, Mr. and Mrs. Owunka, Israel Usonegbu, Gift Usonegbu, Esume Vome, Ovie Godson Ohwonohwo, Ugochukwu Peter, Ikuku Oniovosa, Ogheneovo Precious, Emamode Ogeh, Oghenegweke Prince, Onome Sajere, Ajawobu Bright, Edoghogho Abiamum, Gideon Moses, Mr. Michael, Omaju Brown, Goodness, Ufuoma Samuel, Ifiogho Ogeh, Jude Odiaka, David Asiekweve, Eze Kinsley, Joel Ezemonye, Onotoghene Aziakpono, Tijani Momoh, Caleb Ojogan, John Emeka, Feastus Samuel, Michael Oghenero, Nwachukwu Onyedikjah, Onyemaechi Azike, Ologbo Emmanuel, Alex Emefe, Salvation Emeke, Wisdom Odin, Oghenewegba Great-Nelson, Celestine Egboduku, Triumph, Devotion Ediowele, Clinton Amrevutere, Oise Alabi, Isaac Alabi, Nzubejah Milton, Fedelis Okaka, Owubigho Chidozie, Okoro Onoriode, Abraham Okoro, Freedom, George Ottanna, Quincy Adeoti, Victory Enogue, Francess Ikponmwosa, Iyewunmi Cherish, Jennifer Mensa, Damisa Chukwuka, Olive Chukwuka, Victoria Chukwuka, Pearl Oghenekume, Evioghene Aziakpono, Charity Ibanga, Linda Enifome, Comfort, Peace, Eunice, Francess, Amarachi Favour, Rutafe Vincent, Josiah Marvelous, Egbeme Daniel, Ona Gideon, Olue Ruth, Miracle Ifon, Ogeh Precious, Adeagba Justice, Iritare Great, Dozo Justus, Eride Precious,

Obriki Daniel, Godstime, Jimmy, the Ogbekile and Pierre family, and countless others, thank you for your steadfast support and friendship.

Lastly, to my beloved family, Mr. Felix Uwhuseba, Mr. Prosper Uwhuseba, Mr and Mrs. Itimi, and Mr and Mrs. Edebe, your unwavering love, sacrifices, and encouragement sustained me through the challenges of this academic pursuit. The completion of this journey belongs to us all, and I am eternally grateful.

TABLE OF CONTENTS

LIST OF TABLES

LIST OF FIGURES

LIST OF PLATES

ABSTRACT

Estuarine ecosystems in industrial regions like the Niger Delta face increasing threats from pollution, habitat loss, and biological stress, highlighting the need for integrated environmental assessments. This study assessed the ecological and biological integrity of the Ubeji axis of the Warri River, Delta State by combining physicochemical and biological data with multivariate and environmental risk analyses. Sampling was from April to December 2024 and focused on water and sediment quality, heavy metal levels, and biological responses of five *Macrobrachium* species: *M. macrobrachion*, *M. rosenbergii*, *M. vollenhovenii*, *M. equidens*, and *M. dux.*

Physicochemical parameters such as Water Temperature, pH, Electric Conductivity were measured *in situ* while heavy metals were tested for in the Laboratory using standard analytical methods. Canonical Correspondence Analysis (CCA) were used to examine species–environment relationships. Pollution levels and ecological risks were evaluated using Contamination Factor (CF), Geoaccumulation Index (Igeo), Enrichment Factor (EF), Pollution Load Index (PLI), and Potential Ecological Risk Index (PERI). The Distribution coefficient (Kd) was calculated to ascertain the bioavailability of the metals.

Results revealed clear seasonal variability in surface water quality driven by rainfall and anthropogenic inputs. Dissolved oxygen (3.85–4.50 mg/L) remained below WHO, US EPA, and FMev thresholds, while pH, conductivity, and nutrients stayed within acceptable limits. Strong and species-dependent Pearson correlations demonstrated that sediment is the dominant exposure route for all *Macrobrachium* species. Iron (Fe) showed strong correlations in *M. rosenbergii* ($r = 0.722$, $p < 0.05$), *M. vollenhovenii* ($r = 0.989$, $p < 0.001$), and *M. equidens* ($r = 0.661$, $p < 0.05$), while *M. macrobrachion* showed a weak, non-significant association ($r = 0.181$, $p > 0.05$). Zinc (Zn) correlated significantly only in *M. vollenhovenii* ($r = 0.917$, $p < 0.001$); correlations in *M. macrobrachion* ($r = 0.547$, $p > 0.05$), *M. rosenbergii* ($r = 0.131$, $p > 0.05$), and *M. equidens* ($r = 0.491$, $p > 0.05$) were weak or non-significant. Canonical Correspondence Analysis (CCA) explained 79.88% of species–environment variation, identifying sediment texture and metal loading as the main ecological drivers. Distribution coefficients (Kd) showed strong sediment retention for chromium (55) and iron (66.89) in June, while cadmium remained predominantly

mobile across months. Risk indices revealed ultra-high enrichment for cadmium (EF > 5), though the geo-accumulation index indicated sediments were unpolluted (Igeo < 0). The Pollution Load Index remained low (PLI = 0.103), and ecological risk assessment showed cadmium posed the highest but still low overall ecological risk (mean PERI = 45.67). In conclusion, the river maintains good ecological integrity with low metal contamination, but cadmium enrichment signals early anthropogenic influence. Although sediments are currently unpolluted, continuous monitoring is recommended to prevent future ecological impairment.

CHAPTER ONE

INTRODUCTION

1.1. Background of Study

Freshwater prawns, particularly those belonging to the genus *Macrobrachium*, serve as keystone species within tropical and subtropical aquatic ecosystems. They play essential roles in nutrient cycling, regulating benthic invertebrate populations, and supporting food web dynamics, thereby sustaining aquatic biodiversity and water quality. Through activities like bioturbation, freshwater prawns enhance habitat complexity and promote ecological resilience in riverine systems (Umehai and Ekelemu, 2023)

In the Warri River, especially the Ubeji Axis of Delta State, Nigeria, five *Macrobrachium* species are prominent: *M. rosenbergii*, *M. macrobrachion*, *M. equidens*, *M. vollenhovenii*, and *M. dux* (Isibor and Freeman, 2016). Each species exhibits distinct ecological traits, including variations in growth rates, reproductive strategies, and habitat preferences, allowing them to occupy specialized niches. Their presence not only stabilizes aquatic food webs but also supports economically valuable fish species and water birds (Oyebola *et al.* 2024).

Globally, the cultivation of freshwater prawns has contributed significantly to food security and economic development. Species like *M. rosenbergii* have been successfully farmed due to their adaptability and high market value (Akinwunmi *et al.* 2022). However, despite Nigeria's vast freshwater resources, prawn aquaculture remains underdeveloped. Challenges such as overfishing, habitat degradation from industrial pollution, and the lack of science-based aquaculture practices have stunted the growth of the prawn industry in regions like Delta State (Onwubiko *et al.* 2020). A major constraint is the scarcity of localized data; bridging the ecological and biological information on native *Macrobrachium* species. Understanding ecological distribution, the patterns

of prawn occurrence across habitats and seasons, and biological characteristics , such as growth rates, reproductive cycles, and feeding habits , is fundamental for effective management. These parameters are often shaped by environmental factors like water quality, salinity, temperature, and habitat complexity (Sintondji *et al.* 2020; Oyebola *et al.* 2024). Without this knowledge, conservation efforts and sustainable aquaculture initiatives cannot be properly formulated.

Although *M. vollenhovenii* has been recognized for its aquaculture potential and ecological adaptability, much less is known about the biology and ecological requirements of *M. equidens, M. dux*, and others. This knowledge gap is particularly concerning in the Ubeji Axis, where freshwater habitats are increasingly impacted by oil spills, urban runoff, and industrial effluents , stressors that can alter prawn populations and their ecological roles (Onwubiko *et al.* 2020).

Given these concerns, a comprehensive assessment of the ecological and biological parameters of these five prawn species is critical. Such research will help establish baseline data necessary for sustainable resource management, habitat restoration, and the design of aquaculture systems tailored to local species and environmental conditions.

Accordingly, this study seeks to investigate the ecological requirements of *M. rosenbergii*, *M. Macrobrachium*, *M. equidens*, *M. vollenhovenii,* and *M. dux* across different habitats and seasons in the Ubeji Axis. It also examine key biological characteristics such as size structure, reproductive status, and growth patterns of the prawns, and analyse how environmental variables such as water quality, habitat type, and seasonal variations influence prawn population dynamics.

By addressing these objectives, the study will not only fill critical knowledge gaps but also contribute to the sustainable development of freshwater prawn fisheries and aquaculture in Delta State, thereby supporting both biodiversity conservation and rural economic revitalization.

1.2. Statement of Research Problem

The freshwater prawn industry in Nigeria has faced marked stagnation over the past decade, with declining production and export volumes, particularly in southern regions like Delta State (Onwubiko *et al.* 2020). Indigenous species such as *Macrobrachium rosenbergii*, *M. Macrobrachium*, and *M. vollenhovenii* in the Ubeji Axis of the Warri River possess significant commercial potential for both domestic consumption and international trade (Akinwunmi *et al.* 2022). However, their contribution remains underexploited, largely due to minimal domestication efforts and continued reliance on wild capture fisheries.

A major barrier to sustainable prawn aquaculture is the insufficient scientific understanding of the biological traits and ecological needs of local *Macrobrachium* populations. Key parameters such as reproductive cycles, growth patterns, and habitat preferences remain poorly documented within the Ubeji River system (Sintondji *et al.* 2020), limiting the ability of farmers and practitioners to adopt science-based management practices.

Environmental degradation, particularly from oil pollution and industrial discharge, has further stressed wild prawn populations in the Ubeji Axis, leading to declining catch per unit effort (CPUE) and unsustainable harvesting trends (Oyebola *et al.* 2024). Combined with limited technical expertise and poor access to species-adapted aquaculture technologies, these pressures have resulted in inconsistent production, overexploitation, and reduced income security for local fishing communities.

Addressing these challenges requires localized research on the distribution, reproductive biology, and growth dynamics of dominant *Macrobrachium* species. Without such baseline data, efforts to enhance aquaculture practices, establish breeding programs, or implement effective conservation strategies will remain inadequate. Therefore, this study seeks to fill critical knowledge gaps and

provide the ecological and biological insights essential for promoting sustainable prawn aquaculture, strengthening livelihoods, and safeguarding freshwater biodiversity in Delta State.

1.3. Justification of Study

Prawn farming in Nigeria, particularly in Delta State remains underdeveloped despite the presence of economically valuable species. Existing studies, such as those by Isibor and Freeman (2016), Anani and Olomukoro (2019), Ifemeje and Destiny (2022), and Umehai and Ekelemu (2023), have investigated environmental drivers and the effects of pollution on prawns. However, critical gaps persist in our understanding of the biological requirements, reproductive cycles, and environmental conditions that optimize prawn growth and survival. This study seeks to address these gaps by conducting a comprehensive ecological and biological assessment of *Macrobrachium* species in the River Ubeji, with a focus on both environmental interactions and species-specific growth parameters.

The importance of this research extends beyond academic inquiry. Locally, it will generate essential data to support the development of sustainable freshwater prawn aquaculture in Delta State. By improving knowledge of species biology and environmental needs, the study can help enhance food security through increased availability of high-quality protein, stimulate economic growth by creating livelihood opportunities especially in rural communities and promote poverty alleviation.

Furthermore, this research aligns with global efforts to improve aquaculture sustainability. Insights gained can be applied to similar tropical and subtropical regions facing comparable challenges, contributing to international goals of biodiversity conservation and reduced ecological impact of

aquaculture. The emphasis on best practices in prawn farming, water resource management, and habitat protection also supports long-term ecosystem health.

Practically, the findings will inform the design of targeted training programs for local farmers, equipping them with the technical skills needed for efficient and environmentally responsible prawn farming. They may also guide policymakers in formulating evidence-based regulations and strategies to support sustainable aquaculture development.

Ultimately, this study aims to empower riverine communities, foster resilient livelihoods, and contribute to the broader objectives of food security, environmental conservation, and socio-economic development in Delta State and beyond.

1.4. Aim and Objectives

The aim of this study is to investigate and document the ecological requirement and biological characteristics of prawns in the Ubeji Axis of Warri River.

The objectives of the study were to:

i. assess species composition, diversity, and abundance, including their spatial and temporal distribution patterns across sampling stations;
ii. characterize morphological, meristic, and biometric traits of the sampled prawns, including length-weight relationships and condition factors, and examine how these vary across locations and seasons;
iii. investigate reproductive biology and feeding ecology, focusing on gonadal development, fecundity, and diet composition across different stations and sampling periods;
iv. analyze environmental variables, including physicochemical parameters of water and sediment, heavy metal concentrations, and bioaccumulation potential in prawn tissues; and

v. investigate the relationships between environmental factors and biological traits of prawns using correlative and multivariate statistical analyses.

CHAPTER TWO

LITERATURE REVIEW

2.1. Freshwater Prawns and Their Ecological Roles

Early research on *Macrobrachium* species emphasized their ecological significance in tropical and subtropical freshwater ecosystems. Holthuis (1980) provided one of the foundational taxonomic classifications of *Macrobrachium* species, highlighting their widespread distribution and importance as benthic organisms. Although detailed ecological roles were not deeply explored at the time, Holthuis' work remains a baseline for subsequent ecological studies. Building on these early insights, later research revealed that *Macrobrachium* species, including *M. rosenbergii* and *M. vollenhovenii*, contribute significantly to ecosystem functioning. Covich, *et al*. (1999) described freshwater decapods such as *Macrobrachium* as keystone species that modify habitats through their burrowing and foraging activities, thereby influencing sediment structure and nutrient availability.

Progressing further, contemporary studies have expanded the understanding of these roles. Freeman *et al*. (2007) demonstrated that *Macrobrachium* prawns significantly influence algal biomass and detrital accumulation by predating on grazing invertebrates, a process that enhances ecosystem productivity and stability, and underscores the prawns' integral role in maintaining trophic balance. In the context of Nigerian freshwater systems, Ogbogu (2000) and more recent assessments by Aransiola *et al*. (2024) confirmed that native *Macrobrachium* species contribute to the regulation of benthic community structure and the recycling of organic matter, thereby playing a pivotal role in sustaining ecosystem dynamics.

As research into freshwater ecosystem processes advanced, the impact of *Macrobrachium* species on nutrient cycling, sediment mixing, and food webs became increasingly evident. March and Pringle (2003) observed that the bioturbation activities of freshwater prawns accelerate nutrient release from sediments, enhancing the availability of critical elements like nitrogen and phosphorus in the water column, which is essential for primary productivity. Reinforcing this perspective, Crowl *et al*. (2012) conducted mesocosm experiments in Caribbean streams and found that the removal of *Macrobrachium* prawns led to sediment build-up and altered nutrient dynamics, thereby demonstrating their essential ecosystem engineering roles.

In tropical African contexts, particularly in Nigerian inland waters, freshwater prawns of the genus *Macrobrachium* play critical ecological roles that extend beyond trophic interactions. Akin-Oriola (2006), study identified *Macrobrachium vollenhovenii* as the most abundant and largest of three prawn species sampled, highlighting its dominance and adaptability within riverine habitats. In the Osun River, Adeyemo and Ogunbiyi (2018) further emphasized that prawns facilitate organic matter breakdown and microbial decomposition, processes essential for nutrient recycling in nutrient-poor freshwater environments. The ecological significance of freshwater shrimps in regulating stream ecosystem processes has been highlighted (e.g., Pringle et al., 1993). In their study of tropical montane streams, they showed that shrimp assemblages influence sediment removal, sessile invertebrates and algal biomass processes that in turn affect water-quality and ecosystem resilience.

2.2. Biological Characteristics of *Macrobrachium* Species

Understanding the biological characteristics of *Macrobrachium* species is fundamental for effective resource management, biodiversity conservation, and aquaculture development. Globally, Holthuis (1980) conducted taxonomic studies across the Indo-Pacific and West African

regions, laying the foundation for the morphological classification of freshwater prawns, especially based on rostral formula, chelae structure, and carapace ratios. New (2002), working primarily in Southeast Asia, documented detailed reproductive and growth traits of *Macrobrachium rosenbergii*, emphasizing sexually dimorphic growth patterns where males attain significantly greater sizes. His work formed the basis for breeding programs in tropical aquaculture. Similarly, Short (2004) carried out ecological and reproductive studies on *Macrobrachium* species in Northern Australia (Northern Territory rivers), revealing that reproductive timing, gonad maturation, and larval development are highly sensitive to environmental cues like temperature, photoperiod, and freshwater discharge.

In tropical Africa, particularly in West African river systems, biological investigations have expanded on these foundational works. Marte (2003) studied *M. vollenhovenii* in Cameroonian rivers, reporting that reproductive cycles are closely linked to seasonal hydrology and sediment transport. Togue *et al*. (2019) in southern Benin (Ouémé River Basin) found that *M. macrobrachion* shows peak Gonadosomatic Index (GSI) values between July and October, matching periods of high rainfall and food abundance. Adeyemi *et al*. (2019), working in the Lower Volta River, Ghana, reported that oocyte diameter, fecundity, and spawning frequency vary seasonally, suggesting strong environmental control over reproductive investment.

In Nigeria, freshwater studies have progressively deepened our understanding of the biological traits, growth patterns, and ecological adaptations of *Macrobrachium* species. Abohweyere (2008), investigating *M. vollenhovenii* in the Lagos–Lekki lagoon system, reported sex-specific length–weight relationships: males exhibited negative allometric growth ($a = -4.72$, $b = 2.92$), while females showed positive allometry ($a = -4.98$, $b = 3.01$), with high condition factors ($K \approx 1.46$) across sexes, indicating favorable physiological status. In the same year, the same author also

found that *M. vollenhovenii* fed on algae, detritus, and invertebrates, with seasonal shifts in diet composition reflecting omnivorous and opportunistic feeding behaviour. Odulate (2015) studied *M. vollenhovenii* in the Ogun River, Abeokuta, reporting total lengths ranging from 8.0 to 18.2 cm (mean 14.81 ± 0.28 cm) and weights from 6.1 to 105.0 g (mean 36.48 ± 1.16 g). Morphometric traits including carapace, rostrum, and limb lengths were documented to support population and taxonomic differentiation. Kingdom *et al*. (2014), working in Lower Taylor Creek (Bayelsa State), examined *M. felicinum*, *M. macrobrachion*, and *M. vollenhovenii*, with average total lengths of 4.88 ± 0.25 cm, 5.22 ± 0.19 cm, and 6.56 ± 0.12 cm respectively. Strong linear relationships between total and carapace lengths were observed: *M. vollenhovenii* ($TL = 1.18 + 3.21$ CL; $r = 0.98$), *M. macrobrachion* ($TL = 0.67 + 3.98$ CL; $r = 0.92$), and *M. felicinum* ($TL = 1.51 + 2.87$ CL; $r = 0.92$), alongside species-specific growth types, positive allometry in *M. vollenhovenii* and *M. felicinum*, and isometry in *M. macrobrachion,* and condition factors ($\bar{K}$) ranging from 1.06 to 1.26. Adeyemo and Ogunbiyi (2018), studying populations in Osun River, reported omnivory as a key adaptive trait in *Macrobrachium* species, facilitating resilience to environmental fluctuations through a varied diet. Most recently, Akinwunmi *et al*. (2023) conducted meristic and morphometric comparisons of *M. vollenhovenii* populations across Badagry and Epe Lagoons, observing negligible variation in total length, cheliped length, and rostral teeth counts across salinity gradients. These suggest morphometric stability but leave open the possibility of genetic divergence. Altogether, these Nigerian studies offer critical biological matrices, including length–weight relationships, growth patterns, condition indices, and feeding ecology, that define the ecological fitness, fisheries value, and adaptive strategies of *Macrobrachium* species in freshwater ecosystems.

2.3 Environmental Factors Influencing Prawn Biology

The relationship between environmental parameters and the biology of freshwater prawns has long been a critical focus in aquaculture and ecological studies. The ecological significance of freshwater shrimp assemblages in regulating stream processes has been highlighted by Pringle and Blake (1994), who through exclusion experiments demonstrated that reduced shrimp densities lead to increased sediment accumulation and enhanced algal biomass in tropical montane streams. Building on global cultivation practices, the Food and Agriculture Organization (FAO, 2002) published cultivation manuals that established optimal environmental thresholds for prawn farming, particularly in Southeast Asia. These included maintaining pH between 7.0 and 8.5, dissolved oxygen above 5 mg/L, and water temperatures between 28–31 °C. Deviations from these ranges were associated with reduced survival, slower growth, and impaired reproduction in *Macrobrachium* species.

New (2002), working extensively on *Macrobrachium rosenbergii* in farm ponds across Malaysia and Thailand, corroborated FAO recommendations and highlighted the species' high sensitivity to even slight fluctuations in temperature and dissolved oxygen. These changes influenced molting intervals, growth, and fertility. In the same work, New also addressed sediment impacts, observing that fine particles and turbidity interfered with prawn burrowing, feeding, and locomotion. Similar findings emerged in a different region: Huenemann and Dibble (2012), through studies in North American streams, demonstrated that increased turbidity reduces visual prey capture among freshwater prawns.

In the African context, Omoniyi and Bakare (2013) conducted controlled laboratory experiments using *Macrobrachium vollenhovenii* sourced from Lagos State. They discovered that water temperatures exceeding 31 °C significantly increased embryonic and larval mortality, emphasizing

the thermal sensitivity of African species. Later, Huong *et al*. (2010), studying juvenile *M. rosenbergii* in brackish farms in Vietnam's Mekong Delta, found that elevated salinity levels delayed molting and impaired growth, reinforcing the importance of maintaining freshwater conditions for optimal development. More recently, Singh *et al*. (2023) observed in Kerala's tropical river systems that high sediment loads correlated with decreased prawn abundance and stunted growth, likely due to disruptions in feeding and substrate quality.

Acidification has also emerged as a growing concern. Liew *et al*. (2022), working in Malaysian tropical waters, demonstrated that low pH levels impair larval development, posing a significant threat to aquaculture sustainability. Notably, these findings align with and extend those of earlier FAO and Southeast Asian studies. Although combined assessments of sediment and acidification are limited, Liew *et al*. (2022) suggested that acidic, sediment-laden river conditions may synergistically worsen stress levels in developing prawns.

In Nigeria's oil-producing Niger Delta region, Akinrotimi *et al*. (2011) conducted laboratory and field assessments using specimens from estuaries and freshwater streams around Port Harcourt and Warri, showing that chronic exposure to petroleum hydrocarbons resulted in prawn bioaccumulation, reduced fecundity, and increased mortality. Their controlled exposure experiments revealed physiological and behavioural disruptions, including respiratory distress, depigmentation, and high mortality ($LC_{50} \approx 4–5$ mg/L), in both *M. macrobrachion* and *M. vollenhovenii* sourced from Delta State waterways. Beyond pollution, sediment, turbidity, and salinity also influence prawn biology The environmental and biological dynamics of *Macrobrachium* species in the Warri River region have drawn increasing scientific attention over the past decade, particularly regarding pollution and habitat quality. Isibor and Freeman (2016) provided one of the earliest focused assessments, analyzing heavy metals and total petroleum

hydrocarbons (TPHs) in water and in *Macrobrachium vollenhovenii* from the Egboko River, a tributary within the Warri estuarine system. Their findings revealed alarming concentrations of cadmium, lead, and chromium in both the environment and prawn tissues, exceeding national and international safety limits. This suggested not only significant pollution but also active bioaccumulation, potentially affecting prawn health, reproductive capability, and growth patterns. Building on this concern, Ifemeje and Destiny (2022) expanded the analysis to include PAHs and additional aquatic organisms, crabs, crayfish, and fish, collected from the Ekpan and Ogunu Rivers, which are also linked to the Warri River system. Their study confirmed that these tributaries, heavily impacted by crude oil exploitation, harbored aquatic fauna with elevated levels of PAHs and heavy metals in muscle tissues. Although their data included multiple taxa, *Macrobrachium* species were again noted for their sensitivity to pollution, with probable consequences such as oxidative stress, impaired osmoregulation, and disrupted molting cycles, all of which can compromise population stability and aquaculture viability. More recently, Umehai and Ekelemu (2023) shifted focus to a relatively less-disturbed site: the Ase River, which flows into the Warri River system. Their work assessed both water quality parameters and *Macrobrachium* population structure. Unlike the polluted tributaries, Ase River maintained near-neutral pH, adequate dissolved oxygen levels, and lower contaminant loads. These conditions supported healthier populations of *M. vollenhovenii*, with improved abundance and apparent reproductive success. The contrast with earlier studies underscores how site-specific environmental quality within the broader Warri system can directly influence prawn biology, ranging from survival and growth to reproductive output.

Together, these studies form a chronological narrative highlighting the ecological pressures on *Macrobrachium* species in the Warri River region. From early signs of bioaccumulation in 2016,

through the multi-species contamination profiles of 2022, to the more optimistic conditions observed in 2023, the evidence strongly suggests that environmental degradation, particularly due to hydrocarbons and metals, remains a key threat. However, cleaner sub-systems like Ase River provide valuable insights into the biological potential of *Macrobrachium* when environmental conditions are favorable, making them critical benchmarks for conservation and aquaculture development in Nigeria's oil-impacted deltaic ecosystems.

2.4 Prawn Aquaculture in Nigeria and Global Context

The development of prawn aquaculture in Nigeria remains at an early stage compared to global practices, despite the country's favorable ecological conditions. Early records of aquaculture activities in Nigeria focused largely on fish species such as catfish and tilapia, with very limited attention given to freshwater prawns. Studies by Adewumi and Olaleye (2011) highlighted the dominance of finfish culture and noted that crustacean aquaculture was virtually absent in national development plans, mainly due to lack of technical knowledge, seed stock availability, and investment incentives. Unlike countries in Asia and Latin America, where farming of *Macrobrachium rosenbergii* has been systematically integrated into rural economies and export markets, Nigeria's freshwater prawn farming remained largely experimental and small-scale through the 2000s (New, 2002).

Initial attempts at cultivating *Macrobrachium vollenhovenii*, a native West African species, were reported sporadically in research settings but lacked commercial scaling. In a review of aquaculture in sub-Saharan Africa, FAO (2016) acknowledged that while Nigeria possesses abundant water resources conducive to prawn farming, infrastructural limitations, poor hatchery technologies, and low farmer awareness severely constrained progress. Furthermore, most

aquaculture research institutions focused efforts on boosting fish production to address protein shortages, often sidelining potential diversification into prawns.

In Delta State specifically, the situation mirrors broader national challenges but also presents unique opportunities. The region's vast network of rivers, estuaries, and wetlands provides suitable habitats for freshwater prawns, yet commercial exploitation remains minimal. Anyanwu *et al*. (2007) noted that despite the region's aquaculture potential, key obstacles include environmental degradation from oil exploration, lack of access to prawn juveniles, absence of prawn-specific feeds, and inadequate extension services. Moreover, most aquaculture activities in Delta State are smallholder-driven, with minimal government intervention targeting species diversification beyond tilapia and catfish. However, recent environmental management initiatives aimed at ecosystem restoration, alongside growing interest in high-value aquaculture products, offer new opportunities for promoting freshwater prawn culture. Properly harnessed, prawn farming could complement fish culture, create jobs, and contribute to poverty reduction efforts in rural and peri-urban areas of Delta State.

Comparisons with global regions that share similar tropical conditions reveal valuable lessons. In Bangladesh, for instance, the deliberate promotion of *Macrobrachium rosenbergii* farming through farmer training, hatchery development, and market integration significantly boosted rural incomes and nutritional security (Ahmed *et al*, 2008). Integrated farming models where prawns were cultured alongside rice or fish diversified risks and improved resource use efficiency. Similarly, in Thailand and Vietnam, technological innovations such as improved hatchery protocols, development of prawn-specific feeds, and farmer cooperatives helped scale up production from smallholder farms to major export-oriented industries (New and Nair, 2012). These success stories suggest that for Nigeria, particularly Delta State, key interventions would

include establishing hatcheries specialized in indigenous prawns like *M. rosenbergii and M. vollenhovenii*, investing in farmer training programs focused on sustainable prawn husbandry, and building value chains that connect small producers to domestic and regional markets.

It is also noteworthy that environmental management practices integrated into prawn aquaculture in these countries emphasize water quality control, disease management, and sediment management strategies to sustain productivity. These innovations could be adapted to Nigeria's socio-ecological context, where environmental challenges such as oil pollution necessitate a strong focus on ecosystem health alongside aquaculture development. Overall, while prawn aquaculture in Nigeria remains nascent, the convergence of ecological suitability, increasing awareness of aquaculture diversification, and lessons from other tropical regions provides a foundation for its strategic expansion, particularly in resource-rich but underutilized areas such as Delta State.

2.5 Impacts of Pollution on Freshwater Ecosystems and Prawn Health

Pollution has been a longstanding threat to freshwater ecosystems, with significant implications for aquatic organisms such as prawns. Early studies by Mason (1991) outlined how pollution from industrial and agricultural sources degraded freshwater habitats, leading to reduced biodiversity and altered ecosystem processes. In polluted environments, prawns,being benthic and detritivorous,are particularly vulnerable to the accumulation of contaminants. Environmental degradation caused by pollutants alters key water quality parameters such as dissolved oxygen, turbidity, and pH, which in turn affect prawn health and population stability (Mason, 1991). Building on this, Chapman (2001) demonstrated that sediment contamination and eutrophication significantly degrade estuarine and riverine benthic habitats,a pattern likely to reduce nursery suitability and recruitment success of freshwater prawns in adjoining coastal and inland waters.

The issue of bioaccumulation of heavy metals in prawns has attracted increasing attention over the last few decades. Heavy metals such as cadmium (Cd), mercury (Hg), and lead (Pb) persist in aquatic systems, often binding to sediments where prawns forage. Research by Rainbow (2002) emphasized that decapod crustaceans like *Macrobrachium* species bioaccumulate metals through both water and dietary exposure, posing risks not only to their health but also to predators higher up the food chain, including humans. Supporting this, regional studies in Nigeria,particularly in oil-impacted areas,have reported considerable heavy metal contamination in both water and sediments. For example, Omoigberale and Ogbeibu (2005) and Oribhabor and Ogbeibu (2009) recorded elevated levels of lead, cadmium, and zinc in rivers and creeks receiving oil exploration discharges in the Niger Delta. Similarly, Imiuwa *et al*. (2014) and Ogbeibu *et al*. (2014) found evidence of moderate to high metal accumulation in bottom sediments of the Ikpoba and Benin Rivers, indicating persistent inputs from urban and industrial sources.

Such sediment enrichment has direct consequences for resident macroinvertebrates, including prawns. In Nigerian freshwater systems, studies by Oguzie and Ehigiator (2011) and Ukamaka *et al*. (2024) have documented significant bioaccumulation of heavy metals (e.g. Pb, Fe, Mn) in wild-caught *Macrobrachium* prawns, with concentrations sometimes exceeding international safety thresholds, raising concern for potential physiological effects such as impaired growth or molting, as well as food safety risks for local communities. Heavy metal toxicity further compounds risks to prawn survival and reproductive success. According to Rainbow (2002), sub-lethal concentrations of metals can cause oxidative stress, immunosuppression, and endocrine disruption in crustaceans, thereby affecting vital processes like gametogenesis and larval development. Experimental evidence by Revathi *et al*. (2011) demonstrated that cadmium chloride exposure in intact prawns resulted in decreased gonadosomatic index (GSI), inhibited ovarian maturation, and

histopathological changes in the gills, hepatopancreas, and ovarian tissues, directly linking metal exposure to reproductive impairment in *Macrobrachium rosenbergii*.

Recent studies by Anani and Olomukoro (2021) and Ukamaka *et al*. (2024) have reinforced this pattern, reporting significant bioaccumulation of trace and heavy metals in freshwater prawns from oil-impacted creeks in the Niger Delta, with tissue metal burdens surpassing safe consumption limits. These findings imply systemic toxicity and histopathological alterations in vital organs, corroborating earlier evidence of metal-induced physiological stress in *Macrobrachium* species.

The cumulative evidence,including local assessments by Omoigberale and Ogbeibu (2005), Oribhabor and Ogbeibu (2009), Imiuwa *et al*. (2014), and Ogbeibu *et al*. (2014),underscores that pollution-induced habitat degradation, sediment metal enrichment, and associated bioaccumulation pose multifaceted threats to freshwater prawn health in Nigerian rivers and creeks. Given that prawns also play critical roles in nutrient cycling, sediment mixing, and food web stability, the degradation of their populations can trigger cascading ecological effects, ultimately compromising the resilience of freshwater ecosystems. The persistence of these threats highlights the urgent need for integrated environmental management approaches,including pollution control, habitat restoration, and routine biomonitoring,to safeguard prawn populations and the broader health of freshwater systems.

2.6 Biological and Reproductive Ecology of *Macrobrachium* Species

Species within the genus *Macrobrachium*, such as *M. rosenbergii*, *M. macrobrachion*, *M. vollenhovenii*, *M. equidens*, and *M. dux*, exhibit notable biological and reproductive variations that significantly affect their ecological functions, taxonomic classification, and aquaculture viability. Early morphological and taxonomic work by Holthuis (1950) laid the foundation for species identification, which was further refined by De Grave *et al*. (2008), who elaborated on key

morphological features, including cheliped asymmetry, elongated rostrum, and body segmentation. These traits have proven critical for distinguishing closely related species. In Nigeria, Lawal-Are and Owolabi (2012), studying prawns in the Lagos Lagoon, reported interspecific differences in body coloration, size, and claw structure, noting that *M. rosenbergii*, an exotic species introduced for aquaculture, can reach sizes of 30 cm and displays marked sexual dimorphism, while *M. macrobrachion* and *M. vollenhovenii* are medium-sized and endemic to West African fresh and brackish waters.

Nigerian studies have paid increasing attention to the spatial distribution and ecological tolerances of native species. For instance, Ibim (2023), investigating estuarine prawn communities in the Bonny River system (Rivers State), observed that *M. equidens* and *M. dux* are smaller species (under 8 cm), predominantly occupying turbid brackish zones where they face higher predation and salinity stress. These habitat preferences shape their reproductive strategies and population structure. In Warri River (Delta State), Umehai and Ekelemu (2023) identified four coexisting *Macrobrachium* species and noted that reproductive timing and species composition were seasonally influenced by rainfall and nutrient levels.

Reproductive ecology, especially spawning periodicity, has long been a subject of ecological inquiry. In one of the earliest Nigerian studies, Marioghae (1982) documented peak ovigerous (egg-bearing) activity in *M. macrobrachion* and *M. vollenhovenii* during the wet season (July–September) in the Lagos coastal systems. Organ *et al* (2005), in a complementary study of *M. macrobrachion* in Lagos Lagoon, described a spawning window from May to November, characterized by fortnightly oviposition and a positive relationship with increasing rainfall. These patterns are consistent with findings from the Cross River Estuary by Nwosu and Holzlöhner (2016), who confirmed that hydrological cycles, particularly rainfall and salinity dilution, act as

primary cues for spawning in *M. vollenhovenii*, *M. equidens*, and *M. dux*. Similar wet-season breeding trends were reported by Oben *et al*. (2015) in the Sanaga River, Cameroon, supporting the regional influence of rainfall on reproductive timing. All species exhibit maternal brood care, wherein fertilized eggs are carried under the pleopods of females until hatching, a strategy that increases embryonic oxygenation and survival. This behaviour has been well-documented in *M. rosenbergii* (Valenti and New, 2000, 2000; CABI, 2024), and is now confirmed among native Nigerian species like *M. vollenhovenii* and *M. macrobrachion*.

Fecundity rates vary widely across species and are closely linked to body size and habitat conditions. *M. rosenbergii* remains the most fecund, producing between 20,000 and 75,000 eggs per spawning (Cavallo *et al*. 2001), whereas *M. vollenhovenii*, studied in Cross River Estuary by Nwosu and Holzlöhner (2016), yields an average of 23,943 eggs per brood, ranging from 1,744 to 46,141. In contrast, *M. macrobrachion* produces fewer eggs (mean = 2,490; range = 270–4,710), and *M. equidens* has even lower fecundity, averaging 2,359 eggs per spawn.

Quantitative indices like the gonadosomatic index (GSI) and hepatosomatic index (HSI) are valuable for understanding reproductive investment and physiological readiness in *Macrobrachium* populations. Liew *et al*. (2022) examined how low water pH affects the growth and early developmental stages of *M. rosenbergii* larvae. Although their research specifically addressed pH, it underscores the broader influence of environmental conditions on prawn development. Similarly, Organ *et al*. (2005) found that *M. macrobrachion* in the Lagos Lagoon exhibited higher GSI values during the rainy season when food availability and dissolved oxygen concentrations were more favorable.

Environmental variables, particularly temperature, rainfall, salinity, and substrate type, play pivotal roles in reproductive success. Elevated water temperatures have been linked to accelerated

gonadal development in *M. rosenbergii* and *M. macrobrachion* (D'Abramo *et al*. 2001; Organ *et al*. 2005). In flood-prone systems such as the Warri River, Isibor and Freeman (2016) showed that heavy metals and petroleum hydrocarbons can suppress fecundity in *M. vollenhovenii* by disrupting endocrine function. Further downstream in Ekpan and Ogunu Rivers (Warri), Ifemeje and Destiny (2022) reported that oil pollution negatively affects egg-carrying frequency and larval survival across multiple crustacean species, including *Macrobrachium*. These studies underscore that while hydrology supports breeding, anthropogenic pollution threatens reproductive integrity and species survival.

2.7 Research Gaps, Knowledge Deficiencies, and Conceptual Framework

Although freshwater prawns of the genus *Macrobrachium* have been extensively studied globally (New, 2002; Valenti and New 2006), significant knowledge gaps persist, particularly regarding species-specific biological and ecological characteristics in tropical African systems. In Nigeria, foundational studies by Powell *et al*. (1982) provided baseline taxonomic records of aquatic macroinvertebrates in the Niger Delta region but lacked detailed analysis of growth dynamics, reproductive biology, or responses to localized environmental conditions. More recently, Akinrotimi *et al*. (2011) emphasized the aquaculture potential of *Macrobrachium* species in Nigeria, yet few studies have linked this biological potential with ecosystem-level drivers in polluted estuarine systems.

Within the Warri River system, especially the Ubeji axis, research has primarily focused on water and sediment quality (Isibor and Freeman, 2016; Anani and Olomukoro, 2019), as well as bioaccumulation of heavy metals in fish and gastropods (Chindah *et al*. 2003; Ifemeje and Destiny, 2022). However, these studies often neglect freshwater prawns, despite their ecological and

economic importance. Furthermore, existing studies on prawns within the Warri River, such as those by Isibor and Freeman (2016), have been limited to distributional surveys, leaving a critical gap in understanding how pollution and habitat alteration affect core biological functions like feeding patterns, reproduction, and growth performance. For instance, there is little to no documentation on the length-weight relationships, condition factor, gonadosomatic indices, or food habits of *Macrobrachium* species in this environment, parameters that are vital for assessing health and aquaculture viability.

Additionally, environmental assessments in the region have often been decoupled from biological observations. While studies such as Omoregie and Ufodike (1990) and Chindah *et al*. (2003) have highlighted the ecological risks posed by hydrocarbon pollution and heavy metals, there is a dearth of empirical studies correlating these stressors with physiological or reproductive disruptions in *Macrobrachium* species. This disconnect hampers the ability to develop predictive ecological models or identify thresholds of environmental stress that lead to biological impairment.

To bridge these gaps, this study introduces an integrative conceptual framework combining biological, ecological, and environmental dimensions. The framework draws from ecosystem theory (Odum, 1983) and is supported by empirical studies by Ogbeibu and Oribhabor (2002), who demonstrated that aquatic fauna, including crustaceans, are sensitive indicators of environmental degradation. His research in the Warri River system and other parts of the Niger Delta revealed that industrial discharges, including crude oil and effluent pollution, significantly alter macroinvertebrate community structure, indicating broader ecological stress. These findings affirm that prawn population dynamics are closely tied to shifts in environmental quality, particularly under industrial stress conditions.

Ultimately, this framework underpins the study's objectives: to profile the biological characteristics of *Macrobrachium* species, evaluate the environmental health of their habitat, and establish causal relationships between anthropogenic stressors and prawn population health. The findings aim to inform sustainable management practices and policy interventions in the Warri River system and other comparable estuarine ecosystems across the Niger Delta.

CHAPTER THREE

MATERIAL AND METHODS

3.1. Material and Methods

The study was conducted at Ubeji Axis of the Warri, Delta State from April to December 2024. Laboratory examinations and analysis were conducted at the Ecotoxicology and Forensics Laboratory situated at the University of Benin, Benin City.

3.2. Description of the Study Area

3.2.1 Geographical Location

The Ubeji area of Warri lies approximately between 5.51000–5.52500° N latitude and 5.74000–5.76000° E longitude, lies within the tropical swamp forest zone of southern Nigeria (Figure 1). The Ubeji axis of the Warri River is characterized by distinct seasonal variations associated with alternating wet and dry periods, influenced further by tidal fluctuations. The river's upstream region exhibits freshwater conditions bordered by dense forest vegetation, whereas the downstream section transitions into a brackish environment dominated by sparse mangrove flora (Okoye and Iteyere. 2014). This riparian zone supports a wide array of petroleum-related operations, including oil exploration, exploitation, refining, and distribution, all of which have imposed significant anthropogenic pressures on the aquatic ecosystem. Notable among these are alterations in physicochemical water parameters and disruptions to the aquatic biota. The cumulative impact of these activities continues to degrade water quality and threaten biodiversity within the Ubeji River system.

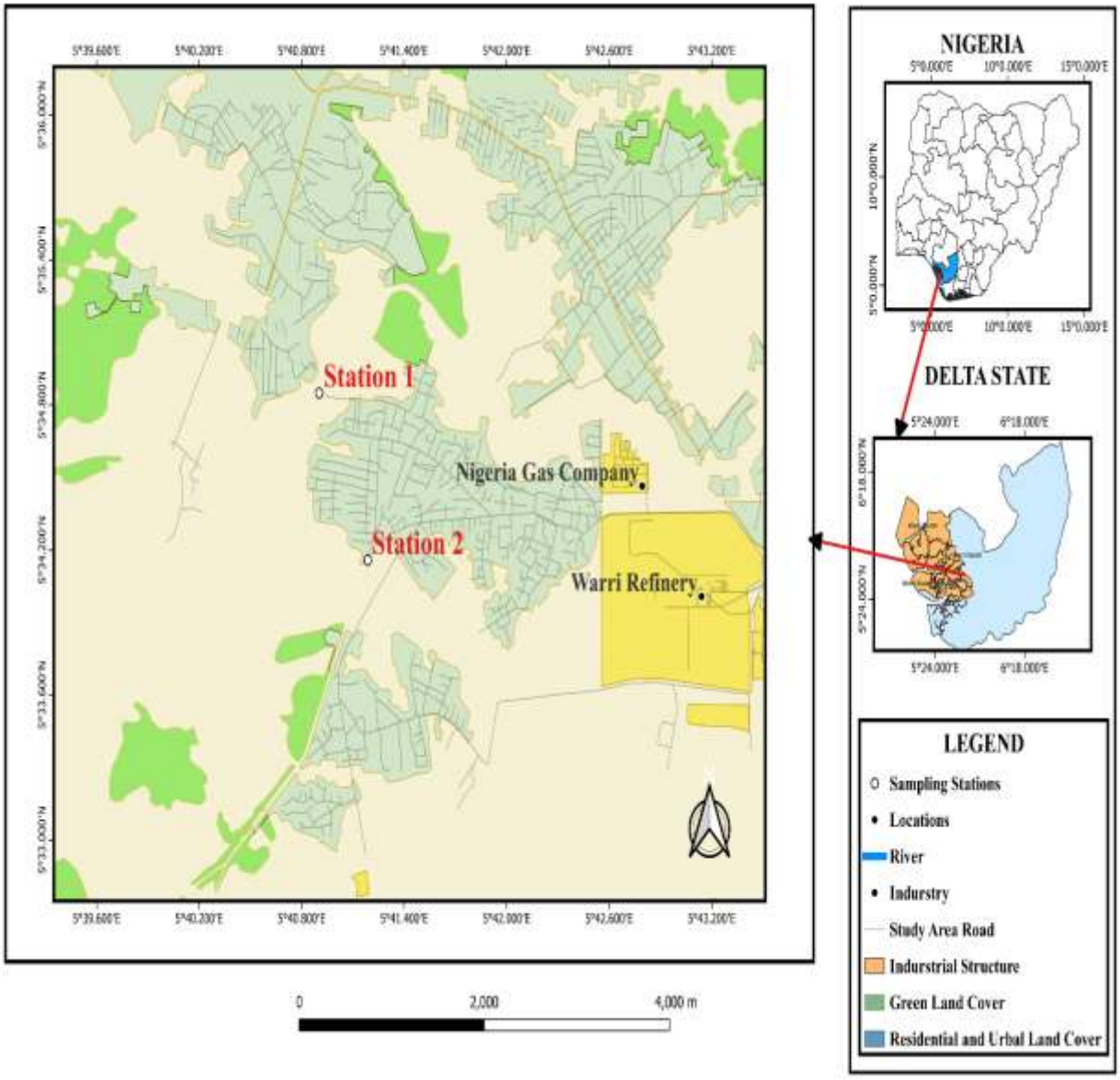

Figure 1: Study Area Showing the Sampling Stations during Study Duration

3.2.2. Vegetation

The Ubeji River corridor exhibits a mosaic of vegetation types characteristic of the tropical swamp forest zone. The riparian landscape is primarily composed of secondary growth interspersed with economically important plant species and anthropogenically altered flora. Common vegetation includes oil palm (*Elaeis guineensis*), raffia palm (*Raphia hookeri*), and pawpaw (*Carica papaya*). In less disturbed patches, bamboo (*Bambusa vulgaris*), male fern (*Dryopteris filix-mas*), and slender dayflower (*Commelina erecta*) thrive, adding to the habitat complexity.

Aquatic and semi-aquatic plant species are also well-represented along the riverbanks and in stagnant zones of the water body. Notable among these are water hyacinth (*Eichhornia crassipes*), duckweed (*Lemna paucicostata*), water lily (*Nymphaea lotus*), and floating fern (*Salvinia nymphellula*).

3.2.3 Human Activities

The Ubeji River and its adjoining landscape are intensely influenced by a range of human activities, primarily driven by the area's strategic role in Nigeria's petroleum sector. The river hosts multiple oil-related operations, including crude oil exploration, drilling, refining, and pipeline transportation. These activities are centered on major facilities such as the Warri Refining and Petrochemical Company and Nigeria Gas Company, both of which contribute to environmental perturbations through thermal discharges, hydrocarbon leaks, and effluent release.

Beyond petroleum operations, the region supports small-scale fishing, boat traffic, and domestic wastewater discharge from surrounding communities. Industrial effluents, untreated sewage, and stormwater runoff containing hydrocarbons and heavy metals have led to substantial alterations in

the river's physicochemical properties. These stressors have resulted in habitat degradation, reduced water quality, and disruption of native aquatic fauna.

Moreover, urban encroachment and population growth in Ubeji and the larger Warri metropolis have intensified anthropogenic pressure on the river system. Informal waste disposal along riverbanks, as well as runoff from residential and commercial zones, introduces further contaminants into the aquatic environment. The cumulative impact of these activities underscores the river's vulnerability and highlights the urgent need for integrated watershed management and sustainable industrial practices**.**

3.3. Description of Study Stations

The study was conducted in the upper reaches of the Warri Ubeji River, specifically between two designated sampling stations, Station 1 and Station 2.

3.3.1. Sampling Stations

Station 1

The first sampling station was located in Egbokodo Itsekiri at Latitude 5.5783149 and Longitude 5.6816127 (Plate 1). One side of Station 1 is densely forested, while the opposite side is influenced by human and anthropogenic activities, including fishing, washing, swimming, and transport activities involving goods and people. Floating macrophytes such as water hyacinth, water lily, and water lettuce were observed at this station.

Station 2

Station 2 is located 2.3 km from Station 1 in the Ubeji community, directly opposite the Deeper Life camp ground, at Latitude 5.569925 and Longitude 5.6870405 (Plate 2). This station is also influenced by human and anthropogenic activities, with a higher intensity of petrochemical operations on one side and a less dense forest on the other, compared to Station 1. Unlike Station 1, floating macrophytes were not observed at Station 2 due to the high level of disturbance caused by petrochemical and other commercial activities in the area.

3.4. Sample Collection and Identification

Prawns of *Macrobrachium* species were then collected fortnightly from two designated river sampling stations from April – December 2024, using basket traps as described by Akinwunmi and Lawal-Are (2019). After collection, the prawns were sorted and preserved in 10% formalin solution and transported to Tobejay Technologies Lab for biological examination. Selected samples were rinsed with deionized water, treated with 1 ml of nitric acid (HNO_3) per 100 ml of deionized water to maintain sample integrity for heavy metal analysis, and transported to the Ecotoxicology laboratory at the Department of Animal and Environmental Biology, University of Benin, for further analysis. Identification of the prawn species was carried out following the FAO species identification guide (Holthuis, 1980), Powell (1980), and Marioghae (1982).

3.5. Biophysical Assessment

3.5.1 Identification, Abundance, distribution and Sex determination

Specimens of *Macrobrachium* prawns collected were identified to species level using diagnostic morphological characteristics described by the FAO species identification guide (Holthuis, 1980), Powell (1980), and Marioghae (1982). Abundance and distribution were determined by counting

the prawns collected from each sampling station. Thereafter, the specimens were sorted by sex. Sex determination followed the method described by Anetekhai (1990) and Edokpayi (1990), using specific morphological features that distinguish males from females. Key characteristics include the presence of the appendix masculina on the second pleopod in males, the joining or separation of pleopods, the reproductive chamber in females, and the presence of genital openings (gonopores): males typically have openings at the base of the fifth pereiopod (walking leg), while females have theirs at the base of the third pereiopod. Additional features such as nubs on the first abdominal segment may also aid identification.

3.5.2. Morphometric and Meristic analysis

Morphometric measurements (Figure 2) follows Carrillo (1968) and Jimoh *et al*. (2002), were

1. Total length (TL),
2. Dorsal cephalothorax length (DCL),
3. Cephalothorax height (CH),
4. Dorsal rostral length (DRL),
5. Abdomen length (AL),
6. Telson length (tsl),
7. Uropod length (UL),
8. Eye diameter (ED) and
9. Body weight (BW) .

Meristic counts will be:

1. Number of spines on the upper face of the rostrum (DRS)
2. Number of spines on the lower face of the rostrum (VRS).

Plate 1: Station 1 (Ugbokodo – itsekiri) and its surrounding vegetation

Plate 2: Station 2 (Ubeji opposite deeper life camping ground)

3.5.3. Length-Weight Relationship

The relationship between the weight and length of the specimen will determined also using:

$W = a L^b$

Where W = weight in gram;

L = length in centimetre,

a = regression constant;

b = regression coefficient.

The length–weight regression equation was generated by generalized linear regression on log transformed data performed with SPSS v23.0 software. The degree of variation between the length and weight of the prawns was also estimated by R^2 (coefficient of determination). The regression ANOVA was employed to test the isomeric (b=3) and alometric (b≠3) nature of the prawns at 0.05 level of significance.

3.5.4. Condition Factors

Data obtained from the length and weight measurements was used to calculate the condition factor (K) from the relationship.

$$K = \frac{W}{L^3} \times 100$$

Where K = condition factor

L = Total Length

W = Weight in gram.

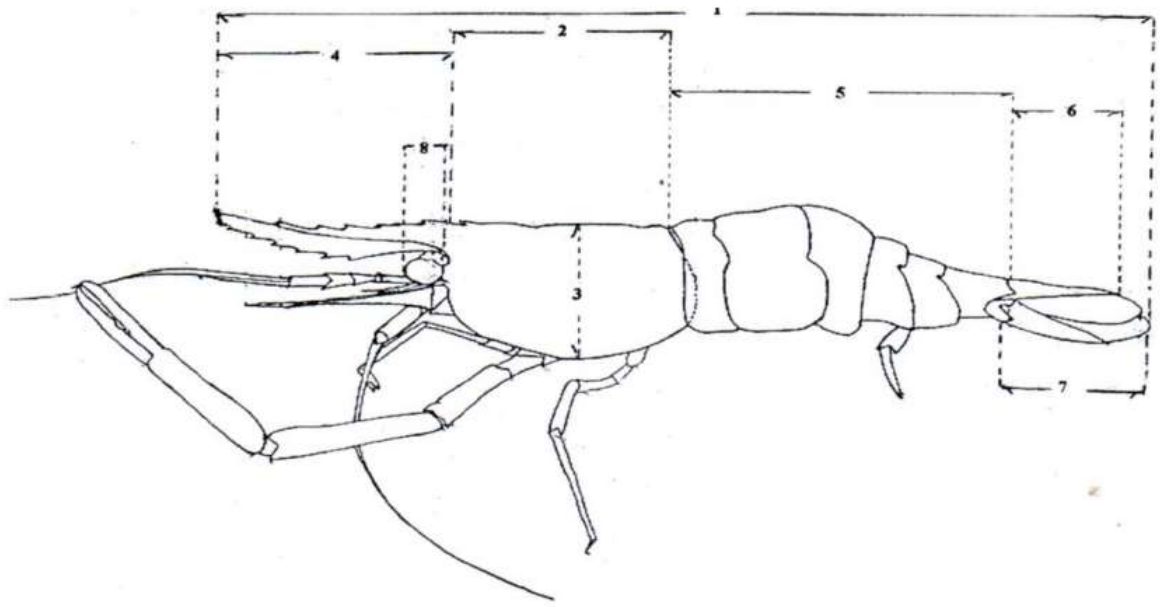

Source: Adite *et al*. 2013

Figure 2: Morphometric measurements used in describing *M.Macrobrachium* : 1 = total length, 2 = dorsal cephalothorax length, 3 = cephalothorax height, 4 = dorsal rostral length, 5 = abdomen length, 6 = telson length, 7 = uropod length, 8 = eye diameter.

3.5.5 Gonadosomatic Index (GSI)

A ripe female specimen was collected and the weight and total body length was recorded. Ripe gonad was determined following Nikolsky (1963) classification. It was dissected and the ripe ovaries will be exposed and taken out. Weight of gonads was taken and finally GSI value of female specimen was calculated. This was done as percentage of the gonad weight (GW) in terms of body weight (BW) of the prawn (Afonso-Dias *et al.* 2005)

$$\text{GSI} = \frac{GW}{BW} \times 100$$

3.5.6 Hepatosomatic Index (HSI)

The HSI was calculated according to the method of Rajaguru, (1992) by determining the weight of hepatopancreas as a percentage of the total weight of the prawn.

$$\text{HSI} = \frac{LW}{BW} \times 100$$

Where, LW and BW are liver weight and total weight of the prawn, respectively.

3.5.7. Feeding Intensity

The feeding intensity was determined by dissecting and the entire gut and emptying it into the Petri dish, and allotting scores 0/4, 1/4, 2/4, 3/4, 4/4 according to their fullness of stomach.

a. $^4/_4$ Full stomach: A stomach in which the food items occupying the entire cavity of the stomach.
b. ¾ Full Stomach: A stomach in which the food items occupying ¾ of the stomach
c. $^1/_2$ Full Stomach: A stomach in which the food items occupying ½ of the stomach
d. ¼ Full Stomach: A stomach in which the food items occupying ¼ of the stomach
e. $^0/_4$ Empty stomach: There will be no food item in the stomach. A little digested secretion may be present.

Gravimetric method will be used to quantitatively determine the gut content and express as a percentage of the total weight of stomach contents.

3.6. Collection and Analysis of Water Samples

Monthly water quality parameters were obtained using pooled (composite) sampling, following the protocol described by the U.S. Environmental Protection Agency (USEPA, 2017). Equal-volume aliquots were collected from multiple points within each sampling station and combined to obtain a representative sample for each month. Analytical procedures followed the APHA (2023) Standard Methods for the Examination of Water and Wastewater. Physicochemical parameters such as Water Temperature, pH, Electrical Conductivity, Salinity, Oxygen Reduction Potential and Total Dissolved Solids were analyzed *in-situ* using Digital Meter (OEM TPH01139). Dissolved Oxygen (DO) and Biological Oxygen Demand (BOD_5) were determined using Winkler`s method. Nutrients (Nitrate, Phosphate and Sulphate) and Heavy metals where analyzed using Atomic Absorption Spectrophotometry (AAS, Model AA240FS, Varian Inc.).

3.7. Sediment Samples

Sediment samples were collected using an Van veen grab sampler to ensure the retrieval of undisturbed surface sediments. Immediately after collection, the samples were transferred into labeled, acid-washed polyethylene bags, preserved in an ice-filled cooler, and transported to the laboratory. Upon arrival, samples were stored at 4°C until analysis. For preparation, the sediment samples were thawed and oven-dried at 100°C for 24 hours to eliminate moisture. A 1 g portion of the dried, finely ground, and homogenized sediment was accurately weighed to the nearest 0.01 mg and placed in a 100 mL Erlenmeyer flask. Acid digestion was carried out by adding 20 mL of

concentrated nitric acid (HNO_3) and 10 mL of perchloric acid ($HClO_4$) to the sample. The mixture was digested on a hot plate at temperatures ranging from 200 to 250°C for no less than five hours, until a clear solution was obtained, following the method of Van Loon (1980). The digest was then diluted to a final volume of 50 mL using double-distilled water. Heavy metal concentrations in both water and sediment samples were determined using a Atomic Absorption Spectrophotometry (AAS, Model AA240FS, Varian Inc.), with specific cathode lamps and wavelengths for each metal. Concentrations were reported in parts per million (ppm), calculated as:

Concentration (ppm) = (A - B) × 100

Where:

• *A* = Concentration of the metal in the sample

• *B* = Concentration of the metal in the blank sample

• 100 = Final volume of the extract

3.7.1. Determination of Heavy Metal Concentrations in Whole Prawn Samples

Collected prawn specimens were preserved in ice and transported to the laboratory, where they were allowed to thaw at ambient room temperature (26–27°C). Each specimen was thoroughly rinsed with deionized water to remove external debris. The whole prawn was used for analysis; each specimen was weighed using a precision analytical balance and then oven-dried at 105°C for one hour to eliminate moisture content. The dried prawn samples were pulverized using a sterilized porcelain mortar and pestle and sieved through a 1 mm mesh to obtain a homogenous powdered form. A 0.5 g subsample of the powdered whole prawn was transferred into a digestion flask, followed by the addition of 0.5 ml of concentrated nitric acid (HNO_3). The mixture was diluted with deionized water to a final volume of 100 ml and heated in a water bath under a fume hood until the solution was reduced to approximately 20 ml. After cooling, the digested solution was

filtered through Whatman No. 42 filter paper. The filtrate was then made up to 100 ml with deionized water in a calibrated flask and stored in acid-washed polyethylene bottles for further analysis. Heavy metal concentrations, including cadmium (Cd), lead (Pb), copper (Cu), chromium (Cr), zinc (Zn), nickel (Ni), manganese (Mn), and iron (Fe),in the digested prawn samples were quantified using Atomic Absorption Spectrophotometry (AAS, Model AA240FS, Varian Inc.).

3.8. Statistical Analysis

Statistical analysis was carried out to assess spatial patterns, relationships, and potential ecological implications of the measured variables in water, sediment, and biological samples. Statistical tools were employed to interpret the physico-chemical parameters, sediment contamination indices, and prawn biological metrics. Descriptive statistics (mean, standard deviation) were computed using SPSS. Inferential statistics, t-test was performed to evaluate significant differences in heavy metal concentrations in water, sediment. One-Way ANOVA was used to test for significant difference between prawn species. All statistical analyses were performed using SPSS v23.0 (Ogbeibu, 2014).

3.9. Bivariate Analysis

3.9.1. Correlation Analysis

Pearson's correlation coefficient (r) was computed to assess the strength and direction of linear relationships between water and sediment heavy metal concentrations and prawn biological parameters, including condition factor (K), gonadosomatic index (GSI), and tissue bioaccumulation levels (Ogbeibu, 2014). This analysis was used to preliminarily identify metals

that may influence prawn health and accumulation patterns. Variables were considered statistically significant at $p < 0.05$.

3.9.2 Multivariate Analysis

Canonical Correspondence Analysis (CCA) was performed using PAST software Version 4 to explore relationships between physicochemical parameters and factors such as abundance, distribution, feeding intensity, and fecundity. Additionally, CCA was applied to examine relationships between morphometric and meristic features and biological indices such as the gonadosomatic index, body weight, and hepatosomatic index (Ogbeibu, 2014).

3.10. Evaluation of Environmental Risk Assessment

3.10.1 Calculation of Geo-Accumulation Index (*Igeo*)

The Geo-accumulation Index (*Igeo*) was utilized to assess the level of metal contamination in sediments, using the method outlined by Ogbeibu *et al*. 2014. This index compares observed metal concentrations with baseline values, providing insight into pollution levels relative to natural background concentrations.

It is calculated using the following formula:

$$Igeo = log2\,(Csample\ /\ (1.5 \times Cbackground))$$

Where:

$Csample$ represents the concentration of the heavy metal in the sediment sample, and $Cbackground$ represents the geochemical background concentration (mg kg−1) of the heavy metal.

Background values for metals in the study area were sourced from prior research utilized the average concentration in the earth crust. The Igeo values for each metal were calculated at each sampling station, enabling the classification of pollution severity by comparing the observed values to the natural baseline concentrations (Table 3.1).

3.10.2 Contamination Factors (CF)

The Contamination Factor (CF) is a valuable tool for assessing metal contamination in sediments, as it compares the measured metal concentrations to their background levels found in coastal shale. A key advantage of CF is that it offers a straightforward, quantitative assessment of contamination, which aids in evaluating the environmental impact of specific metals. By identifying areas with higher contamination levels, CF can inform targeted remediation strategies. The formula used is:

$$CF = Ci / Cn$$

In this equation, C_i signifies the metal content within the sediment, and C_n denotes the background value for that specific metal. The computed CF values were classified according to Hakanson's 1980 classification scheme (Table 3.1).

3.10.3 Pollution Load Index (PLI)

The Pollution Load Index (PLI) is a tool for evaluating the overall pollution level of sediments, derived from the contamination factor values of different metals. It is calculated by finding the geometric mean of these CF values across all analyzed metals:

The formula for calculating the PLI is as follows:

$$PLI = \sqrt{(CF1 \times CF2 \times CF3 \times \ldots \times CFn)}$$

In this equation, *CF*1, *CF*2, *CF*3...*CFn* denotes the contamination factors for each metal found in the sediment. These CF values are determined by comparing the metal concentration in the sediment to their corresponding background levels.

This empirical index offers a straightforward way to compare and evaluate the level of heavy metal pollution.

When PLI > 1, it means that a pollution exists; otherwise,

If PLI < 1, there is no metal pollution.

The PLI offers a singular numerical representation of the overall pollution level present in sediment by considering the cumulative impact of various metals. Elevated PLI values denote higher levels of pollution, whereas lower values imply reduced pollution levels.

3.10.4 Contamination degree (CD)

This parameter encompasses all factors contributing to contamination, offering insight into the overall extent of sediment pollution at a specific location. It is expressed as:

$$CD = \sum_{i=1}^{n} CF_i$$

The CD value is interpreted as follows: less than 6 indicates a low level of contamination, values ranging from 6 to less than 12 indicate moderate contamination levels, those between 12 and less than 24 denote considerable contamination, while a Cd value of at least 24 signifies a very high degree of contamination (Håkanson,1980).

Table 3.1. The enrichment factor (EF), contamination factor and geo-accumulation index (*Igeo*) classes in relation to sediment quality

EF Class[a]	Sediment Quality	CF Class[b]	Sediment Quality	*Igeo* Class [c]	Sediment Quality
EF< 1	Indicating depletion in sediment composition.	CF < 1	Low contamination,	<0	Unpolluted
EF≥ 1	Suggesting some level of enrichment.	1 ≤ CF ≤ 3	Moderate contamination	0–1	Unpolluted to moderately polluted
EF≥1.5	Indicates enrichment primarily from anthropogenic or non-natural sources.	3 ≤ CF ≤ 6	Considerable contamination	1–2	Moderately polluted
EF>2	Signifies significant enrichment levels.	CF > 6	High contamination	2–3	Moderately to highly polluted
				3–4	Highly polluted
				4–5	Highly to very highly polluted
				>5	Very highly polluted

a- Mmolawa *et al*. (2011)
b- Hakanson (1980)
c- Muller *et al*. (1969)

3.10.5 Potential ecological risk index (PERI)

The Potential Ecological Risk Index (PERI) assesses the ecological risks posed by heavy metals in sediments, taking into account both their toxicity and concentrations compared to background levels. The formula used to calculate the individual potential ecological risk for each metal is as follows:

$$E_r^i = T_r^i \times CF_i$$

Where E_r^i is the individual metal potential risks, T_r^i is the toxic response factor for a given substance and CF is the contamination factor.

The designated toxic response factors for the heavy metals utilized in calculating PERI are as follows: Zn is 1, Cr is 2, Cd is 30, Pb stands at 5, Mn has a value of 1, Cu also registers at 5 and Ni matches with a factor of 5 (Håkanson, 1980). PERI is the summation of the individual potential risks (E_r^i). It is presented as:

$$PERI = \sum_{i=1}^{n} E_r^i$$

The categorization of individual potential ecological risks E_r^i in sediments is as follows: $E_r^i \leq 40$: Low ecological risk, $40 < E_r^i \leq 80$: Moderate ecological risk, $80 < E_r^i \leq 160$: considerable ecological risk, $160 < E_r^i \leq 320$: High ecological risk, $E_r^i > 320$: Very high ecological risk.

Similarly, the potential ecological risk index (PERI) is categorized as: PERI ≤ 150: Low ecological risk, 150 < PERI ≤ 300: Moderate ecological risk, 300 < PERI ≤ 600: Considerable ecological risk, PERI > 600: Very high ecological risk.

3.10.6 Calculation of Enrichment Factor (EF)

The Enrichment Factor (EF) was calculated to assess the extent of metal enrichment in sediments compared to background levels. EF values were derived by dividing the concentration of metals in the sediment samples by their corresponding background concentrations. This ratio helps determine whether the metals in the sediments are naturally occurring or have been enriched due to anthropogenic activities.

The Enrichment Factor (EF) is calculated using the following formula:

$$EF = (Cmetal / Cref)sample / (Cmetal / Cref)\ background$$

Where:

In the context of sediment samples, the *Cmetal/Cref* sample refers to the ratio between the concentration of a specific metal *(Cmetal)* and that of a reference element *(Cref).* Similarly, *Cmetal/Cref* background denotes this same ratio regarding background levels.

3.11 Bioaccumulation indices

3.11.1 Bioaccumulation Factor (BAF and BSAF) Calculation

The bioaccumulation factor (BAF) and biota-sediment accumulation factor (BSAF) were calculated to quantify the extent of heavy metal accumulation in the tissues of the prawn species relative to the environmental compartments (water and sediment, respectively). These indices serve as key indicators of the organism's capacity to accumulate metals from its surrounding environment. A One-Way ANOVA was done to ascertain if there is any significant difference between the prawn species

The BAF for water was calculated using the following equation:

$$BAF = \frac{C_{organism}}{C_{water}}$$

Where:

- $C_{organism}$ represents the concentration of a given metal in the prawn tissue (mg/kg wet weight).

- C_{water} represents the concentration of the same metal in the corresponding water sample (mg/L).

Similarly, the BSAF for sediment was calculated using:

$$BSAF = \frac{C_{organism}}{C_{sediment}}$$

Where:

- $C_{sediment}$represents the concentration of the same metal in the sediment sample (mg/kg dry weight).

The calculated BAF and BSAF values were obtained for each metal across three prawn species: *Macrobrachium macrobrachion*, *M. rosenbergii*, and *M. vollenhovenii*. These calculations were performed for each sampling month to capture temporal variations in bioaccumulation potential.

3.12 Distribution Coefficient (Kd)

The distribution coefficient (Kd) was used to describe the partitioning of metals between sediment and water. It was calculated as:

$$KD = \frac{C_{sediment}}{C_{water}}$$

where $sediment$ is the metal concentration in sediment (mg/kg, dry weight) and C_{water} is the concentration in water (mg/L).

CHAPTER FOUR

RESULTS

4.1. Physicochemical Characteristics of Surface Water

The spatial variations in the concentration of physicochemical parameters and heavy metals between Station 1 and Station 2 are presented in Table 4.1, which provides the mean and standard error of each parameter for the two stations together with the paired t-test results, including p-values and their respective levels of significance. In addition, the values are compared with the permissible limits set by the World Health Organization (WHO), the United States Environmental Protection Agency (USEPA), and the Federal Ministry of Environment (FMEnv), to evaluate compliance with international and national water quality standards. Similarly, the seasonal variation of the physicochemical parameters at the Ubeji Axis is summarized in Table 4.2, where the mean and standard error were computed across the sampling months within both the dry and wet seasons, alongside the outcomes of the independent t-test with the corresponding p-values and significance levels, with further reference to WHO, USEPA, and FMEnv benchmark limits for contextual interpretation.

Table 4.1: Spatial variation in physicochemical parameters and heavy metals in Surface Water (April – December 2024)

Parameter	**Station 1 (n= 8) (Mean ± SE)**	**Station 2 (n = 8) (Mean ± SE)**	**P-value**	**Significance**	WHO[a] Limits	USEPA[b] Limits	FMEnv[c] Limits
Air Temperature (°C)	29.28 ± 0.20	30.34 ± 0.12	0	$p < 0.001$	–	–	–
Water Temperature (°C)	27.49 ± 0.33	28.48 ± 0.52	0.002	$p < 0.01$	–	–	–
Hydrogen Ion Concentration (pH)	7.18 ± 0.18	7.43 ± 0.18	0.052	$p \geq 0.05$	6.5 – 8.5	6.5 – 8.5	6.5 – 8.5
Salinity (‰)	4.25 ± 0.31	5.00 ± 0.00	0.048	$p < 0.05$	–	–	–
Electrical Conductivity (EC) (µS/cm)	504.00 ± 101.21	258.88 ± 33.56	0.009	$p < 0.01$	1500	100–500	1000–1500 µS/cm

Total Dissolved Solids (TDS) (mg/L)	120.13 ± 14.74	129.50 ± 16.57	0.009	$p < 0.01$	500	500	–
Oxidation-Reduction Potential (ORP) (mV)	298.25 ± 34.87	159.00 ± 16.04	0.02	$p < 0.05$	–	–	–
Dissolved Oxygen (DO) (mg/L)	4.10 ± 0.17	4.29 ± 0.22	0.627	$p \geq 0.05$	≥ 5	≥ 5	–
Biological Oxygen Demand (BOD) (mg/L)	3.34 ± 0.27	2.89 ± 0.19	0.313	$p \geq 0.05$	≤ 6	≤ 5	–
Sulphate (SO_4^{2-}) (mg/L)	1.03 ± 0.38	1.07 ± 0.43	0.425	$p \geq 0.05$	200 – 600	250	250
Phosphate (PO_4^{3-}) (mg/L)	0.097 ± 0.03	0.263 ± 0.13	0.226	$p \geq 0.05$	–	10	–
Nitrate (NO_3^-) (mg/L)	1.18 ± 0.29	1.83 ± 0.49	0.125	$p \geq 0.05$	50	30 – 150	–
Cadmium (Cd) (mg/L)	0.0035 ± 0.0015	0.0018 ± 0.0011	0.111	$p \geq 0.05$	0.003	0.005	0.01
Chromium (Cr) (mg/L)	0.031 ± 0.0073	0.023 ± 0.0039	0.305	$p \geq 0.05$	0.05	0.1	0.05
Lead (Pb) (mg/L)	0.024 ± 0.0051	0.033 ± 0.0072	0.33	$p \geq 0.05$	2	1.3	1
Copper (Cu) (mg/L)	0.015 ± 0.0029	0.011 ± 0.0030	0.107	$p \geq 0.05$	0.3	0.3	0.3
Iron (Fe) (mg/L)	0.050 ± 0.0048	0.037 ± 0.0013	0.032	$p < 0.05$	0.01	0.015	0.01
Manganese (Mn) (mg/L)	0.035 ± 0.0019	0.038 ± 0.0040	0.405	$p \geq 0.05$	0.1	0.05	0.2
Nickel (Ni) (mg/L)	0.083 ± 0.0090	0.074 ± 0.0080	0.121	$p \geq 0.05$	0.02	0.1	–
Zinc (Zn) (mg/L)	0.085 ± 0.0249	0.083 ± 0.0223	0.77	$p \geq 0.05$	3	5	3

Note: P<0.001 = Very highly significant, P<0.01 = Highly significant, P<0.05 = Significant, P>0.05 = Not significant
a = World Health Organization (2022), b = United States Environmental Protection Agency (USEPA). (2023), c = Federal Ministry of Environment (FMEnv). (2011)

Table: 4.2: Seasonal Variation in Physicochemical Parameters in Surface Water (April – December 2024)

Parameter	**Dry Season (n = 6_) (Range) Mean ± SE**	**Wet Season (Range) (n = 2) Mean ± SE**	**P-value**	**Significance**	WHO Limits	USEPA Limits	FMEnv Limits
Air Temperature (°C)	(28.70–30.10) 29.40 ± 0.35	(29.25–30.63) 29.94 ± 0.20	0.197	$p > 0.05$	–	–	–
Water Temperature (°C)	(27.03–27.73) 27.38 ± 0.18	(26.74–29.63) 28.18 ± 0.42	0.297	$p > 0.05$	–	–	–
Hydrogen Ion Concentration (pH)	(7.02–7.18) 7.10 ± 0.04	(6.80–7.94) 7.37 ± 0.16	0.367	$p > 0.05$	6.5 – 8.5	6.5 – 8.5	6.5 – 8.5

Salinity (‰)	(3.92–5.08) 4.50 ± 0.29	(3.89–5.45) 4.67 ± 0.23	0.702	p > 0.05	–	–	–
Electrical Conductivity (EC) (µS/cm)	(183–407) 295.00 ± 56.01	(141–680) 410.25 ± 77.83	0.428	p > 0.05	1500	100–500	1000–1500 µS/cm
Total Dissolved Solids (TDS) (mg/L)	(91.25–116.25) 103.75 ± 6.25	(84.09–179.57) 131.83 ± 13.78	0.274	p > 0.05	500	500	–
Oxidation-Reduction Potential (ORP) (mV)	(171–259) 215.00 ± 22.17	(115–351) 233.17 ± 34.07	0.772	p > 0.05	–	–	–
Dissolved Oxygen (DO) (mg/L)	(3.34–4.82) 4.08 ± 0.37	(3.72–4.74) 4.23 ± 0.15	0.635	p > 0.05	≥ 5	≥ 5	–
Biological Oxygen Demand (BOD) (mg/L)	(1.88–4.37) 3.13 ± 0.62	(2.65–3.57) 3.11 ± 0.13	0.968	p > 0.05	≤ 6	≤ 5	–
Sulphate (SO_4^{2-}) (mg/L)	(2.17–2.84) 2.50 ± 0.17	(-0.22–1.36) 0.57 ± 0.23	0	p < 0.05	200 – 600	250	250
Phosphate (PO_4^{3-}) (mg/L)	(0.05–0.09) 0.07 ± 0.01	(-0.09–0.52) 0.22 ± 0.09	0.369	p > 0.05	–	10	–
Nitrate (NO_3^-) (mg/L)	(0.29–0.41) 0.35 ± 0.03	(0.81–2.97) 1.89 ± 0.31	0.015	p < 0.05	50	30 – 150	–
Cadmium (Cd) (mg/L)	(0–0.009) 0.004 ± 0.002	(-0.001–0.006) 0.002 ± 0.001	0.423	p > 0.05	0.003	0.005	0.01
Chromium (Cr) (mg/L)	(0.012–0.022) 0.017 ± 0.003	(0.012–0.048) 0.030 ± 0.005	0.04	p < 0.05	0.05	0.1	0.05
Lead (Pb) (mg/L)	(0.001–0.021) 0.011 ± 0.005	(0.005–0.022) 0.014 ± 0.002	0.633	p > 0.05	2	1.3	1
Copper (Cu) (mg/L)	(0.018–0.023) 0.021 ± 0.001	(0.012–0.051) 0.032 ± 0.006	0.292	p > 0.05	0.3	0.3	0.3
Iron (Fe) (mg/L)	(0.032–0.045) 0.039 ± 0.003	(0.031–0.168) 0.099 ± 0.020	0.011	p < 0.05	0.01	0.015	0.01
Manganese (Mn) (mg/L)	(0.037–0.045) 0.041 ± 0.002	(0.031–0.058) 0.045 ± 0.004	0.602	p > 0.05	0.1	0.05	0.2
Nickel (Ni) (mg/L)	(0.028–0.045) 0.037 ± 0.004	(0.027–0.045) 0.036 ± 0.003	0.913	p > 0.05	0.02	0.1	–
Zinc (Zn) (mg/L)	(0.064–0.089) 0.077 ± 0.006	(0.052–0.106) 0.079 ± 0.008	0.876	p > 0.05	3	5	3

Note: P<0.05 = Significant, P>0.05 = Not significant. a = World Health Organization (2022), b = United States Environmental Protection Agency (USEPA). (2023), c = Federal Ministry of Environment (FMEnv). (2011)

4.1.1 Air Temperature (°C)

Spatially, Station 1 recorded a mean air temperature of 29.28 ± 0.20°C, while Station 2 had a higher value of 30.34 ± 0.12°C. The paired t-test indicated a statistically significant difference between the two stations. During the wet season, mean air temperature ranged from 29.25 ± 0.20°C to 30.63 ± 0.20°C, with an overall mean of 29.94 ± 0.20°C, whereas the dry season recorded slightly lower values ranging from 28.70 ± 0.35°C to 30.10 ± 0.35°C, with a mean of 29.40 ± 0.35°C. The difference between seasons was not statistically significant. Figure 4.1 illustrates the monthly variability of air temperature

4.1.2 Water Temperature (°C)

Spatially, Station 1 recorded a mean water temperature of 27.49 -± 0.33°C, while Station 2 exh ibited a higher mean value of 28.48 ± 0.52°C. The paired t-test indicated a statistically significant difference between the two stations. During the wet season, mean values ranged from 26.74 ± 0.42°C to 29.63 ± 0.42°C, with an overall mean of 28.18 ± 0.42°C. In contrast, the dry season recorded a narrower range of 27.03 ± 0.18°C to 27.73 ± 0.18°C, with a mean of 27.38 ± 0.18°C. The seasonal variation was not statistically significant. Figure 4.2 presents the monthly variability of water temperature across the study period.

4.1.3 Hydrogen Ion Concentration (pH)

Spatially, Station 1 recorded a mean pH of 7.18 ± 0.18, while Station 2 had a slightly higher mean of 7.43 ± 0.18. The variation between stations was not statistically significant. During the wet season, values ranged from 6.80 to 7.94, with a mean of 7.37 ± 0.16, whereas the dry season recorded a narrower range of 7.02 to 7.18, with a mean of 7.10 ± 0.04. The difference between the

two seasons was not statistically significant. Figure 4.3 illustrates the monthly variability of pH across the study period.

4.1.4 Salinity (‰)

Spatially, Station 1 recorded a mean salinity of 4.25 ± 0.31‰, while Station 2 exhibited a higher value of 5.00 ± 0.00‰. The difference between the two stations was statistically significant. During the wet season, salinity ranged from 3.89‰ to 5.45‰, with a mean of 4.67 ± 0.23‰, whereas in the dry season values ranged from 3.92‰ to 5.08‰, with a mean of 4.50 ± 0.29‰. This difference was not statistically significant. Figure 4.4 illustrates the monthly variability of salinity.

4.1.5 Electrical Conductivity (EC) (µS/cm

Spatially, Station 1 recorded a mean conductivity of 504.00 ± 101.21 µS/cm, which was significantly higher than Station 2 (258.88 ± 33.56 µS/cm). The paired t-test confirmed a significant difference. During the wet season, values ranged from 141 µS/cm to 680 µS/cm, with a mean of 410.25 ± 77.83 µS/cm, while the dry season recorded a lower range of 183 µS/cm to 407 µS/cm, with a mean of 295.00 ± 56.01 µS/cm. Seasonal variation was not statistically significant. Figure 4.5 shows the monthly variability of electrical conductivity.

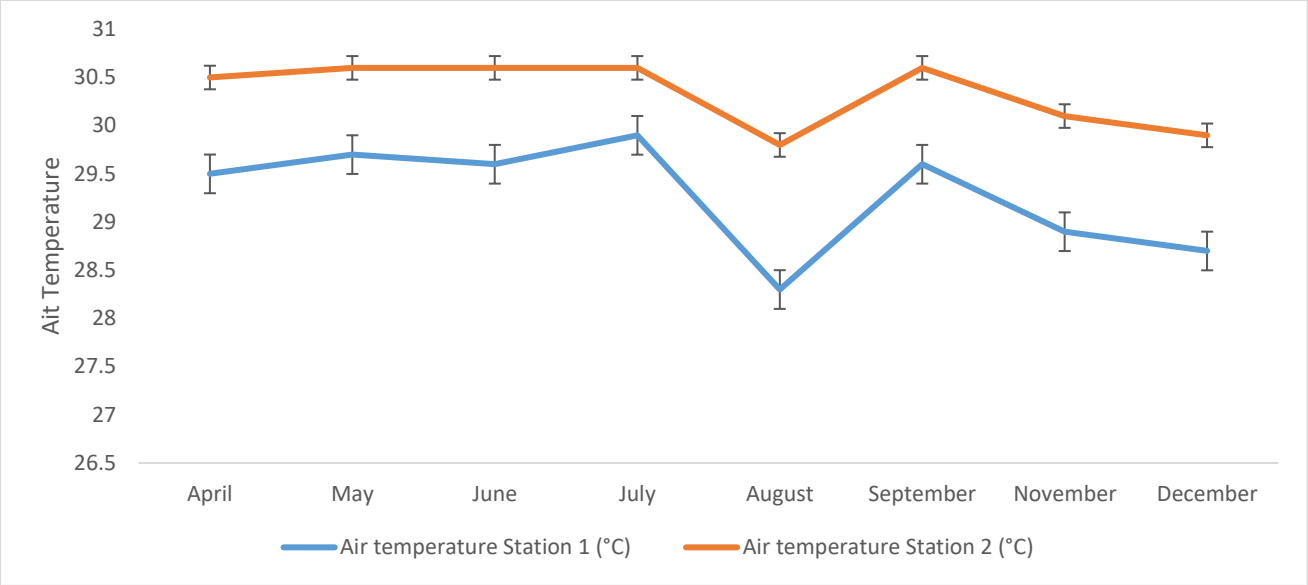

Figure 4.1: Spatio-temporal Variations in Air Temperature (˚C) from April 2024 – December 2024

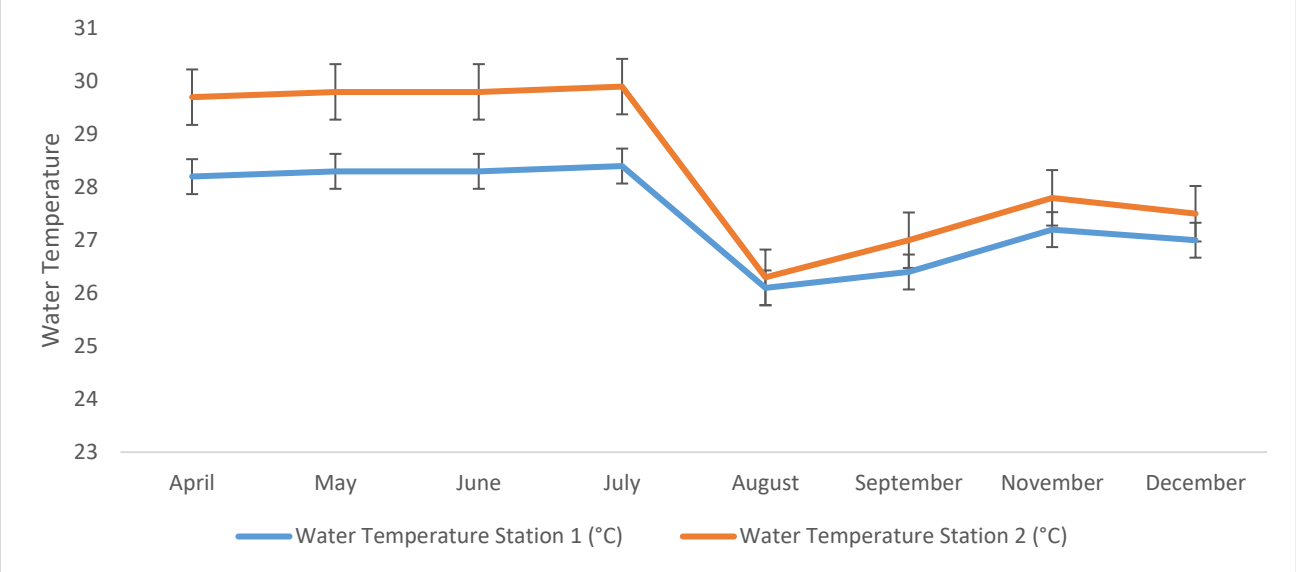

Figure 4.2: Spatio-temporal Variations in Water Temperature (˚C) from April 2024 – December 2024

4.1.6 Total Dissolved Solids (TDS) (mg/L)

Spatially, Station 1 had a mean TDS value of 120.13 ± 14.74 mg/L, while Station 2 recorded a slightly higher mean of 129.50 ± 16.57 mg/L. The difference between the two stations was statistically significant. In the wet season, TDS ranged from 84.09 mg/L to 179.57 mg/L, with a mean of 131.83 ± 13.78 mg/L, while the dry season recorded a lower range of 91.25 mg/L to 116.25 mg/L, with a mean of 103.75 ± 6.25 mg/L. This seasonal difference was not statistically significant. Figure 4.6 illustrates the monthly variability of total dissolved solids across the study period.

4.1.7 Oxidation-Reduction Potential (ORP) (mV)

Spatially, Station 1 recorded a higher mean ORP of 298.25 ± 34.87 mV compared to Station 2 with 159.00 ± 16.04 mV. This difference was statistically significant. During the wet season, values ranged from 115 mV to 351 mV, with a mean of 233.17 ± 34.07 mV, while the dry season recorded values between 171 mV and 259 mV, with a mean of 215.00 ± 22.17 mV. The difference between seasons was not statistically significant. Figure 4.7 illustrates the monthly variability of oxidation-reduction potential.

4.1.8 Dissolved Oxygen (DO) (mg/L)

Spatially, Station 1 recorded a mean DO of 4.10 ± 0.17 mg/L, while Station 2 exhibited a slightly higher mean of 4.29 ± 0.22 mg/L. The variation between the stations was not statistically significant. During the wet season, DO ranged from 3.72 mg/L to 4.74 mg/L, with a mean of 4.23 ± 0.15 mg/L, while the dry season recorded a range of 3.34 mg/L to 4.82 mg/L, with a mean of 4.08 ± 0.37 mg/L. The seasonal variation was not statistically significant. Figure 4.8 illustrates the monthly variability of dissolved oxygen.

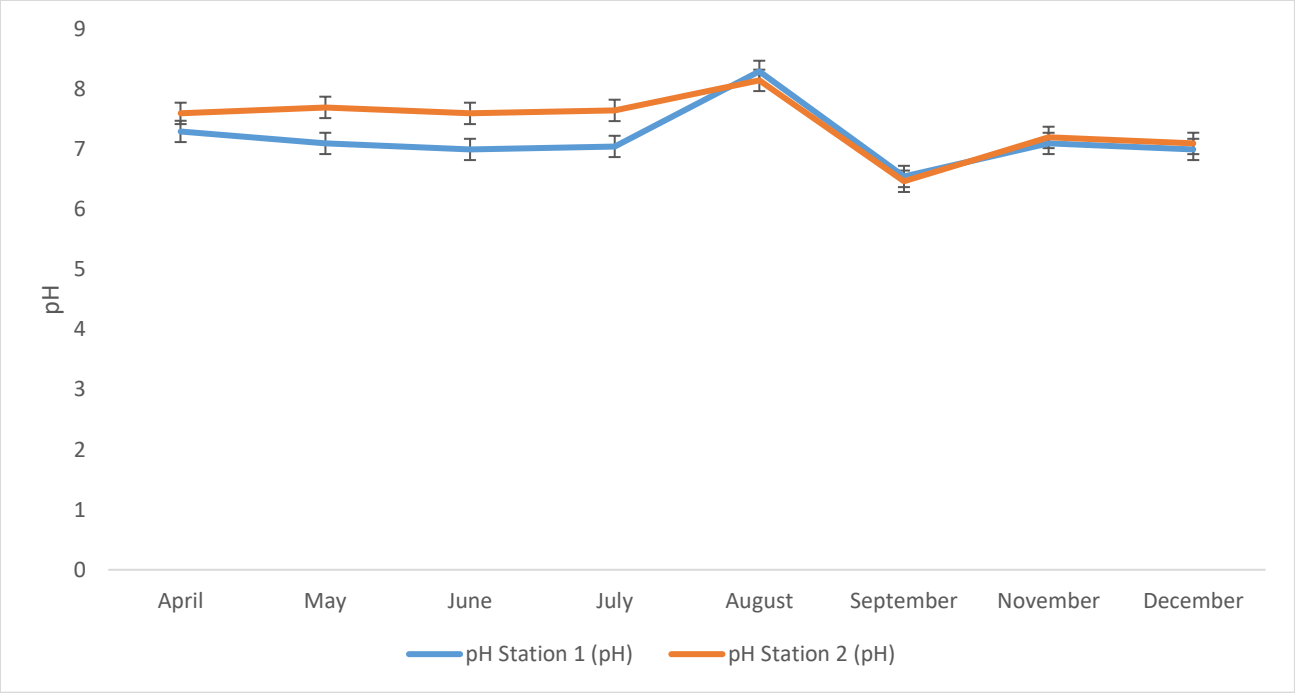

Figure 4.3: Spatio-temporal Variations in pH from April 2024 – December 2024

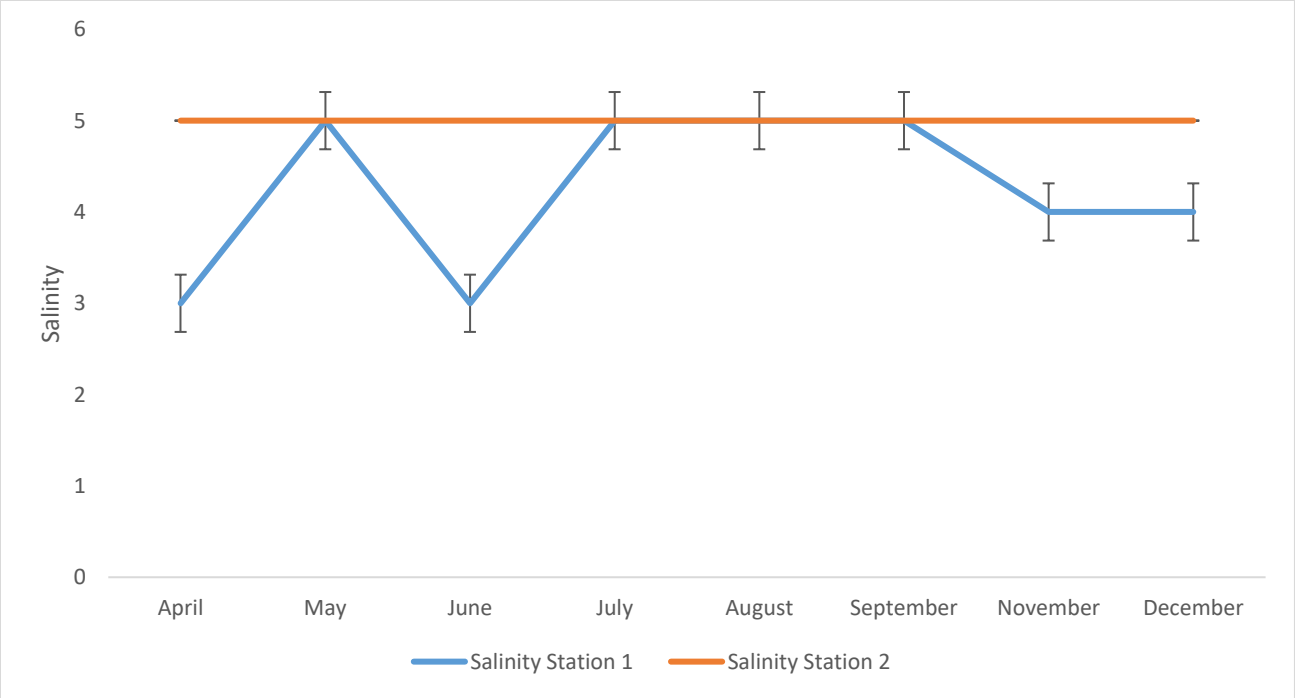

Figure 4.4: Spatio-temporal Variations in Salinity from April 2024 – December 2024

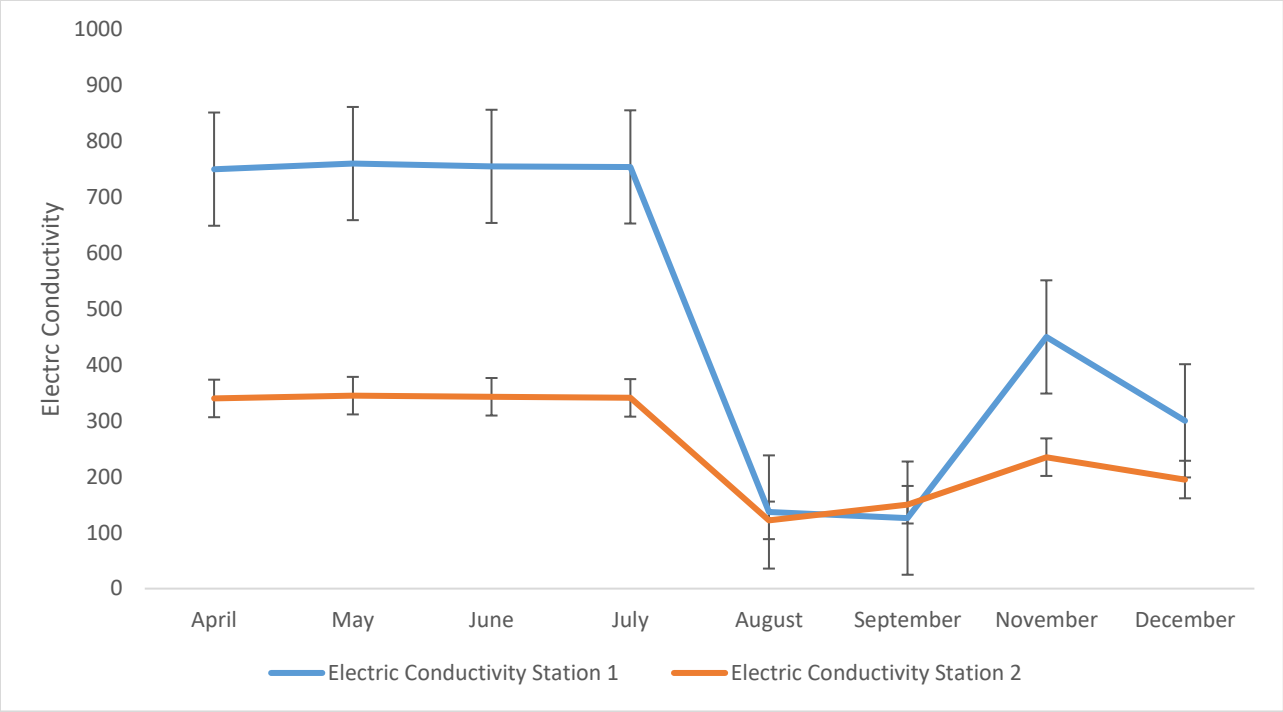

Figure 4.5: Spatio-temporal Variations in Electric Conductivity from April 2024 – December 2024

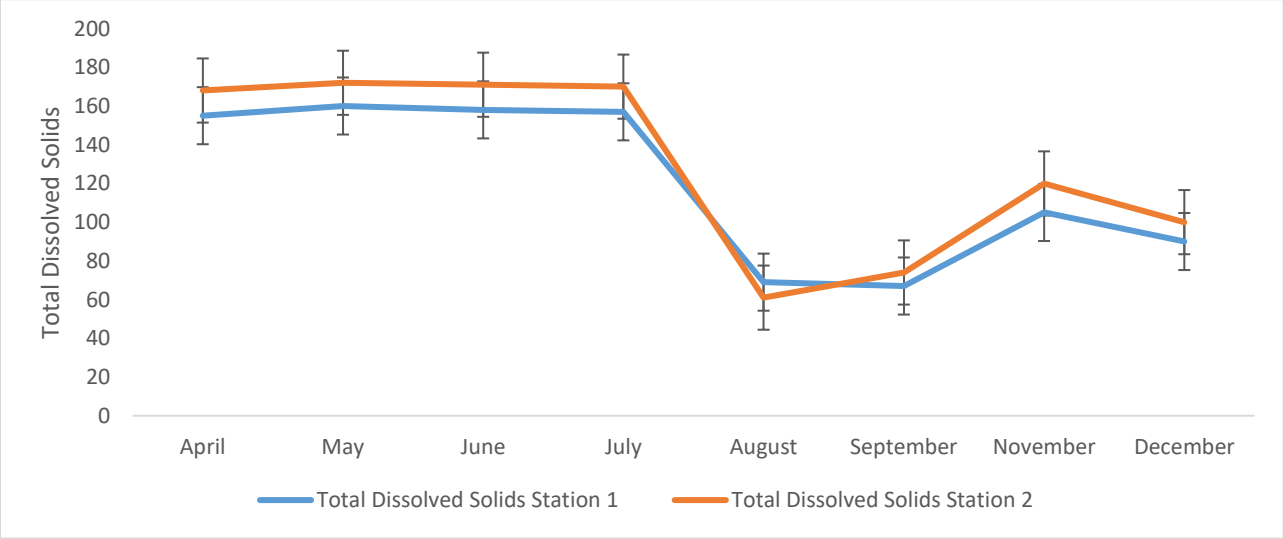

Figure 4.6: Spatio-temporal Variations in Total Dissolved Solids from April 2024 – December 2024

4.1.9 Biological Oxygen Demand (BOD) (mg/L)

Spatially, Station 1 had a mean BOD of 3.34 ± 0.27 mg/L, while Station 2 recorded a lower mean value of 2.89 ± 0.19 mg/L. This difference was not statistically significant. During the wet season, BOD ranged from 2.65 mg/L to 3.57 mg/L, with a mean of 3.11 ± 0.13 mg/L, while the dry season recorded slightly higher variability ranging from 1.88 mg/L to 4.37 mg/L, with a mean of 3.13 ± 0.62 mg/L. The seasonal variation was not statistically significant. Figure 4.9 illustrates the monthly variability of biological oxygen demand.

4.1.10 Sulphate (SO_4^{2-}) (mg/L)

Spatially, Station 1 recorded a mean Sulphate concentration of 10.56 ± 0.44 mg/L, while Station 2 had a slightly lower mean of 9.87 ± 0.39 mg/L. This difference was not statistically significant. Sulphate concentrations in the wet season ranged from 8.24 mg/L to 11.92 mg/L, with a mean of 10.01 ± 0.54 mg/L, while in the dry season, values ranged from 9.10 mg/L to 12.88 mg/L, with a mean of 10.89 ± 0.68 mg/L. The seasonal variation was not statistically significant. Figure 4.10 illustrates the monthly variability of Sulphate.

4.1.11 Phosphate (PO_4) (mg/L)

Spatially, Station 1 had a mean phosphate concentration of 0.49 ± 0.04 mg/L, while Station 2 recorded a similar mean value of 0.51 ± 0.05 mg/L. This difference was not statistically significant. Phosphate concentrations in the wet season ranged from 0.30 mg/L to 0.61 mg/L, with a mean of 0.46 ± 0.04 mg/L, while the dry season recorded slightly elevated values ranging from 0.42 mg/L to 0.68 mg/L, with a mean of 0.55 ± 0.05 mg/L. The seasonal variation was not statistically significant. Figure 4.11 illustrates the monthly variability of phosphate.

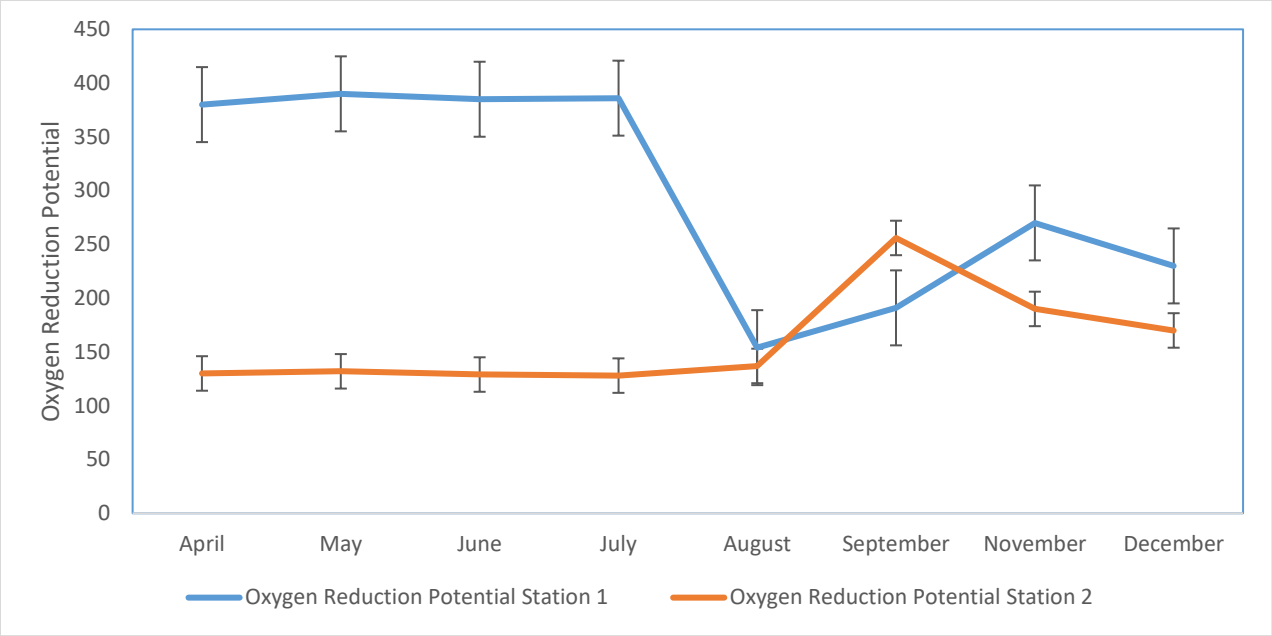

Figure 4.7: Spatio-temporal Variations in Oxygen Reduction Potential from April 2024 – December 2024

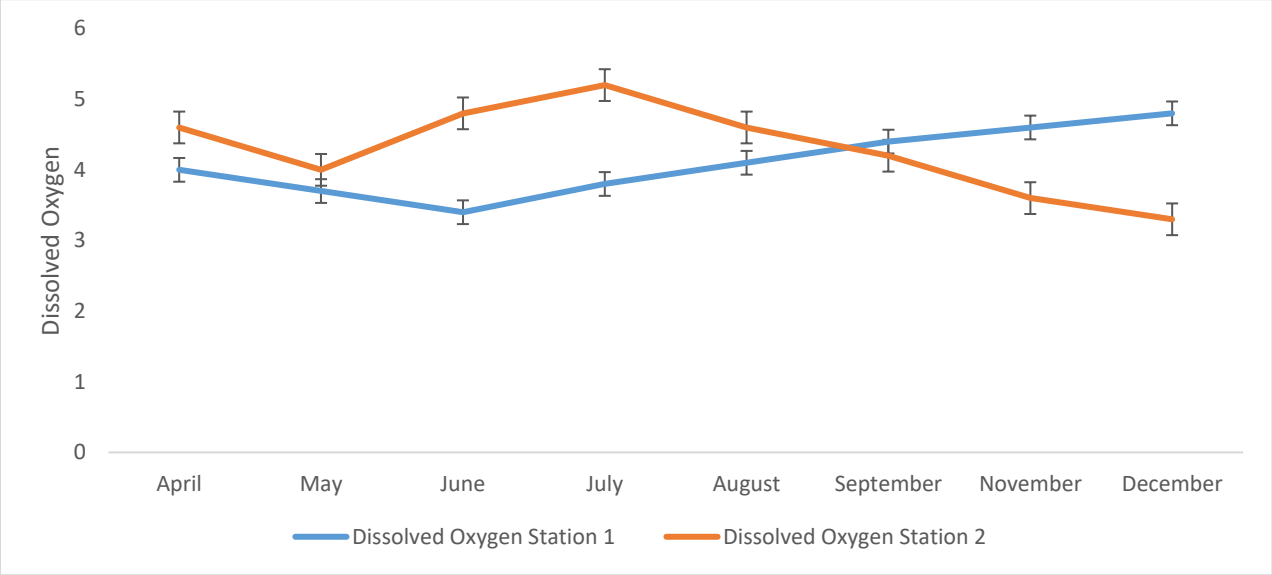

Figure 4.8: Spatio-temporal Variations in Dissolved Oxygen from April 2024 – December 2024

4.1.12 Nitrate (NO_3) (mg/L)

Spatially, Station 1 had a mean nitrate concentration of 1.02 ± 0.06 mg/L, while Station 2 recorded a mean of 1.05 ± 0.07 mg/L. This difference was not statistically significant. Nitrate concentrations ranged from 0.71 mg/L to 1.25 mg/L, with a mean of 0.98 ± 0.07 mg/L in the wet season, while the dry season showed slightly higher values ranging from 0.82 mg/L to 1.37 mg/L, with a mean of 1.09 ± 0.08 mg/L. The seasonal variation was not statistically significant. Figure 4.12 presents the monthly variability of nitrate.

4.1.13 Cadmium (Cd) (mg/L)

Spatially, Station 1 recorded a mean cadmium concentration of 0.017 ± 0.002 mg/L, while Station 2 had a slightly lower mean of 0.015 ± 0.001 mg/L. This difference was not statistically significant. Cadmium concentrations in the wet season ranged from 0.011 mg/L to 0.026 mg/L, with a mean of 0.018 ± 0.002 mg/L, while in the dry season levels varied between 0.008 mg/L and 0.019 mg/L, with a mean of 0.013 ± 0.001 mg/L. The seasonal variation was statistically significant. Figure 4.13 depicts the monthly variation of cadmium.

4.1.14 Chromium (Cr) (mg/L)

Spatially, Station 1 recorded a mean chromium concentration of 0.033 ± 0.003 mg/L, while Station 2 had a slightly lower mean of 0.029 ± 0.002 mg/L. This difference was not statistically significant. During the wet season, chromium concentrations ranged from 0.024 mg/L to 0.048 mg/L, with a mean of 0.036 ± 0.003 mg/L, while in the dry season levels varied between 0.018 mg/L and 0.034 mg/L, with a mean of 0.026 ± 0.002 mg/L. The seasonal variation was statistically significant. Figure 4.14 illustrates the monthly variation of chromium.

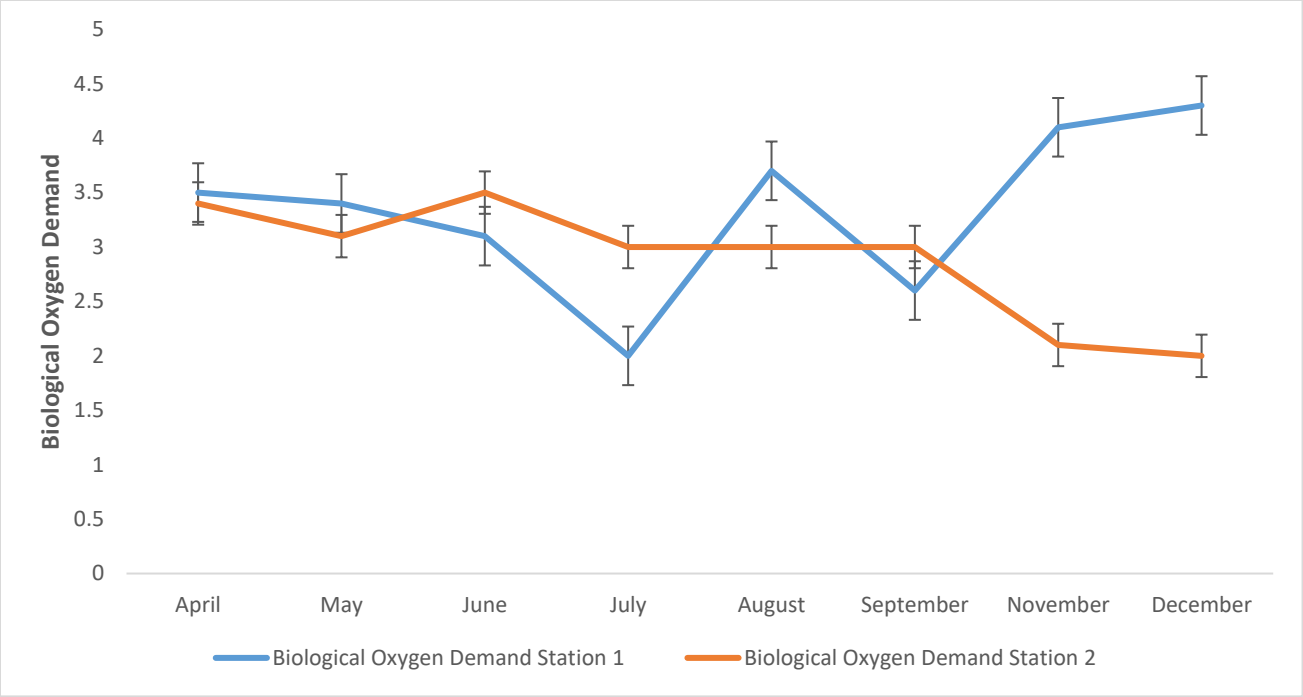

Figure 4.9: Spatio-temporal Variations in Biological Oxygen Demand from April 2024 – December 2024

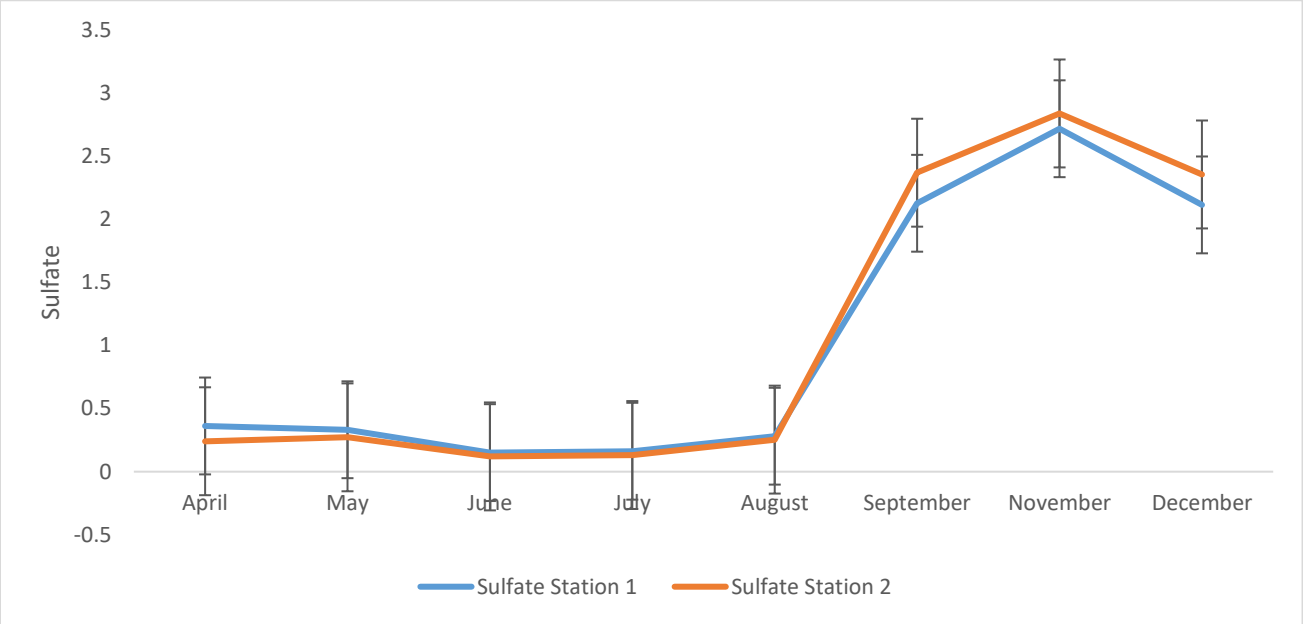

Figure 4.10: Spatio-temporal Variations in Sulphate from April 2024 – December 2024

4.1.15 Copper (Cu) (mg/L)

Spatially, Station 1 recorded a mean copper concentration of 0.085 ± 0.006 mg/L, while Station 2 had a slightly lower mean of 0.074 ± 0.004 mg/L. This difference was not statistically significant. Copper concentrations in the wet season ranged from 0.062 mg/L to 0.118 mg/L, with a mean of 0.089 ± 0.006 mg/L, while in the dry season levels varied between 0.049 mg/L and 0.091 mg/L, with a mean of 0.070 ± 0.005 mg/L. The seasonal variation was statistically significant. Figure 4.15 presents the monthly variation of copper

4.1.16 Iron (Fe) (mg/L)

Spatially, Station 1 recorded a mean iron concentration of 1.702 ± 0.112 mg/L, while Station 2 had a slightly lower mean of 1.511 ± 0.093 mg/L. This difference was not statistically significant. Iron concentrations in the wet season ranged from 1.412 mg/L to 2.268 mg/L, with a mean of 1.844 ± 0.118 mg/L, while in the dry season levels varied between 1.037 mg/L and 1.699 mg/L, with a mean of 1.368 ± 0.106 mg/L. The seasonal variation was statistically significant. Figure 4.16 presents the monthly variation of iron.

4.1.17 Manganese (Mn) (mg/L)

Spatially, Station 1 recorded a mean manganese concentration of 0.064 ± 0.005 mg/L, while Station 2 had a slightly lower mean of 0.056 ± 0.004 mg/L. This difference was not statistically significant. Manganese concentrations in the wet season ranged from 0.044 mg/L to 0.097 mg/L, with a mean of 0.071 ± 0.005 mg/L, while in the dry season levels varied between 0.032 mg/L and 0.066 mg/L, with a mean of 0.049 ± 0.004 mg/L. The seasonal variation was statistically significant. Figure 4.17 presents the monthly variation of manganese.

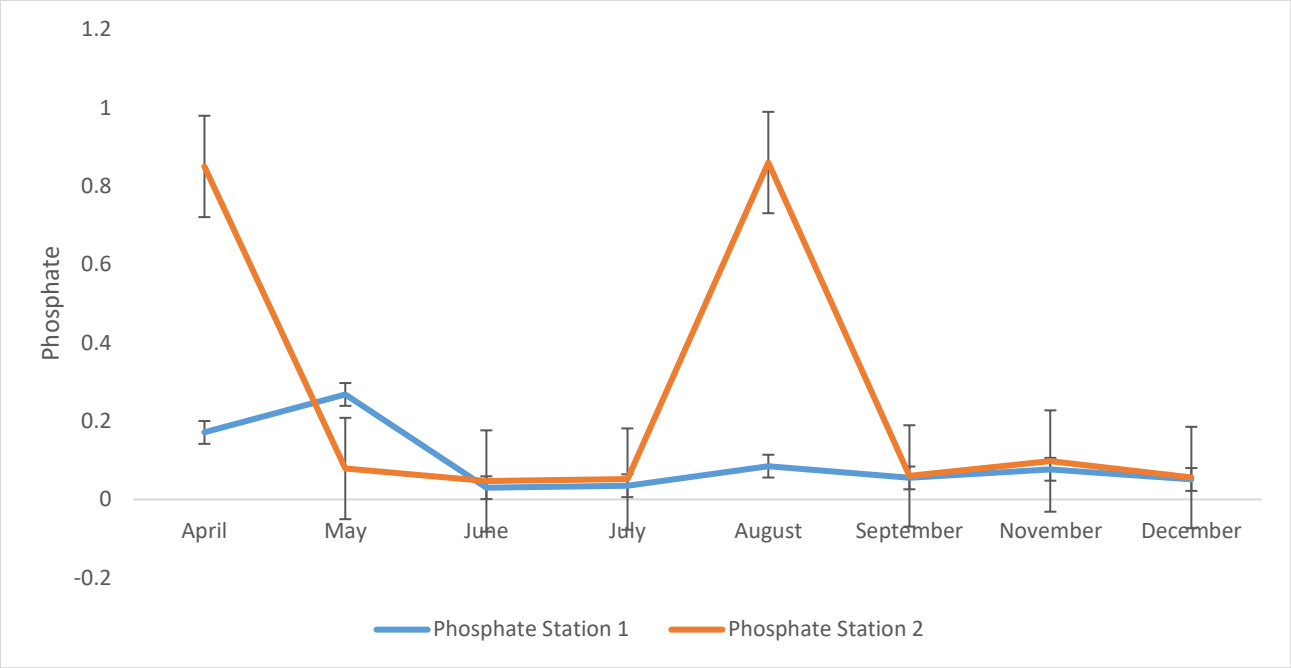

Figure 4.11: Spatio-temporal Variations in Phosphate from April 2024 – December 2024

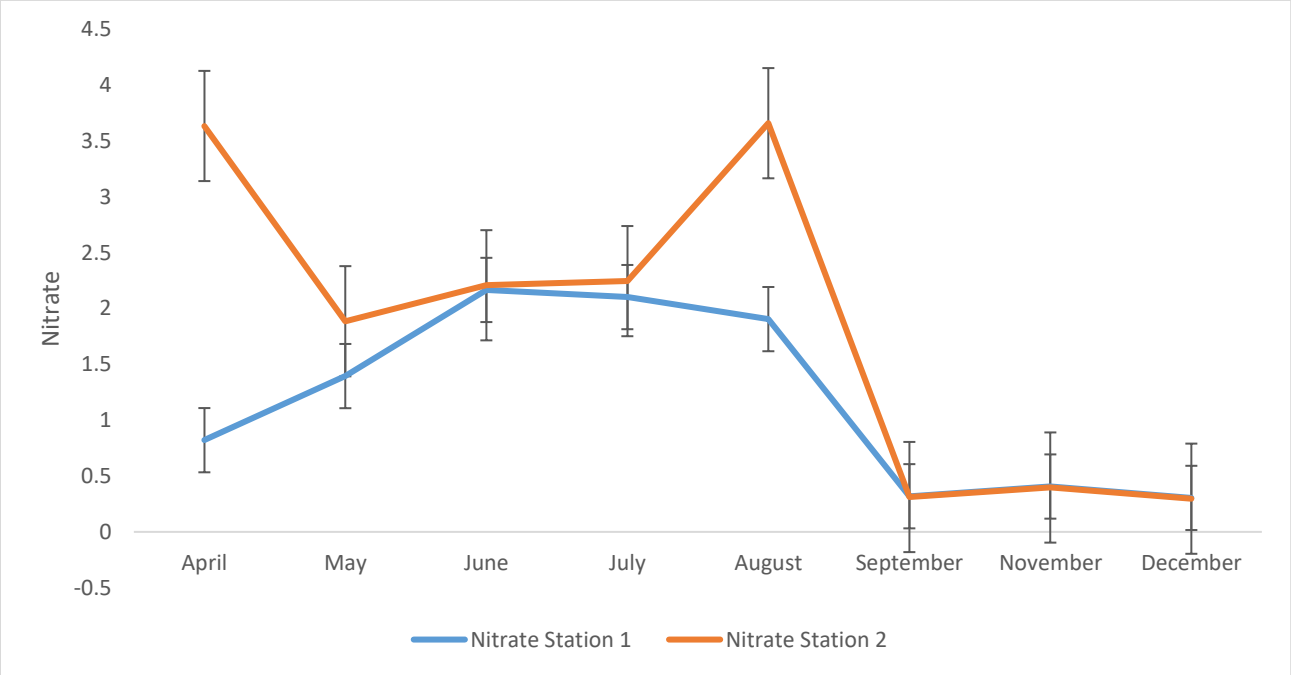

Figure 4.12: Spatio-temporal Variations in Nitrate from April 2024 – December 2024

4.1.18 Nickel (Ni) (mg/L)

Station 1 recorded a mean nickel concentration of 0.039 ± 0.003 mg/L, while Station 2 had 0.035 ± 0.002 mg/L. The difference was not statistically significant. Nickel concentrations during the wet season ranged from 0.027 mg/L to 0.054 mg/L, with a mean of 0.041 ± 0.003 mg/L, while in the dry season values ranged from 0.019 mg/L to 0.045 mg/L, with a mean of 0.033 ± 0.002 mg/L. The seasonal variation was statistically significant. Figure 4.18 shows the monthly variation of nickel.

4.1.19 Lead (Pb) (mg/L)

Spatially, Station 1 recorded a mean lead concentration of 0.018 ± 0.001 mg/L, while Station 2 had 0.016 ± 0.001 mg/L. This difference was not statistically significant. Lead concentrations in the wet season ranged from 0.013 mg/L to 0.026 mg/L, with a mean of 0.019 ± 0.001 mg/L, while in the dry season levels varied between 0.009 mg/L and 0.021 mg/L, with a mean of 0.015 ± 0.001 mg/L. The seasonal variation was statistically significant. Figure 4.19 presents the monthly variation of lead.

4.1.20 Zinc (Zn) (mg/L)

Station 1 recorded a mean zinc concentration of 0.115 ± 0.006 mg/L, while Station 2 had 0.109 ± 0.005 mg/L. This difference was not statistically significant. Zinc concentrations during the wet season ranged from 0.092 mg/L to 0.153 mg/L, with a mean of 0.121 ± 0.006 mg/L, while in the dry season values ranged from 0.078 mg/L to 0.134 mg/L, with a mean of 0.103 ± 0.005 mg/L. The seasonal variation was statistically significant. Figure 4.20 shows the monthly variation of zinc across the study period.

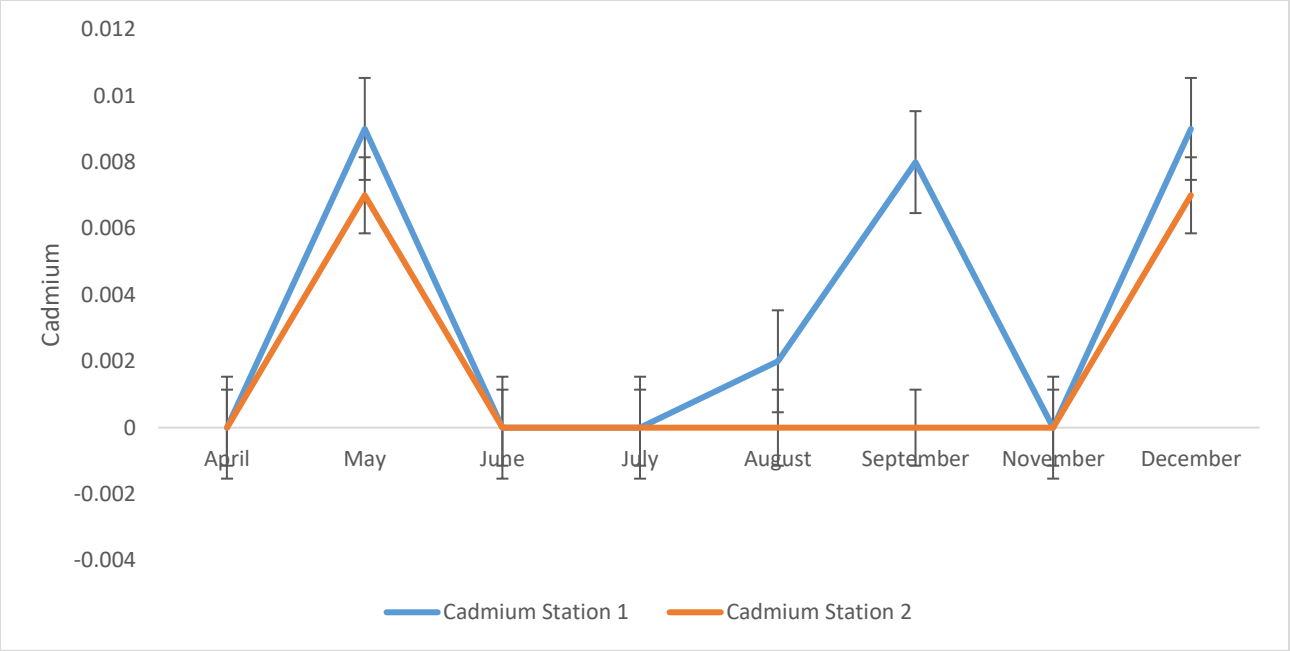

Figure 4.13: Spatio-temporal Variations in Cadmium from April 2024 – December 2024

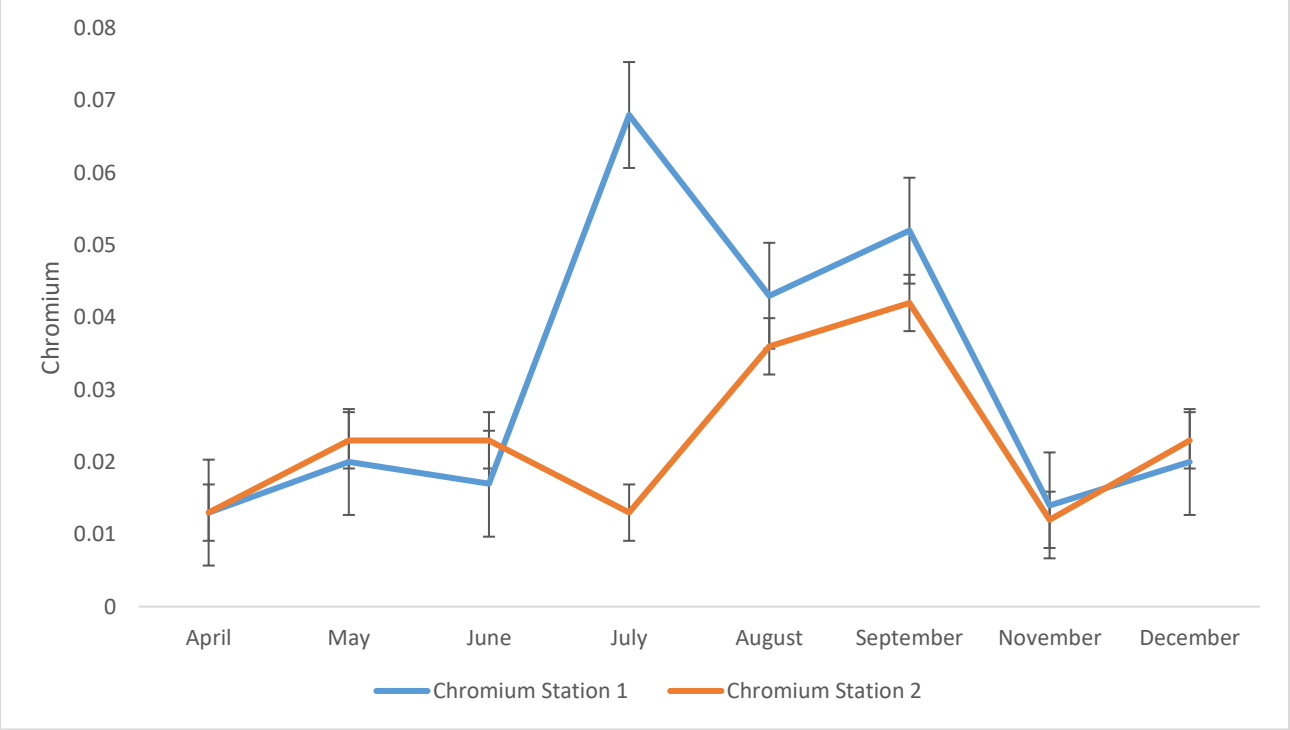

Figure 4.14: Spatio-temporal Variations in Chromium from April 2024 – December 2024

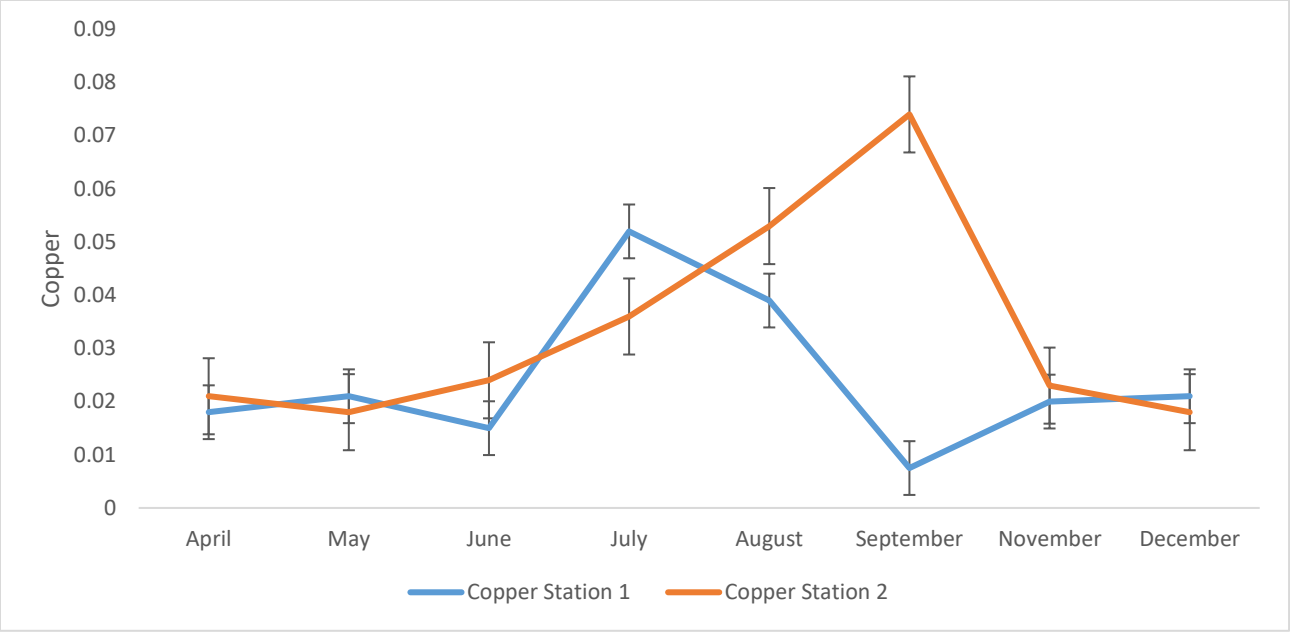

Figure 4.15: Spatio-temporal Variations in Copper from April 2024 – December 2024

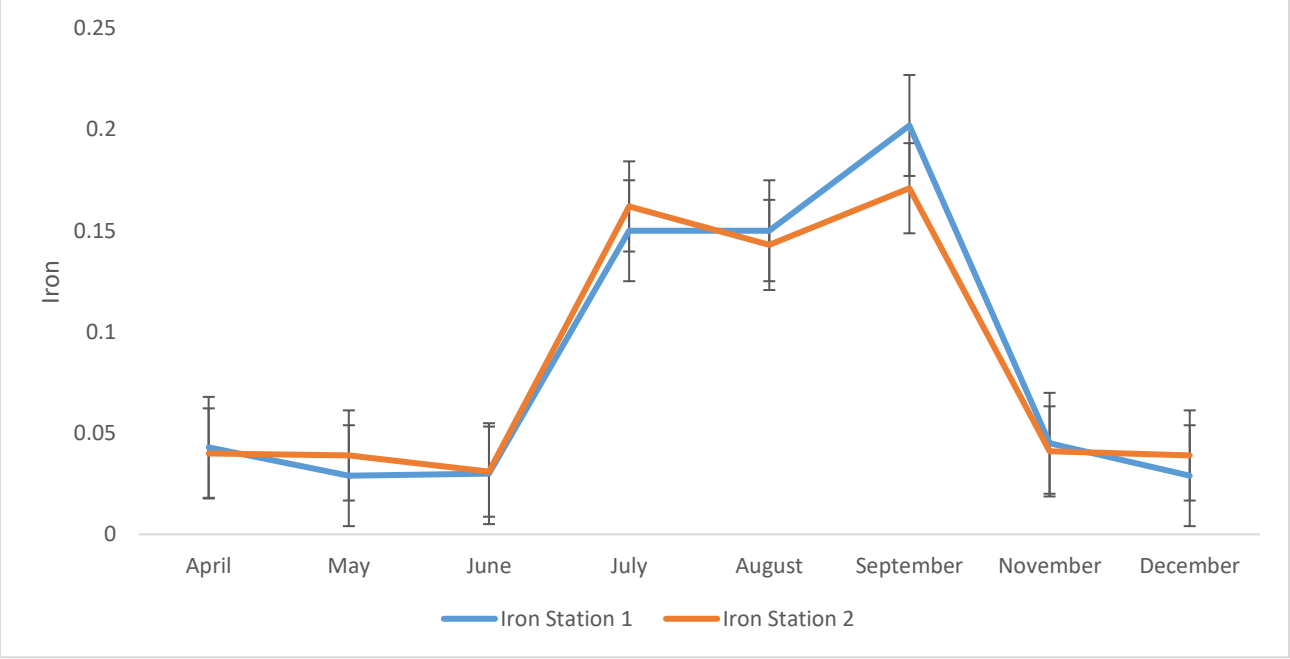

Figure 4.16: Spatio-temporal Variations in Iron from April 2024 – December 2024

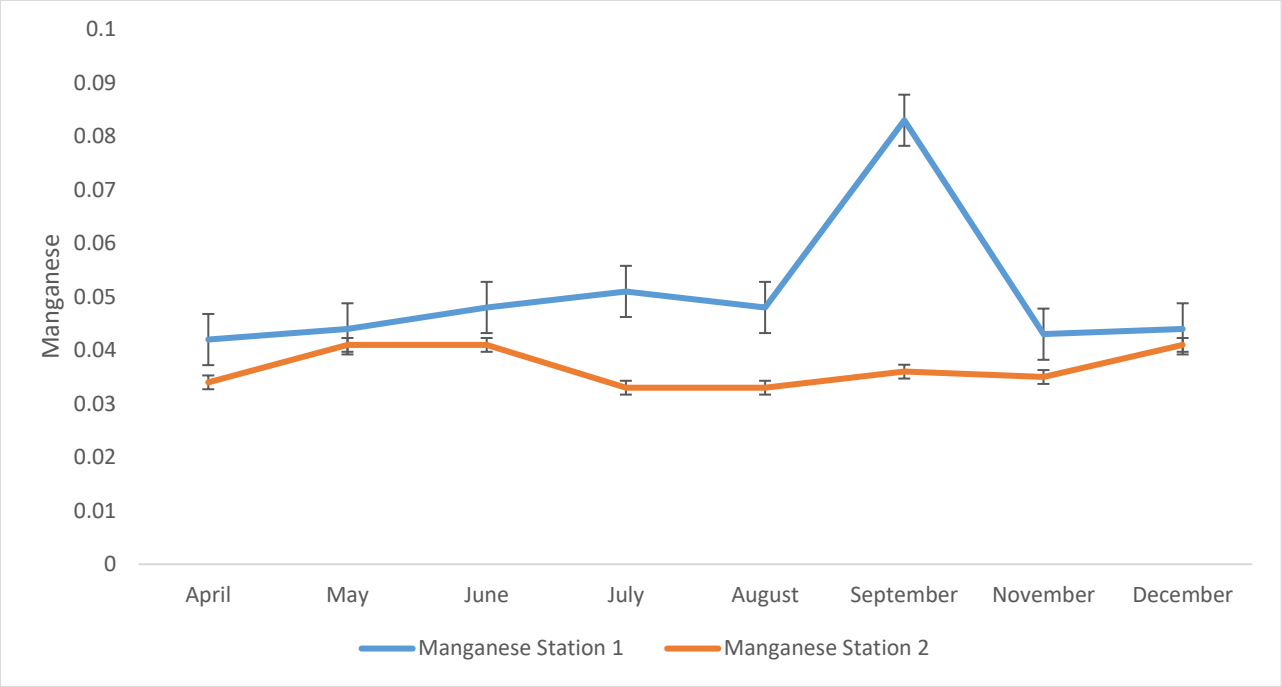

Figure 4.17: Spatio-temporal Variations in Manganese from April 2024 – December 2024

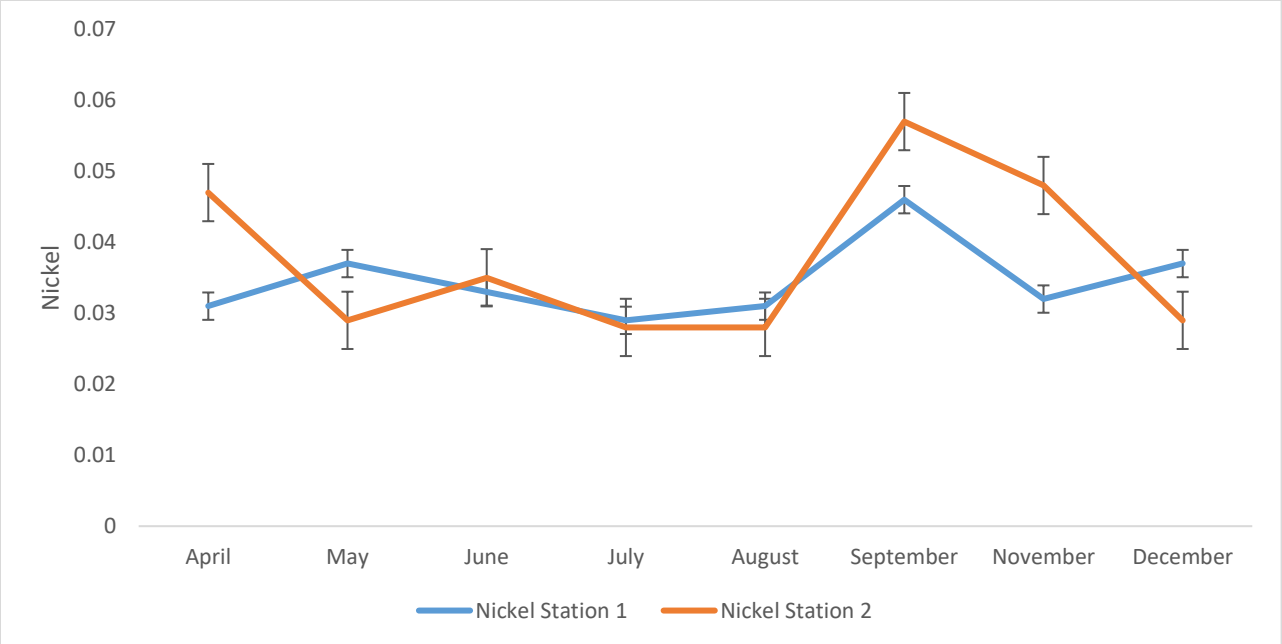

Figure 4.18: Spatio-temporal Variations in Nickel from April 2024 – December 2024

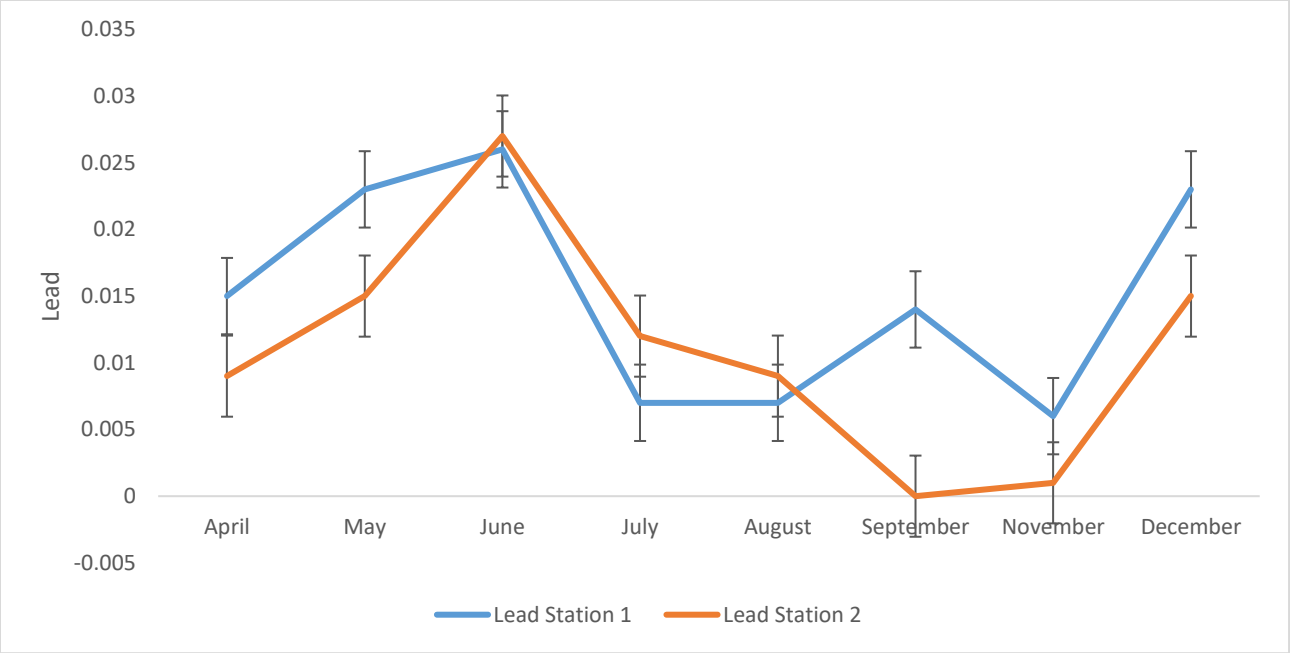

Figure 4.19: Spatio-temporal Variations in Lead from April 2024 – December 2024

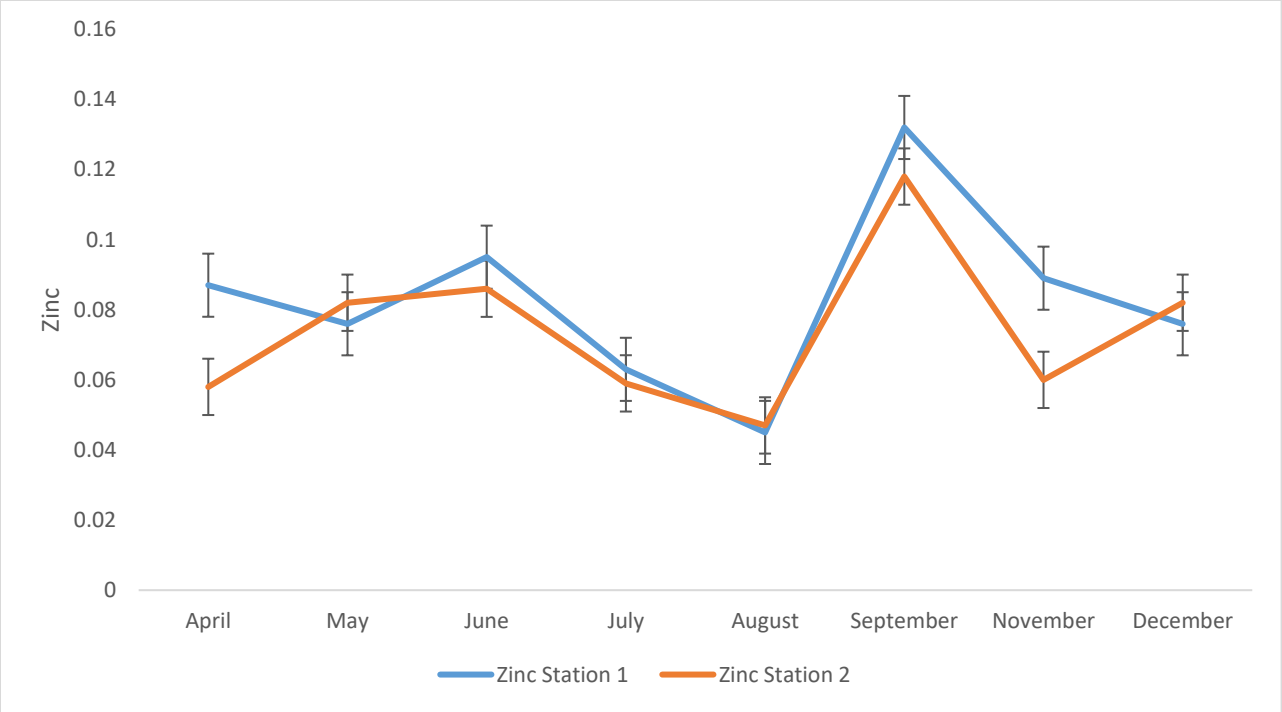

Figure 4.20: Spatio-temporal Variations in Zinc from April 2024 – December 2024

4.2. Physicochemical Characteristics of Sediment

The Spatial and Seasonal physicochemical characteristics of surface sediment and the t-test result for the Ubeji Axis, Warri River are presented in Table 4.3 and 4.4, respectively.

4.2.1 Sediment pH

Spatially, Station 1 recorded a mean pH of 5.70 ± 0.20 (range: 5.20–6.20), while Station 2 had 5.24 ± 0.07 (range: 5.10–5.70), with the difference being statistically significant. Sediment pH during the wet season ranged from 5.0 to 6.0, with a mean of 5.50 ± 0.09, while it ranged from 5.1 to 5.7, with a mean of 5.38 ± 0.14 in the dry season. The seasonal variation was not statistically significant. Figure 4.21 shows the monthly variation in Sediment pH

4.2.2 Conductivity (µS/cm)

Station 1 recorded 121.11 ± 1.70 µS/cm (range: 118.0–123.7 µS/cm), and Station 2 had 110.24 ± 3.02 µS/cm (range: 107.2–116.3 µS/cm), with a statistically significant spatial variation. Conductivity in the wet season ranged from 107.2 to 123.7 µS/cm, with a mean of 115.92 ± 1.69 µS/cm, while the dry season ranged from 107.8 to 122.9 µS/cm, with a mean of 114.95 ± 3.83 µS/cm. No significant seasonal difference was observed. Figure 4.22 illustrates the monthly variation in Sediment Conductivity.

4.2.3 Moisture (%)

Station 1 had 13.44 ± 0.27% (range: 13.0–13.8), and Station 2 had 12.73 ± 0.29% (range: 12.4–12.9), with a significant spatial difference. Wet season sediment moisture ranged from 12.3 to 13.8%, with a mean 13.11 ± 0.13, while dry season values ranged from 12.4 to 13.7%, mean 13.00 ± 0.27, showing no significant seasonal difference. Figure 4.23 illustrates the monthly variation in Moisture content.

Table 4.3: Spatial Variation in Physicochemical properties in Sediment

Parameter	Station 1 (n = 8) (Range; Mean ± SE)	Station 2 (n = 8) (Range; Mean ± SE)	p-value	Significance	Limit
pH	5.20–6.20; 5.70 ± 0.20	5.10–5.70; 5.24 ± 0.07	0.001	< 0.05	6.5 – 8.5[a]
Conductivity (µS/cm)	118.0–123.7; 121.11 ± 1.70	107.2–116.3; 110.24 ± 3.02	0.000	< 0.05	-
Moisture (%)	13.0–13.8; 13.44 ± 0.27	12.4–12.9; 12.73 ± 0.29	0.000	< 0.05	-
Cadmium (mg/kg)	0.005–0.020; 0.010 ± 0.002	0.007–0.018; 0.010 ± 0.002	0.763	≥ 0.05	0.6 [b]
Chromium (mg/kg)	0.31–1.10; 0.50 ± 0.16	0.019–0.09; 0.43 ± 0.16	0.290	≥ 0.05	52.3[b]
Copper (mg/kg)	0.09–0.40; 0.37 ± 0.15	0.018–0.376; 0.36 ± 0.16	0.754	≥ 0.05	18.7[b]
Iron (mg/kg)	1.10–2.90; 1.45 ± 0.29	0.025–2.088; 1.46 ± 0.30	0.802	≥ 0.05	-
Lead (mg/kg)	0.025–0.041; 0.027 ± 0.004	0.019–0.032; 0.027 ± 0.004	0.470	≥ 0.05	30.2[b]
Manganese (mg/kg)	0.11–0.18; 0.131 ± 0.016	0.035–0.15; 0.134 ± 0.015	0.168	≥ 0.05	-
Nickel (mg/kg)	0.095–0.16; 0.105 ± 0.013	0.03–0.11; 0.108 ± 0.013	0.133	≥ 0.05	15.9[b]
Zinc (mg/kg)	0.183–1.082; 0.405 ± 0.119	0.069–0.274; 0.412 ± 0.126	0.548	≥ 0.05	124[b]

Note: a = NESREA / WHO Environmental Guideline, b = [b] CCME / NOAA Sediment Quality Guidelines (TEL – Threshold Effect Level), P < 0.001 = Very Significant, P<0.05 = Significant, P>0.05 = Not significant

Table 4.4: Seasonal variation in physicochemical properties in Sediment

Parameter	**Wet Season (n = 6) (Range) Mean ± SE**	**Dry Season (n = 2) (Range) Mean ± SE**	**p-value**	**Significance**
Sediment pH	(5.0–6.0) 5.50 ± 0.09	(5.1–5.7) 5.38 ± 0.14	0.497	P > 0.05
Conductivity	(107.2–123.7) 115.92 ± 1.69	(107.8–122.9) 114.95 ± 3.83	0.794	P > 0.05
Moisture (%)	(12.3–13.8) 13.11 ± 0.13	(12.4–13.7) 13.00 ± 0.27	0.696	P > 0.05
Cd (mg/kg)	(0.001–0.020) 0.0098 ± 0.0016	(0.007–0.018) 0.0120 ± 0.0027	0.505	P > 0.05
Cr (mg/kg)	(0.055–1.10) 0.602 ± 0.119	(0.019–0.09) 0.054 ± 0.020	0.021	P < 0.01
Cu (mg/kg)	(0.09–1.429) 0.451 ± 0.132	(0.018–0.21) 0.114 ± 0.055	0.033	P < 0.05
Fe (mg/kg)	(1.10–2.90) 1.74 ± 0.18	(0.025–1.20) 0.60 ± 0.33	0.029	P < 0.01
Pb (mg/kg)	(0.010–0.041) 0.0277 ± 0.0031	(0.019–0.032) 0.0255 ± 0.0032	0.714	P > 0.05
Mn (mg/kg)	(0.11–0.18) 0.146 ± 0.0070	(0.035–0.15) 0.091 ± 0.031	0.177	P < 0.05
Ni (mg/kg)	(0.095–0.16) 0.119 ± 0.0066	(0.03–0.11) 0.068 ± 0.021	0.093	P < 0.01
Zn (mg/kg)	(0.183–1.082) 0.489 ± 0.101	(0.069–0.274) 0.168 ± 0.057	0.099	P < 0.05

Note: P<0.01 = Highly significant, P<0.05 = Significant, P>0.05 = Not significant

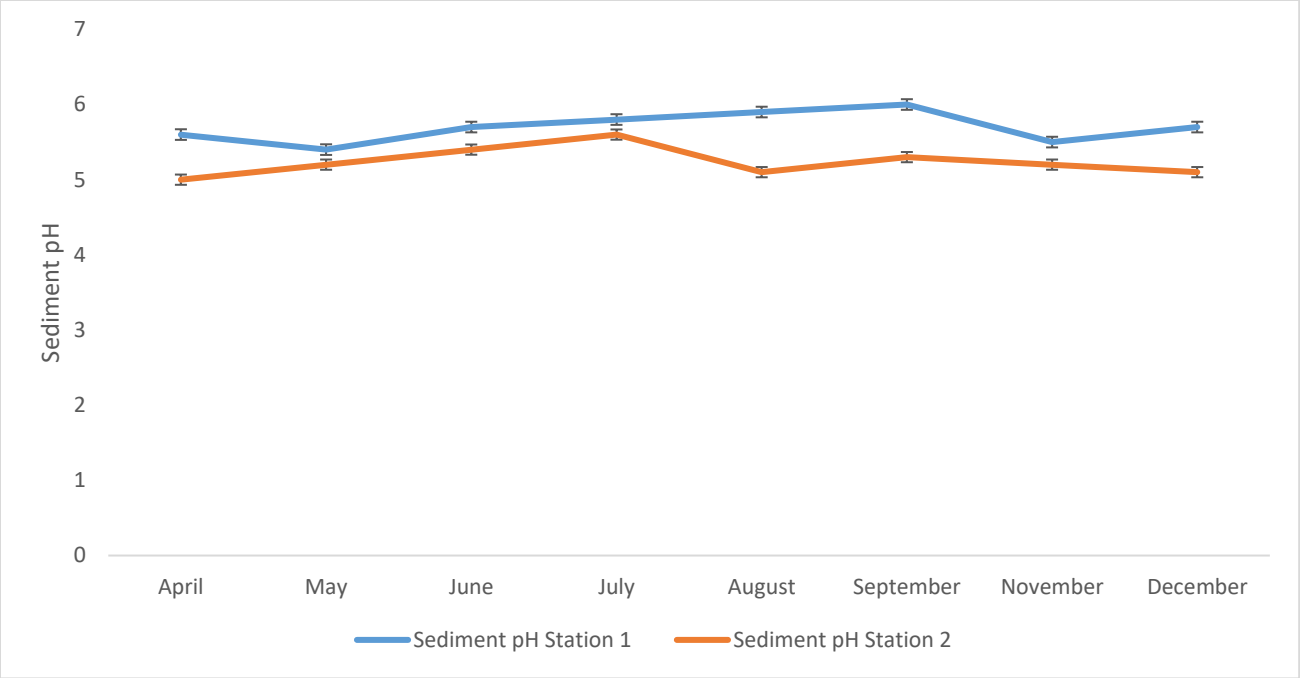

Figure 4.21: Spatio-temporal Variations in Sediment pH from April 2024 – December 2024

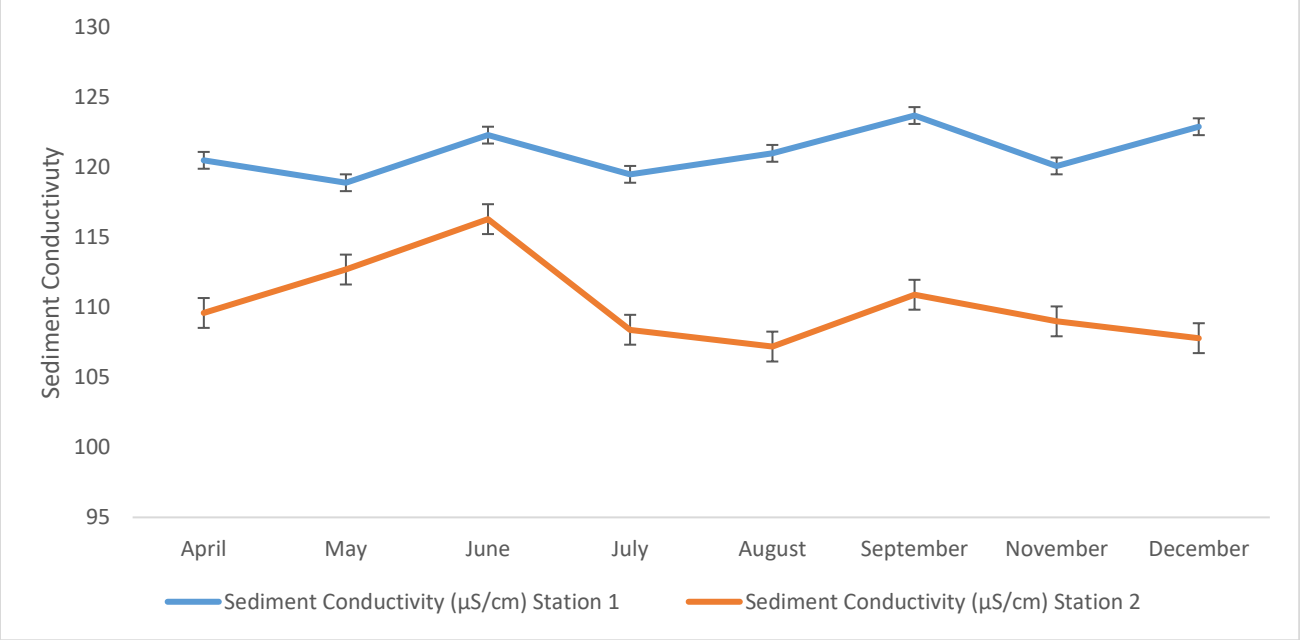

Figure 4.22: Spatio-temporal Variations in Sediment Conductivity from April 2024 – December 2024

4.2.4 Cadmium (Cd, mg/kg)

Spatially, Station 1 recorded 0.010 ± 0.002 mg/kg (range: 0.005–0.020), and Station 2 also had 0.010 ± 0.002 mg/kg (range: 0.007–0.018), with no significant. Cadmium levels during the wet season ranged from 0.001 to 0.020 mg/kg, mean 0.0098 ± 0.0016, while in the dry season they ranged from 0.007 to 0.018 mg/kg, mean 0.0120 ± 0.0027. No significant seasonal variation was observed. Figure 4. 24 illustrates the monthly variation in Cadmium concentration

4.2.5 Chromium (Cr, mg/kg)

Spatially, Station 1 recorded 0.50 ± 0.16 mg/kg (range: 0.31–1.10), and Station 2 had 0.43 ± 0.16 mg/kg (range: 0.019–0.09), with no significant spatial difference. Chromium concentrations in the wet season ranged from 0.055 to 1.10 mg/kg, mean 0.602 ± 0.119, while dry season levels were 0.019–0.09 mg/kg, mean 0.054 ± 0.020, a significant seasonal variation. Figure 4.25 illustrates the monthly variation in Chromium Concentration

4.2.6 Copper (Cu, mg/kg)

Station 1 recorded 0.37 ± 0.15 mg/kg (range: 0.09–0.40), and Station 2 had 0.36 ± 0.16 mg/kg (range: 0.018–0.376), with no significant spatial difference. Wet season copper ranged from 0.09 to 1.429 mg/kg, with a mean of 0.451 ± 0.132, while dry season values ranged from 0.018 to 0.21 mg/kg, with a mean of 0.114 ± 0.055, and showing significant seasonal variation. Figure 4.26 illustrates the monthly variation in Copper Concentration.

4.2.7 Iron (Fe, mg/kg)

Station 1 had 1.45 ± 0.29 mg/kg (range: 1.10–2.90), and Station 2 1.46 ± 0.30 mg/kg (range: 0.025–2.088), with no spatial difference. Iron during the wet season ranged from 1.10 to 2.90 mg/kg, mean 1.74 ± 0.18, and dry season from 0.025 to 1.20 mg/kg, mean 0.60 ± 0.33, with significant seasonal variation. Figure 4.27 shows the monthly variation in Iron Concentration.

4.2.8 Lead (Pb, mg/kg)

Station 1 and Station 2 both had 0.027 ± 0.004 mg/kg (ranges: 0.025–0.041 and 0.019–0.032, respectively), with no significant spatial difference. Lead ranged from 0.010 to 0.041 mg/kg in the wet season (mean 0.0277 ± 0.0031) and 0.019–0.032 mg/kg in the dry season (mean 0.0255 ± 0.0032), with no significant seasonal difference. Figure 4.28 shows the monthly variation in Lead Concentration.

4.2.9 Manganese (Mn, mg/kg)

Spatially, Station 1 had 0.131 ± 0.016 mg/kg (range: 0.11–0.18), and Station 2 0.134 ± 0.015 mg/kg (range: 0.035–0.15), with no significant spatial difference. Manganese levels during the wet season ranged from 0.11 to 0.18 mg/kg (mean 0.146 ± 0.0070), while dry season values ranged from 0.035 to 0.15 mg/kg (mean 0.091 ± 0.031), showing a significant seasonal difference. Figure 4.29 illustrates the monthly variation in Sediment Manganese concentration.

4.2.10 Nickel (Ni, mg/kg)

Station 1 recorded 0.105 ± 0.013 mg/kg (range: 0.095–0.16), and Station 2 0.108 ± 0.013 mg/kg (range: 0.03–0.11), with no significant spatial difference. Nickel ranged from 0.095 to 0.16 mg/kg in the wet season (mean 0.119 ± 0.0066) and 0.03–0.11 mg/kg in the dry season (mean 0.068 ± 0.021), showing significant seasonal variation. Figure 4.30 shows the monthly variation in Nickel Concentration.

4.2.11 Zinc (Zn, mg/kg)

Station 1 had 0.405 ± 0.119 mg/kg (range: 0.183–1.082), and Station 2 0.412 ± 0.126 mg/kg (range: 0.069–0.274), with no significant spatial difference. Zinc concentrations during the wet season ranged from 0.183 to 1.082 mg/kg, mean 0.489 ± 0.101, while in the dry season values ranged from 0.069 to 0.274 mg/kg, mean 0.168 ± 0.057, with significant seasonal variation. Figure 4.31 shows the monthly variation in Zinc Concentration.

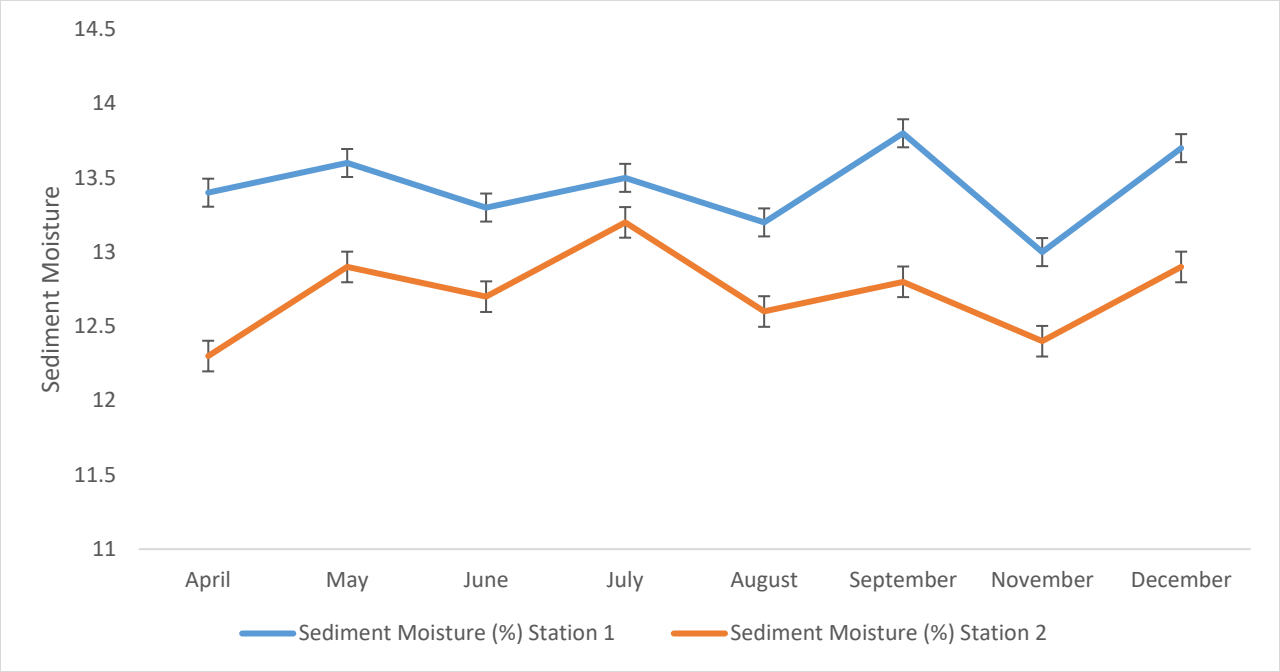

Figure 4.23: Spatio-temporal Variations in Sediment Moisture from April 2024 – December 2024

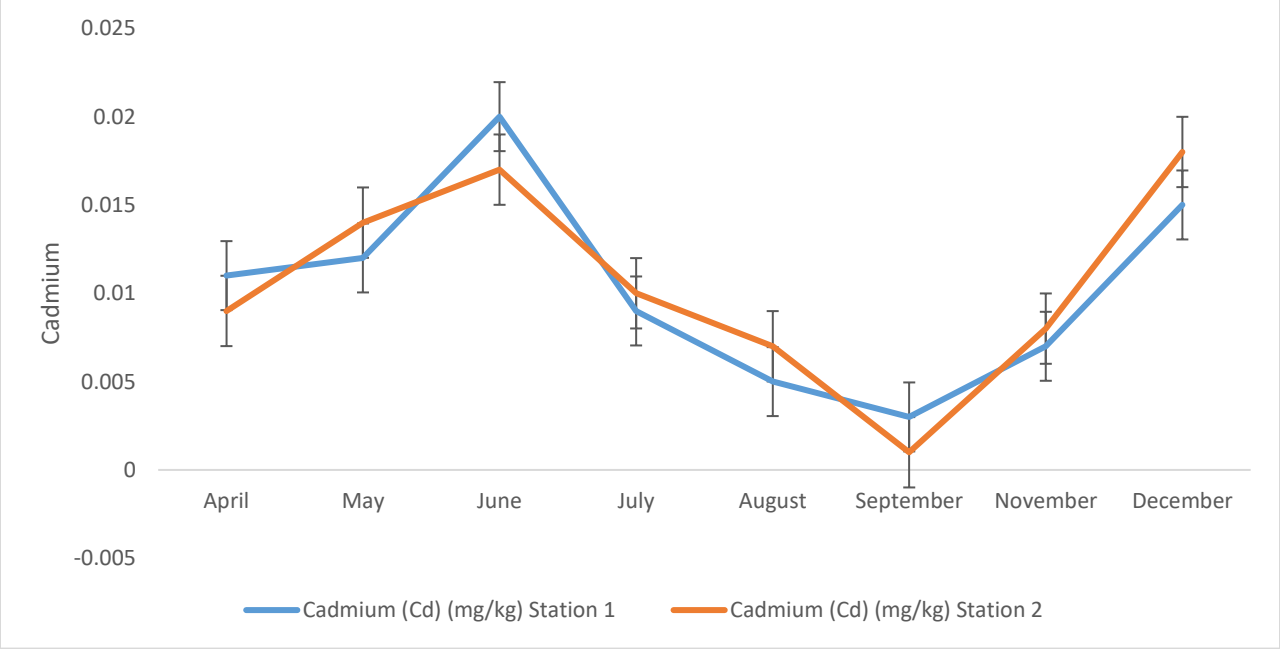

Figure 4.24: Spatio-temporal Variations in Cadmium from April 2024 – December 2024

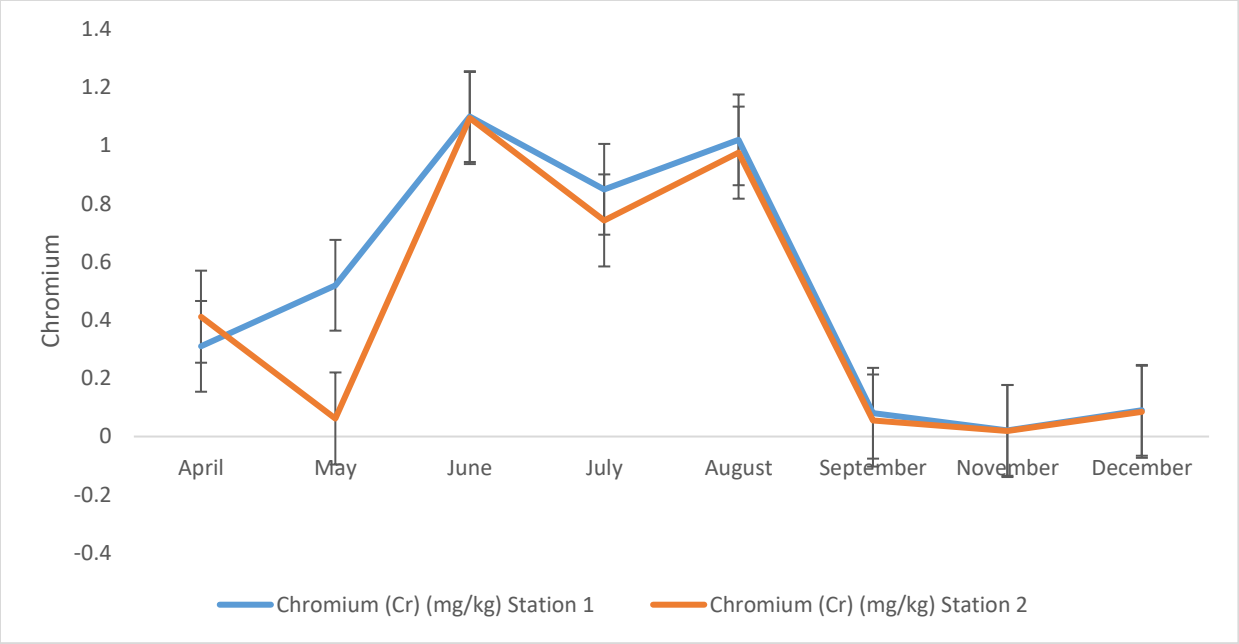

Figure 4.25: Spatio-temporal Variations in Chromium from April 2024 – December 2024

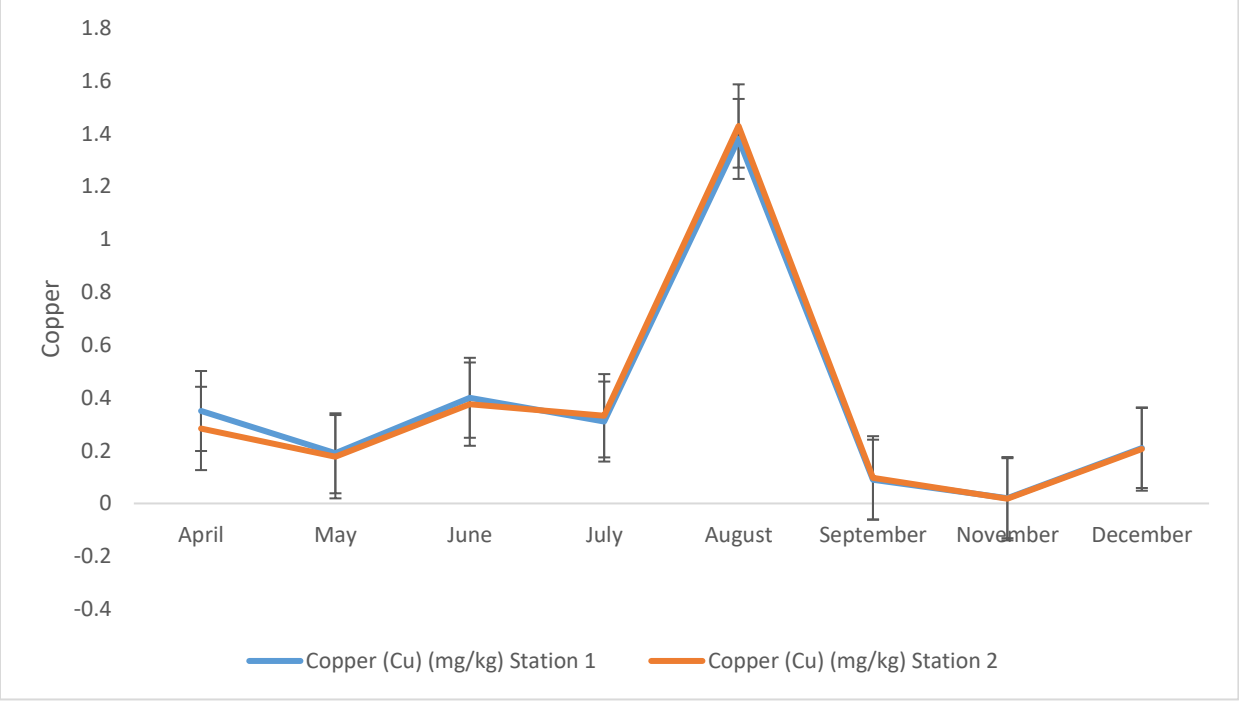

Figure 4.26: Spatio-temporal Variations in Copper from April 2024 – December 2024

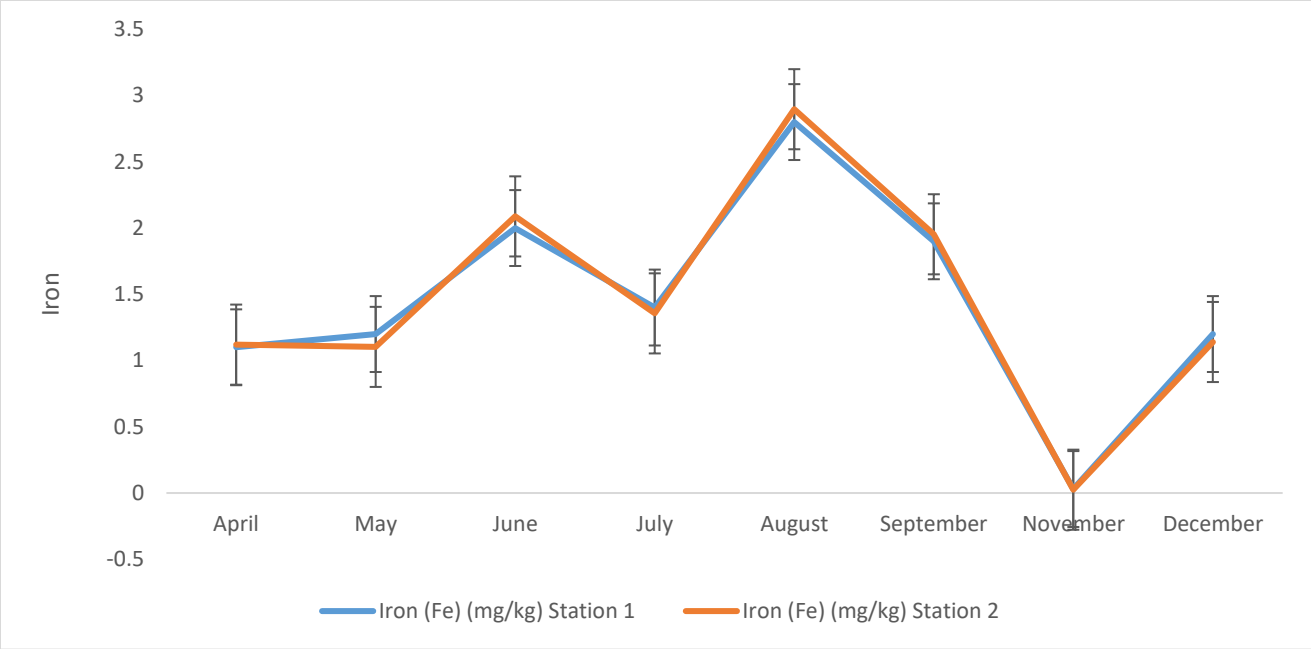

Figure 4.27: Spatio-temporal Variations in Iron from April 2024 – December 2024

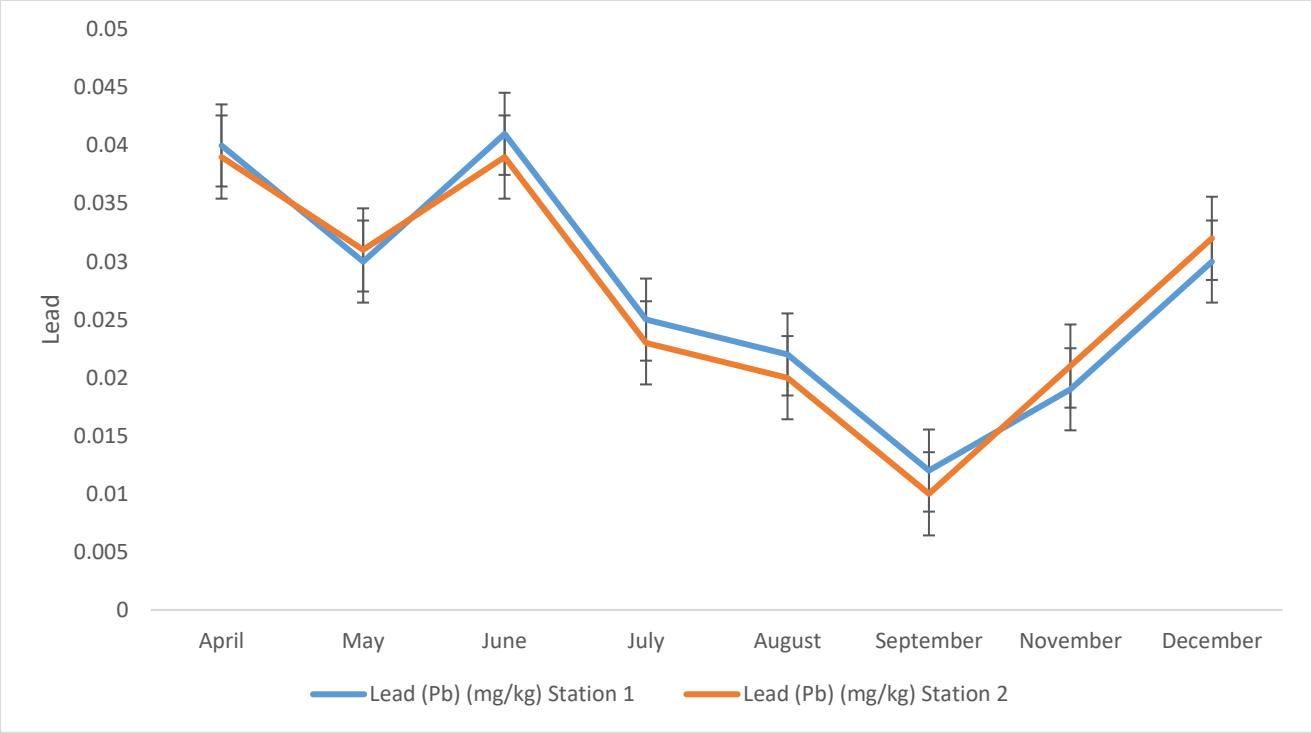

Figure 4.28: Spatio-temporal Variations in Lead from April 2024 – December 2024

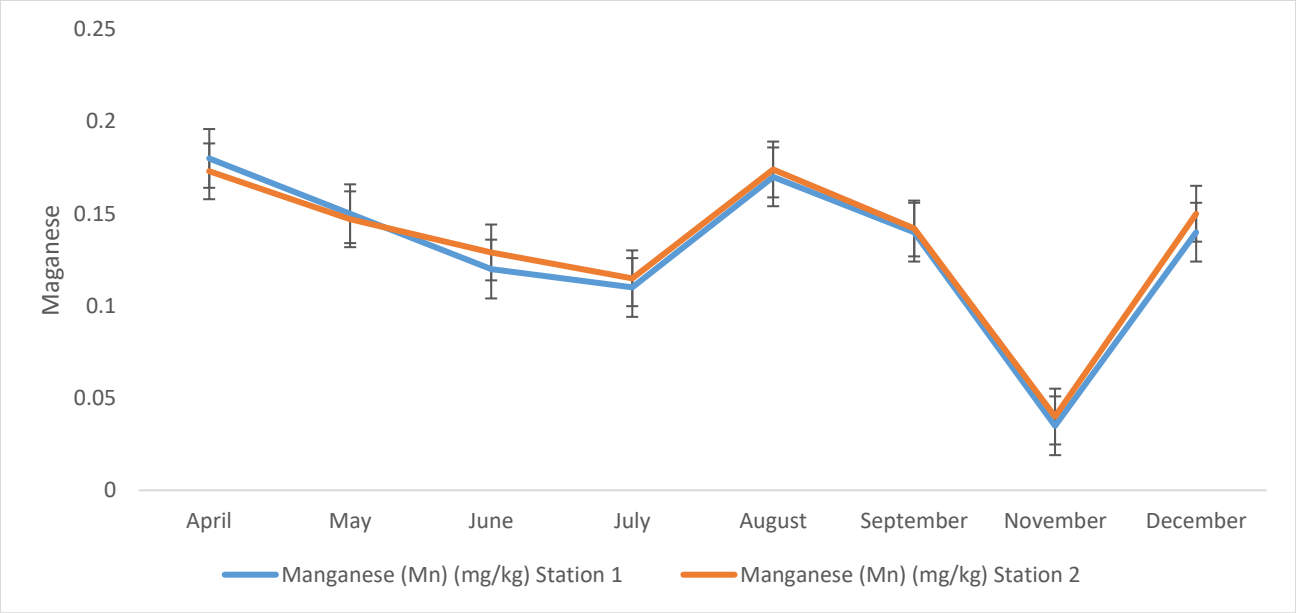

Figure 4.29: Spatio-temporal Variations in Manganese from April 2024 – December 2024

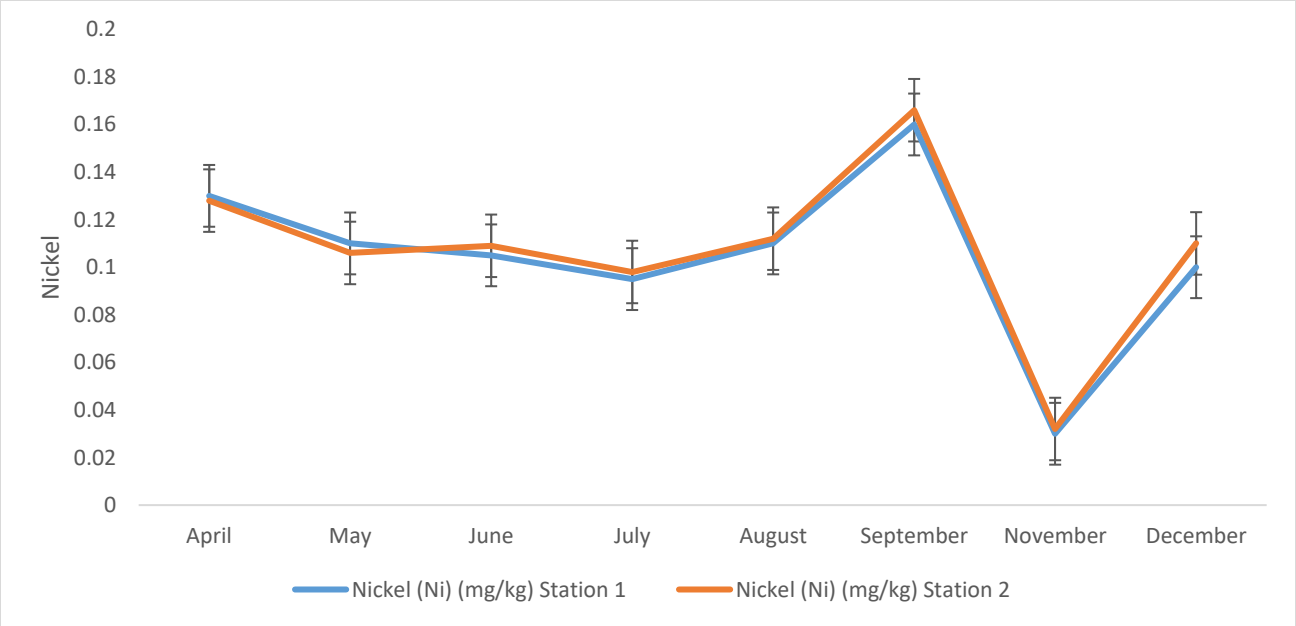

Figure 4.30: Spatio-temporal Variations in Nickel from April 2024 – December 2024

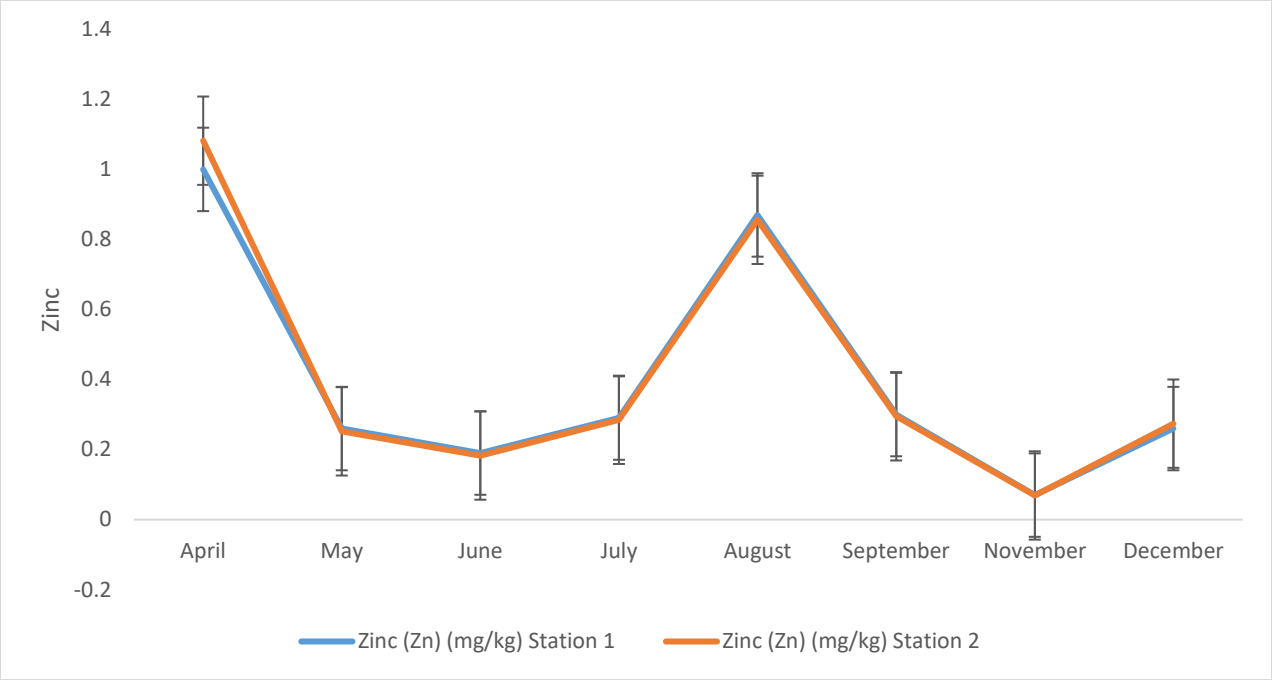

Figure 4.31: Spatio-temporal Variations in Zinc from April 2024 – December 2024

4.3 Prawn Species Composition and Abundance

A total of 1969 individual freshwater prawns, representing five (5) species, were recorded across all sampling stations (Table 4.5). These prawns all belong to the order Decapoda and the family Palaemonidae. The species identified were *Macrobrachium macrobrachion, Macrobrachium rosenbergii, Macrobrachium vollenhovenii, Macrobrachium equidens,* and *Macrobrachium dux*. All five species were present across the sampling stations, though their abundance varied spatially.

4.3.1 Community Structure

The prawn community structure in the study area showed a moderate level of species richness, with all five species belonging to a single order (Decapoda) but differing in morphological characteristics and size distribution. *M. rosenbergii* and *M. macrobrachion* were the most frequently encountered species, together accounting for over half of the total prawn population recorded. *M. rosenbergii*, a species commonly cultured in aquaculture, was also observed in relatively high numbers. All species displayed distinct coloration patterns irrespective of size, suggesting that pigmentation is a consistent characteristic among the prawns of this ecosystem. While coloration intensity and hue may vary with age, sex, and environmental conditions, no individuals were observed to be entirely colorless at any life stage.

Macrobrachium equidens and *M. dux* were less frequently encountered and showed more site-specific distributions. The consistent presence of all five species across stations highlights the ecological complexity and resilience of the freshwater prawn assemblage in the study area.

Table 4.5: Taxonomic Classification of Reported Prawn Species

Phylum	Class	Order	Family	Species	Authority
Arthropoda	Malacostraca	Decapoda	Palaemonidae	*Macrobrachium macrobrachion*	Herklots, 1851
				Macrobrachium rosenbergii	De Man, 1879
				Macrobrachium vollenhovenii	Herklots, 1857
				Macrobrachium dux	De Man, 1912
				Macrobrachium equidens	Dana, 1852

Plate 4.1: Prawn species collected during the sampling duration

4.3.2: Composition, Distribution and Abundance of Prawn

The prawn community structure within the Ubeji Axis of the Warri River was composed of five *Macrobrachium* species. Among them, *Macrobrachium macrobrachion* was the most dominant, with 905 individuals accounting for 46% of the total population (Table 4.6).

Macrobrachium rosenbergii ranked second in abundance, contributing 375 individuals or 19% of the total. It was closely followed by *Macrobrachium vollenhovenii*, which made up 18% of the community with 362 individuals. *Macrobrachium equiden*s recorded 246 individuals, comprising 12% of the overall count. The least represented species was *Macrobrachium dux*, with just 81 individuals, accounting for 4% of the total prawn population.

The spatial analysis of prawn species across the two sampling stations showed relatively balanced distributions, with Station 1 yielding 988 individuals and Station 2 yielding 981, summing to a total of 1,969 individuals (Table 4.6). At Station 1, *M. macrobrachion* was the most abundant species with 406 individuals (41.1%), followed by *M. rosenbergii* (204 individuals, 20.6%) and *M. vollenhovenii* (206 individuals, 20.9%). *M. equidens* and *M. dux* were less represented, accounting for 13.3% and 4.1% respectively. At Station 2, *M. macrobrachion* also maintained dominance with 499 individuals (50.9%), while *M. rosenbergii* (171 individuals, 17.4%) and *M. vollenhovenii* (156 individuals, 15.9%) followed. *M. equidens* contributed 115 individuals (11.7%), and *M. dux* remained the least abundant with 40 individuals (4.1%).

The distribution pattern confirms that *M. macrobrachion* is ecologically dominant in both stations. However, diversity indices reveal subtle differences between the two sites. Species richness (Taxa_S = 5) was identical across both stations, indicating no difference in the number of species present. Shannon-Wiener diversity (H = 1.448 vs. 1.323) was higher at Station 1, suggesting slightly greater diversity compared to Station 2. Margalef's richness index was very similar at both

stations (0.5801 vs. 0.5807), while dominance (D = 0.2743 vs. 0.3298) was lower at Station 1, indicating less dominance by a single species. Evenness calculated as H/S was higher at Station 1 (0.2836) than at Station 2 (0.2646), showing that individuals were more evenly distributed among species at Station 1.

4.3.3. Temporal Analysis of Prawn Species

The temporal analysis of *Macrobrachium* species across both stations from April to December revealed seasonal variations in abundance, with significant interspecific and monthly differences (Table 4.7). A total of 1,969 individuals were recorded over the sampling period. *Macrobrachium macrobrachion* was the most dominant species, comprising 895 individuals, which accounted for approximately 45% of the total catch. It reached its highest abundance in April with 243 individuals (19% of total monthly catch) and remained prominent through May (158) and June (153), followed by lower but steady numbers in subsequent months, with 68 individuals recorded in December. *Macrobrachium rosenbergii* showed moderate abundance and stability, contributing 375 individuals (19%) of the total count. It peaked in April with 74 individuals and maintained a relatively consistent presence across all months, ranging between 37 and 52 individuals. *Macrobrachium vollenhovenii* exhibited pronounced temporal fluctuations, with a total count of 362 individuals (18%). Abundance was low from April to June but surged sharply in August (83 individuals) and September (70), contributing significantly to the total catch during those months (12% each). A similarly high number was recorded in November (72). *Macrobrachium equidens* was moderately represented with 244 individuals (12%). The species showed a relatively even distribution across months, peaking in May (38) and April (36), and displaying slight declines in later months. *Macrobrachium dux* had the lowest abundance, contributing only 91 individuals

(5%) to the total. It was consistently the least represented species each month, with minor peaks in December (15 individuals) and May (10). The temporal cohort analysis of prawns across the Ubeji Axis from April to December revealed distinct growth and population patterns at both stations. Length-class analysis showed that the majority of individuals were consistently found in the 5–8 cm intervals. For instance, the 5–6 cm interval had the highest counts across nearly all months, with values such as 29 and 47 in April for St1 and St2, respectively, and similarly high counts in May (12 and 37), June (20 and 38), and July (10 and 24). The 6–7 cm cohort was also well represented, with April counts of 49 and 57, and consistently high values in subsequent months. This indicates that medium-sized prawns dominated the population, while smaller (<3 cm) and larger (>10 cm) individuals were comparatively rare. Linking cohort data to species-specific population trends, *Macrobrachium macrobrachion* clearly drove the abundance in these medium-sized classes. With a total of 895 individuals (45% of the total catch), it reached its peak in April (243 individuals) and maintained high numbers through May (158) and June (153). These months coincide with the largest cohort counts in the 5–8 cm intervals, indicating that growth and recruitment of this species contributed substantially to the population structure. By December, its abundance declined to 68 individuals. *Macrobrachium rosenbergii* (375 individuals, 19%) and *M. equidens* (244 individuals, 12%) displayed moderate but stable population trends, contributing mainly to the 5–8 cm length classes. For example, cohort counts for 5–6 cm and 6–7 cm intervals in April–June aligned closely with the presence of these species, supporting the observation that their populations were composed primarily of medium-length individuals.

Macrobrachium vollenhovenii (362 individuals, 18%) showed marked seasonal fluctuations. Its abundance surged in August (83 individuals) and September (70), with November recording 72,

corresponding to high counts in the 5–8 cm cohorts (August 5–6 cm: 19 and 14; 6–7 cm: 40 and 22; September 5–6 cm: 16 and 13; 6–7 cm: 30 and 26). These peaks reflect seasonal recruitment or growth events that concentrated individuals in medium-length categories, making *M. vollenhovenii* a key driver of cohort variability during these months.

Finally, *Macrobrachium dux*, the least abundant species (91 individuals, 5%), contributed modestly to small and medium cohorts, with minor peaks such as in December 0–1 cm (3 individuals) and 4–5 cm (6–7). Overall, the analysis demonstrates that the increase in population observed from April to December was predominantly within the medium-sized cohort ranges of 5–8 cm

Table 4.6: Spatial Variation in Prawn Species in the Ubeji Axis, Warri River

Species	Station 1	Station 2	Total	Percentage
Macrobrachium dux	41	40	81	4%
Macrobrachium equidens	131	115	246	12%
Macrobrachium macrobrachion	406	499	905	46%
Macrobrachium rosenbergii	204	171	375	19%
Macrobrachium vollenhovenii	206	156	362	18%
Total per Station	988	981	1969	100%
Species richness (Taxa_S)	5	5		
Shannon-Wiener Index (H)	1.448	1.323		
Margalef	0.5801	0.5807		
Dominance_D	0.2743	0.3298		
Evenness H/S	0.2836	0.2646		

Table 4.7: Pooled Temporal Variation of Prawn Species in Ubeji Axis, Warri River

Month	*M. dux*	*M. equidens*	*M. macrobrachion*	*M. rosenbergii*	*M. vollenhovenii*	Total	Percentage
April	7	36	243	74	16	376	19%
May	10	38	158	52	31	289	15%
June	11	32	153	51	16	263	13%
July	9	28	60	40	49	186	9%
August	7	32	78	41	83	241	12%
September	12	31	79	37	70	229	12%
November	10	27	66	41	72	216	11%
December	15	22	68	39	25	169	9%

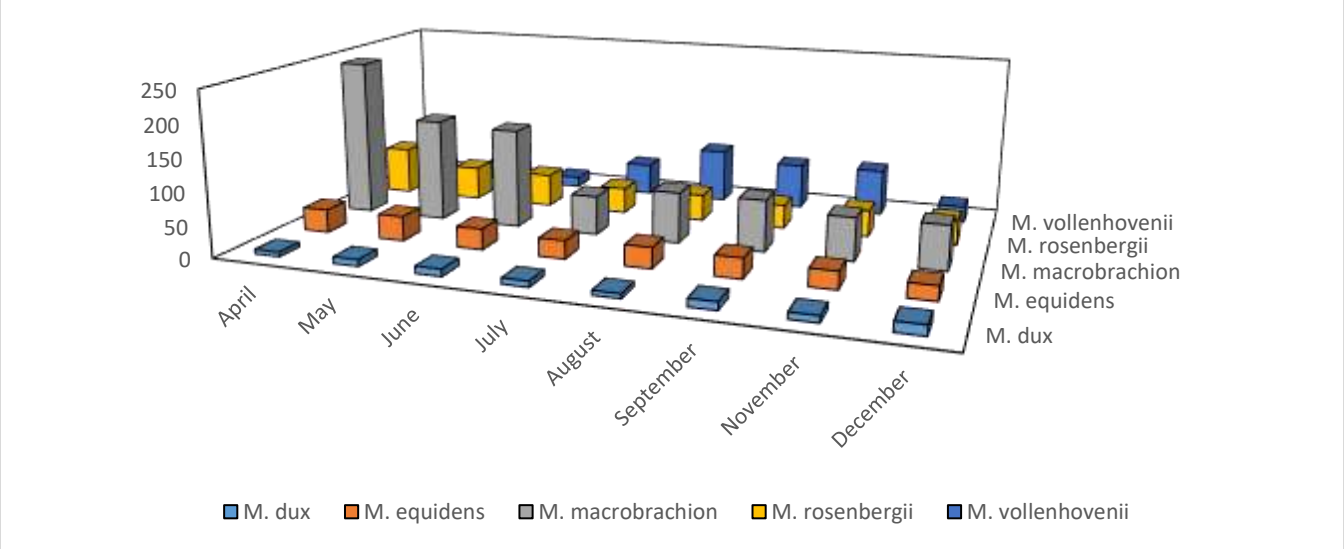

Figure 4.32: Monthly Variation of Prawn Species in Ubeji Axis, Warri River from April – December 2024

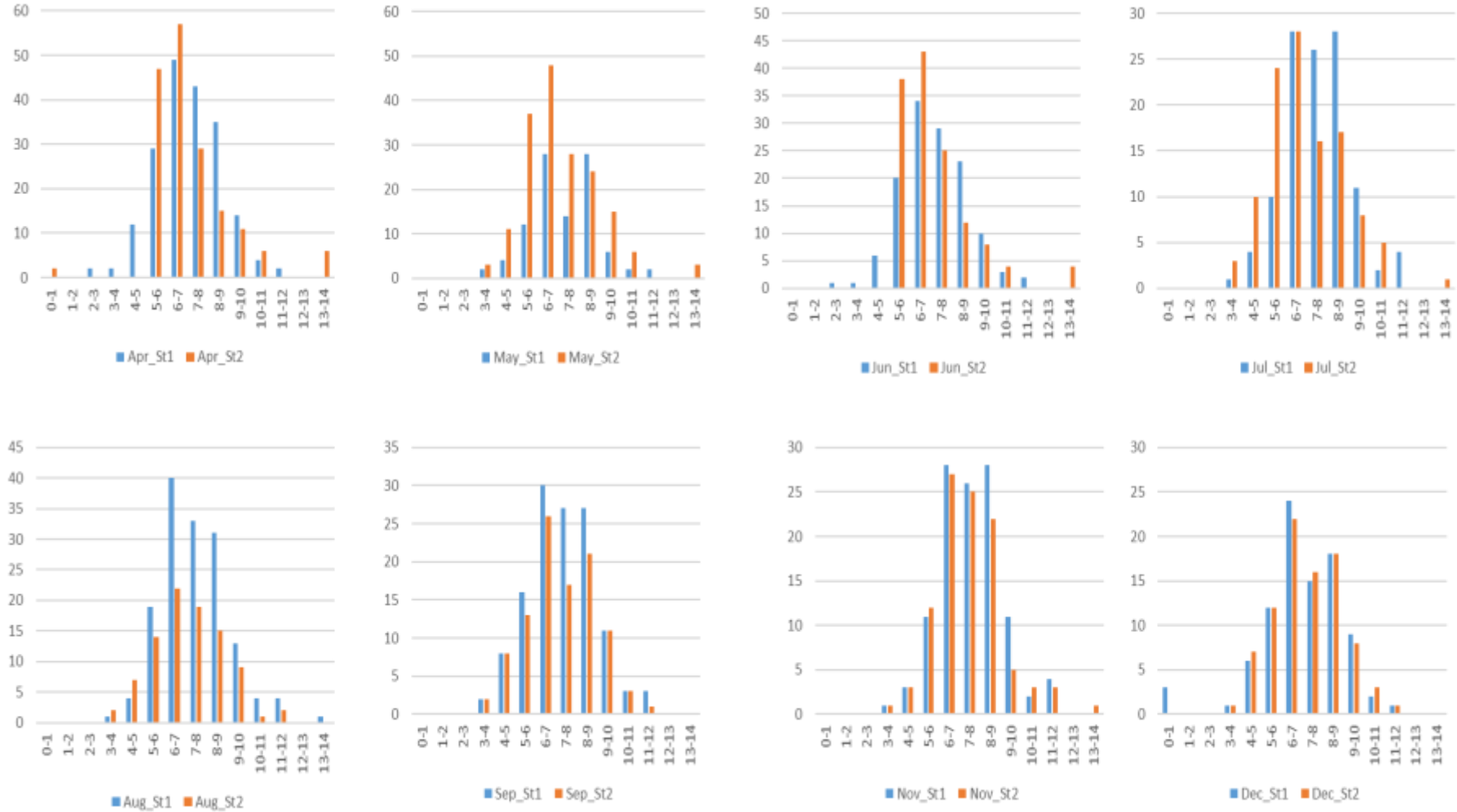

Plate 4.2: Pooled Length-class analysis of *Macrobrachium* Species from April – December 2024

4.4. Morphological and Meristic Characteristics

4.4.1 Total Length (TL)

The total length of *Macrobrachium* species across stations and months is presented in Table 4.8. *Macrobrachium dux* exhibited moderate variation at Station 1, with values ranging from 7.58 ± 0.60 cm in August to 8.45 ± 0.30 cm in September, while in Station 2 measurements ranged from 6.53 ± 0.36 cm in June to 8.23 ± 0.07 cm in August, with the species completely absent in April. The difference in total length between stations for this species was statistically significant ($p = 0.033$). *M. equidens* remained relatively stable at Station 1, where total length ranged from 6.56 ± 0.25 cm in April to 7.03 ± 0.27 cm in July and November. At Station 2, values fluctuated between 6.32 ± 0.33 cm in August and 7.49 ± 0.32 cm in April. There was no significant difference in total length between stations for this species ($p = 0.988$). For *M. macrobrachion*, Station 1 recorded values ranging from 6.85 ± 0.14 cm in April to 7.69 ± 0.29 cm in July and November. At Station 2, lengths were slightly lower, ranging from 6.22 ± 0.23 cm in July to 7.22 ± 0.26 cm in November. The difference in total length between stations was statistically significant ($p = 0.000$). *M. rosenbergii* recorded some of the highest values across all species, with Station 1 ranging from 8.02 ± 0.25 cm in April to 8.82 ± 0.34 cm in August. Station 2 exhibited higher values in some months, peaking at 10.23 ± 0.43 cm in April and remaining above 8.50 cm through the remaining sampled months. The difference in total length between stations was statistically significant ($p = 0.002$). *M. vollenhovenii* showed moderate variation at Station 1, ranging from 6.83 ± 0.25 cm in June to 7.60 ± 0.42 cm in May. Station 2 recorded values between 6.69 ± 0.25 cm in July and 8.11 ± 0.42 cm in December. There was no significant difference in total length between stations for this species ($p = 0.387$).

Table 4.8: Monthly Variation in Total Length (cm) of *Macrobrachium* Species

Species & Station	**April (Mean ± SE)**	**May (Mean ± SE)**	**June (Mean ± SE)**	**July (Mean ± SE)**	**August (Mean ± SE)**	**September (Mean ± SE)**	**November (Mean ± SE)**	**December (Mean ± SE)**	**Overall p – value (S1 vs S2)**
M. dux S1	8.09 ± 0.71	8.10 ± 0.12	8.09 ± 0.71	8.10 ± 0.12	7.58 ± 0.60	8.45 ± 0.30	8.10 ± 0.12	7.90 ± 0.16	0.033
M. dux S2	0.00 ± 0.00	7.92 ± 0.14	6.53 ± 0.36	7.98 ± 0.48	8.23 ± 0.07	7.16 ± 0.53	7.73 ± 0.28	7.16 ± 0.53	
M. equidens S1	6.56 ± 0.25	6.95 ± 0.29	6.64 ± 0.32	7.03 ± 0.27	6.94 ± 0.24	6.64 ± 0.27	7.03 ± 0.27	6.57 ± 0.35	0.988
M. equidens S2	7.49 ± 0.32	6.78 ± 0.25	7.29 ± 0.29	6.40 ± 0.29	6.32 ± 0.33	6.48 ± 0.32	6.84 ± 0.27	6.35 ± 0.33	
M. macrobrachion S1	6.85 ± 0.14	7.10 ± 0.21	6.94 ± 0.16	7.69 ± 0.29	7.22 ± 0.26	6.98 ± 0.26	7.69 ± 0.29	6.97 ± 0.25	0.000
M. macrobrachion S2	6.51 ± 0.08	6.37 ± 0.13	6.51 ± 0.11	6.22 ± 0.23	6.60 ± 0.22	6.69 ± 0.23	7.22 ± 0.26	6.70 ± 0.24	
M. rosenbergii S1	8.02 ± 0.25	8.61 ± 0.35	8.11 ± 0.34	8.62 ± 0.34	8.82 ± 0.34	8.73 ± 0.34	8.62 ± 0.34	8.41 ± 0.31	0.002
M. rosenbergii S2	10.23 ± 0.43	8.96 ± 0.36	9.00 ± 0.55	8.63 ± 0.47	8.99 ± 0.36	8.58 ± 0.29	8.88 ± 0.38	8.59 ± 0.31	
M. vollenhovenii S1	6.84 ± 0.20	7.60 ± 0.42	6.83 ± 0.25	7.24 ± 0.22	7.26 ± 0.17	7.30 ± 0.29	7.26 ± 0.21	7.49 ± 0.35	0.387
M. vollenhovenii S2	7.13 ± 0.30	7.33 ± 0.31	6.96 ± 0.31	6.69 ± 0.25	7.19 ± 0.37	7.71 ± 0.41	6.97 ± 0.26	8.11 ± 0.42	

4.4.2. Dorsal Carapace Length (DCL)

The monthly variation in dorsal carapace length of *Macrobrachium* species is shown in Table 4.9. *Macrobrachium dux* recorded values ranging from 1.88 ± 0.17 cm in August to 2.10 ± 0.08 cm in September at Station 1. Station 2 measurements ranged from 1.57 ± 0.05 cm in June to 2.00 ± 0.12 cm in July. There was no statistically significant difference in dorsal carapace length between stations for this species ($p = 0.071$). *M. equidens* showed moderate monthly variation, with Station 1 values fluctuating between 1.59 ± 0.06 cm in April and 1.74 ± 0.06 cm in July and November. At Station 2, values ranged from 1.58 ± 0.09 cm in July and December to 1.89 ± 0.07 cm in April. There was no statistically significant difference in dorsal carapace length between stations for this species ($p = 0.602$). For *M. macrobrachion*, Station 1 recorded values between 1.64 ± 0.04 cm in April and 1.83 ± 0.09 cm in July and November. Station 2 exhibited slightly lower values, ranging from 1.47 ± 0.06 cm in July to 1.75 ± 0.07 cm in November. The difference in dorsal carapace length between stations was statistically significant ($p = 0.000$). *M. rosenbergii* showed higher DCL values relative to other species, with Station 1 values ranging from 2.07 ± 0.08 cm in April to 2.33 ± 0.14 cm in August. Station 2 measurements ranged from 2.11 ± 0.14 cm in July to 2.75 ± 0.13 cm in April. There was no statistically significant difference in dorsal carapace length between stations for this species ($p = 0.116$). *M. vollenhovenii* exhibited consistent values across stations, with Station 1 measurements ranging from 1.64 ± 0.08 cm in April to 1.93 ± 0.12 cm in May, while Station 2 recorded values from 1.62 ± 0.06 cm in July to 1.97 ± 0.09 cm in December. There was no statistically significant difference in dorsal carapace length between stations for this species ($p = 0.126$).

Table 4.9: Dorsal Carapace Length (cm) of *Macrobrachium* Species

Species & Station	April (Mean ± SE)	May (Mean ± SE)	June (Mean ± SE)	July (Mean ± SE)	August (Mean ± SE)	September (Mean ± SE)	November (Mean ± SE)	December (Mean ± SE)	Overall p-value (S1 vs S2)
M. dux S1	1.91 ± 0.19	2.00 ± 0.06	1.91 ± 0.19	2.00 ± 0.06	1.88 ± 0.17	2.10 ± 0.08	2.00 ± 0.06	1.94 ± 0.06	0.071
M. dux S2	0.00 ± 0.00	1.95 ± 0.05	1.57 ± 0.05	2.00 ± 0.12	2.00 ± 0.10	1.75 ± 0.14	1.85 ± 0.10	1.75 ± 0.14	
M. equidens S1	1.59 ± 0.06	1.72 ± 0.07	1.66 ± 0.08	1.74 ± 0.06	1.72 ± 0.06	1.63 ± 0.07	1.74 ± 0.06	1.60 ± 0.10	0.602
M. equidens S2	1.89 ± 0.07	1.70 ± 0.07	1.82 ± 0.07	1.58 ± 0.09	1.59 ± 0.09	1.60 ± 0.09	1.69 ± 0.07	1.58 ± 0.09	
M. macrobrachion S1	1.64 ± 0.04	1.70 ± 0.06	1.69 ± 0.05	1.83 ± 0.09	1.72 ± 0.07	1.66 ± 0.07	1.83 ± 0.09	1.72 ± 0.07	0.000
M. macrobrachion S2	1.59 ± 0.02	1.52 ± 0.03	1.59 ± 0.03	1.47 ± 0.06	1.64 ± 0.06	1.63 ± 0.06	1.75 ± 0.07	1.65 ± 0.07	
M. rosenbergii S1	2.07 ± 0.08	2.29 ± 0.16	2.15 ± 0.12	2.29 ± 0.16	2.33 ± 0.14	2.31 ± 0.17	2.29 ± 0.16	2.12 ± 0.13	0.116
M. rosenbergii S2	2.75 ± 0.13	2.22 ± 0.11	2.36 ± 0.17	2.11 ± 0.14	2.39 ± 0.21	2.14 ± 0.13	2.31 ± 0.14	2.15 ± 0.14	
M. vollenhovenii S1	1.64 ± 0.08	1.93 ± 0.12	1.65 ± 0.10	1.81 ± 0.06	1.81 ± 0.05	1.81 ± 0.08	1.83 ± 0.06	1.88 ± 0.10	0.126
M. vollenhovenii S2	1.80 ± 0.15	1.78 ± 0.07	1.71 ± 0.10	1.62 ± 0.06	1.76 ± 0.09	1.90 ± 0.10	1.72 ± 0.07	1.97 ± 0.09	

4.4.3. Carapace Height (CH)

The monthly variation in carapace height of *Macrobrachium* species is presented in Table 4.10. *Macrobrachium dux* recorded values ranging from 1.13 ± 0.11 cm in April to 1.32 ± 0.07 cm in September at Station 1. Station 2 measurements ranged from 0.98 ± 0.11 cm in June to 1.33 ± 0.07 cm in August. There was no statistically significant difference in carapace height between stations for this species ($p = 0.406$). *M. equidens* showed relatively small carapace heights, with Station 1 values fluctuating between 0.91 ± 0.05 cm in April and 1.01 ± 0.04 cm in August. At Station 2, values ranged from 0.90 ± 0.05 cm in August to 1.19 ± 0.05 cm in April. The difference in carapace height between stations was statistically significant ($p = 0.002$). For *M. macrobrachion*, Station 1 recorded stable values ranging from 1.00 ± 0.02 cm in April to 1.13 ± 0.04 cm in July and November. Station 2 exhibited similar values, ranging from 0.99 ± 0.05 cm in July to 1.10 ± 0.04 cm in November. There was no statistically significant difference in carapace height between stations ($p = 0.778$). *M. rosenbergii* showed the highest carapace heights across species, with Station 1 values ranging from 1.24 ± 0.04 cm in April to 1.37 ± 0.07 cm in September. Station 2 measurements ranged from 1.32 ± 0.06 cm in June to 1.45 ± 0.05 cm in April. The difference in carapace height between stations was statistically significant ($p = 0.024$). *M. vollenhovenii* exhibited intermediate and consistent values, with Station 1 measurements ranging from 1.09 ± 0.04 cm in July and November to 1.22 ± 0.06 cm in April. Station 2 recordings ranged from 1.05 ± 0.05 cm in November to 1.28 ± 0.17 cm in April. There was no statistically significant difference in carapace height between stations ($p = 0.557$).

Table 4.10: Carapace Height (cm) of *Macrobrachium* Species

Species & Station	April (Mean ± SE)	May (Mean ± SE)	June (Mean ± SE)	July (Mean ± SE)	August (Mean ± SE)	September (Mean ± SE)	November (Mean ± SE)	December (Mean ± SE)	Overall p-value (S1 vs S2)
M. dux S1	1.13 ± 0.11	1.25 ± 0.09	1.13 ± 0.11	1.25 ± 0.09	1.23 ± 0.10	1.32 ± 0.07	1.25 ± 0.09	1.23 ± 0.08	0.406
M. dux S2	0.00 ± 0.00	1.27 ± 0.04	0.98 ± 0.11	1.28 ± 0.08	1.33 ± 0.07	1.10 ± 0.11	1.17 ± 0.08	1.10 ± 0.11	
M. equidens S1	0.91 ± 0.05	0.98 ± 0.04	0.94 ± 0.06	0.98 ± 0.04	1.01 ± 0.04	0.92 ± 0.04	0.98 ± 0.04	0.92 ± 0.06	0.002
M. equidens S2	1.19 ± 0.05	1.08 ± 0.05	1.16 ± 0.05	1.00 ± 0.07	0.90 ± 0.05	0.92 ± 0.05	0.96 ± 0.05	0.92 ± 0.06	
M. macrobrachion S1	1.00 ± 0.02	1.02 ± 0.03	1.02 ± 0.03	1.13 ± 0.04	1.08 ± 0.04	1.05 ± 0.04	1.13 ± 0.04	1.10 ± 0.05	0.778
M. macrobrachion S2	1.04 ± 0.02	1.00 ± 0.02	1.03 ± 0.02	0.99 ± 0.05	1.06 ± 0.04	1.05 ± 0.04	1.10 ± 0.04	1.05 ± 0.04	
M. rosenbergii S1	1.24 ± 0.04	1.35 ± 0.07	1.25 ± 0.06	1.35 ± 0.07	1.36 ± 0.06	1.37 ± 0.07	1.35 ± 0.07	1.33 ± 0.07	0.024
M. rosenbergii S2	1.45 ± 0.05	1.37 ± 0.04	1.32 ± 0.06	1.35 ± 0.05	1.44 ± 0.05	1.38 ± 0.06	1.36 ± 0.07	1.38 ± 0.07	
M. vollenhovenii S1	1.22 ± 0.06	1.20 ± 0.10	1.18 ± 0.08	1.09 ± 0.04	1.10 ± 0.03	1.11 ± 0.05	1.09 ± 0.04	1.18 ± 0.06	0.557
M. vollenhovenii S2	1.28 ± 0.17	1.15 ± 0.06	1.22 ± 0.10	1.08 ± 0.04	1.14 ± 0.06	1.19 ± 0.07	1.05 ± 0.05	1.26 ± 0.05	

4.4.4. Dorsal Rostrum Length (DRL)

The dorsal rostrum length of *Macrobrachium* species across stations and months is presented in Table 4.11. *Macrobrachium dux* showed moderate variation at Station 1, with values ranging from 1.70 ± 0.12 cm in August to 1.95 ± 0.17 cm in September. At Station 2, measurements ranged from 1.47 ± 0.09 cm in June to 1.86 ± 0.16 cm in July. There was no statistically significant difference in dorsal rostrum length between stations for this species ($p = 0.104$). *M. equidens* exhibited relatively stable values, with Station 1 ranging from 1.46 ± 0.08 cm in April to 1.56 ± 0.10 cm in May, July, and November. At Station 2, values fluctuated between 1.36 ± 0.11 cm in August and 1.73 ± 0.07 cm in April. The difference between stations was not statistically significant ($p = 0.378$). For *M. macrobrachion*, Station 1 values ranged from 1.56 ± 0.07 cm in September to 1.73 ± 0.08 cm in July and November, while Station 2 values ranged from 1.42 ± 0.06 cm in July to 1.64 ± 0.06 cm in November. A significant difference was observed between stations ($p = 0.000$). *M. rosenbergii* recorded the largest dorsal rostrum lengths, with Station 1 ranging from 1.89 ± 0.06 cm in June to 2.07 ± 0.10 cm in August. At Station 2, values ranged from 1.96 ± 0.07 cm in September to 2.62 ± 0.14 cm in April. The difference between stations was statistically significant ($p = 0.000$). *M. vollenhovenii* showed consistent rostrum lengths across months, with Station 1 ranging from 1.42 ± 0.07 cm in June to 1.67 ± 0.10 cm in September, and Station 2 ranging from 1.55 ± 0.08 cm in November to 1.85 ± 0.14 cm in December. There was no significant difference in dorsal rostrum length between stations for this species ($p = 0.736$)).

Table 4.11: Dorsal Rostrum Length (cm) of *Macrobrachium* Species

Species & Station	**April (Mean ± SE)**	**May (Mean ± SE)**	**June (Mean ± SE)**	**July (Mean ± SE)**	**August (Mean ± SE)**	**September (Mean ± SE)**	**November (Mean ± SE)**	**December (Mean ± SE)**	**Overall p-value (S1 vs S2)**
M. dux S1	1.83 ± 0.25	1.75 ± 0.09	1.83 ± 0.25	1.75 ± 0.09	1.70 ± 0.12	1.95 ± 0.17	1.75 ± 0.09	1.74 ± 0.06	0.104
M. dux S2	0.00 ± 0.00	1.72 ± 0.06	1.47 ± 0.09	1.86 ± 0.16	1.83 ± 0.07	1.59 ± 0.13	1.68 ± 0.08	1.59 ± 0.13	
M. equidens S1	1.46 ± 0.08	1.55 ± 0.10	1.46 ± 0.10	1.56 ± 0.10	1.56 ± 0.08	1.47 ± 0.09	1.56 ± 0.10	1.47 ± 0.11	0.378
M. equidens S2	1.73 ± 0.07	1.57 ± 0.05	1.69 ± 0.06	1.48 ± 0.07	1.36 ± 0.11	1.47 ± 0.09	1.55 ± 0.10	1.44 ± 0.10	
M. macrobrachion S1	1.58 ± 0.04	1.62 ± 0.06	1.61 ± 0.05	1.73 ± 0.08	1.62 ± 0.07	1.56 ± 0.07	1.73 ± 0.08	1.60 ± 0.07	0
M. macrobrachion S2	1.51 ± 0.02	1.46 ± 0.04	1.51 ± 0.03	1.42 ± 0.06	1.54 ± 0.06	1.56 ± 0.06	1.64 ± 0.06	1.58 ± 0.06	
M. rosenbergii S1	1.90 ± 0.05	1.97 ± 0.08	1.89 ± 0.06	1.97 ± 0.08	2.07 ± 0.10	1.98 ± 0.07	1.97 ± 0.08	1.93 ± 0.08	0
M. rosenbergii S2	2.62 ± 0.14	2.19 ± 0.11	2.25 ± 0.17	2.09 ± 0.14	2.04 ± 0.05	1.96 ± 0.07	2.10 ± 0.11	1.97 ± 0.08	
M. vollenhovenii S1	1.44 ± 0.06	1.64 ± 0.14	1.42 ± 0.07	1.63 ± 0.07	1.65 ± 0.05	1.67 ± 0.10	1.63 ± 0.07	1.65 ± 0.11	0.736
M. vollenhovenii S2	1.58 ± 0.19	1.65 ± 0.09	1.59 ± 0.12	1.54 ± 0.06	1.61 ± 0.09	1.75 ± 0.13	1.55 ± 0.08	1.85 ± 0.14	

4.4.5. Abdominal Length (AL)

The abdominal length of *Macrobrachium* species across stations and months is presented in Table 4.12. *Macrobrachium dux* exhibited moderate variation at Station 1, with values ranging from 2.51 ± 0.27 cm in April and June to 2.80 ± 0.04 cm in September. At Station 2, abdominal lengths ranged from 2.27 ± 0.15 cm in June to 2.90 ± 0.10 cm in August, with the species absent in April. The difference in abdominal length between stations for this species was not statistically significant ($p = 0.455$). *M. equidens* showed relatively stable abdominal lengths at Station 1, ranging from 2.18 ± 0.08 cm in December to 2.30 ± 0.08 cm in July, August, and November. Station 2 values fluctuated between 2.10 ± 0.06 cm in December and 2.61 ± 0.14 cm in April. There was no significant difference in abdominal length between stations for this species ($p = 0.161$). For *M. macrobrachion*, Station 1 recorded values ranging from 2.29 ± 0.08 cm in December to 2.63 ± 0.10 cm in July and November. At Station 2, abdominal lengths were slightly lower, ranging from 2.21 ± 0.10 cm in July to 2.47 ± 0.10 cm in November. The difference in abdominal length between stations was statistically significant ($p = 0.001$). *M. rosenbergii* consistently exhibited the largest abdominal lengths, with Station 1 values ranging from 2.83 ± 0.07 cm in April and June to 3.01 ± 0.10 cm in August. Station 2 measurements ranged from 2.93 ± 0.17 cm in June to 3.30 ± 0.14 cm in April. The difference in abdominal length between stations was statistically significant ($p = 0.019$). *M. vollenhovenii* displayed intermediate lengths, with Station 1 ranging from 2.28 ± 0.06 cm in June to 2.53 ± 0.15 cm in December, while Station 2 ranged from 2.32 ± 0.10 cm in November to 2.65 ± 0.16 cm in December. There was no significant difference in abdominal length between stations for this species ($p = 0.768$).

Table 4.12: Abdominal Length (cm) of *Macrobrachium* Species

Species & Station	April (Mean ± SE)	May (Mean ± SE)	June (Mean ± SE)	July (Mean ± SE)	August (Mean ± SE)	September (Mean ± SE)	November (Mean ± SE)	December (Mean ± SE)	Overall p-value (S1 vs S2)
M. dux S1	2.51 ± 0.27	2.75 ± 0.03	2.51 ± 0.27	2.75 ± 0.03	2.58 ± 0.19	2.80 ± 0.04	2.75 ± 0.03	2.73 ± 0.10	0.455
M. dux S2	0.00 ± 0.00	2.75 ± 0.08	2.27 ± 0.15	2.64 ± 0.14	2.90 ± 0.10	2.48 ± 0.18	2.67 ± 0.08	2.48 ± 0.18	
M. equidens S1	2.27 ± 0.06	2.26 ± 0.06	2.28 ± 0.07	2.30 ± 0.07	2.30 ± 0.08	2.20 ± 0.06	2.30 ± 0.07	2.18 ± 0.08	0.161
M. equidens S2	2.61 ± 0.14	2.39 ± 0.10	2.53 ± 0.12	2.24 ± 0.12	2.14 ± 0.06	2.15 ± 0.07	2.26 ± 0.07	2.10 ± 0.06	
M. macrobrachion S1	2.31 ± 0.05	2.41 ± 0.08	2.31 ± 0.06	2.63 ± 0.10	2.48 ± 0.09	2.42 ± 0.10	2.63 ± 0.10	2.29 ± 0.08	0.001
M. macrobrachion S2	2.24 ± 0.03	2.23 ± 0.05	2.24 ± 0.04	2.21 ± 0.10	2.25 ± 0.07	2.28 ± 0.09	2.47 ± 0.10	2.26 ± 0.09	
M. rosenbergii S1	2.83 ± 0.07	2.95 ± 0.10	2.83 ± 0.10	2.95 ± 0.10	3.01 ± 0.10	2.99 ± 0.10	2.95 ± 0.10	2.87 ± 0.10	0.019
M. rosenbergii S2	3.30 ± 0.14	3.03 ± 0.12	2.93 ± 0.17	2.97 ± 0.16	3.09 ± 0.12	3.04 ± 0.10	3.00 ± 0.12	3.03 ± 0.11	
M. vollenhovenii S1	2.30 ± 0.05	2.44 ± 0.11	2.28 ± 0.06	2.37 ± 0.08	2.39 ± 0.06	2.42 ± 0.11	2.37 ± 0.08	2.53 ± 0.15	0.768
M. vollenhovenii S2	2.43 ± 0.16	2.45 ± 0.11	2.39 ± 0.15	2.33 ± 0.09	2.42 ± 0.13	2.51 ± 0.14	2.32 ± 0.10	2.65 ± 0.16	

4.4.6. Telson Length (TL)

The telson length of *Macrobrachium* species across stations and months is presented in Table 4.13. *Macrobrachium dux* exhibited moderate variation at Station 1, with values ranging from 1.23 ± 0.15 cm in August to 1.46 ± 0.13 cm in April and June. At Station 2, measurements ranged from 1.00 ± 0.12 cm in June to 1.28 ± 0.02 cm in May, with the species absent in April. The difference in telson length between stations was statistically significant ($p = 0.002$). *M. equidens* showed relatively stable telson lengths across months, with Station 1 values ranging from 1.00 ± 0.06 cm in April to 1.14 ± 0.08 cm in July and November. At Station 2, values ranged from 0.95 ± 0.05 cm in July to 1.10 ± 0.06 cm in April. No significant difference was recorded between stations ($p = 0.103$). For *M. macrobrachion*, Station 1 values ranged from 1.13 ± 0.03 cm in April to 1.27 ± 0.07 cm in July and November, while Station 2 measurements varied between 0.95 ± 0.04 cm in July and 1.19 ± 0.06 cm in November. There was a significant difference between stations ($p = 0.000$). *M. rosenbergii* recorded higher telson lengths relative to other species, with Station 1 ranging from 1.15 ± 0.07 cm in May and July to 1.25 ± 0.06 cm in December. Station 2 measurements ranged from 1.20 ± 0.07 cm in August to 1.30 ± 0.02 cm in April. The difference between stations was statistically significant ($p = 0.034$). *M. vollenhovenii* showed moderate and relatively consistent telson lengths, with Station 1 ranging from 1.20 ± 0.07 cm in April to 1.24 ± 0.08 cm in December, and Station 2 ranging from 1.08 ± 0.04 cm in July to 1.45 ± 0.07 cm in April. There was no significant difference in telson length between stations for this species ($p = 0.132$).

Table 4.13: Telson Length (cm) of *Macrobrachium* Species

Species & Station	April (Mean ± SE)	May (Mean ± SE)	June (Mean ± SE)	July (Mean ± SE)	August (Mean ± SE)	September (Mean ± SE)	November (Mean ± SE)	December (Mean ± SE)	Overall p – value (S1 vs S2)
M. dux S1	1.46 ± 0.13	1.40 ± 0.06	1.46 ± 0.13	1.40 ± 0.06	1.23 ± 0.15	1.38 ± 0.05	1.40 ± 0.06	1.26 ± 0.06	0.002
M. dux S2	0.00 ± 0.00	1.28 ± 0.02	1.00 ± 0.12	1.26 ± 0.07	1.27 ± 0.03	1.15 ± 0.10	1.33 ± 0.06	1.15 ± 0.10	
M. equidens S1	1.00 ± 0.06	1.13 ± 0.08	1.04 ± 0.08	1.14 ± 0.08	1.10 ± 0.06	1.08 ± 0.07	1.14 ± 0.08	1.05 ± 0.09	0.103
M. equidens S2	1.10 ± 0.06	1.00 ± 0.04	1.08 ± 0.06	0.95 ± 0.05	0.98 ± 0.08	1.02 ± 0.08	1.06 ± 0.08	1.00 ± 0.09	
M. macrobrachion S1	1.13 ± 0.03	1.17 ± 0.05	1.16 ± 0.04	1.27 ± 0.07	1.16 ± 0.06	1.13 ± 0.06	1.27 ± 0.07	1.14 ± 0.06	0
M. macrobrachion S2	1.02 ± 0.01	0.98 ± 0.02	1.02 ± 0.02	0.95 ± 0.04	1.03 ± 0.05	1.06 ± 0.05	1.19 ± 0.06	1.07 ± 0.05	
M. rosenbergii S1	1.20 ± 0.04	1.15 ± 0.07	1.19 ± 0.06	1.15 ± 0.07	1.16 ± 0.05	1.19 ± 0.07	1.15 ± 0.07	1.25 ± 0.06	0.034
M. rosenbergii S2	1.30 ± 0.02	1.29 ± 0.03	1.23 ± 0.03	1.27 ± 0.04	1.20 ± 0.07	1.21 ± 0.06	1.20 ± 0.06	1.21 ± 0.06	
M. vollenhovenii S1	1.20 ± 0.07	1.40 ± 0.09	1.25 ± 0.10	1.24 ± 0.05	1.24 ± 0.04	1.23 ± 0.07	1.24 ± 0.05	1.24 ± 0.08	0.132
M. vollenhovenii S2	1.45 ± 0.07	1.20 ± 0.06	1.28 ± 0.08	1.08 ± 0.04	1.14 ± 0.06	1.32 ± 0.08	1.18 ± 0.06	1.41 ± 0.07	

4.4.7. Uropod Length (UL)

The uropod length of *Macrobrachium* species across stations and months is presented in Table 4.14. *Macrobrachium dux* exhibited moderate variation at Station 1, with values ranging from 1.43 ± 0.15 cm in August to 1.83 ± 0.09 cm in April and June. At Station 2, measurements ranged from 1.20 ± 0.12 cm in June to 1.53 ± 0.06 cm in November, with the species absent in April. The difference in uropod length between stations was statistically significant ($p = 0.000$). *M. equidens* showed moderate fluctuations, with Station 1 values ranging from 1.27 ± 0.07 cm in April to 1.42 ± 0.08 cm in July and November. At Station 2, values varied between 1.14 ± 0.04 cm in July and 1.34 ± 0.09 cm in November. There was a significant difference between stations ($p = 0.002$). For *M. macrobrachion*, Station 1 values ranged from 1.34 ± 0.03 cm in April to 1.50 ± 0.07 cm in July and November, while Station 2 measurements ranged from 1.16 ± 0.04 cm in July to 1.39 ± 0.06 cm in November, showing a significant station difference ($p = 0.000$). *M. rosenbergii* recorded consistently higher uropod lengths relative to other species, with Station 1 ranging from 1.41 ± 0.07 cm in May and July to 1.49 ± 0.06 cm in December. Station 2 values ranged from 1.43 ± 0.04 cm in June to 1.52 ± 0.03 cm in May, with no significant difference between stations ($p = 0.227$). *M. vollenhovenii* exhibited moderate variation across months, with Station 1 ranging from 1.43 ± 0.06 cm in August and November to 1.59 ± 0.08 cm in May, and Station 2 ranging from 1.30 ± 0.04 cm in July to 1.65 ± 0.07 cm in December. No significant difference was observed between stations ($p = 0.255$).

Table 4.14: Uropod Length (cm) of *Macrobrachium* Species

Species & Station	April (Mean ± SE)	May (Mean ± SE)	June (Mean ± SE)	July (Mean ± SE)	August (Mean ± SE)	September (Mean ± SE)	November (Mean ± SE)	December (Mean ± SE)	Overall p-value (S1 vs S2)
M. dux S1	1.83 ± 0.09	1.60 ± 0.06	1.83 ± 0.09	1.60 ± 0.06	1.43 ± 0.15	1.60 ± 0.06	1.60 ± 0.06	1.49 ± 0.06	0
M. dux S2	0.00 ± 0.00	1.50 ± 0.00	1.20 ± 0.12	1.48 ± 0.08	1.50 ± 0.00	1.35 ± 0.11	1.53 ± 0.06	1.35 ± 0.11	
M. equidens S1	1.27 ± 0.07	1.41 ± 0.08	1.33 ± 0.10	1.42 ± 0.08	1.35 ± 0.06	1.34 ± 0.08	1.42 ± 0.08	1.32 ± 0.10	0.002
M. equidens S2	1.27 ± 0.05	1.18 ± 0.04	1.26 ± 0.05	1.14 ± 0.04	1.25 ± 0.10	1.27 ± 0.09	1.34 ± 0.09	1.25 ± 0.10	
M. macrobrachion S1	1.34 ± 0.03	1.38 ± 0.05	1.38 ± 0.04	1.50 ± 0.07	1.39 ± 0.06	1.34 ± 0.07	1.50 ± 0.07	1.37 ± 0.06	0
M. macrobrachion S2	1.22 ± 0.01	1.19 ± 0.02	1.22 ± 0.02	1.16 ± 0.04	1.24 ± 0.06	1.26 ± 0.05	1.39 ± 0.06	1.26 ± 0.05	
M. rosenbergii S1	1.44 ± 0.05	1.41 ± 0.07	1.44 ± 0.06	1.41 ± 0.07	1.41 ± 0.06	1.44 ± 0.07	1.41 ± 0.07	1.49 ± 0.06	0.227
M. rosenbergii S2	1.50 ± 0.03	1.52 ± 0.03	1.43 ± 0.04	1.50 ± 0.05	1.46 ± 0.08	1.45 ± 0.06	1.45 ± 0.06	1.45 ± 0.06	
M. vollenhovenii S1	1.46 ± 0.05	1.59 ± 0.08	1.48 ± 0.06	1.43 ± 0.06	1.43 ± 0.04	1.44 ± 0.08	1.43 ± 0.06	1.43 ± 0.09	0.255
M. vollenhovenii S2	1.58 ± 0.07	1.43 ± 0.06	1.41 ± 0.07	1.30 ± 0.04	1.37 ± 0.07	1.55 ± 0.08	1.38 ± 0.06	1.65 ± 0.07	

4.4.8. Eye Diameter (ED)

The eye diameter of *Macrobrachium* species across stations and months is presented in Table 4.15. *Macrobrachium dux* exhibited moderate variation, with Station 1 values ranging from 0.16 ± 0.02 cm in April and June to 0.20 ± 0.00 cm in May, July, September, November, and December. At Station 2, measurements ranged from 0.00 ± 0.00 cm in April to 0.20 ± 0.00 cm in August, with intermediate values in other months. The difference in eye diameter between stations was statistically significant ($p = 0.017$). *M. equidens* showed relatively stable eye diameter across months, ranging from 0.13 ± 0.01 cm in August and December to 0.14 ± 0.01 cm in April, May, June, July, and November at Station 1. Station 2 values ranged from 0.11 ± 0.01 cm in May and July to 0.13 ± 0.01 cm in April and June. A significant difference between stations was observed ($p = 0.007$). For *M. macrobrachion*, Station 1 measurements ranged from 0.14 ± 0.00 cm in April, June, and December to 0.16 ± 0.01 cm in July and November, while Station 2 values varied from 0.10 ± 0.00 cm in April to 0.14 ± 0.01 cm in November and December, with a statistically significant difference ($p = 0.000$). *M. rosenbergii* recorded slightly higher eye diameters, with Station 1 ranging from 0.16 ± 0.01 cm in most months to 0.17 ± 0.01 cm in June and September, and Station 2 ranging from 0.15 ± 0.01 cm in June to 0.19 ± 0.01 cm in August. No significant difference was observed between stations ($p = 0.389$). *M. vollenhovenii* exhibited relatively consistent eye diameter across months, with Station 1 values ranging from 0.15 ± 0.01 cm in June, July, August, September, and November to 0.17 ± 0.01 cm in May and 0.16 ± 0.02 cm in April. At Station 2, values ranged from 0.14 ± 0.01 cm in July to 0.18 ± 0.04 cm in April and 0.18 ± 0.01 cm in December, with no significant difference between stations ($p = 0.841$).

Table 4.15: Eye Diameter (cm) of *Macrobrachium* Species

Species & Station	**April (Mean ± SE)**	**May (Mean ± SE)**	**June (Mean ± SE)**	**July (Mean ± SE)**	**August (Mean ± SE)**	**September (Mean ± SE)**	**November (Mean ± SE)**	**December (Mean ± SE)**	**Overall p – value (S1 vs S2)**
M. dux S1	0.16 ± 0.02	0.20 ± 0.00	0.16 ± 0.02	0.20 ± 0.00	0.18 ± 0.03	0.20 ± 0.00	0.20 ± 0.00	0.20 ± 0.00	0.017
M. dux S2	0.00 ± 0.00	0.15 ± 0.02	0.10 ± 0.00	0.16 ± 0.02	0.20 ± 0.00	0.16 ± 0.02	0.17 ± 0.02	0.16 ± 0.02	
M. equidens S1	0.14 ± 0.01	0.14 ± 0.01	0.14 ± 0.01	0.14 ± 0.01	0.13 ± 0.01	0.13 ± 0.01	0.14 ± 0.01	0.13 ± 0.01	0.007
M. equidens S2	0.13 ± 0.01	0.11 ± 0.01	0.12 ± 0.01	0.11 ± 0.01	0.12 ± 0.01	0.12 ± 0.01	0.12 ± 0.01	0.12 ± 0.01	
M. macrobrachion S1	0.14 ± 0.00	0.15 ± 0.01	0.14 ± 0.01	0.16 ± 0.01	0.14 ± 0.01	0.14 ± 0.01	0.16 ± 0.01	0.14 ± 0.01	0
M. macrobrachion S2	0.10 ± 0.00	0.12 ± 0.00	0.11 ± 0.00	0.11 ± 0.01	0.13 ± 0.01	0.13 ± 0.01	0.14 ± 0.01	0.14 ± 0.01	
M. rosenbergii S1	0.16 ± 0.01	0.16 ± 0.01	0.17 ± 0.01	0.16 ± 0.01	0.16 ± 0.01	0.17 ± 0.01	0.16 ± 0.01	0.16 ± 0.01	0.389
M. rosenbergii S2	0.18 ± 0.01	0.17 ± 0.01	0.15 ± 0.01	0.17 ± 0.01	0.19 ± 0.01	0.17 ± 0.01	0.16 ± 0.01	0.17 ± 0.01	
M. vollenhovenii S1	0.16 ± 0.02	0.17 ± 0.01	0.15 ± 0.02	0.15 ± 0.01	0.15 ± 0.01	0.15 ± 0.01	0.15 ± 0.01	0.16 ± 0.01	0.841
M. vollenhovenii S2	0.18 ± 0.04	0.15 ± 0.01	0.15 ± 0.03	0.14 ± 0.01	0.16 ± 0.01	0.17 ± 0.01	0.15 ± 0.01	0.18 ± 0.01	

4.5. Condition Indices

4.5.1. Length-Weight Relationship and Condition Factor of *Macrobrachium* Species

Table 4.16 summarizes the length-weight relationship and condition factors for the prawn species recorded. In April, male specimens at Station 1 exhibited a negative allometric growth pattern (b = 2.9757) with a high coefficient of determination (R^2 = 0.913), suggesting a reliable length–weight relationship. Their condition factor ranged from 0.791 to 1.507 with a mean of 1.150 ± 0.240, indicating a good physiological state. Conversely, Station 2 males also showed negative allometry (b = 1.7957) with an exceptionally strong R^2 value of 0.999. However, their condition factor (mean K = 0.863 ± 0.249) was lower than their Station 1 counterparts, reflecting a poorer physiological state. Female individuals at Station 1 likewise demonstrated negative allometric growth (b = 1.6686, R^2 = 0.554), but with a relatively higher condition factor (K = 1.141 ± 0.501), which suggests good body robustness despite the weak model fit. At Station 2, females maintained a negative allometric trend (b = 1.3135) with a stronger R^2 of 0.650. Their K factor (1.119 ± 0.423) was comparable to Station 1, indicating generally good condition despite spatial variation.

May revealed a shift in male growth dynamics, particularly at Station 1 where a positive allometric growth (b = 3.4316) was observed, coupled with a strong R^2 of 0.713. This suggests rapid weight increase relative to length, likely influenced by favorable environmental or nutritional conditions. The mean condition factor was 1.148 ± 0.281, further reinforcing this inference. In contrast, Station 2 males retained a negative allometric trend (b = 1.9502, R^2 = 0.869), with a moderate condition factor of 0.996 ± 0.319. Females from both stations sustained a negative allometric profile: Station 1 (b = 1.7696, R^2 = 0.708, K = 1.203 ± 0.630) and Station 2 (b = 1.4816, R^2 = 0.662, K = 1.252 ± 0.646), both with good body condition and moderate correlation strengths

Table 4.16: Length-weight relationship and Fulton Condition factor (K) of *Macrobrachium* sp (April – December)

Month	Sex	N_1	a_1	b_1	R^2_1	Station 1 K (Range) Mean ± SD	Growth type	Fulton K	N_2	a_2	b_2	R^2_2	Station 2 K (Range) Mean ± SD	Growth type	Fulton K
April	Male	13	84.51	2.9757x	0.913	(0.791–1.507) 1.150 ± 0.240	Negative allometric	Good	17	11.46	1.7957x	0.999	(0.562–1.136) 0.863 ± 0.249	Negative allometric	Poor
	Female	186	6.81	1.6686x	0.554	(0.579–3.698) 1.141 ± 0.501	Negative allometric	Good	160	3.68	1.3135x	0.65	(0.354–2.368) 1.119 ± 0.423	Negative allometric	Good
May	Male	15	220.66	3.4316x	0.713	(0.641–1.507) 1.148 ± 0.281	Positive allometric	Good	31	13.33	1.9502x	0.869	(0.562–2.344) 0.996 ± 0.319	Negative allometric	Poor
	Female	99	8.12	1.7696x	0.708	(0.611–3.698) 1.203 ± 0.630	Negative allometric	Good	144	4.84	1.4816x	0.662	(0.354–3.698) 1.252 ± 0.646	Negative allometric	Good
June	Male	40	32.94	2.4633x	0.81	(0.636–2.026) 1.105 ± 0.322	Negative allometric	Good	43	5.65	1.5119x	0.757	(0.354–2.368) 1.045 ± 0.379	Negative allometric	Good
	Female	89	5.78	1.5926x	0.532	(0.579–3.698) 1.146 ± 0.507	Negative allometric	Good	91	3.93	1.3421x	0.611	(0.354–2.664) 1.127 ± 0.432	Negative allometric	Good
July	Male	42	13.82	2.0537x	0.721	(0.611–3.545) 1.157 ± 0.506	Negative allometric	Good	35	5.5	1.5519x	0.675	(0.562–3.698) 1.333 ± 0.720	Negative allometric	Good
	Female	72	11.92	1.9571x	0.71	(0.611–3.476) 1.095 ± 0.431	Negative allometric	Good	77	4.69	1.4827x	0.638	(0.354–3.826) 1.317 ± 0.743	Negative allometric	Good
August	Male	43	13.49	2.0233x	0.724	(0.562–3.545) 1.130 ± 0.508	Negative allometric	Good	24	9.49	1.8484x	0.817	(0.611–3.545) 1.223 ± 0.616	Negative allometric	Good

	Female	107	8.83	1.7948x	0.684	(0.354–3.939) 1.099 ± 0.444	Negative allometric	Good	67	10.07	1.8685x	0.719	(0.579–3.083) 1.181 ± 0.473	Negative allometric	Good
September	Male	47	10.86	1.9247x	0.672	(0.611–3.272) 1.221 ± 0.510	Negative allometric	Good	41	17.68	2.1580x	0.757	(0.611–2.344) 1.090 ± 0.365	Negative allometric	Good
	Female	80	9.67	1.8608x	0.752	(0.521–3.258) 1.121 ± 0.440	Negative allometric	Good	61	6.94	1.6783x	0.678	(0.579–2.747) 1.207 ± 0.503	Negative allometric	Good
November	Male	46	12.88	2.0051x	0.721	(0.521–2.375) 1.099 ± 0.379	Negative allometric	Good	40	10.62	1.9022x	0.672	(0.482–2.562) 1.126 ± 0.416	Negative allometric	Good
	Female	68	13.39	2.0200x	0.689	(0.531–2.926) 1.093 ± 0.403	Negative allometric	Good	62	7.34	1.7089x	0.663	(0.354–2.909) 1.103 ± 0.446	Negative allometric	Good
December	Male	15	19.1	2.2121x	0.61	(0.483–2.184) 1.131 ± 0.390	Negative allometric	Good	34	15.18	2.0836x	0.717	(0.611–2.344) 1.091 ± 0.385	Negative allometric	Good
	Female	76	13.86	2.0178x	0.758	(0.579–2.602) 1.088 ± 0.377	Negative allometric	Good	54	7.69	1.7371x	0.662	(0.579–2.909) 1.222 ± 0.518	Negative allometric	Good

Key: N_1, N_2: Sample size for Station 1 and Station 2, respectively. a_1, a_2: Intercept constants of length–weight regression for Station 1 and Station 2. b_1, b_2: Slope coefficients of length–weight regression for Station 1 and Station 2. R^2_1, R^2_2: Coefficient of determination (goodness-of-fit) for Stations 1 and 2. K (Range) Mean ± SD: Fulton's condition factor (minimum–maximum range, mean ± standard deviation) for each station. Growth type: Classification of growth pattern based on b value (negative allometric if $b < 3$, isometric if $b \approx 3$, positive allometric if $b > 3$). Fulton K: Qualitative assessment of condition factor (Good, Poor)

In June, male prawns at Station 1 demonstrated negative allometric growth (b = 2.4633, R^2 = 0.810), with a mean condition factor of 1.105 ± 0.322. Station 2 males showed a lower growth coefficient (b = 1.5119) and R^2 = 0.757, with a slightly reduced K value (1.045 ± 0.379). This indicates slower weight accumulation at Station 2. Female growth patterns continued the negative allometric trend: b = 1.5926 (Station 1) and b = 1.3421 (Station 2), with condition factors of 1.146 ± 0.507 and 1.127 ± 0.432, respectively. While growth remained length-biased, the good K values suggest overall satisfactory physiological health in both stations.

In July, Station 1 males maintained a negative allometric pattern (b = 2.0537, R^2 = 0.721), with a K range of 0.611–3.545 and mean of 1.157 ± 0.506. Station 2 males were similar (b = 1.5519, R^2 = 0.675), but displayed a higher mean K of 1.333 ± 0.720, suggesting superior condition, potentially due to localised resource abundance or reduced competition. Female prawns from both stations also conformed to negative allometric growth: Station 1 (b = 1.9571, R^2 = 0.710, K = 1.095 ± 0.431), Station 2 (b = 1.4827, R^2 = 0.638, K = 1.317 ± 0.743).

August maintained the trend of negative allometric growth across all groups. Station 1 males showed b = 2.0233, R^2 = 0.724, and a mean K of 1.130 ± 0.508. Their Station 2 counterparts, while still exhibiting negative allometry (b = 1.8484), showed higher model fit (R^2 = 0.817) and K = 1.223 ± 0.616. Female prawns similarly displayed negative allometric coefficients: Station 1 (b = 1.7948, R^2 = 0.684, K = 1.099 ± 0.444) and Station 2 (b = 1.8685, R^2 = 0.719, K = 1.181 ± 0.473), suggesting consistent energy allocation trends with no evidence of weight-dominant growth.

In September, male prawns from Station 1 continued a negative allometric pattern (b = 1.9247, R^2 = 0.672), with their highest mean condition factor (1.221 ± 0.510). Station 2 males had a slightly elevated b = 2.1580 (R^2 = 0.757), but also reflected negative allometric growth, with a K of 1.090 ± 0.365. Females mirrored this growth pattern: Station 1 (b = 1.8608, R^2 = 0.752, K = 1.121 ±

0.440), Station 2 (b = 1.6783, R^2 = 0.678, K = 1.207 ± 0.503), again supporting a prevailing trend of length-prioritized growth but generally good condition.

By November, all groups continued to display negative allometry. Station 1 males had b = 2.0051, R^2 = 0.721, and K = 1.099 ± 0.379, while Station 2 males recorded b = 1.9022, R^2 = 0.672, and K = 1.126 ± 0.416. Female values for b remained consistent with previous months: Station 1 (b = 2.0200, R^2 = 0.689, K = 1.093 ± 0.403) and Station 2 (b = 1.7089, R^2 = 0.663, K = 1.103 ± 0.446). In December, males at Station 1 had b = 2.2121 (R^2 = 0.610) and a K of 1.131 ± 0.390. Station 2 males recorded b = 2.0836, R^2 = 0.717, with a slightly lower K (1.091 ± 0.385). Female growth remained negative allometric, with Station 1 having b = 2.0178 (R^2 = 0.758, K = 1.088 ± 0.377) and Station 2 recording b = 1.7371 (R^2 = 0.662, K = 1.222 ± 0.518).

Across all months and stations, the length–weight relationship of the population consistently exhibited negative allometric growth, with 'b' values less than 3 in nearly all groups, indicating that length increased at a greater rate than weight. The only deviation from this pattern occurred in Station 1 males during May, where a positive allometric relationship (b = 3.4316) was recorded, representing the highest growth exponent observed in the dataset. In contrast, the lowest 'b' value was documented among females at Station 2 in April (b = 1.3135), marking the most pronounced case of negative allometry.

The coefficient of determination (R^2) varied across months and groups, ranging from moderate to high levels of model fit. Male specimens at Station 2 in April presented the strongest R^2 (0.999), while the weakest was observed in Station 1 females for the same month (R^2 = 0.554). R^2 values above 0.7 were more frequently recorded among males than females, particularly at Station 1, indicating more consistent length–weight relationships in males at that location.

In terms of condition factor (K), values were generally within the acceptable physiological range, with monthly means typically falling between 1.0 and 1.3. The highest mean condition factor was recorded for Station 2 males in July (K = 1.333 ± 0.720), while the lowest occurred in Station 2 males in April (K = 0.863 ± 0.249). Across both stations and sexes, female individuals more often displayed slightly higher mean condition factors than their male counterparts, although this trend was not uniform across all months.

Temporal variations were evident, with both 'b' and K values fluctuating across months. However, spatial patterns were also apparent: Station 1 males showed a wider range of 'b' values across months, including the highest and some of the more moderate values, while Station 2 males tended to exhibit lower 'b' coefficients more consistently. Female groups from both stations displayed similar ranges of 'b' values, although Station 1 females generally presented slightly higher R^2 values.

4.5.2. Hepatosomatic index

Figure 4.33 presents the monthly mean hepatosomatic index (HSI) of *Macrobrachium* species (males and females) sampled from Stations 1 and 2 between April and December. A sex-specific pattern is evident in the dataset. Females generally exhibited higher HSI values relative to males, particularly during May, June, and December. At Station 1 in May, female HSI (5.89) was higher than that of males (4.32), while a similar female dominance occurred in June (5.87 vs. 5.28) and in December at Station 2 (6.23 vs. 5.42). Males, however, recorded pronounced HSI elevations at Station 2 during the early wet season, with the highest mean in April (7.65 compared with 5.67 at Station 1).

Inter-station contrasts further underscore ecological differences. Male HSI values were consistently higher at Station 2 than Station 1 in April, May, and June, indicating a more favorable

physiological condition in the early wet season at Station 2. The monthly sequence of male HSI at Station 2 followed: April > June > May > July > November > December > September > August, whereas at Station 1 it was: April > September > August > July > June > November > December > May. Among females, inter-station differences were less pronounced. Station 1 females surpassed those at Station 2 in May (5.89 vs. 5.69), whereas higher values were recorded at Station 2 in September (5.88 vs. 5.32) and December (6.23 vs. 5.71). December represented the overall maximum female mean HSI (6.23 at Station 2). Female rankings at Station 1 followed: May > December > June > August > November > July > April > September, while at Station 2 they followed: December > June ≈ September > August > May > April > November > July. These results emphasize December as a critical period of hepatopancreatic renewal in females, particularly in Station 2.

4.6. Reproductive Biology

4.6.1. Sex Distribution

Table 4.17 presents the spatio-temporal distribution of male and female *Macrobrachium* species collected from the Ubeji axis of the Warri River. The results reveal distinct temporal and spatial variations in sex composition throughout the sampling period. In April, both stations exhibited a markedly skewed sex ratio strongly favoring females. Station 1 recorded 186 females and 13 males, yielding a ratio of 1:14.3, while Station 2 had 160 females and 17 males (1:9.4). This represents the greatest degree of female dominance recorded during the study, particularly at Station 1. By May, although the female-biased pattern persisted, the disparity had reduced. Station 1 recorded a sex ratio of 1:6.6, while Station 2 recorded 1:4.6, indicating a modest increase in the proportion of males. In June, the sex composition exhibited a progressive shift toward equilibrium. Station 1 reported 40 males and 89 females (1:2.2), and Station 2 had 43 males and 91 females (1:2.1), reflecting increased male occurrence. The transition toward a more balanced sex

ratio continued in July, with Station 1 recording 42 males and 72 females (1:1.7) and Station 2 recording 35 males and 77 females (1:2.2). This trend was sustained in August, where the ratios remained moderately female-biased at 1:2.5 (Station 1) and 1:2.8 (Station 2). From September to November, the sex ratios were most closely approximated to parity across both stations. In Station 1, values ranged from 1:1.5 to 1:1.7, while Station 2 exhibited ratios of 1:1.5 to 1:1.6. Notably, September and November at Station 2 (41 males to 61 females, and 40 males to 62 females, respectively) reflect the closest alignment to a 1:1 sex ratio, signifying the least deviation from sex parity during the study. In December, however, the sex structure diverged once more. Station 1 exhibited a renewed female-biased ratio of 1:5.1 (15 males and 76 females), while Station 2 remained comparatively balanced at 1:1.6.

4.6.1.1 Sex ratio of *Macrobrachium dux*

Figure 4.34 illustrates the monthly sex composition of *Macrobrachium dux* across two stations over the eight-month sampling period. In April, only Station 1 yielded specimens, with a strongly female-biased ratio of 1:7. No individuals were recorded at Station 2. May continued this trend, with females exclusively present in both stations, reinforcing early-season female dominance. By June, sex ratios became more balanced, Station 1 had a 1:1.3 ratio (3 males, 4 females), while Station 2 showed complete parity (2 males, 2 females). July revealed divergence: Station 1 showed male dominance (3:1), while Station 2 remained slightly female-biased (2:3). August marked a return to near parity in both stations, with ratios of 1:1 and 1:2, respectively. September maintained this trend, with Station 1 at 1:1 and Station 2 mildly skewed towards females (1:1.7). A shift occurred in November, where both stations showed male dominance,3:1 in Station 1 and 2:1 in Station 2,the only month where this pattern was observed concurrently. In December, sex ratios again approached balance, with Station 1 slightly male-biased (1.3:1) and Station 2 leaning female (1:1.7).

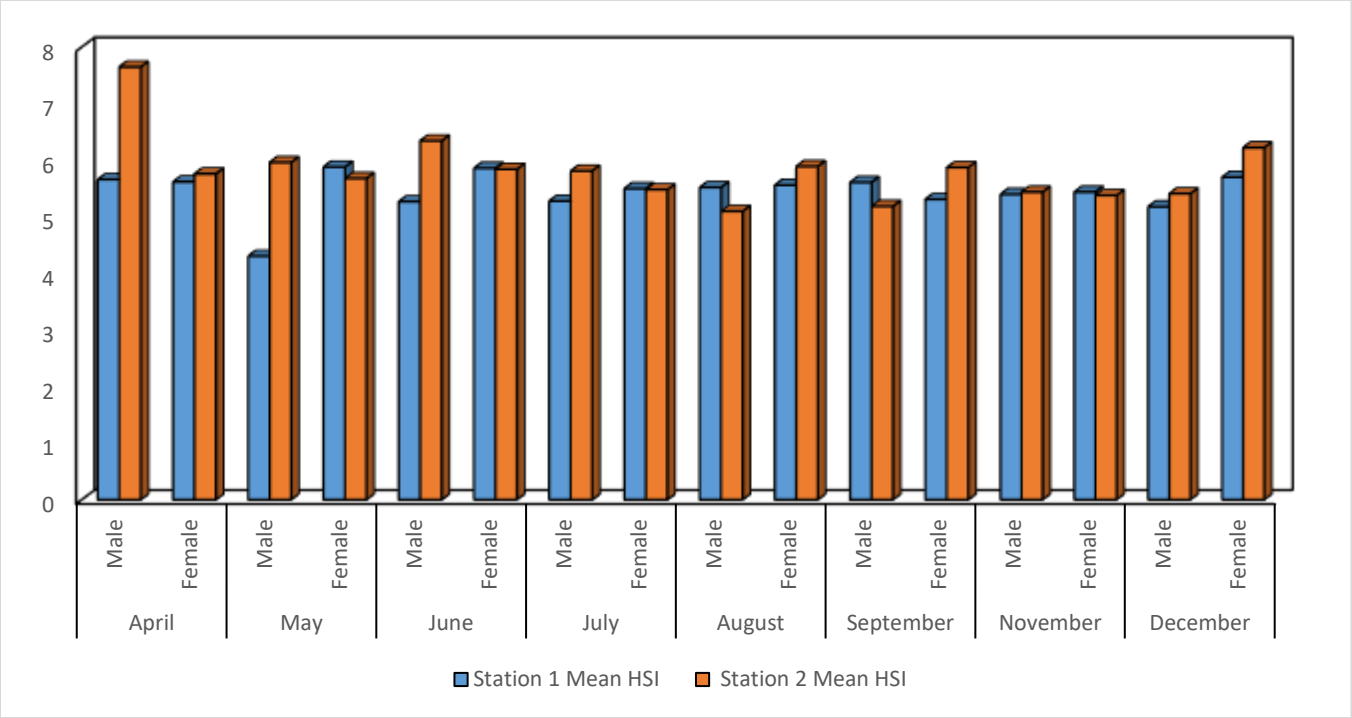

Figure 4.33: Pooled Mean Hepatosomatic Index (HSI) of *Macrobrachium* Species Table 4.17:

Pooled spatio-temporal ratio of *Macrobrachium* sp. in the Ubeji Axis, Warri River

Month	Station	Male (n)	Female (n)	Total (n)	Sex Ratio (M:F)
April	1	13	186	199	1:14.3
	2	17	160	177	1:9.4
May	1	15	99	114	1:6.6
	2	31	144	175	1:4.6
June	1	40	89	129	1:2.2
	2	43	91	134	1:2.1
July	1	42	72	114	1:1.7
	2	35	77	112	1:2.2
August	1	43	107	150	1:2.5
	2	24	67	91	1:2.8
September	1	47	80	127	1:1.7
	2	41	61	102	1:1.5
November	1	46	68	114	1:1.5
	2	40	62	102	1:1.6
December	1	15	76	91	1:5.1
	2	34	54	88	1:1.6

4.6.1.2 Sex distribution of *Macrobrachium equidens*

Figure 4.35 illustrates the monthly sex distribution of *Macrobrachium equidens* across Stations 1 and 2, highlighting notable temporal and spatial variations. In April, both stations exhibited strong female dominance,most pronounced at Station 1 with a 1:9 ratio (2 males, 18 females), the highest female skew observed. Station 2 also showed a notable female bias (1:2.2). This trend persisted into May, with ratios of 1:7 and 1:2.1 at Stations 1 and 2, respectively, reinforcing early-season female prevalence.

Sex ratios began to shift toward equilibrium by June, with Station 1 at 1:1.3 (6 males, 8 females) and Station 2 at 1:1.6 (7 males, 11 females). July exhibited near parity,1:1.3 in Station 1 and 1:1.2 in Station 2,representing the closest balance in sex composition during the study. In August, female dominance returned, particularly in Station 2 (1:5), while Station 1 recorded a ratio of 1:1.9.

September marked a reversal in Station 1, showing a male-biased composition (11 males, 7 females; 1.6:1), contrasting with Station 2's slight female bias (1:1.6). In November, Station 1 maintained a near-balanced ratio (1:1.3), whereas Station 2 recorded its highest male skew (1.8:1), the only month with male dominance at this site. December saw a return to female dominance in both stations,most notably at Station 1 (1:4.5) and a milder skew at Station 2 (1:3).

Overall, *M. equidens* displayed marked female dominance in the early months (April–May), relative parity mid-year (June–July), and sporadic male-biased ratios later in the season. The highest female dominance occurred in April at Station 1 (1:9), while the strongest male dominance appeared in September at Station 1 (1.6:1) and November at Station 2 (1.8:1). The closest approach to sex parity was in July, particularly at Station 2 (1:1.2), indicating a mid-season phase of reproductive balance.

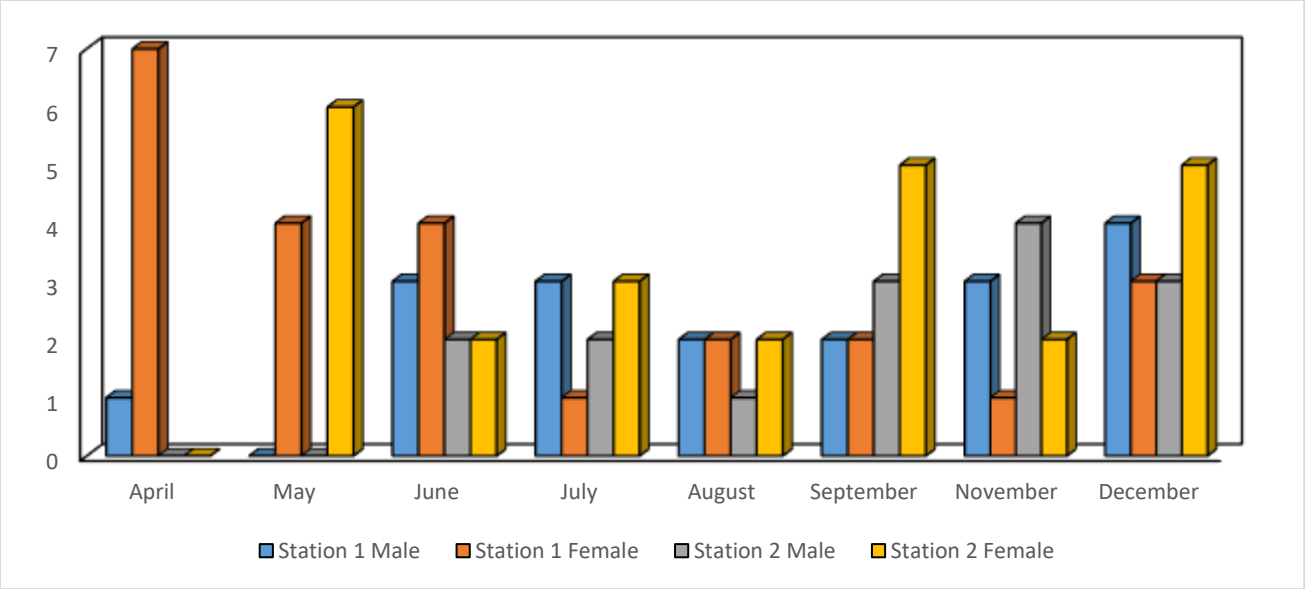

Figure 4.34**:** Monthly sex distribution of *M. dux*

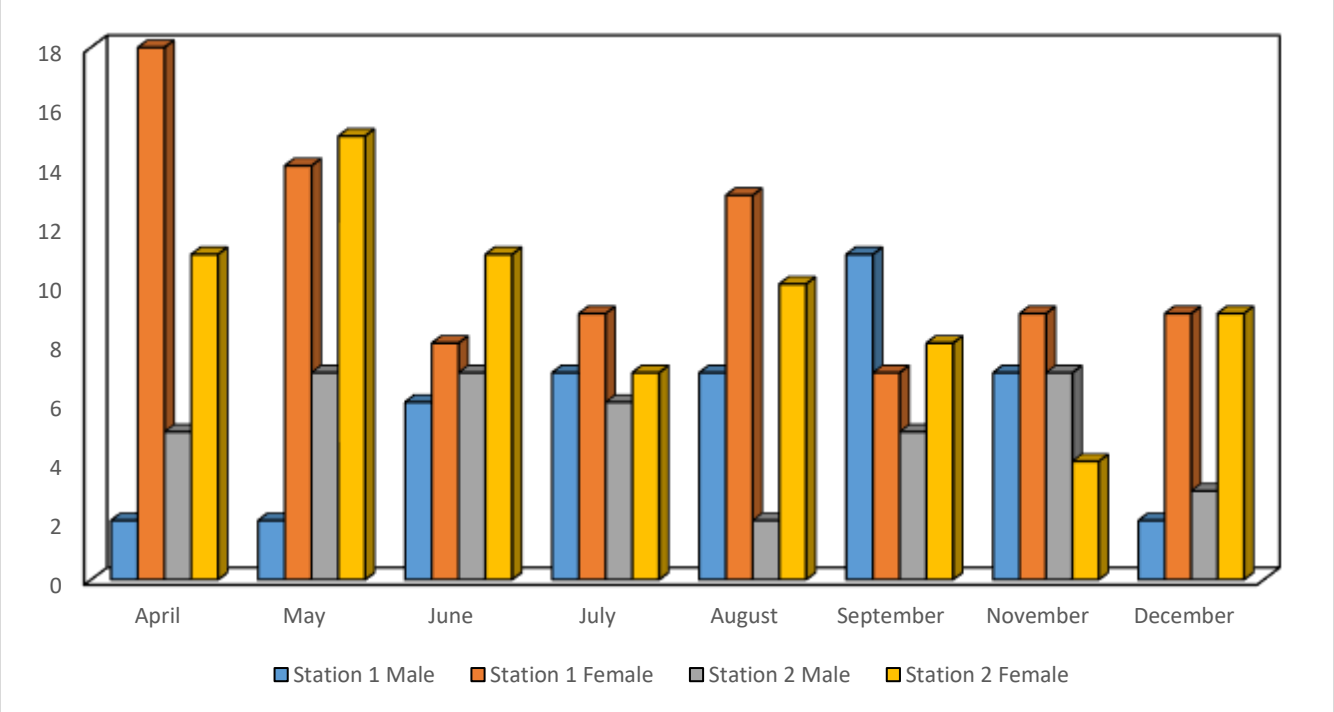

Figure 4.35: Monthly sex distribution of *M. equidens*

4.6.1.3 Sex distribution of *Macrobrachium macrobrachion*

Figure 4.36 presents the monthly sex distribution of *Macrobrachium macrobrachion* from Stations 1 and 2, revealing significant temporal and spatial variations. In April and May, both stations exhibited pronounced female dominance. Station 1 recorded 5 males to 107 females (1:21.4) in April and 4:56 (1:14) in May, while Station 2 had 6:125 (1:20.8) in April and 9:89 (1:9.9) in May, indicating the strongest female-skewed ratios during the study. By June, sex ratios began to moderate. Station 1 had 16 males to 58 females (1:3.6), and Station 2 recorded 23:56 (1:2.4), reflecting a shift towards more balanced distributions. In July, both stations exhibited improved parity, Station 1 with 9:21 (1:2.3) and Station 2 with 8:22 (1:2.8). August maintained this trend with moderate female bias at Station 1 (9:27; 1:3) and Station 2 (5:37; 1:7.4). September marked a relative peak in male contribution. Station 1 recorded 15 males to 21 females (1:1.4), and Station 2 had 16:27 (1:1.7), reflecting the closest sex ratio balance of the year. In November, the pattern remained relatively balanced with ratios of 10:20 (1:2) at Station 1 and 11:25 (1:2.3) at Station 2. December showed a return to female dominance, Station 1 had 3:35 (1:11.7), while Station 2 showed a less skewed 15:25 (1:1.7). Overall, *M. macrobrachion* populations showed strong female dominance early in the sampling period (April–May), progressing towards greater sex ratio balance mid-year (June–September), with slight reversion to female-skewed compositions by December. The most balanced sex ratios occurred in September at both stations, especially at Station 1 (1:1.4).

4.6.1.4 Sex distribution of *Macrobrachium rosenbergii*

Figure 4.37 illustrates the monthly sex composition of *Macrobrachium rosenbergii* at Stations 1 and 2, revealing dynamic but generally female-skewed trends with intermittent parity and male dominance. In April, both stations displayed strong female dominance: Station 1 recorded 2 males to 48 females (1:24), while Station 2 had 6 males and 24 females (1:4), marking the most female-biased month of the study. In May, sex ratios shifted slightly. Station 1 recorded 6:14 (1:2.3) and Station 2 had 10:32 (1:3.2), continuing a pattern of female predominance. June showed a trend toward more balanced distributions, Station 1 with 12 males to 16 females (1:1.3), and Station 2 with 8:15 (1:1.9). By July, parity was observed at Station 1 (10:10; 1:1), while Station 2 maintained a moderate female bias (5:14; 1:2.8). August sustained this trend with Station 1 recording 10:17 (1:1.7) and Station 2 showing a female skew (3:11; 1:3.7). September reflected greater balance, with Station 1 at 6:12 (1:2) and Station 2 at 8:11 (1:1.4). In November, male representation peaked. Station 1 showed a male-biased ratio of 11:9 (1.2:1), while Station 2 exhibited near parity with 11:10 (1.1:1), the closest male-to-female balance recorded. In December, a strong female bias re-emerged at Station 1 (4:27; 1:6.8), while Station 2 maintained a milder skew (8:10; 1:1.3).

Overall, *M. rosenbergii* populations displayed early and late-season female dominance, with mid-season (June–November) periods showing more balanced or male-leaning compositions. The most pronounced female bias was in April at Station 1 (1:24), while the highest male dominance occurred in November at Station 1 (1.2:1). July at Station 1 marked the only instance of complete sex parity.

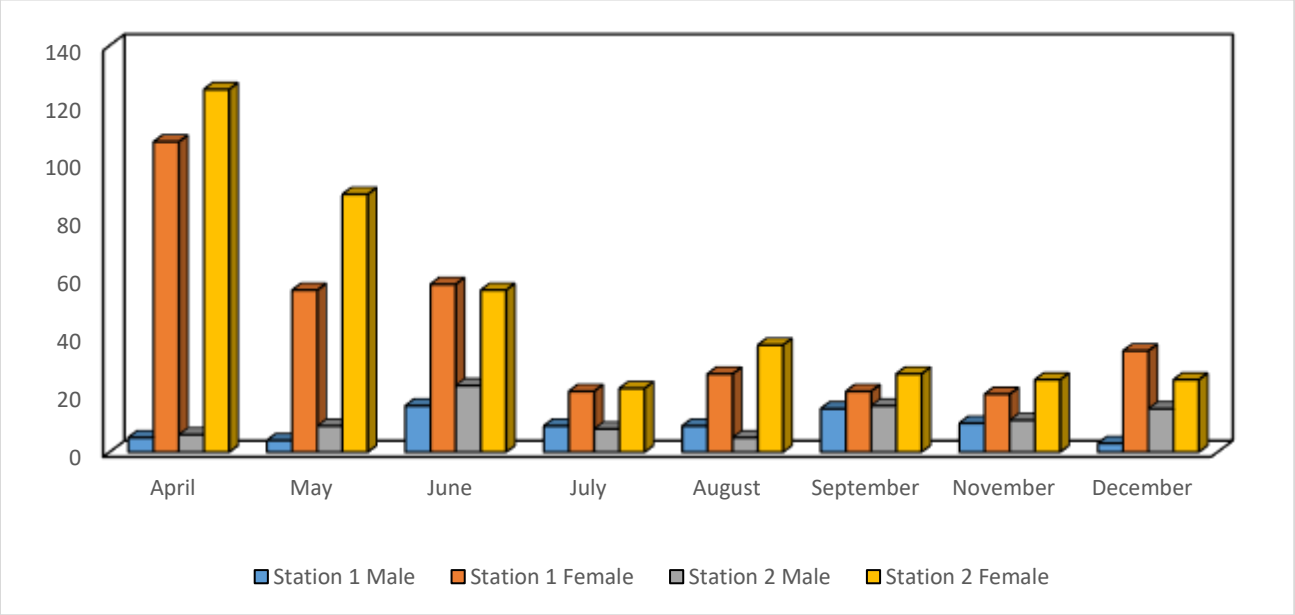

Figure 4.36: Monthly sex distribution of *M. macrobrachion*

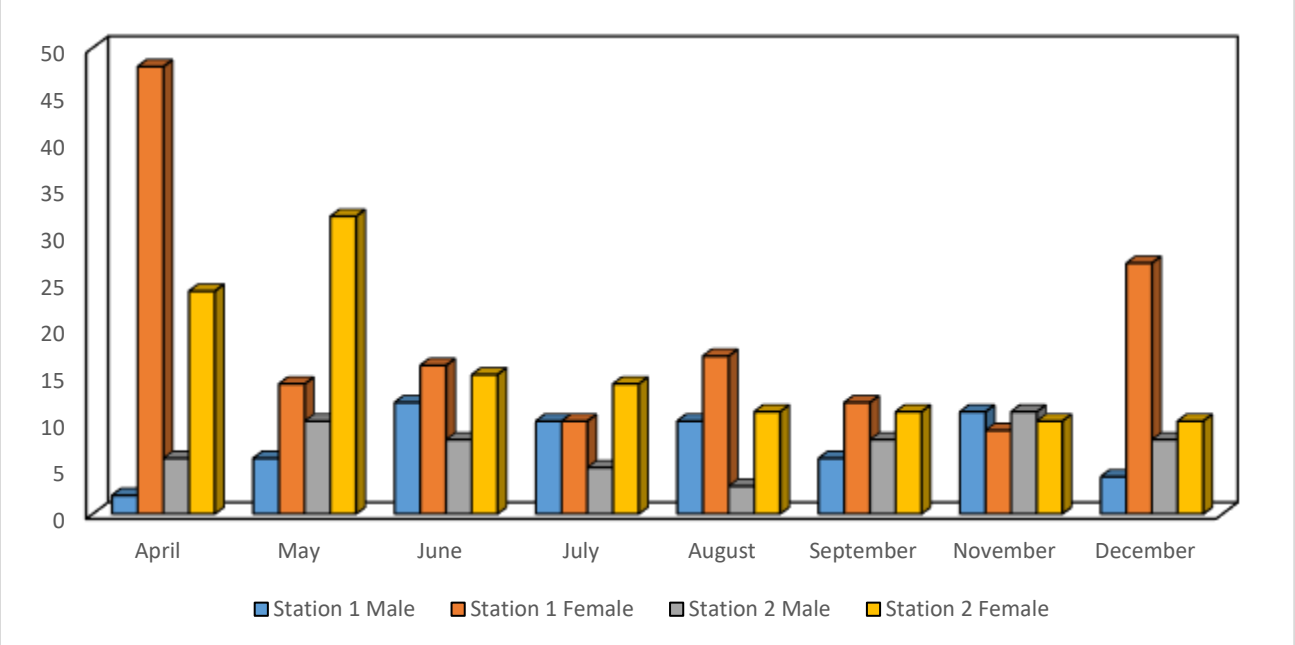

Figure 4.37: Monthly sex distribution of *M. rosenbergii*

4.6.1.5 Sex distribution of *Macrobrachium vollenhovenii*

Figure 4.38 shows the sex composition of *Macrobrachium vollenhovenii* across two stations over eight months, revealing moderate female dominance interspersed with periods of parity and male bias. In April, Station 1 recorded 2 males and 8 females (1:4), while Station 2 had no males and 6 females, indicating complete female exclusivity at that station and strong early-season skewness. In May, both stations continued to show female-biased distributions,Station 1 with 3:11 (1:3.7) and Station 2 with 5:12 (1:2.4). June marked the first instance of near parity. Station 1 recorded an equal number of males and females (3:3), while Station 2 showed a moderate female bias (3:7; 1:2.3). July exhibited increased male presence but still retained female dominance. Station 1 had 13 males and 31 females (1:2.4), while Station 2 recorded 14:31 (1:2.2). In August, Station 1 maintained a similar ratio (14:49; 1:3.5), but Station 2 reversed the trend, with 13 males to 7 females (1.9:1), representing the strongest male dominance of the dataset.

In September, both stations again leaned female-biased: Station 1 with 13:38 (1:2.9) and Station 2 with 9:10 (1:1.1), indicating near sex parity at Station 2. November featured mixed trends. Station 1 showed 15 males to 29 females (1:1.9), while Station 2 recorded 7:21 (1:3), sustaining the female-skewed pattern. By December, both stations showed moderate female dominance: Station 1 with 2:12 (1:6) and Station 2 with 5:11 (1:2.2), re-establishing the early-season trend of female predominance. Overall, *M. vollenhovenii* populations across months and stations generally exhibited female-biased sex ratios, particularly in April, May, and December. The strongest female dominance occurred in April at Station 2 (0 males to 6 females), while the most notable male bias appeared in August at Station 2 (1.9:1). The closest approach to sex parity was observed in June at Station 1 (1:1), and in September at Station 2 (1:1.1).

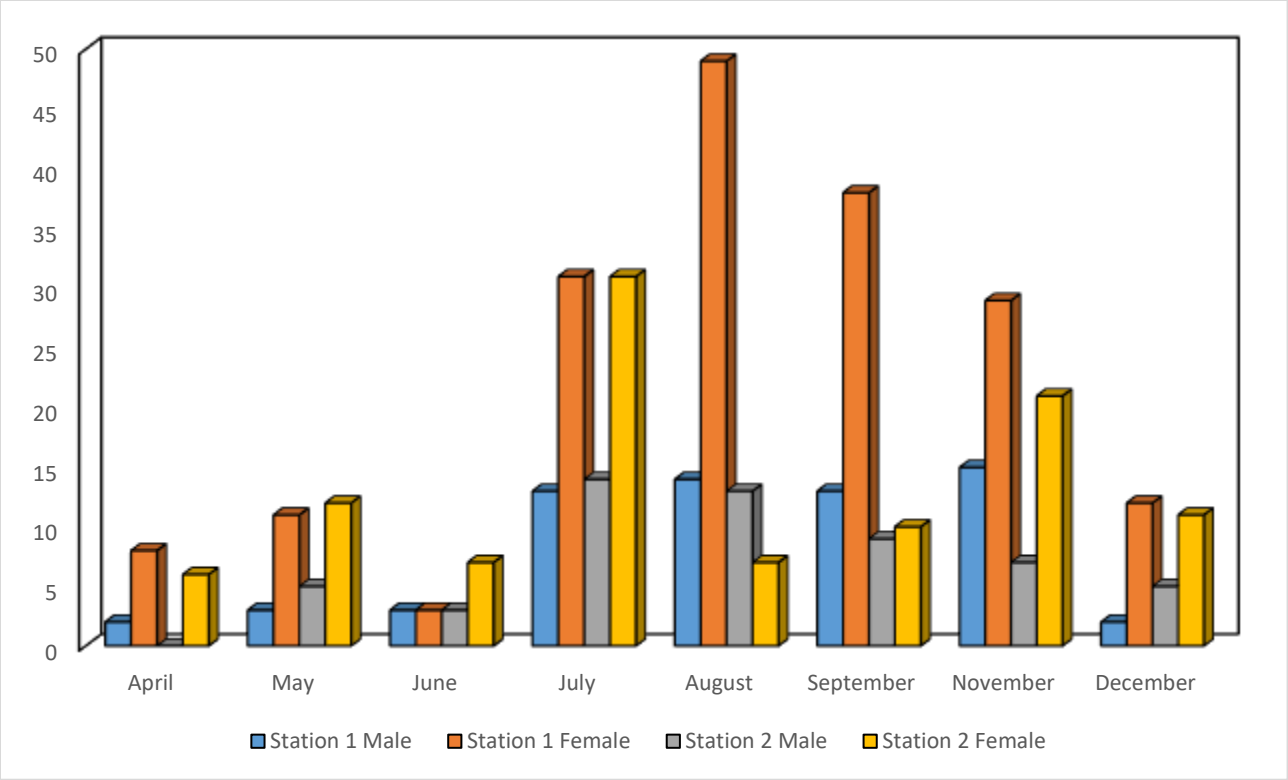

Figure 4.38: Monthly sex distribution of *M. vollenhovenii*

4.6.2. Gonadal Maturity of *Macrobrachium* Species

The pooled monthly distribution of gonadal maturity stages of *Macrobrachium* species across the Ubeji Axis (Figure 4.39) revealed marked temporal and spatial variations between stations. At Station 1, the Virgin and Development stages dominated in April (45% and 34%, respectively), with only minor representation of the Ripe (12%), Ripe Running (4%), and Spent (5%) stages. In contrast, Station 2 was exclusively characterized by 100% Virgin individuals, indicating reproductive immaturity at the onset of the study.

By May, Station 1 exhibited a notable increase in reproductive progression, with 44% of individuals in the Development stage and 23% in the Ripe stage, alongside 19% in the Ripe Running stage. This pattern suggests active gonadal development and readiness for spawning. Conversely, Station 2 remained largely dominated by Virgin prawns (98%), with only a minimal presence of developing individuals (2%), highlighting a delayed reproductive progression relative to Station 1.

In June, Station 1 was dominated by individuals in the Development stage (47%), followed by Virgin (27%) and Ripe (16%) stages, reflecting active gonadal maturation. Station 2 displayed a broader spread across Virgin (43%), Development (22%), Spent (24%), and minor proportions of Ripe and Ripe Running stages (5% each), suggesting asynchronous reproductive activity, including post-spawning individuals.

The distribution in July highlighted further divergence between stations. At Station 1, Virgin prawns (38%) predominated, although advanced stages were also represented, with 16% Ripe and 11% Ripe Running. In contrast, Station 2 was dominated by reproductively mature and post-reproductive individuals, with 31% Ripe, 16% Ripe Running, and 33% Spent, indicating peak spawning activity.

August reflected reproductive advancement at both stations. Station 1 was dominated by Ripe Running (35%) and Spent (30%) individuals, while Station 2 exhibited a more balanced distribution across Ripe (25%), Virgin (24%), Development (21%), and Ripe Running (21%), with fewer Spent individuals (9%). This suggests Station 1 had reached peak spawning, whereas Station 2 remained in active reproductive progression.

By September, both stations displayed a dominance of post-spawning individuals. At Station 1, the Spent stage (38%) was most represented, followed by Development (24%) and Ripe (20%). Similarly, Station 2 was characterized by 36% Spent and 26% Virgin individuals, with the remaining stages distributed more evenly. This shift indicates the onset of a post-reproductive phase across the system.

In November, reproductive activity peaked again. Station 1 showed a dominance of Ripe Running individuals (47%) and a substantial proportion of Spent prawns (26%), with minimal Virgin (10%) and Development (6%) stages. Station 2 mirrored this trend, with high proportions of Ripe Running (35%) and Spent (32%), indicating synchronized reproductive activity across both stations.

By December, contrasting dynamics were observed. Station 1 displayed a relatively even distribution across stages, with Virgin (28%), Spent (25%), Development (22%), Ripe (14%), and Ripe Running (11%), suggesting overlapping cohorts in various stages of reproductive progression. Station 2, however, was dominated by Spent individuals (56%) alongside 29% Virgin, and much lower representation of Ripe (4%) and Development (11%), with Ripe Running absent. This indicates Station 2 had largely transitioned into a post-spawning state, while Station 1 maintained active reproductive heterogeneity.

The pooled analysis of stomach stages across the five *Macrobrachium* species revealed distinct temporal dynamics. The Virgin stage exhibited a gradual increase in frequency from the early months (April–June) towards the later part of the study (September–December), In contrast, the Developing stage showed moderate fluctuations, with a noticeable peak around the mid-year months (July–August). The Mature stage displayed a progressive increase from the onset of the wet season, reaching its highest occurrence during the peak reproductive months, before declining towards the end of the year. Conversely, the Spent stage remained relatively low in frequency overall, but increased slightly in the months following peak maturity, indicating post-spawning individuals within the stock.

4.6.2.1. Gonadal maturity of *Macrobrachium dux*

The monthly distribution of gonadal maturity stages (A–E) of *Macrobrachium dux* at Station 1 and Station 2, revealed distinct spatial and temporal variations (Figure 4.40). At Station 1, virgin (Stage A) and developing (Stage B) stages dominated, with Stage B peaking in April and May (3 each), and Stage A reaching its highest in June (3). Ripe (Stage C) individuals appeared only in December (1), ripe running (Stage D) was recorded solely in November (1), while spent (Stage E) stages occurred in April, August, and September. Station 2 exhibited a strong virgin peak in May (6), ripe running (Stage D) peaked in July (3), and spent (Stage E) peaked in December (3). Notably, September showed the broadest maturity spectrum (A–E) at Station 2, indicating the highest gonadal diversity. Based on the total number of gonadal occurrences across stages and months, the monthly reproductive activity followed the order: September > December > April > May > July > November > June > August. Overall, the stage frequency across all months and stations followed the order: A > B > E > D > C, highlighting a reproductive pattern skewed toward early gonadal development and intermittent spawning events later in the year.

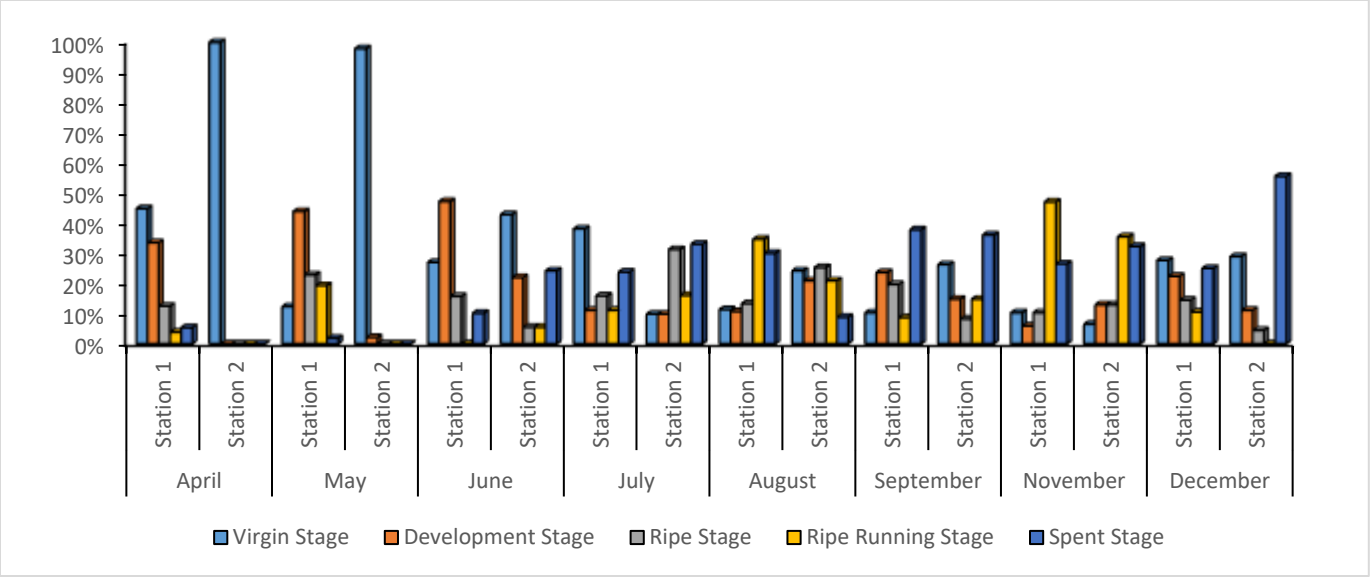

Figure 4.39: Monthly distribution of gonadal maturity stages of *Macrobrachium* Species

4.6.2.2. Gonadal maturity of *Macrobrachium equidens*

The monthly distribution of gonadal maturity stages (A–E) of *Macrobrachium equidens* at Station 1 and Station 2, reflects clear spatial and temporal patterns (Figure 4.41). At Station 1, virgin individuals (Stage A) dominated in April and May, with the highest occurrence recorded in May (12). Developing stages (Stage B) were frequent in April (5) and June (4), while ripe individuals (Stage C) were consistently low (1–2) across all months. Ripe running stages (Stage D) peaked in August and November (4 each), and spent stages (Stage E) were more pronounced in August (4) and December (3). In contrast, Station 2 showed a strong virgin peak in May (15) and April (11), with no ripe or running stages observed in those months. Developing and ripe stages appeared more in August, while spent individuals peaked in September (4) and December (4). The broadest maturity spread at Station 2 occurred in August and September, featuring multiple maturity stages, particularly Stages B, D, and E. Summing all stage frequencies across months, the order of reproductive activity by month was: August > April > May > September > December > June > July > November. Overall, the frequency of stages followed the order: A > B > E > C > D, indicating dominance of early reproductive phases with scattered ripening and spawning events throughout the year.

4.6.2.3. Gonadal maturity of *Macrobrachium macrobrachion*

The monthly distribution of gonadal maturity stages (A–E) of *Macrobrachium macrobrachion* at Station 1 and Station 2, highlights distinct reproductive dynamics across time and space (Figure 4.42). At Station 1, virgin individuals (Stage A) were highest in April (74) and May (37), with a substantial drop in subsequent months. Developing stages (Stage B) peaked in June (27), while ripe stages (Stage C) and ripe running stages (Stage D) reached notable counts in June and

December (10 each). Spent individuals (Stage E) appeared most in August (8). In Station 2, virgin individuals (Stage A) overwhelmingly peaked in April (125) and May (89), followed by a sharp decline from June onwards. Developing and ripe stages were most evident in June (B: 15; C: 2) and August (B: 4; C: 8), while ripe running stages (Stage D) showed distinct peaks in August and September (12 each). Spent stages (Stage E) showed consistent representation, particularly in June and December (11 and 12, respectively). Overall monthly reproductive activity across both stations followed the order: April > May > June > August > December > July > September > November. The frequency of maturity stages summed across all months ranked as: A > B > C > D > E, indicating a dominance of early maturity stages and highlighting seasonal progression toward ripening and spawning phases later in the year.

4.6.2.4. Gonadal maturity of *Macrobrachium rosenbergii*

The monthly gonadal maturity stages (A–E) of *Macrobrachium rosenbergii* across Station 1 and Station 2, reveas spatial and temporal reproductive variation (Figure 4.43). At Station 1, virgin individuals (Stage A) peaked in May (6), while developing stages (Stage B) were highest in June (10). Ripe stages (Stage C) were observed sporadically across months, with low counts (maximum of 3 in September). Ripe running stages (Stage D) reached their highest in August (8), while spent stages (Stage E) showed moderate activity in December (6) and September (6). In contrast, Station 2 exhibited a pronounced virgin peak in April (18) and May (22), followed by fewer individuals in later months. Developing and ripe stages (B and C) were most represented in August and July, respectively, while ripe running (Stage D) and spent (Stage E) stages showed more variation across July to November. The overall monthly reproductive activity across both stations ranked: May > April > June > August > December > July > September > November. Summing frequencies across all months, the general order of maturity stages was: A > B > D > E > C.

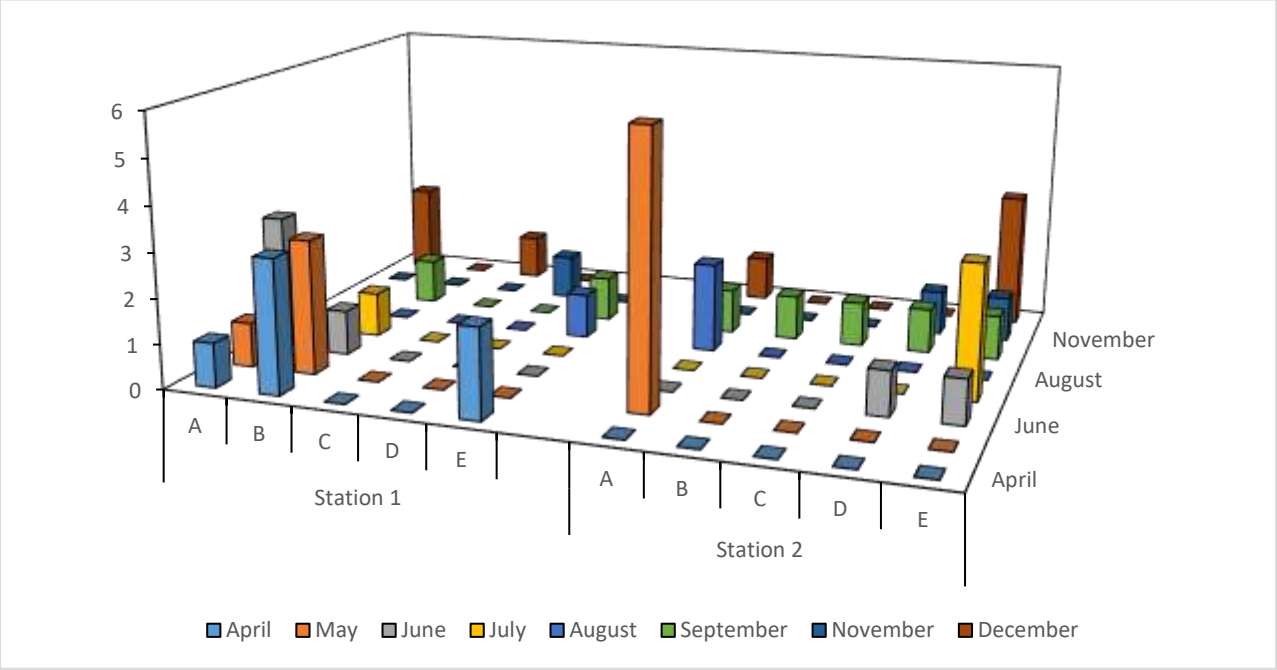

Figure 4.40: Spatio-temporal distribution of Gonadal maturity of *M. dux* for the Ubeji Axis, Warri River

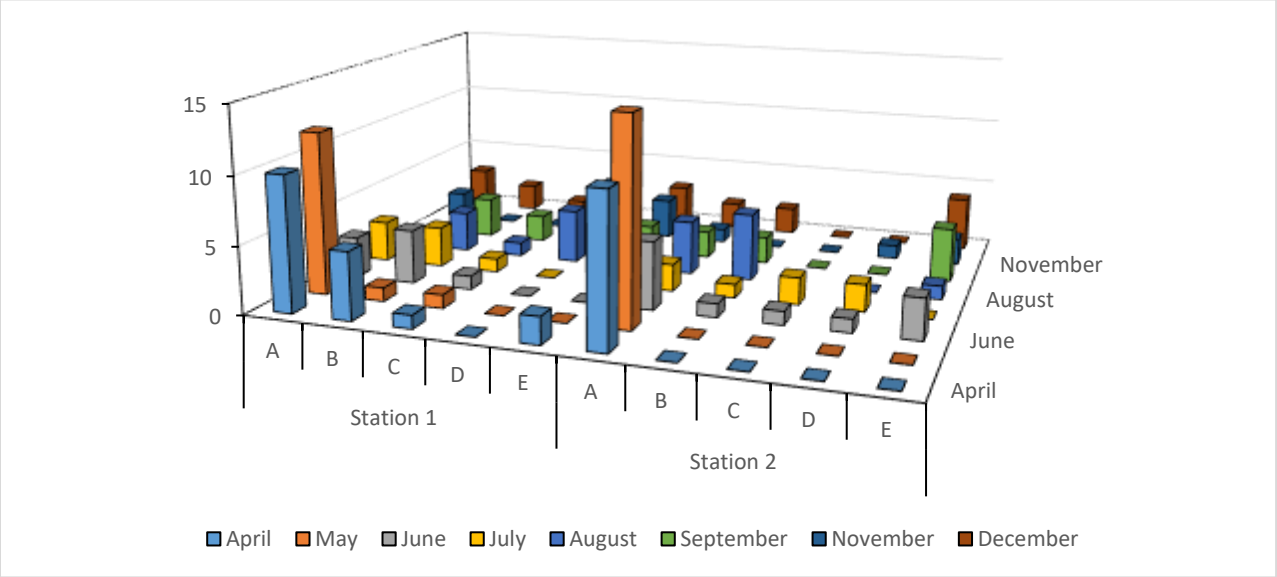

Figure 4.41: Spatio-temporal distribution of Gonadal maturity of *M. equidens for* the Ubeji Axis, Warri River

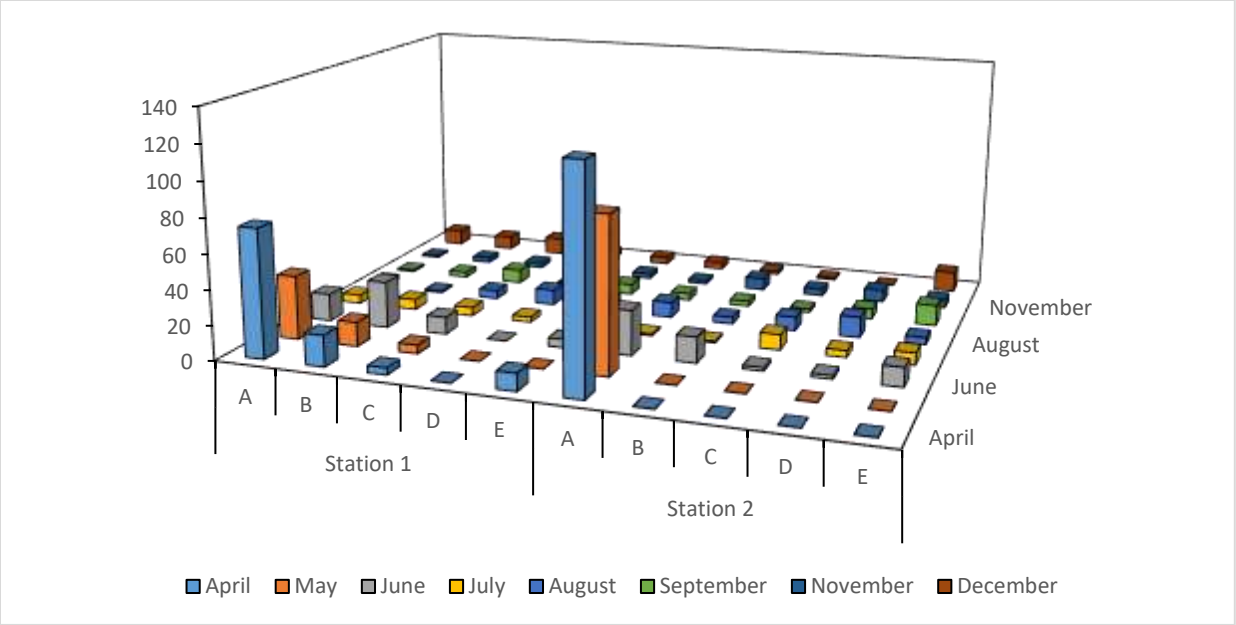

Figure 4.42: Spatio-temporal distribution of Gonadal maturity of *M. macrobrachion* for the Ubeji Axis, Warri River

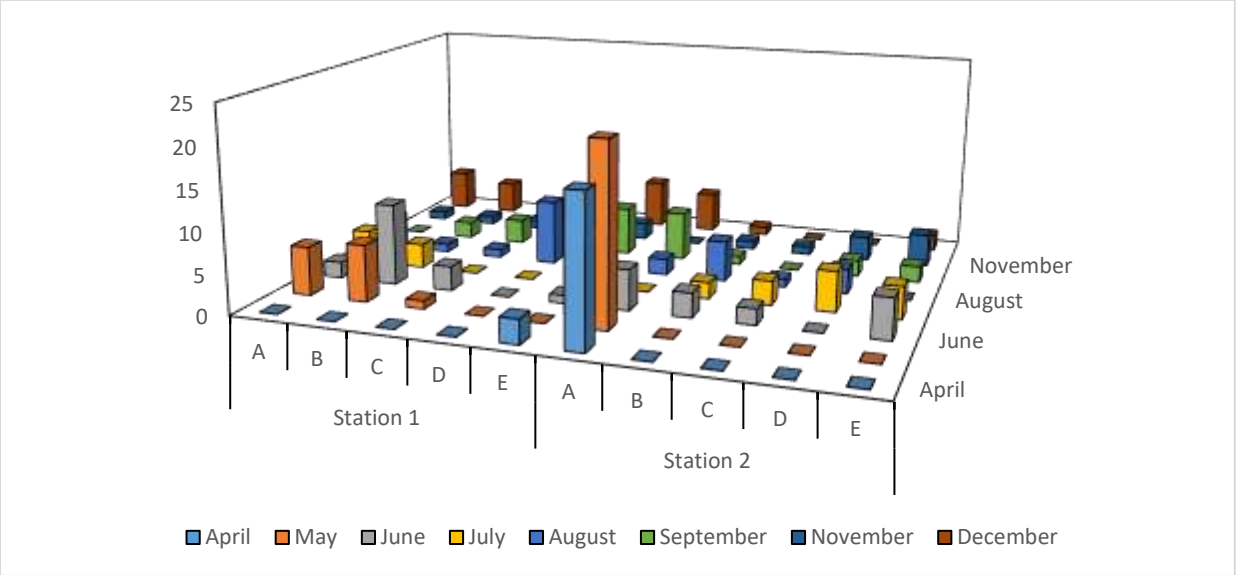

Figure 4.43: Spatio-temporal distribution of Gonadal maturity of *M. rosenbergii* for the Ubeji Axis, Warri River

4.6.2.5. Gonadal maturity of *Macrobrachium vollenhovenii*

The monthly distribution of gonadal maturity stages in *Macrobrachium vollenhovenii* across Station 1 and Station 2, shows marked spatial and temporal variations (Figure 4.44). At Station 1, the highest abundance of virgin individuals (Stage A) occurred in July (12), followed by September (7) and May (5), while no virgin prawns were observed in April, June, or August. Developing stages (Stage B) peaked in September (4), whereas ripe individuals (Stage C)

mostly in July and September (4 and 5, respectively). The ripe running stage (Stage D) was most prominent in November (13), while the spent stage (Stage E) had its maximum in August (16). Station 2 showed a dominant virgin peak in May (12) and April (6), with the highest ripe (Stage C) and ripe running (Stage D) individuals occurring in July (7 and 6, respectively). Notably, the spent stage (Stage E) peaked strongly in July (14). Across months, Station 1 recorded the most reproductive activity in July > September > November > May > December, while Station 2 peaked in July > May > September > November > April. The cumulative reproductive stage ranking across both stations followed: A > E > D > C > B, highlighting the dominance of virgin and post-spawning stages, with moderate presence of fully mature individuals, and relatively fewer developing prawns.

4.6.3. Gonadosomatic Index (GSI)

The pooled Gonadosomatic Index (GSI) of prawns exhibited distinct temporal variations across the study period, reflecting fluctuations in reproductive activity (Figure 4.45). At Station 1, GSI values were consistently low in April and May (0.07 each), but increased sharply to a peak of 0.20 in June, indicating the onset of gonadal development. This was followed by a moderate decline in July (0.12), a subsequent rise in August (0.17), and a pronounced dip in September (0.06). A secondary peak was observed in November (0.18) before the index declined again in December (0.09). At Station 2, GSI was absent in April and May (0.00) but increased in June (0.13) and July (0.14), reaching parity with Station 1 in August (0.17). Thereafter, the values showed a slight decline in September (0.07) and a more marked increase in November (0.14), before dropping completely to 0.00 in December.

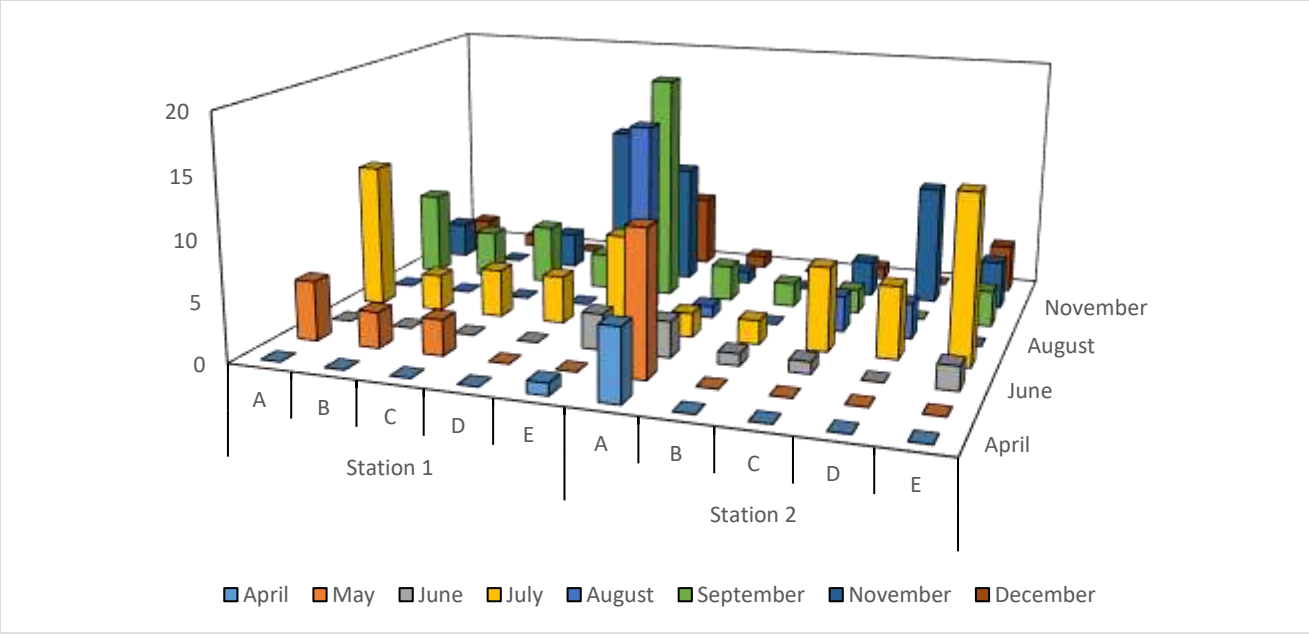

Figure 4.44: Spatio-temporal distribution of Gonadal maturity of *M. vollenhovenii* for the Ubeji Axis, Warri River

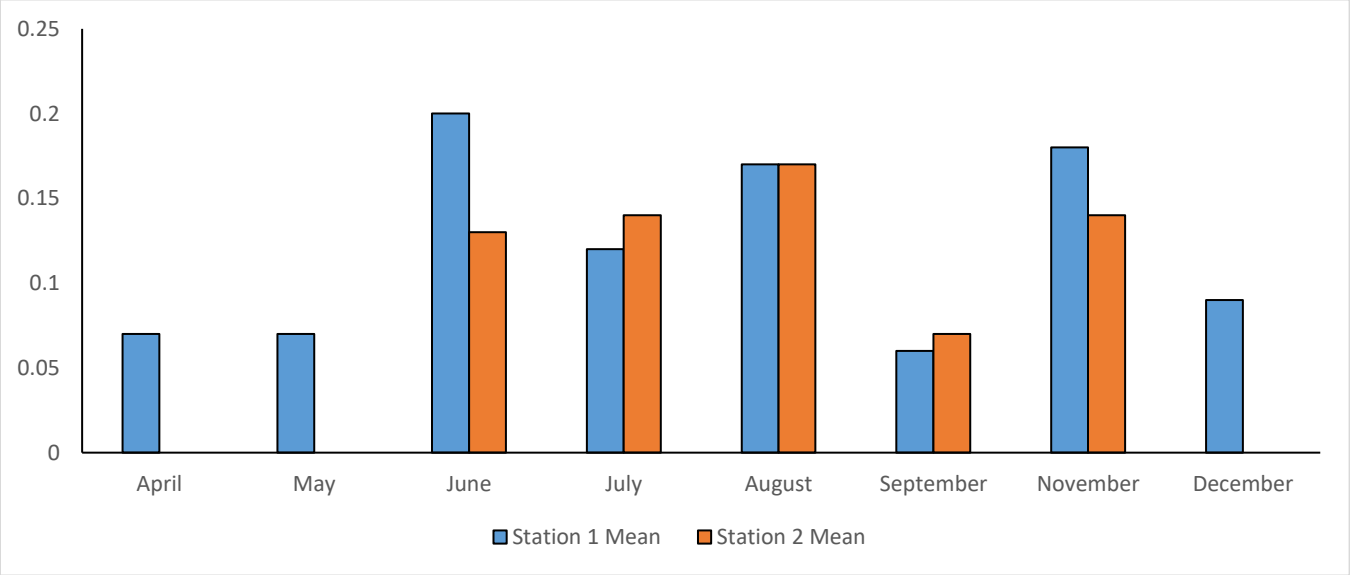

Figure 4.45: Pooled Gonadosomatic Index (GSI) of *Macrobrachium* Species

4.6.3.1. Spatio-temporal mean GSI for *M. dux* for the Ubeji Axis, Warri River

The spatio-temporal mean Gonadosomatic Index (GSI) values for *Macrobrachium dux* along the Ubeji Axis of the Warri River is shown in Figure 4.46. At Station 1, GSI values were generally low or absent, with a mean of 0.12 recorded in April from six individuals, but no individuals or GSI activity was recorded in May. June exhibited a decrease in mean GSI to 0.04 from four individuals, followed by near-zero values in July and August despite some individuals being sampled. September and December also showed no gonadal development with mean GSI values at zero, except November where a relatively high mean GSI of 0.43 was observed, though based on only one individual.

At Station 2, gonadal activity was absent in April and May, with no individuals recorded in April and zero mean GSI in May. In June, a small sample of two individuals exhibited a high mean GSI of 0.66, indicating notable reproductive activity. This was followed by a return to zero mean GSI in July and August despite the presence of individuals, September and November showed moderate mean GSI values of 0.14 and 0.22 respectively, reflecting some ongoing gonadal development. No individuals were recorded in December at Station 2. Ranking the mean GSI values across stations and months, the order of reproductive activity is: June (Station 2: 0.66) > November (Station 1: 0.43) > November (Station 2: 0.22) > September (Station 2: 0.14) > April (Station 1: 0.12) > June (Station 1: 0.04) > other months with zero mean GSI.

4.6.3.2. Spatio-temporal mean GSI for *M. equidens* for the Ubeji Axis, Warri River

The spatio-temporal mean Gonadosomatic Index (GSI) values for *Macrobrachium equidens* is shown in Figure 4.47. At Station 1, mean GSI values were generally low to moderate, with 0.08 recorded in April, followed by a decrease to 0.03 in May. A peak was observed in June with a

mean GSI of 0.20. July, August, September, and December showed no gonadal activity. November showed a notable increase with a mean GSI of 0.24.

At Station 2, gonadal activity was absent in April and May due to zero individuals sampled. In June, a peak mean GSI of 0.21 was recorded, closely matching Station 1. July showed sustained gonadal activity with a mean GSI of 0.22, while August had a lower mean GSI of 0.04. September showed no gonadal activity while November recorded a moderate mean GSI of 0.17. No individuals were sampled in December. Ranking mean GSI values across stations and months, the order is: November (Station 1: 0.24) > July (Station 2: 0.22) ≈ June (Station 2: 0.21) ≈ June (Station 1: 0.20) > November (Station 2: 0.17) > April (Station 1: 0.08) > May (Station 1: 0.03) > August (Station 2: 0.04) > months with zero mean GSI.

4.6.3.3. Spatio-temporal mean GSI for *M. macrobrachion* for the Ubeji Axis, Warri River

The spatio-temporal mean Gonadosomatic Index (GSI) values for *Macrobrachium macrobrachion* is presented in Figure 4.48. At Station 1, mean GSI values were consistently moderate to high throughout the sampling period, with April and May recording 0.07 and 0.09 respectively. Peaks in reproductive activity were observed in June and July, both showing mean GSI values of 0.22. August and September showed slightly lower but still notable mean GSIs of 0.15 and 0.23. November and December recorded mean GSIs of 0.17 and 0.12 respectively, indicating sustained reproductive activity into the late season. At Station 2, no individuals were recorded in April and May. Reproductive activity began in June with a mean GSI of 0.10, which was maintained in July at the same level (0.10). August showed a marked increase with a peak mean GSI of 0.23. This was followed by moderate values in September (0.11) and November (0.14). No individuals were recorded in December at Station 2. Overall, *M. macrobrachion* displayed sustained and relatively strong reproductive activity across both

stations, with Station 1 generally exhibiting higher mean GSI values and larger sample sizes. Ranking mean GSI values across stations and months, the order of reproductive activity is: September (Station 1: 0.23) ≈ August (Station 2: 0.23) ≈ June (Station 1: 0.22) ≈ July (Station 1: 0.22) > November (Station 1: 0.17) > August (Station 1: 0.15) > November (Station 2: 0.14) > September (Station 2: 0.11) ≈ June (Station 2: 0.10) ≈ July (Station 2: 0.10) > December (Station 1: 0.12) > May (Station 1: 0.09) > April (Station 1: 0.07) > months with zero mean GSI.

4.6.3.4. Spatio-temporal mean GSI for *M. rosenbergii* for the Ubeji Axis, Warri River

The spatio-temporal mean Gonadosomatic Index (GSI) values for *Macrobrachium rosenbergii* is shown in Figure 4.49. At Station 1, mean GSI values were generally low throughout the study period, starting with 0.06 in April dropping to 0.02 in May. A peak was observed in June with a mean GSI of 0.16. From July to September, mean GSI values were zero. Reproductive activity resumed moderately in November (0.12) and declined slightly in December (0.08).

At Station 2, no individuals were recorded in April and May. Gonadal activity peaked in July with a mean GSI of 0.18, followed by a decline to 0.11 in August and 0.07 in September. Moderate gonadal development was also observed in June (0.13) and November (0.11). No individuals were recorded in December. Overall, *M. rosenbergii* exhibited distinct reproductive peaks at both stations, with Station 2 showing a higher and more sustained gonadal activity in mid-year months compared to Station 1. Ranking mean GSI values across stations and months, reproductive activity follows the order: July (Station 2: 0.18) > June (Station 1: 0.16) > June (Station 2: 0.13) ≈ November (Station 1: 0.12) ≈ November (Station 2: 0.11) > August (Station 2: 0.11) > December (Station 1: 0.08) > September (Station 2: 0.07) > April (Station 1: 0.06) > May (Station 1: 0.02) > months with zero mean GSI.

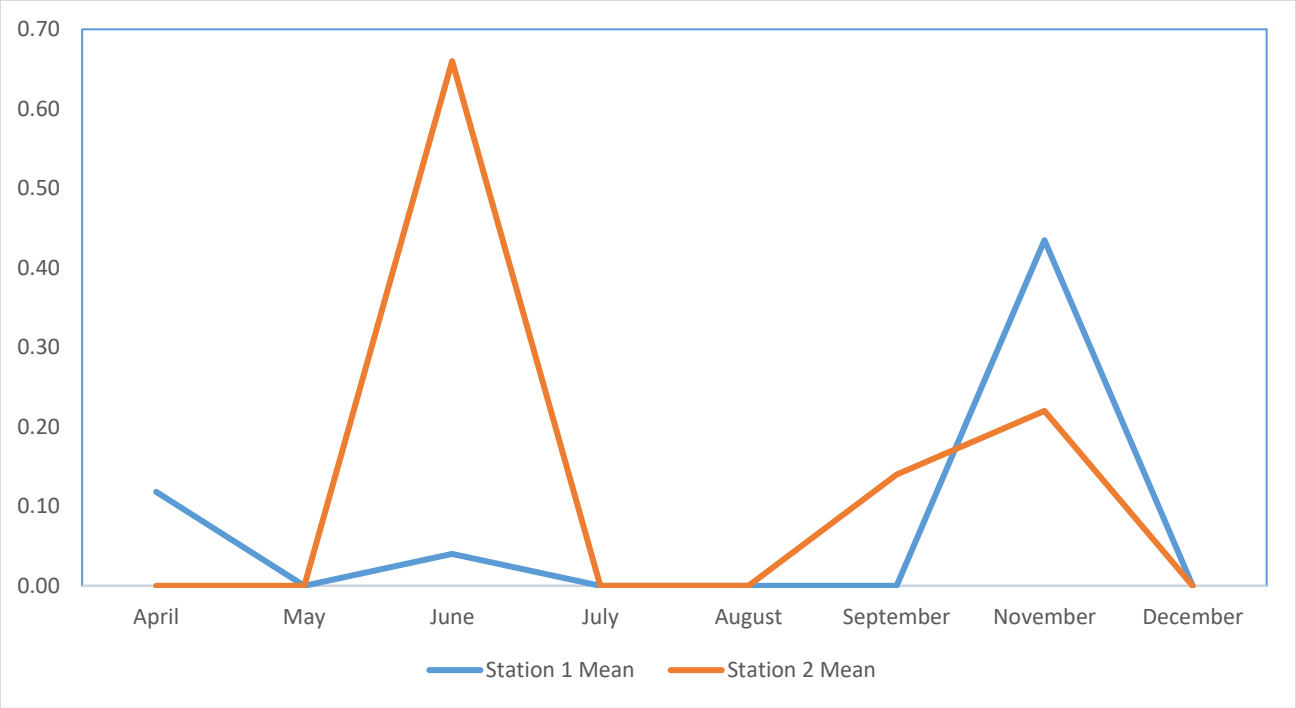

Figure 4.46: Spatio-temporal Mean GSI of *M. dux* for the Ubeji Axis, Warri River

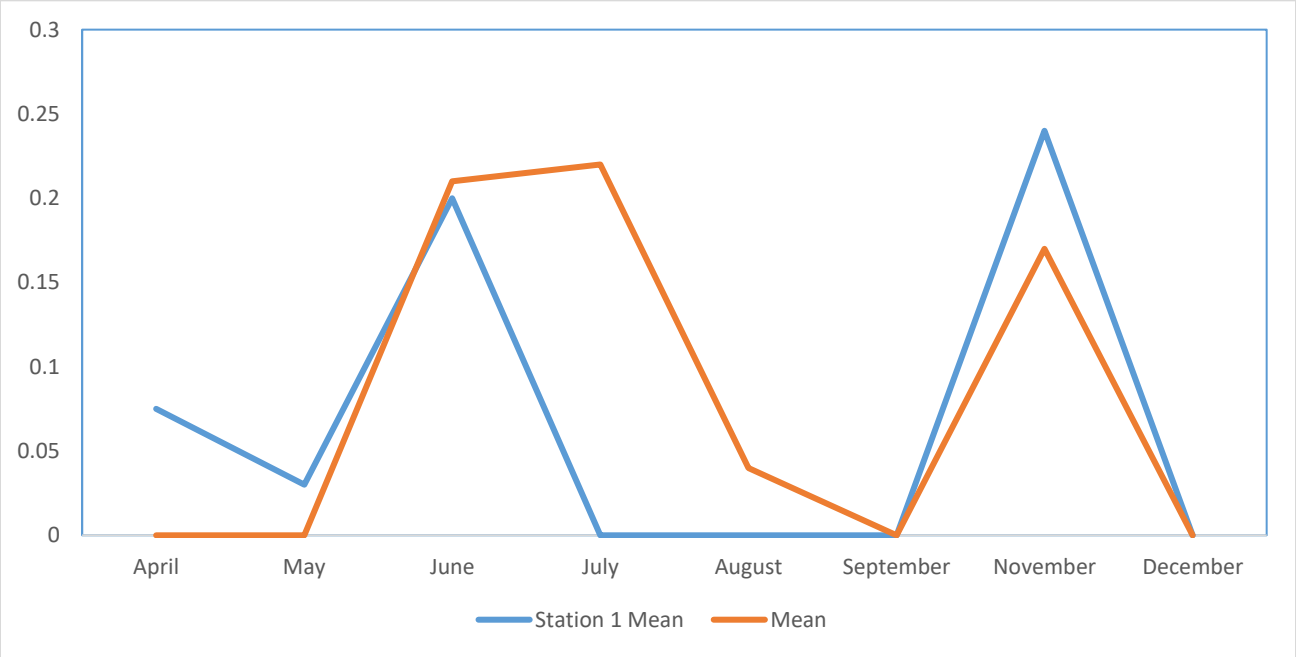

Figure 4.47: Spatio-temporal Mean GSI of *M. equidens* for the Ubeji Axis, Warri River

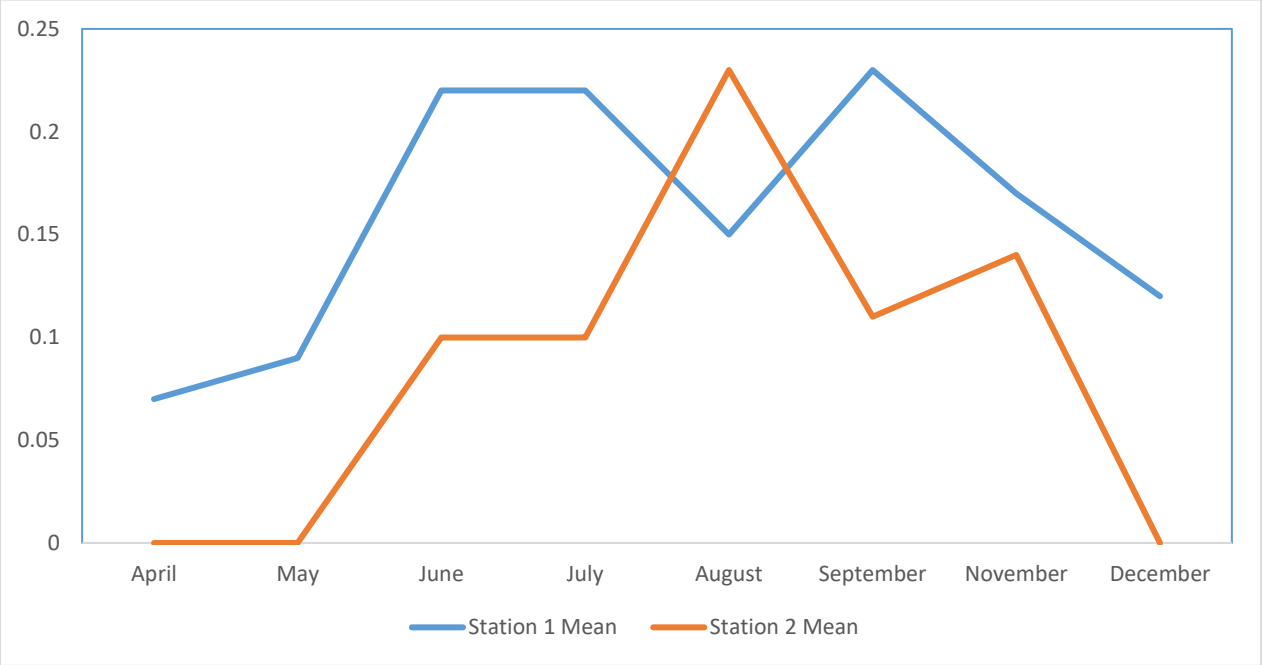

Figure 4.48: Spatio-temporal Mean GSI of *M. macrobrachion* for the Ubeji Axis, Warri River

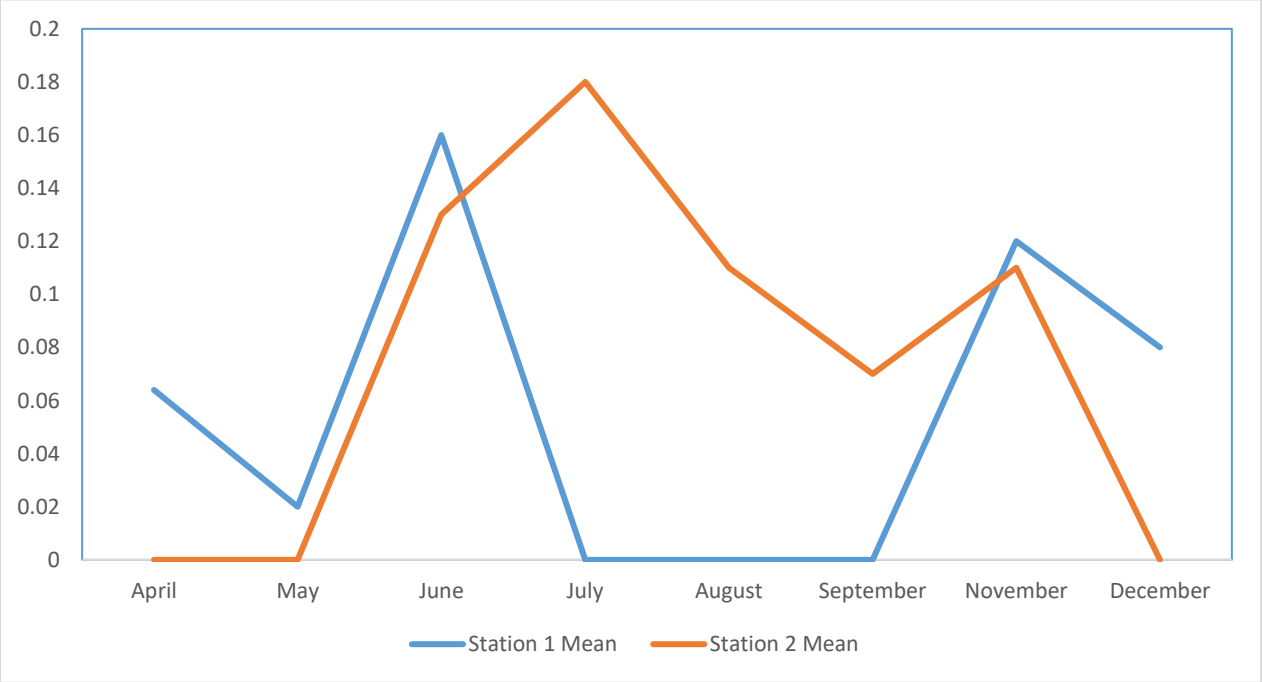

Figure 4.49: Spatio-temporal Mean GSI of *M. rosenbergii* for the Ubeji Axis, Warri River

4.6.3.5. Spatio-temporal mean GSI for *M. vollenhovenii* for the Ubeji Axis, Warri River

Figure 4.50 presents the spatio-temporal mean Gonadosomatic Index (GSI) values for *Macrobrachium vollenhovenii* along the Ubeji Axis of the Warri River, revealing variable reproductive patterns between stations and across months. At Station 1, mean GSI values were generally low in April (0.03) and May (0.05). A notable peak occurred in June with a mean GSI of 0.29, followed by moderately high values in July (0.12) and August (0.15). September saw a sharp decline to 0.05. Reproductive activity rose again in November with a mean GSI of 0.18, then declined to 0.10 in December.

At Station 2, no individuals were recorded in April and May. June showed a moderate mean GSI of 0.11. Reproductive activity increased in July and August, both months showing a mean GSI of 0.16. In September, gonadal activity dropped to zero. November maintained a relatively high mean GSI of 0.15, with no individuals recorded in December.

Overall, *M. vollenhovenii* exhibited two main reproductive peaks at both stations: a strong early peak in June at Station 1 and a sustained peak from July to August at both stations, followed by a secondary peak in November. Ranking mean GSI values across stations and months: June (Station 1: 0.29) > July (Station 2: 0.16) = August (Station 2: 0.16) > August (Station 1: 0.15) = November (Station 2: 0.15) > November (Station 1: 0.18) > July (Station 1: 0.12) > December (Station 1: 0.10) > June (Station 2: 0.11) > May (Station 1: 0.05) > September (Station 1: 0.05) > months with zero mean GSI.

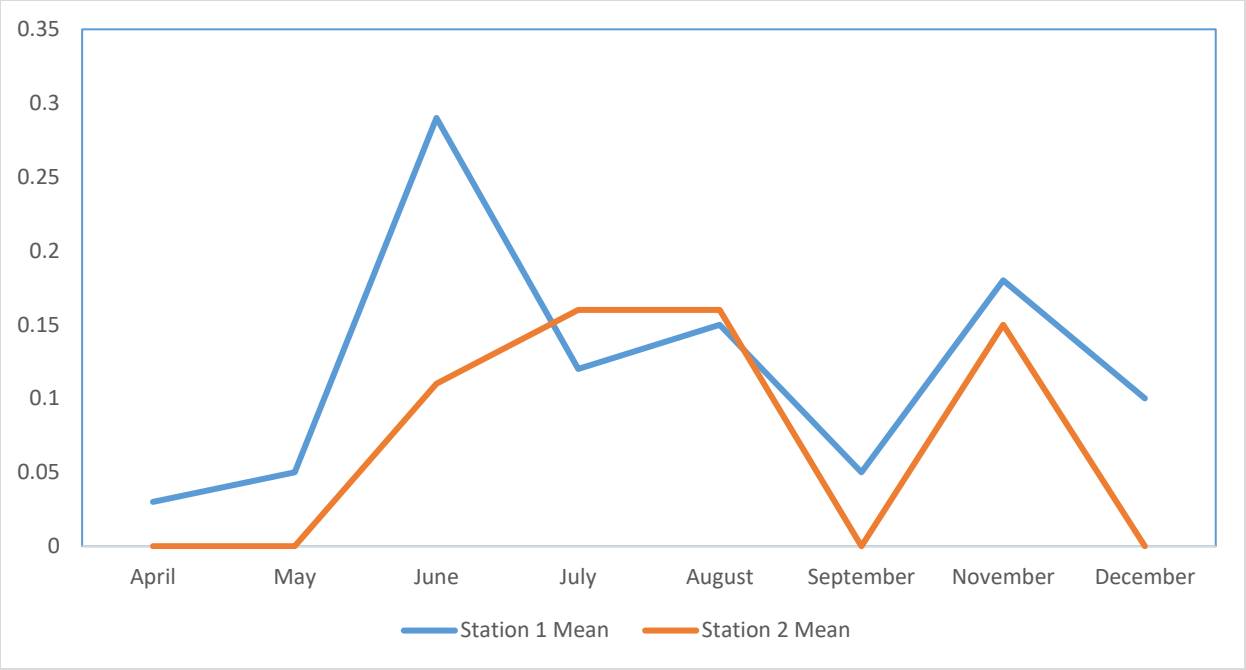

Figure 4.50: Spatio-temporal Mean GSI of *M. vollenhovenii* for the Ubeji Axis, Warri River

4.7 Feeding Intensity

4.7.1. Stomach Fullness

4.7.1.1. Stomach Fullness of *M. dux*

Figure 4.51 presents the monthly Stomach Fullness distribution of *Macrobrachium dux* across Stations 1 and 2, illustrating notable spatio-temporal variations in feeding intensity. At Station 1, no individuals displayed stomach fullness beyond 1/2 for most months, with low activity recorded in April (5 individuals with 1/4, 2 with 1/2), May (4 individuals with 1/4), and July through November showing a similar pattern dominated by trace contents (1/4). A distinct increase in feeding was observed in December, where 1 individual was empty, 3 had 1/4, 1 had 1/2, and 2 had 3/4 stomach fullness, marking the only occurrence of nearly full stomachs at this station.

At Station 2, feeding activity was not reported in April. From May through December, feeding increased modestly with the most active months being September (5 individuals with 1/4, 1 with 1/2) and December (4 individuals with 1/4, 2 with 1/2). While high stomach fullness scores (3/4 and 1) were rare, July and August each recorded one individual with 3/4 stomach fullness.

Overall, feeding intensity remained generally low at both stations, with a slight peak in December at Station 1 and September–December at Station 2. Outliers include the complete absence of feeding in April at Station 2 and the presence of higher Stomach Fullness (3/4) only in July and December, particularly at Station 1. Ranking stomach fullness activity across months (descending order) is Station 1: December > April = June > May = July = August = September = November while Station 2: September > December > May = November > July = August > June > April

4.7.1.2 Stomach Fullness of *M. equidens*

Figure 4.52 presents the monthly distribution of Stomach Fullness for *Macrobrachium equidens* across Stations 1 and 2. At Station 1, feeding activity was most pronounced in April, where 8 individuals were completely empty, but another 12 showed partial feeding, including 4 with 1/4 and 8 with 1/2 stomach fullness. May, June, August, and September maintained relatively high levels of 1/4 and 1/2 scores, with July and September showing slightly elevated activity through the presence of 1 individual each with 3/4 fullness. In contrast, November showed a shift towards empty stomachs (8 individuals), suggesting reduced feeding, while December recorded a mild feeding signal with a majority in the 1/4–1/2 range. At Station 2, the strongest feeding signals occurred in May (12 individuals with empty stomachs, but 10 showing partial feeding), June, August, and September, all characterized by consistent representation in the 1/4 and 1/2 categories. November stood out with the only instance of a 3/4 Stomach Fullness at this station, while December was the only month with a fully fed individual (score of 1), albeit alongside generally moderate activity. Overall, *M. equidens* displayed a consistent pattern of feeding dominated by 1/4 and 1/2 stomach fullness scores across both stations, with few occurrences of higher scores (3/4 and 1). April at Station 1 was notable for the high number of empty stomachs, contrasting with a broader moderate feeding range from May to September. Ranking of feeding activity across months is Station 1: May = August = September > July > June > April > December > November; Station 2: May > September = August = June > July > November > December > April.

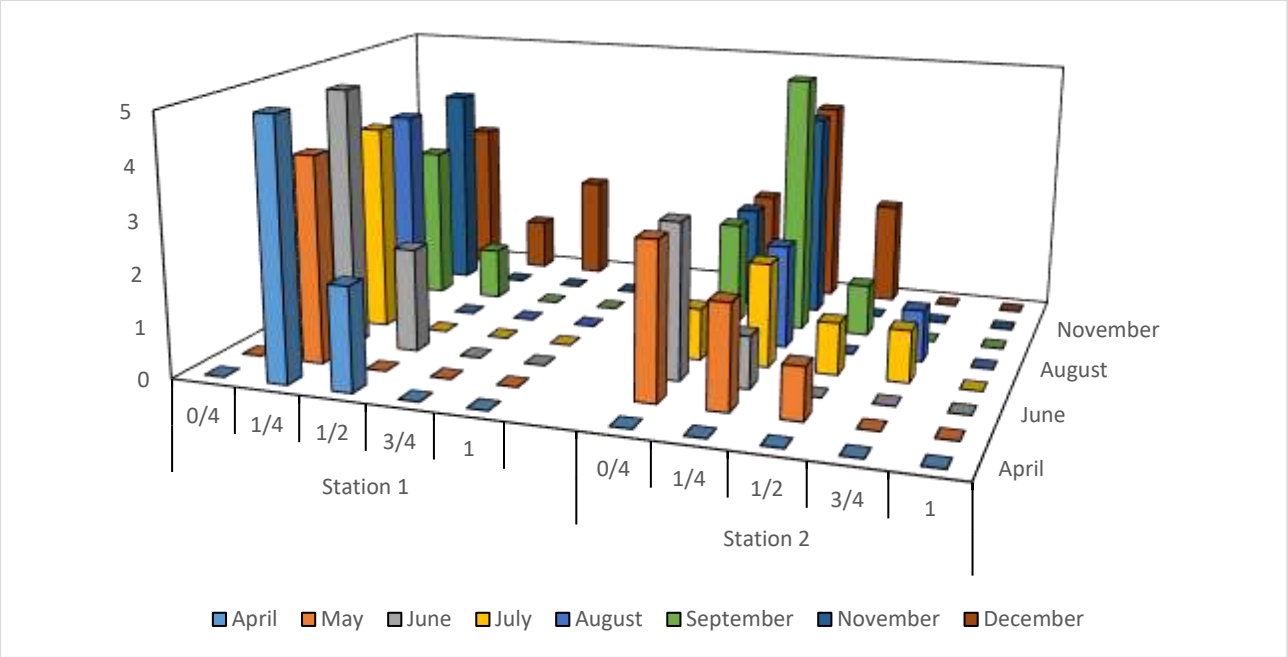

Figure 4.51: Spatio-temporal Stomach Fullness Distribution of *M. dux*

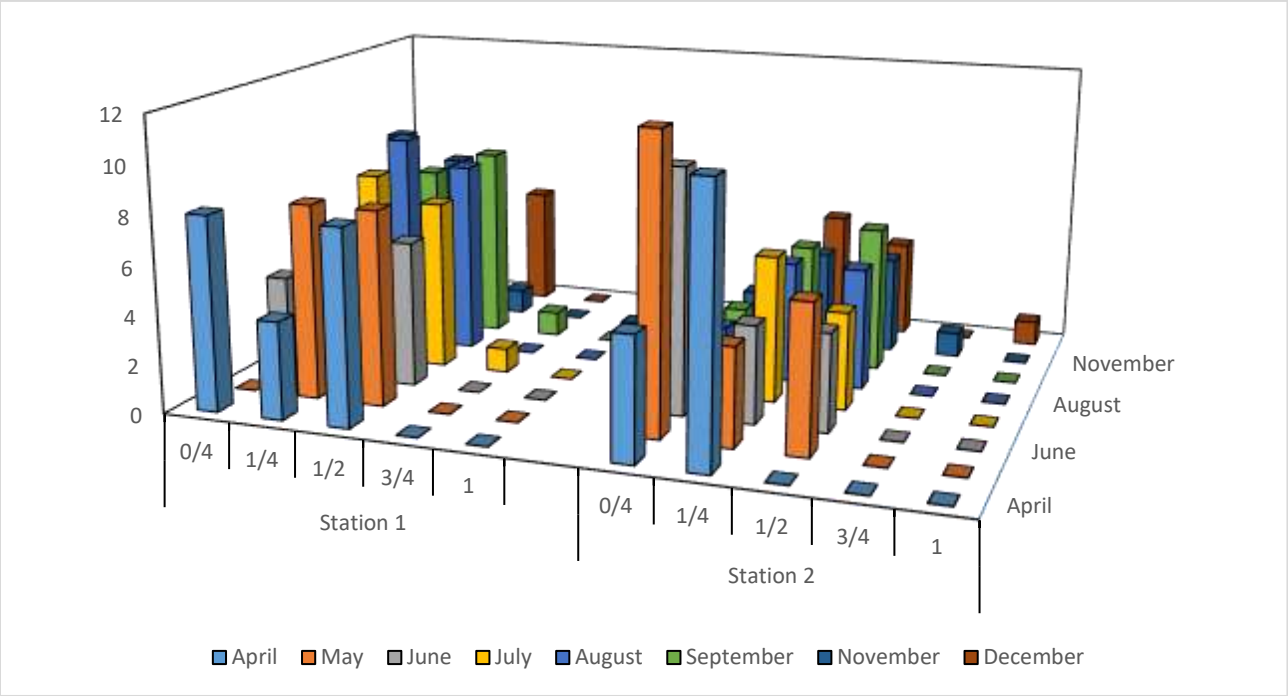

Figure 4.52: Spatio-temporal Stomach Fullness Distribution of *M. equidens*

4.7.1.3. Stomach Fullness of *M. macrobrachion*

Figure 4.53 presents the spatio-temporal Stomach Fullness distribution of *Macrobrachium macrobrachion* along the Ubeji Axis of the Warri River. At Station 1, feeding intensity was highest in April, characterized by a substantial number of individuals with advanced stomach fullness: 34 had 3/4 fullness, 12 had 1/2, and 23 had 1/4, while 41 were empty. Feeding remained moderate in May and June, with the presence of individuals in all Stomach Fullness categories, including two individuals with full stomachs (score of 1) in May. July to December reflected a tapering trend, although some high scores persisted, such as 8–10 individuals with 3/4 stomachs in July and November. Notably, individuals with full stomachs (score of 1) were recorded in May, July, August, September, and November, though in low numbers (1–2 individuals). At Station 2, feeding activity was also highest in April, but with a more extreme skew toward empty stomachs (95 individuals), suggesting post-feeding or migratory behaviour. From May to December, a broader spread of stomach fullness categories was recorded. The months of May, June, and September showed relatively balanced distributions, with moderate numbers across 1/4, 1/2, and 3/4 scores. Full stomachs (score of 1) were rare but increased slightly in September (2 individuals), November (1 individual), and December (5 individuals),the latter being the highest full stomach occurrence at this station. Overall, both stations exhibited high feeding activity in April, a moderate feeding regime from May through September, and a slight resurgence in higher fullness levels by December. Outliers included the very high number of empty individuals in April at Station 2 and the relatively consistent but low presence of fully fed individuals throughout the sampling period. Ranking feeding intensity across months: Station 1: April > June = May > December = November > August = September = July; Station 2: May > June > September > December > November > August > July > April.

4.7.1.4. Stomach Fullness of *M. rosenbergii*

The monthly Stomach Fullness distribution of *Macrobrachium rosenbergii* across Stations 1 and 2 along the Ubeji Axis of the Warri River is presented in Figure 4.54. At Station 1, feeding activity was highest in April, with a total of 40 individuals displaying non-empty stomachs, including 20 with 1/4 fullness, 10 with 1/2, 8 with 3/4, and 2 fully fed. This month marked the peak of feeding intensity. In May and June, moderate activity persisted with 20 and 23 individuals, respectively, exhibiting stomachs between 1/4 and 3/4 fullness, although the number of fully fed individuals remained low,none in May and only one in June. From July to December, feeding levels remained moderate, with slight fluctuations. December recorded 17 individuals with non-empty stomachs but no full stomachs, suggesting a decline in peak feeding intensity toward the end of the year. Notably, full stomachs (score of 1) appeared only in April and June. At Station 2, April also showed feeding activity but at a lower intensity compared to Station 1, with 6 individuals each at 1/4 and 1/2 stomach fullness, and no individuals reaching 3/4 or full capacity. May and June recorded increased feeding, with 17 and 23 individuals respectively showing scores between 1/4 and 3/4. June was the most active feeding month at Station 2, with 4 individuals attaining 3/4 stomach fullness. Feeding remained moderate in July and August but showed improvement in September and November, where 2 and 1 individuals, respectively, reached full stomach capacity, the only months with full stomachs recorded at this station. December recorded 12 individuals with non-empty stomachs, including one fully fed, indicating a mild increase in feeding activity toward the year's end. Ranking monthly feeding intensity in descending order reveals the following trend: Station 1: April > June > May = August = December = November = July = September; Station 2: June = September = November > May = July = December = August > April.

4.7.1.4. Stomach Fullness of *M. vollenhovenii*

The monthly Stomach Fullness distribution of *Macrobrachium vollenhovenii* is presented in Figure 4.55. At Station 1, feeding activity was lowest in April and May, with only 8 and 14 individuals respectively showing non-empty stomachs. No fully fed individuals (score of 1) were recorded throughout the year. Feeding activity increased slightly in June, with 5 individuals showing varying stomach fullness, but a marked rise occurred in July, where 47 individuals had non-empty stomachs, including 10 with 3/4 fullness. August and September maintained high feeding activity, with 63 and 59 individuals, respectively, showing non-empty stomachs. These months represented the peak feeding period for Station 1, with a dominance of moderate to high Stomach Fullness (1/2 and 3/4). November saw a slight decline with 44 individuals across 1/4 to 3/4 scores, while December marked the lowest post-peak feeding intensity, with only 14 individuals showing some degree of stomach fullness. Station 2 displayed negligible feeding in April, as all 6 individuals recorded had empty stomachs. From May through September, feeding activity steadily improved. In May, 8 individuals had non-empty stomachs, including 3 with 3/4 fullness. July recorded 45 individuals with non-empty stomachs, including 8 at 3/4 fullness. August and September maintained similar trends with 20 and 20 individuals respectively showing partial stomach fullness, although only September recorded fully fed individuals (2). November sustained feeding activity with 23 individuals having non-empty stomachs, and December showed moderate feeding with 11 individuals, including one fully fed prawn. Ranking monthly feeding intensity across both stations using observed non-empty stomach totals and presence of higher fullness scores: Station 1: August > September > July > November > May = June > December > April; Station 2: July > September > November > May = August > December > June > April.

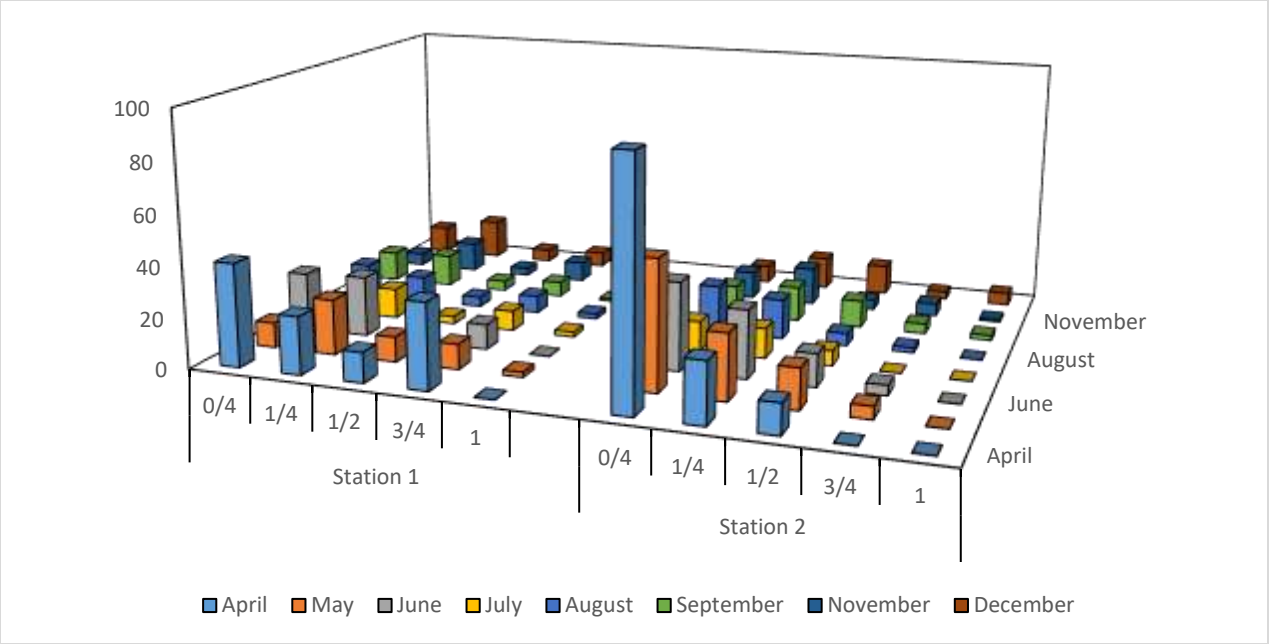

Figure 4.53: Spatio-temporal Stomach Fullness Distribution of *M. macrobrachion*

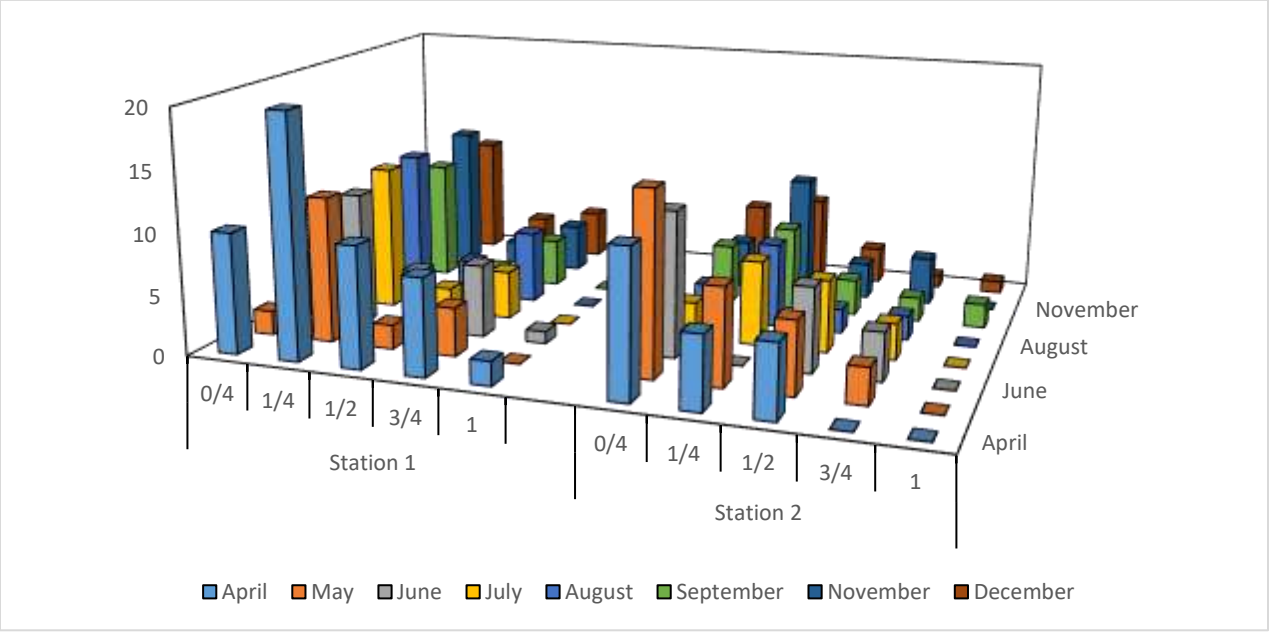

Figure 4.54: Spatio-temporal Stomach Fullness Distribution of *M. rosenbergii*

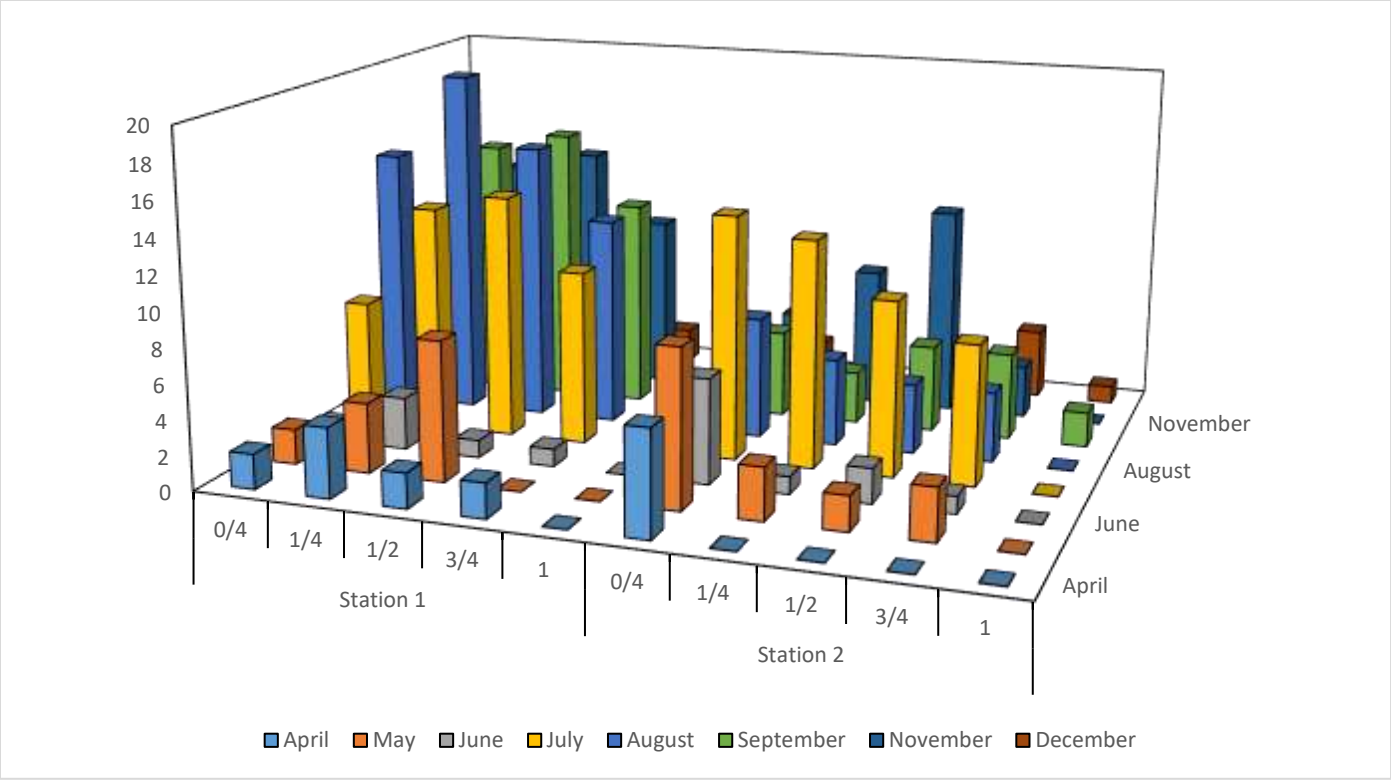

Figure 4.55: Spatio-temporal Stomach Fullness Distribution of *M. vollenhovenii*

4.7.2. Stomach Weight

The mean stomach weight of prawns exhibited both spatial and temporal variation is presented in Figure 4.56. At Station 1, values ranged between 0.054 g (April) and 0.081 g (September), while at Station 2 they ranged between 0.054 g (August) and 0.085 g (December).

In both stations, stomach weight fluctuated moderately across the months. At Station 1, a progressive increase was observed from April (0.054 g) through May (0.072 g) and July (0.073 g), peaking in September (0.081 g) before declining slightly towards December (0.065 g). A similar pattern was noted at Station 2, though the peak value occurred in December (0.085 g), following relatively stable values during mid-year months.

The temporal variation indicates that feeding activity of prawns was generally higher during the rainy season (June–September), and later in December. The spatial comparison shows that Station 2 tended to have slightly higher stomach weights in some months (April, June, December).

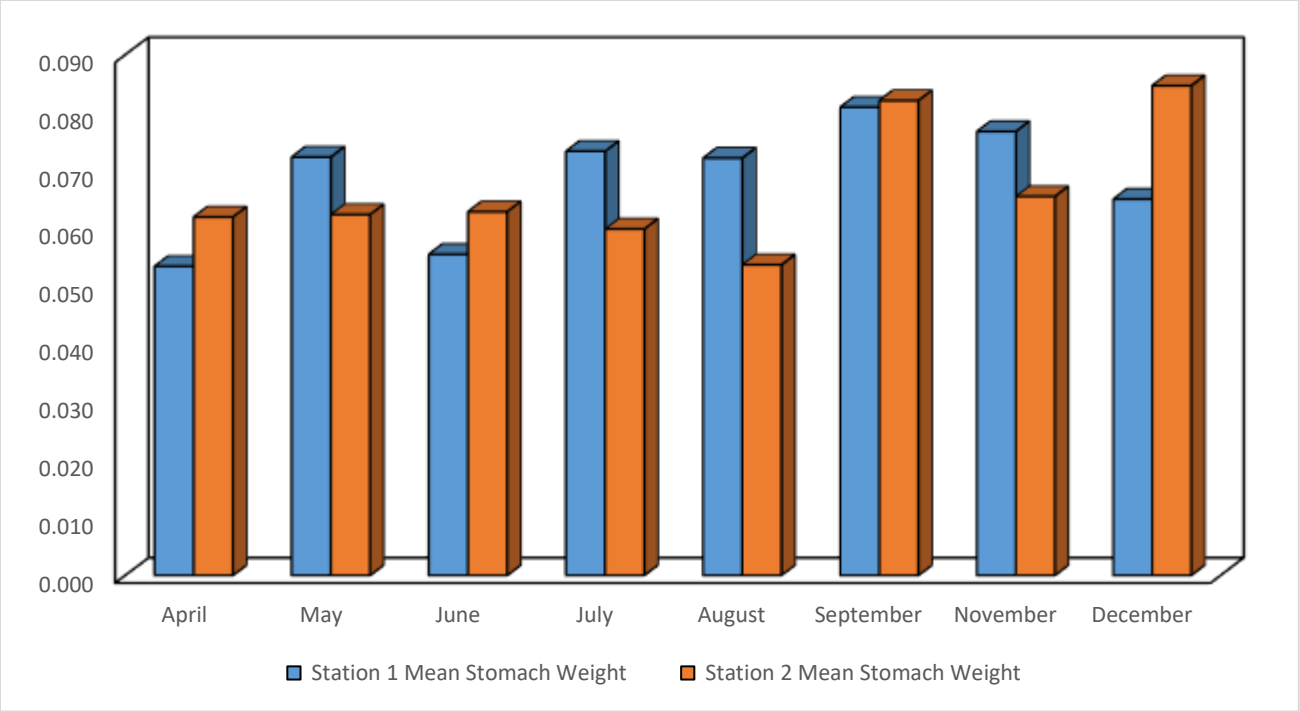

Figure 4.56: Monthly Variation in Mean Stomach Weight of Prawns across Stations

4.7.2.1 Stomach weight of *M. dux*

The spatio-temporal variation in mean stomach weight scores of *Macrobrachium dux* for Station 1 and Station 2 is presented in Figure 4.57. At Station 1, female prawns recorded the highest mean Stomach Fullness in December (0.160). Other notable values occurred in June (0.035), July (0.030), September (0.030), and November (0.030). The lowest mean score appeared in August (0.010). Male values peaked earlier in April (0.070), with moderate scores in September (0.040) and December (0.037) with the lowest male feeding score was in May (0.000).

At Station 2, female *M. dux* showed the highest mean Stomach Fullness in August (0.095), followed by September (0.076), July (0.070), and May (0.070). Male Stomach Fullness remained consistently low, with peak values in June, July, and August (0.030 each), a slight drop in September (0.023), and a complete absence of feeding in April and May (0.000). Feeding activity in females was consistently higher than in males, especially between July and December. Ranking of Female Mean Stomach Fullness across Months follow Station 1: December (0.160) > June (0.035) = September (0.030) = November (0.030) = July (0.030) > April (0.028) > May (0.020) > August (0.010) and Station 2: August (0.095) > September (0.076) > July = May (0.070) > November = December = April (0.030) > June (0.000). Ranking of Male Mean Stomach Fullness across Months shows Station 1: April (0.070) > September (0.040) > December (0.037) > June (0.030) > July = August = November (0.017) > May (0.000) while Station 2: June = July = August (0.030) > September (0.023) > November = December (0.017) > April = May (0.000).

4.7.2.2. Stomach weight of *M. equidens*

The spatio-temporal variation in mean stomach weight scores of *Macrobrachium equidens* for Station 1 and Station 2 is presented in Figure 4.58. At Station 1, female Stomach Fullness peaked in April (0.370). Elevated values were also recorded in May (0.350). A notable decline followed from June (0.030) to November (0.031), with minor fluctuations in December (0.040). The lowest values were observed in July (0.026) and August (0.029). In contrast, male Stomach Fullness at Station 1 remained consistently lower, with a modest peak in May (0.090), followed by moderate values in November (0.070) and July (0.076). Feeding was absent in April and June (0.000). At Station 2, female scores peaked in December (0.100). Secondary highs occurred in September (0.056) and April (0.070). The lowest values appeared in May (0.050) and August (0.033). Males at Station 2 showed the highest Stomach Fullness in November (0.067) and December (0.050), followed by August (0.045). Similar to Station 1, male feeding was absent in April (0.000) and June (0.000). Ranking of Female Mean Stomach Fullness across Months follows Station 1: April (0.370) > May (0.350) > September = December (0.040) > November (0.031) > August (0.029) > July (0.026) > June (0.030) and Station 2: December (0.100) > September (0.056) > April (0.070) > November (0.040) > July (0.042) > June (0.060) > August (0.033) > May (0.050). Ranking of Male Mean Stomach Fullness across Months follows Station 1: May (0.090) > July (0.076) > November (0.070) > August (0.068) > September (0.052) > December (0.030) > April = June (0.000) and Station 2: November (0.067) > December (0.050) > August (0.045) > September (0.034) > July (0.032) > May (0.010) > April = June (0.000).

4.7.2.3. Stomach weight of *M. macrobrachion*

The spatio-temporal variation in mean stomach weight scores of *Macrobrachium macrobrachion* from Station 1 and Station 2 is presented in Figure 4.59. At Station 1, male Stomach Fullness peaked markedly in December (0.230), followed by high values in July and August (0.140) and November (0.130). The lowest mean score occurred in April (0.040). Females at Station 1 exhibited their highest feeding score in August (0.087), followed by July (0.076) and November (0.073). The lowest value was recorded in September (0.040). At Station 2, female prawns had a pronounced Stomach Fullness in April (0.470), standing out as a major outlier and the highest recorded across all groups and month. A secondary peak occurred in December (0.110), while other months such as September (0.087) and May (0.051) exhibited moderate values. Feeding dropped in July (0.031) and August (0.039). Males at Station 2 peaked in November (0.130) and August (0.085), with slightly elevated scores in May (0.090) and September (0.043). Ranking of Female Mean Stomach Fullness across Months follows Station 1: August (0.087) > July (0.076) > November (0.073) > May (0.070) > June (0.058) > December (0.060) > April (0.053) > September (0.040) and Station 2: April (0.470) > December (0.110) > September (0.087) > May (0.051) > November (0.050) > June (0.048) > August (0.039) > July (0.031). Ranking of Male Mean Stomach Fullness across Months follows Station 1: December (0.230) > July = August (0.140) > November (0.130) > May (0.120) > September (0.110) > June (0.053) > April (0.040) and Station 2: November (0.130) > August (0.085) > May (0.090) > September (0.043) > December (0.040) > July (0.034) > June (0.025) > April (0.000).

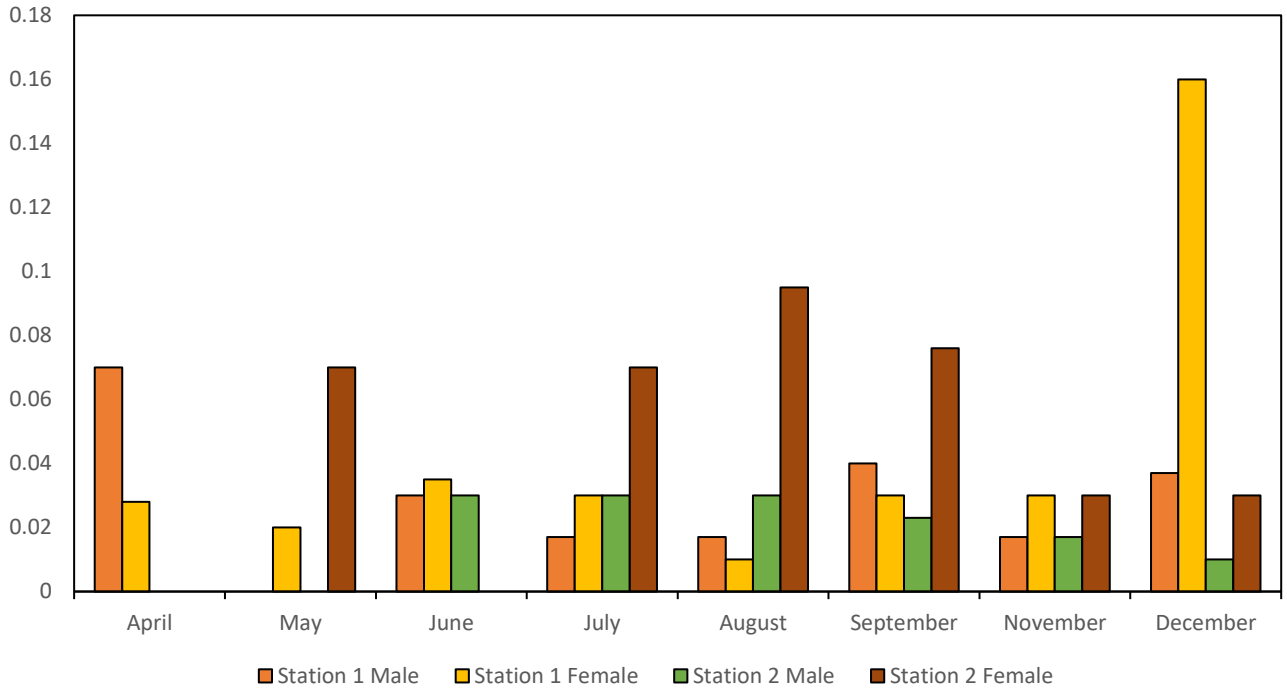

Figure 4.57: Spatio-temporal Stomach weight of *M. dux*

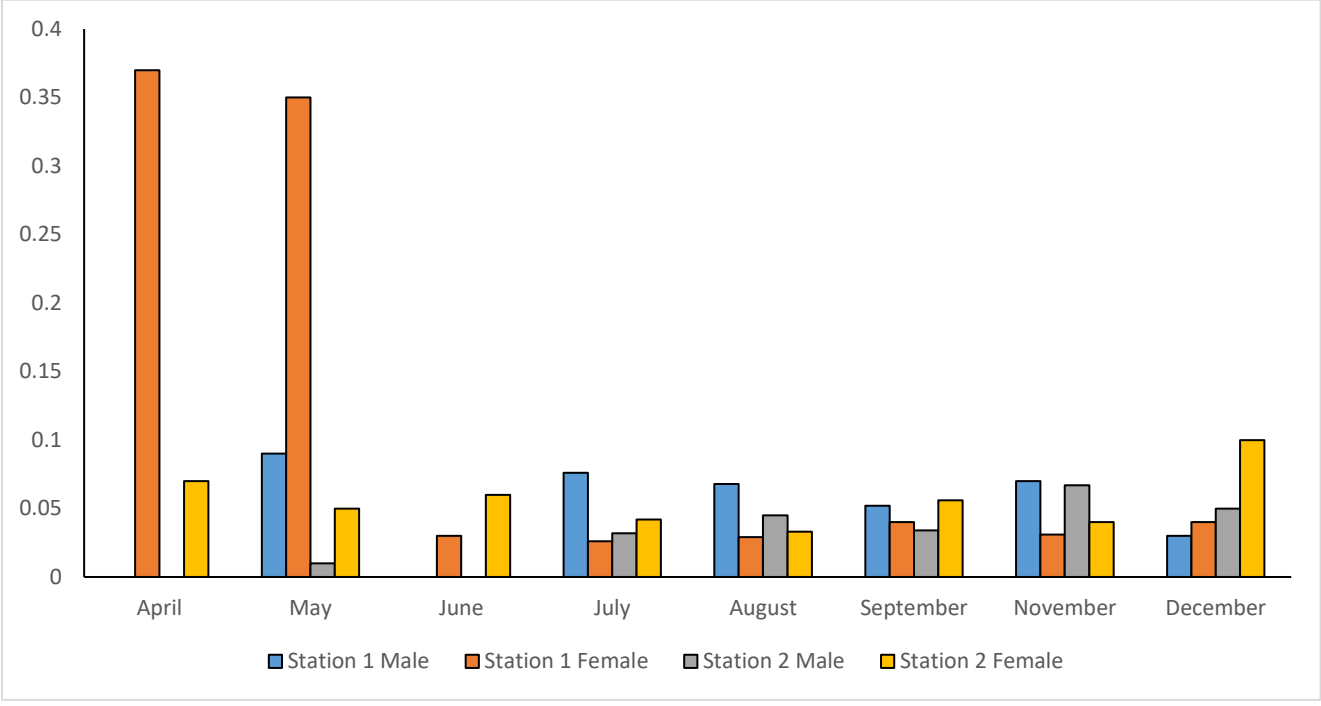

Figure 4.58: Spatio-temporal Stomach weight of *M. equidens*

4.7.2.4. Stomach weight of *M. rosenbergii*

The spatio-temporal variation in mean stomach weight scores of *Macrobrachium rosenbergii* for Station 1 and Station 2 is presented in Figure 4.60. At Station 1, males exhibited relatively stable feeding intensity, with the highest mean score recorded in September (0.070) and the lowest in April (0.000). From May to August, male scores gradually increased (0.060–0.067), reflecting moderate feeding, followed by a decline in November (0.058) and December (0.040). Among females, a striking peak occurred in September (0.180), far exceeding other values and marking a clear outlier. Other elevated female scores were noted in June (0.061), August (0.060), and December (0.070). The lowest value was in July (0.044). At Station 2, male prawns showed the highest feeding score in June (0.096), followed by September (0.074) and December (0.070), while August (0.000) marked the lowest. Female scores peaked in April (0.110) and remained relatively high in June (0.100) and September (0.078). The lowest female feeding was recorded in August (0.020). Ranking of Female Mean Stomach Fullness across Months follows Station 1: September (0.180) > December (0.070) > June (0.061) > August (0.060) > April (0.058) > May (0.053) > November (0.050) > July (0.044) and Station 2: April (0.110) > June (0.100) > September (0.078) > December = May = November = July (0.070/0.070/0.065/0.064) > August (0.020).

Ranking of Male Mean Stomach Fullness across Months follows Station 1: September (0.070) > July = August (0.067) > June (0.066) > May (0.060) > November (0.058) > December (0.040) > April (0.000) and Station 2: June (0.096) > September (0.074) > December (0.070) > July (0.050) > November (0.047) > May (0.027) > April = August (0.000).

4.7.2.5. Stomach weight of *M. vollenhovenii*

The spatio-temporal variation in the mean stomach weight scores of *Macrobrachium vollenhovenii* for Station 1 and Station 2 is shown in Figure 4.61. At Station 1, feeding activity ranged from April (0.020) to a distinct peak in May (0.163), followed by a sharp decline to zero in June. Moderate values were observed again from July to November (0.073–0.093), before declining to 0.045 in December. In females, the stomach weight score also peaked in May (0.150), with relatively high values maintained through April (0.110), July (0.083), September (0.086), and November (0.099). A notable drop occurred in June (0.020), with a slight rebound in subsequent months. At Station 2, male Stomach Fullness peaked in December (0.180) and September (0.150). The lowest value was observed in April and June (0.000). Moderate feeding levels were recorded in July (0.100) and August (0.076). Among females, the highest score appeared in May (0.150), followed by September (0.140) and August (0.083). The lowest values were in April (0.000) and June (0.100). Ranking of Female Mean Stomach Fullness across Months follows Station 1: May (0.150) > April (0.110) > November (0.099) > September (0.086) > July (0.083) > August (0.069) > December (0.060) > June (0.020) and Station 2: May (0.150) > September (0.140) > August (0.083) > November (0.085) > December (0.080) > July (0.078) > June (0.100) > April (0.000). Ranking of Male Mean Stomach Fullness across Months follows Station 1: May (0.163) > August (0.093) > July (0.086) > November (0.085) > September (0.073) > December (0.045) > April (0.020) > June (0.000) and Station 2: December (0.180) > September (0.150) > July (0.100) > August (0.076) > May (0.070) > November (0.045) > April = June (0.000).

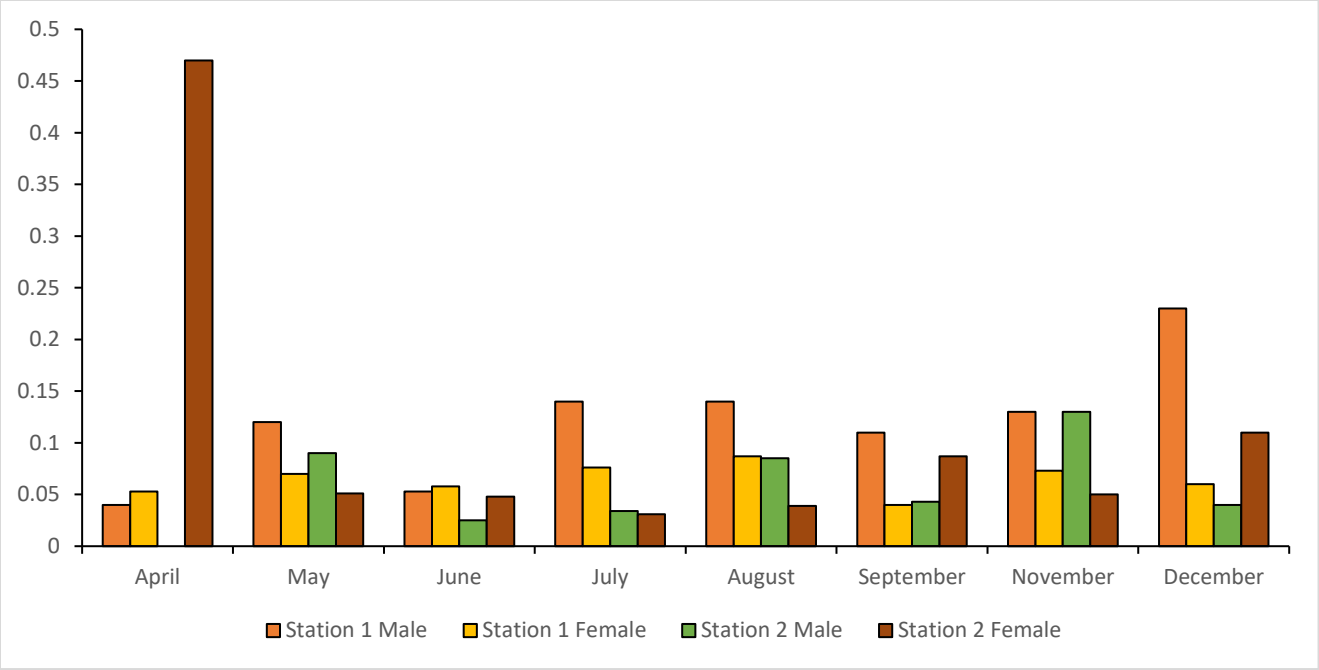

Figure 4.59: Spatio-temporal Stomach weight of *M. macrobrachion*

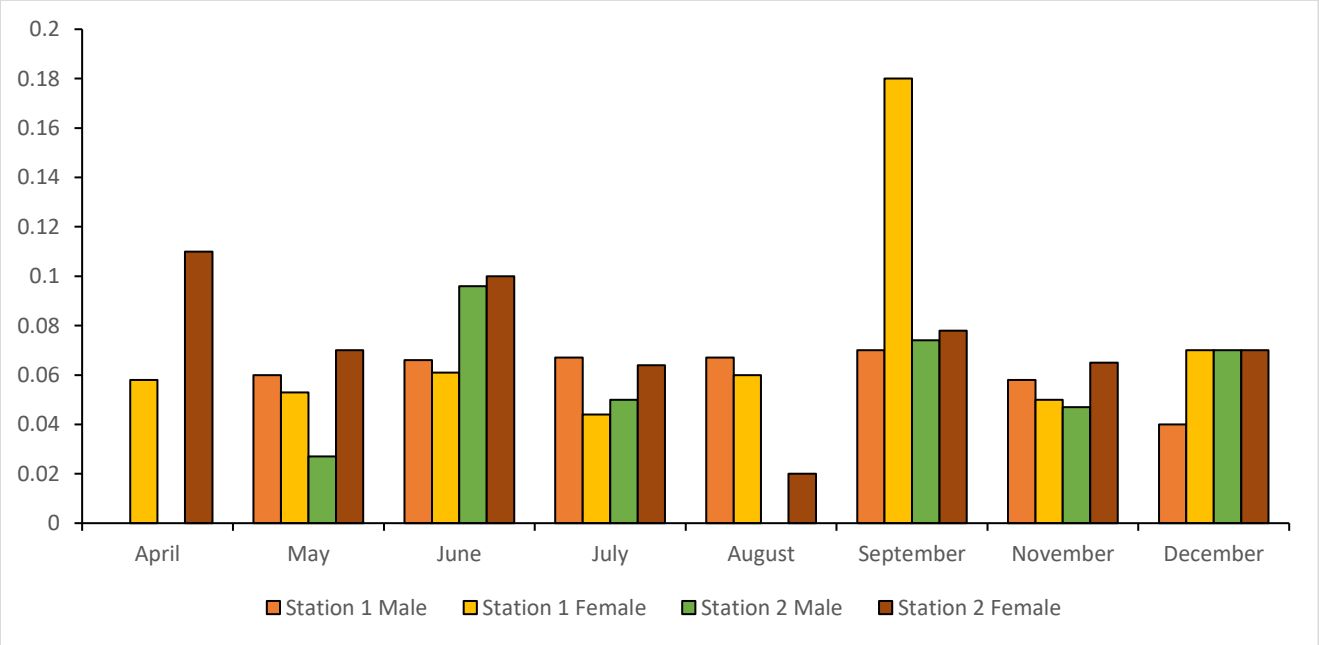

Figure 4.60: Spatio-temporal Stomach weight of *M. rosenbergii*

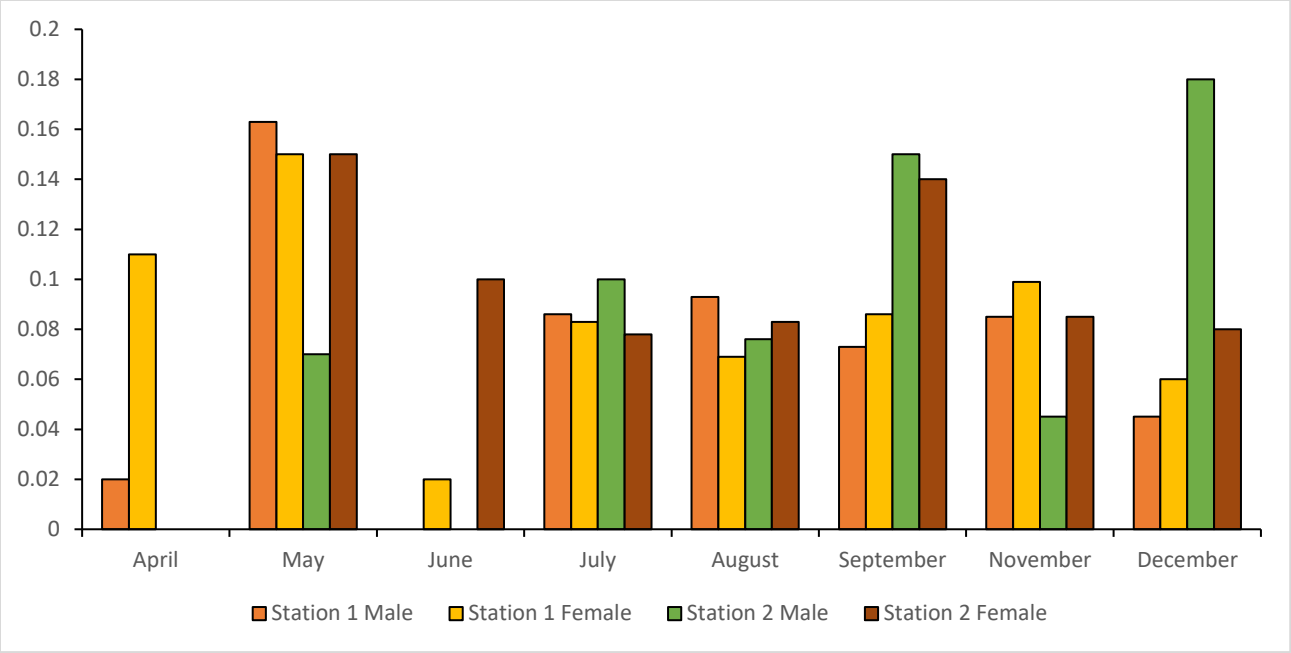

Figure 4.61: Spatio-temporal Stomach weight of *M. vollenhovenii*

4.8. Heavy Metal Concentrations in Prawn Species

4.8.1. Interspecies variation in Heavy metal Concentration

The bioaccumulation of heavy metals for three *Macrobrachium* species is presented in Table 4.18. The concentrations of cadmium in the prawns were low across all species. *Macrobrachium macrobrachion* recorded the highest mean value of 0.099 ± 0.085 mg/kg, whereas *Macrobrachium rosenbergii* and *Macrobrachium vollenhovenii* had considerably lower means of 0.012 ± 0.004 mg/kg and 0.009 ± 0.003 mg/kg respectively. The One-way ANOVA revealed no significant difference in cadmium concentrations was observed for the three species ($p>0.05$). Chromium concentrations followed a similar trend, with values ranging from 0.073 ± 0.020 mg/kg in *Macrobrachium rosenbergii* to 0.085 ± 0.049 mg/kg in *Macrobrachium macrobrachion* and 0.089 ± 0.044 mg/kg in *Macrobrachium vollenhovenii*. The observed differences were not significant ($p>0.05$). Copper concentrations were low, with *Macrobrachium rosenbergii* showing a mean of 0.063 ± 0.018 mg/kg, *Macrobrachium macrobrachion* 0.061 ± 0.027 mg/kg, and *Macrobrachium vollenhovenii* slightly higher at 0.085 ± 0.044 mg/kg. The analysis confirmed no significant difference among species ($p>0.07$). Iron concentrations were higher compared to cadmium, chromium, and copper. *Macrobrachium vollenhovenii* showed the highest mean at 0.250 ± 0.140 mg/kg, followed by *Macrobrachium macrobrachion* at 0.223 ± 0.119 mg/kg, while *Macrobrachium rosenbergii* had the lowest concentration at 0.162 ± 0.052 mg/kg. The variation was not statistically significant ($p>0.05$). Lead concentrations were very low and nearly identical among the species. *Macrobrachium macrobrachion*, *Macrobrachium rosenbergii*, and *Macrobrachium vollenhovenii* recorded mean values of 0.026 ± 0.007 mg/kg, 0.025 ± 0.004 mg/kg, and 0.026 ± 0.004 mg/kg respectively. The differences were negligible, and no significant variation was reported ($p>0.05$). Manganese concentrations were also consistent across species.

Both *Macrobrachium macrobrachion* and *Macrobrachium vollenhovenii* had mean values of 0.017 mg/kg, with standard errors of ± 0.0005 and ± 0.001 respectively, while *Macrobrachium rosenbergii* recorded a slightly lower value of 0.016 ± 0.001 mg/kg. The differences were not significant ($p>0.10$). Nickel showed a different pattern compared to the other metals. *Macrobrachium rosenbergii* had the highest mean concentration at 0.016 ± 0.001 mg/kg, while *Macrobrachium macrobrachion* and *Macrobrachium vollenhovenii* both recorded lower means of 0.013 ± 0.001 mg/kg. Unlike the other metals, the variation in nickel concentrations was statistically significant ($p<0.05$). Zinc was the most abundant of all the metals measured. *Macrobrachium macrobrachion* showed the highest accumulation at 0.334 ± 0.144 mg/kg, followed by *Macrobrachium rosenbergii* at 0.254 ± 0.088 mg/kg, while *Macrobrachium vollenhovenii* recorded a much lower value of 0.039 ± 0.003 mg/kg. The difference was not statistically significant ($p>0.05$). Overall, the ranking of heavy metal accumulation across the prawns followed the order: zinc > iron > cadmium > copper > chromium > lead > nickel > manganese. Among the metals, only nickel exhibited a statistically significant difference across species, with higher accumulation observed in *Macrobrachium rosenbergii*.

Table 4.18: Heavy metal Concentration in *Macrobrachium* Species

Metal	***M. macrobrachion* Mean ± SE**	***M. rosenbergii* Mean ± SE**	***M. vollenhovenii* Mean ± SE**	**Mean Metal Concentration**	**p-value**	**Significance**
Cadmium	0.099 ± 0.085	0.012 ± 0.004	0.009 ± 0.003	0.04	0.36	p>0.05
Chromium	0.085 ± 0.049	0.073 ± 0.020	0.089 ± 0.044	0.082333333	0.958	p>0.06
Copper	0.061 ± 0.027	0.063 ± 0.018	0.085 ± 0.044	0.069666667	0.841	p>0.07
Iron	0.223 ± 0.119	0.162 ± 0.052	0.250 ± 0.140	0.1925	0.849	p>0.08
Lead	0.026 ± 0.007	0.025 ± 0.004	0.026 ± 0.004	0.025666667	0.991	p>0.09
Manganese	0.017 ± 0.0005	0.016 ± 0.001	0.017 ± 0.001	0.016666667	0.404	p>0.10
Nickel	0.013 ± 0.001	0.016 ± 0.001	0.013 ± 0.001	0.014	0.006	p<0.05
Zinc	0.334 ± 0.144	0.254 ± 0.088	0.039 ± 0.003	0.209	0.111	p>0.05

4.9 Bivariate Analysis

4.9.1 Pearson Correlation

4.9.1.1 Environmental Quality and Prawn Abundance

The Pearson correlation analysis of water physicochemical parameters and prawn abundance is shown in Table 4.19. Water temperature showed a positive and significant correlation with *M. macrobrachion* ($r = 0.643$, $p < 0.05$, while no significant relationships were observed with the other two prawns. Dissolved oxygen exhibited a negative but weak and non-significant correlation with all species ($r = –0.181$ to $–0.209$, $p > 0.05$). Salinity showed no significant relationship with the prawns, though the correlation was slightly positive for *M. vollenhovenii* ($r = 0.112$, $p > 0.05$). pH maintained weak non-significant positive correlations with all species, ranging between $r = 0.036$ and 0.172. For the nutrient parameters, nitrate exhibited a strong positive and significant relationship with *M. rosenbergii* ($r = 0.714$, $p < 0.01$) and a moderate positive correlation with *M. vollenhovenii* ($r = 0.412$, $p > 0.05$), while the relationship with *M. macrobrachion* was weak ($r = 0.138$, $p > 0.05$). Phosphate also showed a significant positive correlation with *M. rosenbergii* ($r = 0.687$, $p < 0.01$) and moderate non-significant relationships with the other species. Sulphate displayed consistently weak non-significant negative correlations with all prawns. .

With respect to heavy metals, cadmium was negatively correlated with all three species, strongest in *M. macrobrachion* ($r = –0.562$, $p < 0.05$). Lead exhibited a significant negative relationship with *M. vollenhovenii* ($r = –0.602$, $p < 0.05$) and weaker negative trends with the other prawns. Copper showed a significant negative correlation with *M. rosenbergii* ($r = –0.615$, $p < 0.05$), while zinc and iron maintained mostly weak or moderate positive non-significant correlations across species. Chromium revealed weak positive correlations with all prawns ($r = 0.141–0.264$, $p > 0.05$), while nickel showed consistently negative but non-significant relationships.

Table 4.19: Pearson Correlation Matrix among Physicochemical Parameters and *Macrobrachium* Species Abundance

	Air Temp	**Water Temp**	**pH**	**Salinity**	**EC**	**TDS**	**ORP**	**DO**	**BOD**	**SO_4**	**PO_4**	**NO_3**	**Cd**	**Cr**	**Cu**	**Fe**	**Pb**	**Mn**	**Ni**	**Zn**	***M. dux***	***M. equidens***	***M. macrobrachion***	***M. rosenbergii***	***M. vollenhovenii***
Air Temp	1																								
Water Temp	.178	1																							
pH	.476	-.017	1																						
Salinity	-.366	-.383	.043	1																					
EC	.225	.991**	.076	-.414	1																				
TDS	.226	.995**	.057	-.403	.999**	1																			
ORP	.005	.888**	-.430	-.333	.853**	.861**	1																		
DO	-.295	-.156	.156	.166	-.177	-.185	-.206	1																	
BOD	.808*	-.032	.466	-.548	.048	.037	-.204	-.476	1																
SO_4	-.590	-.558	-.640	.060	-.572	-.576	-.213	-.206	-.201	1															
PO_4	.583	-.135	.688	-.132	-.064	-.081	-.355	.240	.622	-.426	1														
NO_3	.587	.353	.810*	-.081	.399	.392	-.019	.357	.279	-.939**	.589	1													
Cd	-.066	-.139	-.294	.349	-.194	-.168	-.074	-.642	.049	.259	-.253	-.473	1												
Cr	-.276	-.430	-.061	.745*	-.502	-.484	-.368	.593	-.624	-.072	-.122	.081	.013	1											
Cu	-.284	-.448	.201	.700	-.477	-.475	-.468	.769*	-.563	-.142	.096	.261	-.269	.920**	1										
Fe	-.334	-.453	-.055	.686	-.507	-.499	-.354	.745*	-.639	-.006	-.001	.080	-.196	.952**	.959**	1									

Pb	.472	.499	.012	-.440	.469	.490	.331	-.529	.362	-.411	-.225	.200	.339	-.338	-.552	-.575	1								
Mn	-.157	-.339	-.684	.354	-.441	-.413	-.001	.103	-.440	.329	-.432	-.441	.257	.644	.359	.574	-.071	1							
Ni	-.088	-.307	-.738*	-.057	-.353	-.346	.128	-.007	-.105	.598	-.143	-.612	.033	.111	-.036	.219	-.344	.706	1						
Zn	-.070	-.067	-.882**	-.062	-.157	-.133	.334	-.214	-.219	.453	-.508	-.617	.282	.157	-.153	.112	.126	.851**	.837**	1					
M. dux	-.426	-.174	-.691	-.015	-.253	-.229	.023	-.444	-.233	.608	-.753*	-.769*	.639	.014	.310	-.187	.370	.439	.233	.564	1				
M. equidens	.773*	.387	.298	-.016	.412	.414	.331	-.145	.411	-.625	.522	.548	.076	.080	.083	.066	.146	.020		.021	.624	1			
M. macrobrachion	.741*	.573	.156	-.609	.594	.594	.484	-.210	.631	-.509	.533	.418	.106	.537	.539	.500	.401	.266	.065	.035	.401	.739*	1		
M. rosenbergii	.635	.578	.230	-.640	.613	.605	.456	-.094	.601	-.491	.608	.445	.219	.590	.514	.502	.272	.423	.009	.121	.493	.651	.971**	1	
M. vollenhovenii	-.330	-.736*	.120	.660	-.706	-.719*	-.612	.376	-.327	.361	.058	-.141	-.206	.576	.717*	.685	-.806*	.253	.20	-.101	-.221	-.180	-.674	-.637	1

Note: *. Correlation is significant at the 0.05 level (2-tailed), **. Correlation is significant at the 0.01 level (2-tailed).

The Pearson correlation analysis of sediment characteristics and heavy metals with prawn abundance is presented in Table 4.20. Sediment pH showed weak and non-significant associations with all *Macrobrachium* species, with correlations ranging from r = –0.521 (p = 0.186) for *M. macrobrachion* to r = 0.098 (p = 0.818) for *M. dux*. Sediment conductivity also displayed weak, non-significant correlations with the prawns, with the strongest being a positive relationship with *M. dux* (r = 0.405, p = 0.320). Sediment moisture content showed similarly weak associations, with positive correlation with *M. dux* (r = 0.525, p = 0.182) and negative correlations with *M. vollenhovenii* (r = –0.177, p = 0.676), none of which reached statistical significance ($p < 0.05$).

Among sediment heavy metals, cadmium (S) was negatively correlated with *M. vollenhovenii* (r = –0.614, p = 0.106). Lead (S) presented a particularly strong and significant negative relationship with *M. vollenhovenii* (r = –0.880, p = 0.004), while maintaining a strong positive correlation with *M. macrobrachion* (r = 0.769, p = 0.026) and *M. rosenbergii* (r = 0.764, p = 0.027). Manganese (S) displayed positive but non-significant correlations with *M. macrobrachion* and *M. rosenbergii* (r = 0.502 and 0.435, respectively), while its strongest relationship was with *M. equidens* (r = 0.435, p = 0.282). Nickel (S) maintained weak, non-significant associations across all species, with the highest being *M. equidens* (r = 0.408, p = 0.316). Zinc (S) exhibited a moderate positive correlation with *M. rosenbergii* (r = 0.600, p = 0.116) and *M. macrobrachion* (r = 0.526, p = 0.181), but a negative and near-significant correlation with *M. dux* (r = –0.668, p = 0.070), suggesting variability in tolerance across species. Iron (S) correlated positively but weakly with prawns, highest for *M. macrobrachion* (r = –0.043, p = 0.919), while copper (S) showed weak negative correlations with all prawns, none significant. Chromium (S) also revealed weak and inconsistent correlations, including a negative correlation with *M. dux* (r = –0.450, p = 0.263) and near-zero correlations with the others.

Table 4.20: Pearson Correlation Matrix among sediment Parameters and *Macrobrachium* Species Abundance

Variables	Sediment pH	Sed. Conductivity	Sed. Moisture (%)	Cadmium (S)	Chromium (S)	Copper (S)	Iron (S)	Lead (S)	Manganese (S)	Nickel (S)	Zinc (S)	*M. dux*	*M. equidens*	*M. macrobrachion*	*M. rosenbergii*	*M. vollenhovenii*
Sediment pH	1															
Sed. Conductivity	.193	1														
Sed. Moisture (%)	.480	.128	1													
Cadmium (S)	-.242	.206	-.073	1												
Chromium (S)	.421	.167	-.080	.335	1											
Copper (S)	.136	-.265	-.244	.074	.679	1										
Iron (S)	.506	.256	.202	-.048	.679	.764*	1									
Lead (S)	-.514	.310	-.247	.709*	.280	-.034	-.097	1								
Manganese (S)	-.085	.097	.263	.032	.256	.461	.633	.343	1							
Nickel (S)	.340	.386	.500	-.342	.127	.134	.631	-.005	.786*	1						
Zinc (S)	-.220	-.334	-.319	-.162	.251	.603	.403	.250	.716*	.418	1					
M. dux	.098	.405	.525	.327	-.450	-.524	-.193	-.083	-.165	.006	-.668	1				
M. equidens	-.273	.192	-.167	-.339	.229	.158	.223	.298	.435	.408	.432	-.624	1			
M. macrobrachion	-.521	.275	-.289	.098	.095	-.073	-.043	.769*	.502	.337	.526	-.401	.739*	1		
M. rosenbergii	-.555	.083	-.381	.111	.079	-.050	-.144	.764*	.435	.212	.600	-.493	.651	.971**	1	
M. vollenhovenii	.330	-.405	-.177	-.614	-.073	.355	.185	-.880**	-.349	-.191	-.035	-.221	-.180	-.674	-.637	1

Note: *. Correlation is significant at the 0.05 level (2-tailed), **. Correlation is significant at the 0.01 level (2-tailed).

4.9.1.2 Environmental Quality and Bioaccumulation

The Pearson correlation coefficients between heavy metals in water and *Macrobrachium macrobrachion* is presented in Figure 4.21. Among metals in water, chromium showed a very strong positive correlation with both copper (r= 0.920, $p < 0.01$) and iron (r = 0.952, p = $p < 0.01$), while copper and iron were also highly correlated (r = 0.959, $p < 0.01$), all significant at the 0.01 level. Manganese in water was strongly positively correlated with zinc (r = 0.851, $p < 0.01$) and nickel (r = 0.706, $p < 0.01$). Other metals in water exhibited weaker or non-significant correlations with each other. Within *M. macrobrachion*, several strong positive correlations were evident. Copper in the organism was significantly correlated with chromium (r = 0.811, $p < 0.05$) and iron (r = 0.754, $p < 0.01$), while iron showed a very strong positive correlation with chromium (r = 0.943, $p < 0.01$) and manganese (r = 0.947, $p < 0.01$). Lead in the organism correlated significantly with copper (r = 0.866, $p < 0.01$) and showed moderate correlations with other metals, including nickel (r = 0.673, $p < 0.01$). Manganese also displayed strong positive correlations with chromium (r = 0.951, $p < 0.01$) and iron (r = 0.947, $p < 0.01$), and nickel in the organism showed very strong correlations with manganese (r = 0.968, $p < 0.01$) and zinc (r = .954, $p < 0.01$). Zinc was significantly correlated with cadmium (r = 0.916, $p < 0.01$) and nickel (r = 0.954, $p < 0.01$) in the organism. Cross-matrix correlations between metals in water and *Macrobrachium macrobrachion* revealed that cadmium in the organism showed negative correlations with cadmium in water (r = -0.210), iron (r = -0.427), and zinc (r = -0.583). Similarly, chromium in the organism was negatively correlated with chromium in water (r = -0.155), and nickel in the organism had a negative correlation with nickel in water (r = -0.214). In contrast, copper in the organism exhibited a moderate positive correlation with copper in water (r = 0.358), and iron in the organism showed a small positive correlation with iron in water (r = -0.074, $p > 0.05$).

Table 4.21: Pearson Correlation Coefficients between Metals in Water (W) and *M. macrobrachion* (M.m)

	Cd (W)	Cr (W)	Cu (W)	Fe (W)	Pb (W)	Mn (W)	Ni (W)	Zn (W)	Cd (M.m)	Cr (M.m)	Cu (M.m)	Fe (M.m)	Pb (M.m)	Mn (M.m)	Ni (M.m)	Zn (M.m)
Cd (W)	1															
Cr (W)	.013	1														
Cu (W)	-.269	.920**	1													
Fe (W)	-.196	.952**	.959**	1												
Pb (W)	.339	-.338	-.552	-.575	1											
Mn (W)	.257	.644	.359	.574	-.071	1										
Ni (W)	.033	.111	-.036	.219	-.344	.706	1									
Zn (W)	.282	.157	-.153	.112	.126	.851**	.837**	1								
Cd (M.m)	-.210	.377	.567	.381	-.260	-.198	-.370	-.583	1							
Cr (M.m)	-.320	-.155	-.012	.035	-.639	-.018	.363	.104	-.268	1						
Cu (M.m)	-.361	.289	.358	.431	-.598	.256	.294	.199	-.336	.811*	1					
Fe (M.m)	-.427	-.258	-.035	-.074	-.561	-.305	.051	-.191	-.174	.943**	.754*	1				
Pb (M.m)	-.372	.317	.317	.495	-.603	.515	.673	.516	-.426	.674	.866**	.499	1			
Mn (M.m)	-.313	-.392	-.221	-.221	-.485	-.223	.232	-.020	-.213	.951**	.626	.947**	.447	1		
Ni (M.m)	-.215	-.501	-.346	-.385	-.297	-.342	.055	-.108	-.214	.866**	.506	.909**	.251	.968**	1	
Zn (M.m)	-.324	-.436	-.231	-.249	-.522	-.303	.209	-.104	-.113	.916**	.530	.921**	.366	.987**	.954**	1

Note: *. Correlation is significant at the 0.05 level (2-tailed), **. Correlation is significant at the 0.01 level (2-tailed).

The Pearson correlation coefficients between selected heavy metals in water and *Macrobrachium rosenbergii* is presented in Table 4.22. Among metals in water, chromium showed very strong positive correlations with copper ($r = 0.920$, $p < 0.01$) and iron ($r = 0.952$, $p < 0.01$), while copper and iron were also highly correlated ($r = 0.959$, $p < 0.01$). Manganese in water was strongly positively correlated with zinc ($r = 0.851$, $p < 0.01$) and nickel ($r = 0.706$, $p < 0.01$). Other metals in water exhibited weaker or non-significant correlations with each other. Within *M. rosenbergii*, several strong positive correlations were observed. Copper in the organism was highly correlated with chromium ($r = 0.986$, $p < 0.01$) and iron ($r = 0.961$, $p < 0.01$), while iron showed very strong correlations with chromium ($r = 0.952$, $p < 0.01$) and manganese ($r = 0.973$, $p < 0.01$). Lead in the organism was strongly correlated with manganese ($r = 0.872$, $p < 0.01$) and nickel ($r = 0.788$, $p < 0.05$), and zinc also showed moderate positive correlations with manganese ($r = 0.666$) and nickel ($r = 0.664$). Cadmium in the organism displayed a significant negative correlation with cadmium in water ($r = -0.767$, $P < 0.05$), while other correlations between cadmium and water metals were weak or non-significant. Cross-matrix correlations between metals in water and *M. rosenbergii* were generally weak or negative. Cadmium in the organism was negatively correlated with cadmium in water ($r = -0.767$, $p < 0.05$) and weakly with iron ($r = -0.104$) and manganese ($r = -0.072$). Chromium, copper, and iron in the organism showed positive correlations with their respective water metals, though most were not statistically significant. Lead in the organism exhibited moderate positive correlations with manganese ($r = 0.872$, $p < 0.01$) and nickel ($r = .788$, $p < 0.05$) in water.

Table 4.22: Pearson Correlation Coefficients between Metals in Water (W) and *M. rosenbergii* (M.r)

	Cd (W)	Cr (W)	Cu (W)	Fe (W)	Pb (W)	Mn (W)	Ni (W)	Zn (W)	Cd (M.r)	Cr (M.r)	Cu (M.r)	Fe (M.r)	Pb (M.r)	Mn (M.r)	Ni (M.r)	Zn (M.r)
Cd (W)	1															
Cr (W)	.013	1														
Cu (W)	-.269	.920**	1													
Fe (W)	-.196	.952**	.959**	1												
Pb (W)	.339	-.338	-.552	-.575	1											
Mn (W)	.257	.644	.359	.574	-.071	1										
Ni (W)	.033	.111	-.036	.219	-.344	.706	1									
Zn (W)	.282	.157	-.153	.112	.126	.851**	.837**	1								
Cd (M.r)	-.767*	-.289	-.153	-.104	.001	-.072	.401	.351	1							
Cr (M.r)	-.224	-.280	-.163	-.106	-.563	-.005	.457	.174	.265	1						
Cu (M.r)	-.335	-.252	-.119	-.074	-.546	-.013	.414	.154	.382	.986**	1					
Fe (M.r)	-.342	-.419	-.222	-.241	-.492	-.283	.194	-.086	.321	.952**	.961**	1				
Pb (M.r)	-.170	.593	.461	.661	-.410	.872**	.788*	.741*	.757*	.326	.354	.084	1			
Mn (M.r)	-.320	-.413	-.225	-.246	-.456	-.321	.102	-.117	.373	.904**	.926**	.973**	.040	1		
Ni (M.r)	-.355	-.389	-.200	-.259	-.351	-.337	-.004	-.169	.367	.867**	.902**	.960**	.008	.972**	1	
Zn (M.r)	-.529	.171	.344	.293	-.443	-.125	-.156	-.207	.517	.451	.553	.540	.227	.666	.664	1

Note: *. Correlation is significant at the 0.05 level (2-tailed), **. Correlation is significant at the 0.01 level (2-tailed).

The Pearson correlation coefficients between selected heavy metals in water and *Macrobrachium vollenhovenii* is presented in Table 4.23. Among metals in water, chromium showed very strong positive correlations with copper ($r = 0.920$, $p < 0.01$) and iron ($r = 0.952$, $p < 0.01$), while copper and iron were also highly correlated ($r = 0.959$, $p < 0.01$). Manganese in water was strongly positively correlated with zinc ($r = 0.851$, $p < 0.01$) and nickel ($r = 0.706$). Other metals in water exhibited weaker or non-significant correlations with each other.

Within *M. vollenhovenii*, several strong positive correlations were evident. Copper in the organism was highly correlated with chromium ($r = 0.949$, $p < 0.01$) and iron ($r = 0.975$, $p < 0.01$), while iron showed very strong correlations with chromium ($r = 0.983$, $p < 0.01$) and manganese ($r = 0.987$, $p < 0.01$). Manganese in the organism also displayed very strong correlations with chromium (0.977, $p < 0.01$) and iron ($r = 0.987$, $p < 0.01$), and nickel showed very strong correlations with chromium ($r = 0.969$, $p < 0.01$), copper ($r = 0.938$, $p < 0.01$), and iron ($r = 0.981$, $p < 0.01$). Zinc in the organism exhibited significant positive correlations with chromium ($r = .801$, $p < 0.05$), copper ($r = 0.792$, $p < 0.05$), iron ($r = 0.820$, $p < 0.05$), manganese ($r = 0.867$, $p < 0.01$), and nickel ($r = 0.831$, $p < 0.05$). Lead in the organism showed moderate positive correlations with manganese ($r = 0.732$, $p < 0.05$) and nickel ($r = 0.758$, $p < 0.05$).

Cross-matrix correlations between metals in water and *M. vollenhovenii* were generally weak or negative. Cadmium in the organism was negatively correlated with cadmium in water ($r = -.637$), manganese ($r = -.407$), nickel ($r = -.291$), and zinc ($r = -.415$), while chromium in the organism had weak negative correlations with most water metals ($r = -0.319$ with Cd(W), $r = -0.332$ with Cr(W)). Copper and iron in the organism showed very weak or non-significant correlations with water copper and iron, whereas lead in the organism had moderate positive correlations with manganese ($r = 0.732$, $p < 0.05$) and nickel ($r = 0.758$, $p < 0.05$) in water.

Table 4.23: Pearson Correlation Coefficients between Metals in Water (W) and *M. vollenhovenii* (M.v)

	Cd (W)	Cr (W)	Cu (W)	Fe (W)	Pb (W)	Mn (W)	Ni (W)	Zn (W)	Cd (M.v)	Cr (M.v)	Cu (M.v)	Fe (M.v)	Pb (M.v)	Mn (M.v)	Ni (M.v)	Zn (M.v)
Cd (W)	1															
Cr (W)	.013	1														
Cu (W)	-.269	.920**	1													
Fe (W)	-.196	.952**	.959**	1												
Pb (W)	.339	-.338	-.552	-.575	1											
Mn (W)	.257	.644	.359	.574	-.071	1										
Ni (W)	.033	.111	-.036	.219	-.344	.706	1									
Zn (W)	.282	.157	-.153	.112	.126	.851**	.837**	1								
Cd (M.v)	-.637	-.061	.137	.069	-.012	-.407	-.291	-.415	1							
Cr (M.v)	-.319	-.332	-.152	-.141	-.579	-.190	.279	-.014	-.302	1						
Cu (M.v)	-.406	-.191	.000	.000	-.601	-.188	.160	-.077	-.159	.949**	1					
Fe (M.v)	-.383	-.336	-.125	-.150	-.547	-.298	.125	-.140	-.212	.983**	.975**	1				
Pb (M.v)	-.349	.542	.502	.675	-.575	.732*	.758*	.603	-.131	.340	.379	.263	1			
Mn (M.v)	-.402	-.370	-.184	-.201	-.452	-.250	.160	-.062	-.252	.977**	.952**	.987**	.285	1		
Ni (M.v)	-.236	-.342	-.146	-.188	-.519	-.324	.060	-.186	-.339	.969**	.938**	.981**	.164	.962**	1	
Zn (M.v)	-.066	-.416	-.391	-.385	-.051	-.131	.069	.123	-.488	.801*	.792*	.820*	.115	.867**	.831*	1

Note: *. Correlation is significant at the 0.05 level (2-tailed), **. Correlation is significant at the 0.01 level (2-tailed).

The Pearson correlation analysis between sediment metals and bioaccumulated heavy metals in *Macrobrachium macrobrachion* is presented in Table 4.24. Sediment Cadmium (S) was significantly correlated with Lead (S) ($r = 0.709$). Copper (S) exhibited strong positive correlations with Iron (S) ($r = 0.764$, $p < 0.05$) and Chromium (S) ($r = 0.679$). Manganese (S) was significantly associated with Nickel (S) ($r = 0.786$, $p < 0.05$) and Zinc (S) ($r = 0.716$, $p < 0.05$). In terms of bioaccumulation, Cadmium in *M. macrobrachion* showed a very strong positive correlation with sediment Copper (S) ($r = 0.966$, $p < 0.01$) and a notable association with Iron (S) ($r = 0.702$), indicating that Cu- and Fe-rich sediments enhance Cd uptake. Similarly, Copper (M.m) and Iron (M.m) were strongly correlated with sediment Cd ($r = 0.970$, $p < 0.01$ and 0.993, $p < 0.01$, respectively), highlighting multi-metal co-accumulation in the prawns. Lead (M.m) showed weaker correlations with sediment metals, whereas Manganese (M.m) was negatively correlated with sediment Chromium (S) ($r = -0.545$) and Copper (S) ($r = -0.244$). Nickel (M.m) was positively influenced by sediment Cadmium (S) ($r = 0.517$), whereas Zinc (M.m) displayed significant negative correlation with sediment Nickel (S) ($r = -0.785$, $p < 0.05$).

The Pearson correlation analysis for sediment metals and bioaccumulated heavy metals in *Macrobrachium rosenbergii* is presented in Table 4.25. Cadmium (S) was significantly correlated with Lead (S) ($r = 0.709$, $p < 0.05$), while Copper (S) and Iron (S) were strongly interrelated ($r = 0.764$, $p < 0.05$). Manganese (S) showed significant positive correlations with Nickel (S) ($r = 0.786$, $p < 0.05$) and Zinc (S) ($r = 0.716$, $p < 0.05$). In terms of bioaccumulation, Cadmium in *M. rosenbergii* displayed weak to moderate correlations with sediment metals, with the highest being a moderate positive correlation with Lead (S) ($r = 0.315$). Chromium (M.r) was strongly associated with sediment Chromium (S) ($r = 0.796$, $p < 0.05$), Copper (S) ($r = 0.508$), and Iron (S) ($r = 0.612$).

Table 4.24: Pearson Correlation Coefficients between Metals in Sediment (S) and *M. macrobrachion* (M.m)

	Cadmium (S)	Chromium (S)	Copper (S)	Iron (S)	Lead (S)	Manganese (S)	Nickel (S)	Zinc (S)	M.m Cd	M.m Cr	M.m Cu	M.m Fe	M.m Pb	M.m Mn	M.m Ni	M.m Zn
Cadmium (S)	1															
Chromium (S)	.335	1														
Copper (S)	.074	.679	1													
Iron (S)	-.048	.679	.764*	1												
Lead (S)	.709*	.280	-.034	-.097	1											
Manganese (S)	.032	.256	.461	.633	.343	1										
Nickel (S)	-.342	.127	.134	.631	-.005	.786*	1									
Zinc (S)	-.162	.251	.603	.403	.250	.716*	.418	1								
M.m Cd	-.089	.513	.966**	.702	-.233	.350	.072	.543	1							
M.m Cr	-.045	.407	-.023	.019	-.195	-.237	-.054	-.153	-.126	1						
M.m Cu	-.086	.529	.172	.243	-.289	-.136	.046	-.091	.078	.970**	1					
M.m Fe	-.066	.508	.181	.177	-.261	-.154	-.028	-.053	.086	.977**	.993**	1				
M.m Pb	-.245	-.119	-.493	-.500	.017	-.496	-.195	-.063	-.506	.416	.262	.279	1			
M.m Mn	-.235	-.545	-.244	-.385	.116	-.103	-.116	.226	-.121	-.730*	-.800*	-.781*	.289	1		
M.m Ni	.517	.192	-.270	.187	.386	.120	.240	-.522	-.380	-.105	-.094	-.171	-.315	-.314	1	
M.m Zn	-.168	-.111	.272	-.251	.068	-.128	-.396	.547	.349	-.303	-.338	-.261	.317	.679	-.785*	1

Note: *. Correlation is significant at the 0.05 level (2-tailed), **. Correlation is significant at the 0.01 level (2-tailed).

Copper (M.r) was highly correlated with sediment Copper (S) ($r = 0.860$, $p < 0.01$) and Chromium (S) ($r = 0.843$, $p < 0.01$), while Iron (M.r) also showed strong positive correlations with sediment Chromium (S) ($r = 0.907$, $p < 0.01$), Copper (S) ($r = 0.727$, $p < 0.05$), and Iron (S) ($r = 0.722$, P , 0.05). Lead (M.r) was strongly correlated with Cadmium (M.r) ($r = 0.992$, $p < 0.01$), whereas Manganese (M.r) exhibited a significant negative correlation with sediment Iron (S) ($r = -0.748$, $p < 0.05$). Nickel (M.r) showed moderate positive correlations with sediment Chromium (S) ($r = 0.701$) and Iron (S) ($r = 0.557$), while Zinc (M.r) had moderate positive associations with sediment Copper (S) ($r = 0.397$) and Chromium (S) ($r = 0.538$).

The Pearson correlation analysis between sediment metals and bioaccumulated heavy metals in *Macrobrachium vollenhovenii* is shown in Table 4.26. Sediment Cadmium (S) was significantly correlated with Lead (S) ($r = 0.709$, $p < 0.05$), while Copper (S) showed a strong positive correlation with Iron (S) ($r = 0.764$, $p < 0.05$). Manganese (S) was notably associated with Nickel (S) ($r = 0.786$, $p < 0.05$) and Zinc (S) ($r = 0.716$, $p < 0.05$).

In terms of bioaccumulation, Cadmium in *M. vollenhovenii* was positively influenced by sediment Nickel (S) ($r = 0.660$) and Iron (S) ($r = 0.397$). Chromium (M.v) showed weak correlations with sediment metals. Copper (M.v) and Iron (M.v) were highly intercorrelated with Chromium (M.v) ($r = 0.993$, $p < 0.01$ and 0.996, $p < 0.01$, respectively). Lead (M.v) showed moderate positive correlations with Manganese (M.v) ($r = 0.894$, $p < 0.01$), while Manganese (M.v) itself had positive associations with Cadmium (M.v) ($r = 0.504$). Nickel (M.v) displayed a significant negative correlation with sediment Lead (S) ($r = -0.738$, $p < 0.05$), whereas Zinc (M.v) was negatively associated with sediment Zinc (S) ($r = -0.546$).

Table 4.25: Pearson Correlation Coefficients between Metals in Sediment (S) and *M. rosenbergii* (M.r)

	Cadmium (S)	Chromium (S)	Copper (S)	Iron (S)	Lead (S)	Manganese (S)	Nickel (S)	Zinc (S)	Cd (M.r)	Cr (M.r)	Cu (M.r)	Fe (M.r)	Pb (M.r)	Mn (M.r)	Ni (M.r)	Zn (M.r)
Cadmium (S)	1															
Chromium (S)	.335	1														
Copper (S)	.074	.679	1													
Iron (S)	-.048	.679	.764*	1												
Lead (S)	.709*	.280	-.034	-.097	1											
Manganese (S)	.032	.256	.461	.633	.343	1										
Nickel (S)	-.342	.127	.134	.631	-.005	.786*	1									
Zinc (S)	-.162	.251	.603	.403	.250	.716*	.418	1								
Cd (M.r)	.201	.378	-.260	.055	.315	-.254	.064	-.273	1							
Cr (M.r)	.319	.796*	.508	.612	.261	.076	.083	.083	.664	1						
Cu (M.r)	.066	.843**	.860**	.795*	-.096	.189	.105	.326	.208	.814*	1					
Fe (M.r)	.234	.907**	.727*	.722*	.094	.118	.061	.204	.444	.932**	.958**	1				
Pb (M.r)	.130	.374	-.203	.118	.258	-.227	.107	-.222	.992**	.702	.267	.483	1			
Mn (M.r)	.341	-.165	-.426	-.748*	.392	-.340	-.549	-.124	-.077	-.463	-.521	-.433	-.184	1		
Ni (M.r)	.229	.701	.143	.557	.018	.031	.298	-.318	.622	.644	.510	.639	.600	-.285	1	
Zn (M.r)	-.207	.538	.397	.312	-.390	-.090	-.001	.131	-.020	.119	.497	.414	-.034	.119	.426	1

Note: *. Correlation is significant at the 0.05 level (2-tailed), **. Correlation is significant at the 0.01 level (2-tailed).

Table 4.26: Pearson Correlation Coefficients between Metals in Sediment (S) and *M. vollenhovenii* (M.v)

	Cadmium (S)	Chromium (S)	Copper (S)	Iron (S)	Lead (S)	Manganese (S)	Nickel (S)	Zinc (S)	Cd (M.v)	Cr (M.v)	Cu (M.v)	Fe (M.v)	Pb (M.v)	Mn (M.v)	Ni (M.v)	Zn (M.v)
Cadmium (S)	1															
Chromium (S)	.335	1														
Copper (S)	.074	.679	1													
Iron (S)	-.048	.679	.764*	1												
Lead (S)	.709*	.280	-.034	-.097	1											
Manganese (S)	.032	.256	.461	.633	.343	1										
Nickel (S)	-.342	.127	.134	.631	-.005	.786*	1									
Zinc (S)	-.162	.251	.603	.403	.250	.716*	.418	1								
Cd (M.v)	-.323	.345	.043	.397	.071	.335	.660	.405	1							
Cr (M.v)	-.130	.347	.043	-.039	-.248	-.252	-.128	-.027	.286	1						
Cu (M.v)	-.095	.356	-.010	-.025	-.230	-.246	-.088	-.100	.297	.993**	1					
Fe (M.v)	-.085	.416	.048	.053	-.242	-.216	-.055	-.097	.311	.986**	.996**	1				
Pb (M.v)	-.079	.302	-.129	-.022	.132	-.335	-.041	-.001	.665	.189	.183	.181	1			
Mn (M.v)	.242	.605	.113	.061	.341	-.291	-.217	.048	.504	.315	.305	.314	.894**	1		
Ni (M.v)	-.558	-.164	.012	.241	-.738*	.126	.399	-.085	.078	.440	.460	.474	-.441	-.566	1	
Zn (M.v)	.413	.084	-.383	-.107	.187	-.015	.054	-.546	-.165	.317	.413	.416	-.338	-.198	.299	1

Note: *. Correlation is significant at the 0.05 level (2-tailed), **. Correlation is significant at the 0.01 level (2-tailed).

4.9.1.3. Environmental Quality and Prawn Biological Traits

The correlation analysis between water parameters and the biological indices, Gonadosomatic Index (GSI), Hepatosomatic Index (HSI), and Condition Factor (CF), reveals how environmental conditions may influence prawn physiology (Table 4.27). GSI showed a moderate positive correlation with water pH ($r = 0.393$) and nitrate (NO_4^-) ($r = 0.321$). Conversely, GSI was negatively associated with sediment Cadmium (W) ($r = -0.676$). HSI was strongly negatively correlated with salinity ($r = -0.806$, $p < 0.05$). Other water parameters such as air and water temperature showed moderate positive correlations with HSI ($r = 0.499$ and 0.418, respectively). Condition Factor (CF) displayed a strong positive correlation with salinity ($r = 0.826$, $p < 0.05$). CF was also negatively correlated with dissolved Cd (W) ($r = -0.797$, $p < 0.05$). Moderate positive associations of CF with Cu ($r = 0.746$, $p < 0.05$) and Fe ($r = 0.702$) was observed.

The Pearson correlation analysis between sediment characteristics, sediment metals, and biological indices including Gonadosomatic Index (GSI), Hepatosomatic Index (HSI), and Condition Factor (CF) in prawns is presents in Table 4.28. Sediment pH showed moderate positive correlations with Chromium (S) ($r = 0.421$), Iron (S) ($r = 0.506$), and Nickel (S) ($r = 0.340$). Sediment conductivity and moisture exhibited weaker or inconsistent associations with sediment metals. Among the sediment metals, Cadmium (S) was strongly correlated with Lead (S) ($r = 0.709$, $p < 0.05$), while Copper (S) was significantly associated with Iron (S) ($r = 0.764$, $p < 0.05$) and Chromium (S) ($r = 0.679$). Manganese (S) was strongly correlated with Nickel (S) ($r = 0.786$, $p < 0.05$) and Zinc (S) ($r = 0.716$, $p < 0.05$). GSI showed moderate positive correlations with Chromium (S) ($r = 0.617$) and Copper (S) ($r = 0.451$). HSI was strongly positively correlated with Lead (S) ($r = 0.765$, $p < 0.05$). Condition Factor (CF) was positively associated with sediment pH ($r = 0.703$) and sediment moisture ($r = 0.689$), but negatively correlated with Lead (S) ($r = -0.624$) and HSI ($r = -0.644$).

Table 4.27: Pearson Correlation between Water Quality Parameters and Prawn Biological Indices (GSI, HSI, CF)

	Air Temp. (W)	Water Temp. (W)	pH (W)	Salinity (W)	EC (W)	TDS (W)	ORP (W)	DO (W)	BOD (W)	SO4 (W)	PO4 (W)	NO4 (W)	Cd (W)	Cr (W)	Cu (W)	Fe (W)	Pb (W)	Mn (W)	Ni (W)	Zn (W)	GSI	HSI	CF
Air Temp. (W)	1																						
Water Temp. (W)	.178	1																					
pH (W)	.476	-.017	1																				
Salinity (W)	-.366	-.383	.043	1																			
EC (W)	.225	.991**	.076	-.414	1																		
TDS (W)	.226	.995**	.057	-.403	.999**	1																	
ORP (W)	.005	.888**	-.430	-.333	.853**	.861**	1																
DO (W)	-.295	-.156	.156	.166	-.177	-.185	-.206	1															
BOD (W)	.808*	-.032	.466	-.548	.048	.037	-.204	-.476	1														
SO4 (W)	-.590	-.558	-.640	.060	-.572	-.576	-.213	-.206	-.201	1													
PO4 (W)	.583	-.135	.688	-.132	-.064	-.081	-.355	.240	.622	-.426	1												
NO4 (W)	.587	.353	.810*	-.081	.399	.392	-.019	.357	.279	-.939**	.589	1											
Cd (W)	-.066	-.139	-.294	.349	-.194	-.168	-.074	-.642	.049	.259	-.253	-.473	1										
Cr (W)	-.276	-.430	-.061	.745*	-.502	-.484	-.368	.593	-.624	-.072	-.122	.081	.013	1									
Cu (W)	-.284	-.449	.200	.700	-.478	-.475	-.468	.769*	-.563	-.141	.096	.260	-.269	.920**	1								
Fe (W)	-.334	-.453	-.055	.686	-.507	-.499	-.354	.745*	-.639	-.006	-.001	.080	-.196	.952**	.959**	1							
Pb (W)	.472	.499	.012	-.440	.469	.490	.331	-.529	.362	-.411	-.225	.200	.339	-.338	-.552	-.575	1						
Mn (W)	-.157	-.339	-.684	.354	-.441	-.413	-.001	.103	-.440	.329	-.432	-.441	.257	.644	.360	.574	-.071	1					
Ni (W)	-.088	-.307	-.738*	-.057	-.353	-.346	.128	-.007	-.105	.598	-.143	-.612	.033	.111	-.035	.219	-.344	.706	1				
Zn (W)	-.070	-.067	-.882**	-.062	-.157	-.133	.334	-.214	-.219	.453	-.508	-.617	.282	.157	-.152	.112	.126	.851**	.837**	1			
GSI	-.013	-.181	.393	-.020	-.118	-.138	-.292	.305	-.079	-.100	-.103	.321	-.676	.143	.348	.192	-.156	-.176	-.290	-.342	1		
HSI	.499	.418	.108	-.806*	.422	.419	.296	.143	.503	-.391	.486	.378	-.319	-.449	-.407	-.380	.355	-.271	.032	-.015	-.266	1	
CF	-.519	-.076	.015	.826*	-.136	-.121	-.117	.404	-.797*	-.155	-.363	.089	.133	.792*	.746*	.702	-.212	.291	-.303	-.130	.146	-.644	1

Note: *. Correlation is significant at the 0.05 level (2-tailed), **. Correlation is significant at the 0.01 level (2-tailed).

Table 4.28: Pearson Correlation between Sediment Parameters and Prawn Biological Indices (GSI, HSI, CF)

	Sediment pH	Sediment Conductivity (µS/cm)	Sediment Moisture (%)	Cadmium (S)	Chromium (S)	Copper (S)	Iron (S)	Lead (S)	Manganese (S)	Nickel (S)	Zinc (S)	GSI	HSI	CF
Sediment pH	1													
Sediment Conductivity (µS/cm)	.193	1												
Sediment Moisture (%)	.480	.128	1											
Cadmium (S)	-.242	.206	-.073	1										
Chromium (S)	.421	.167	-.080	.335	1									
Copper (S)	.136	-.265	-.244	.074	.679	1								
Iron (S)	.506	.256	.202	-.048	.679	.764*	1							
Lead (S)	-.514	.310	-.247	.709*	.280	-.034	-.097	1						
Manganese (S)	-.085	.097	.263	.032	.256	.461	.633	.343	1					
Nickel (S)	.340	.386	.500	-.342	.127	.134	.631	-.005	.786*	1				
Zinc (S)	-.220	-.334	-.319	-.162	.251	.603	.403	.250	.716*	.418	1			
GSI	.400	.029	-.452	.173	.617	.451	.259	-.178	-.484	-.471	-.184	1		
HSI	-.268	.236	-.290	.290	.195	.015	.051	.765*	.504	.344	.609	-.266	1	
CF	.703	-.298	.689	-.278	.226	.159	.296	-.624	-.078	.125	-.270	.146	-.644	1

Note: *. Correlation is significant at the 0.05 level (2-tailed), **. Correlation is significant at the 0.01 level (2-tail)

The correlation analysis presented in Table 4.29 highlights how the condition indices of *Macrobrachium macrobrachion*, Gonadosomatic Index (GSI), Hepatosomatic Index (HSI), and Condition Factor (CF), relate to bioaccumulated trace metals. For the GSI, positive correlations were observed with cadmium (r = 0.451), chromium (r = 0.326), copper (r = 0.469), and iron (r = 0.417), but none were statistically significant ($p > 0.05$). Negative but non-significant correlations were found with manganese (r = –0.234), nickel (r = –0.112), and zinc (r = –0.011). The HSI showed weak, non-significant positive correlations with all measured metals, including cadmium (r = 0.167), chromium (r = 0.063), copper (r = 0.119), iron (r = 0.085), lead (r = 0.160), manganese (r = 0.032), nickel (r = 0.021), and zinc (r = 0.052), with no associations reaching statistical significance ($p > 0.05$). The CF exhibited negative correlations with cadmium (r = –0.226), chromium (r = –0.066), copper (r = –0.067), iron (r = –0.083), lead (r = –0.457), manganese (r = –0.294), and zinc (r = –0.551). A positive but non-significant correlation was recorded with nickel (r = 0.343). None of these relationships were statistically significant ($p > 0.05$).

The correlation analysis presented in Table 4.30 highlights how the condition indices of *Macrobrachium rosenbergii*, Gonadosomatic Index (GSI), Hepatosomatic Index (HSI), and Condition Factor (CF), relate to bioaccumulated trace metals. For the GSI, a strong and highly significant positive correlation was observed with zinc (r = 1.000, $p < 0.01$). Other positive but non-significant correlations were found with chromium (r = 0.114), copper (r = 0.491), iron (r = 0.409), manganese (r = 0.130), and nickel (r = 0.422). Negative but weak correlations were recorded with cadmium (r = –0.021) and lead (r = –0.036). The HSI showed weak, non-significant correlations with all metals. Negative correlations were found with cadmium (r = –0.023), chromium (r = –0.100), copper (r = –0.094), iron (r = –0.092), lead (r = –0.029), and nickel (r = –0.341). Positive but non-significant correlations occurred with manganese (r = 0.329) and zinc (r

= 0.002). The CF exhibited significant positive correlations with cadmium ($r = 0.771$, $p < 0.05$) and lead ($r = 0.751$, $p < 0.05$). Other positive but non-significant correlations were noted with chromium ($r = 0.530$), iron ($r = 0.314$), manganese ($r = 0.147$), and nickel ($r = 0.276$). Negative, non-significant correlations were observed with copper ($r = 0.091$) and zinc ($r = –0.208$).

The correlation analysis in Table 4.31 highlights how the condition indices of *Macrobrachium vollenhovenii*, Gonadosomatic Index (GSI), Hepatosomatic Index (HSI), and Condition Factor (CF) relate to bioaccumulated trace metals. For the GSI, a significant positive correlation was observed with manganese ($r = 0.712$, $p < 0.05$). Other positive but non-significant correlations were found with chromium ($r = 0.303$), copper ($r = 0.295$), iron ($r = 0.330$), lead ($r = 0.473$), and HSI itself ($r = 0.657$). Negative, non-significant correlations occurred with cadmium ($r = –0.066$), nickel ($r = –0.348$), and zinc ($r = –0.063$). The HSI showed positive but non-significant correlations with most metals, including chromium ($r = 0.533$), copper ($r = 0.496$), iron ($r = 0.494$), lead ($r = 0.436$), manganese ($r = 0.453$), and nickel ($r = 0.073$). Negative correlations were observed with cadmium ($r = –0.031$) and zinc ($r = –0.216$). The CF displayed a significant negative correlation with zinc ($r = –0.728$, $p < 0.05$). Positive but non-significant correlations were noted with cadmium ($r = 0.009$), chromium ($r = 0.117$), copper ($r = 0.025$), iron ($r = 0.025$), lead ($r = 0.486$), manganese ($r = 0.585$), and HSI ($r = 0.665$). A negative, non-significant correlation was observed with nickel ($r = –0.451$).

Table 4.29: Correlation Matrix of Trace Metal Concentrations in *Macrobrachium macrobrachion* (M.m) with Condition Indices

	Cd (M.m)	Cr (M.m)	Cu (M.m)	Fe (M.m)	Pb (M.m)	Mn (M.m)	Ni (M.m)	Zn (M.m)	Mean GSI	Mean HSI	Mean CF
Cd (M.m)	1										
Cr (M.m)	-.126	1									
Cu (M.m)	.078	.970**	1								
Fe (M.m)	.086	.977**	.993**	1							
Pb (M.m)	-.506	.416	.262	.279	1						
Mn (M.m)	-.121	-.730*	-.800*	-.781*	.289	1					
Ni (M.m)	-.380	-.105	-.094	-.171	-.315	-.314	1				
Zn (M.m)	.349	-.303	-.338	-.261	.317	.679	-.785*	1			
Mean GSI	.451	.326	.469	.417	.118	-.234	-.112	-.011	1		
Mean HSI	.167	.063	.119	.085	.160	.032	.021	.052	.160	1	
Mean CF	-.226	-.066	-.067	-.083	-.457	-.294	.343	-.551	-.466	.253	1

Note: *. Correlation is significant at the 0.05 level (2-tailed), **. Correlation is significant at the 0.01 level (2-tailed).

Table 4.30: Correlation Matrix of Trace Metal Concentrations in *Macrobrachium rosenbergii* (M.r) with Condition Indices

	Cd (M.r)	Cr (M.r)	Cu (M.r)	Fe (M.r)	Pb (M.r)	Mn (M.r)	Ni (M.r)	Zn (M.r)	Mean GSI	Mean HSI	Mean CF
Cd (M.r)	1										
Cr (M.r)	.664	1									
Cu (M.r)	.208	.814*	1								
Fe (M.r)	.444	.932**	.958**	1							
Pb (M.r)	.992**	.702	.267	.483	1						
Mn (M.r)	-.077	-.463	-.521	-.433	-.184	1					
Ni (M.r)	.622	.644	.510	.639	.600	-.285	1				
Zn (M.r)	-.020	.119	.497	.414	-.034	.119	.426	1			
Mean GSI	-.021	.114	.491	.409	-.036	.130	.422	1.000**	1		
Mean HSI	-.023	-.100	-.094	-.092	-.029	.329	-.341	.002	.006	1	
Mean CF	.771*	.530	.091	.314	.751*	.147	.276	-.208	-.206	-.267	1

Note: *. Correlation is significant at the 0.05 level (2-tailed), **. Correlation is significant at the 0.01 level (2-tailed).

Table 4.31: Correlation Matrix of Trace Metal Concentrations in *Macrobrachium vollenhovenii* (M.v) with Condition Indices

	Cd (M.v)	Cr (M.v)	Cu (M.v)	Fe (M.v)	Pb (M.v)	Mn (M.v)	Ni (M.v)	Zn (M.v)	Mean GSI	Mean HSI	Mean CF
Cd (M.v)	1										
Cr (M.v)	.286	1									
Cu (M.v)	.297	.993**	1								
Fe (M.v)	.311	.986**	.996**	1							
Pb (M.v)	.665	.189	.183	.181	1						
Mn (M.v)	.504	.315	.305	.314	.894**	1					
Ni (M.v)	.078	.440	.460	.474	-.441	-.566	1				
Zn (M.v)	-.165	.317	.413	.416	-.338	-.198	.299	1			
Mean GSI	-.066	.303	.295	.330	.473	.712*	-.348	-.063	1		
Mean HSI	-.031	.533	.496	.494	.436	.453	.073	-.216	.657	1	
Mean CF	.009	.117	.025	.025	.486	.585	-.451	-.728*	.608	.665	1

Note: *. Correlation is significant at the 0.05 level (2-tailed), **. Correlation is significant at the 0.01 level (2-tailed).

4.10: Multivariate Analysis

4.10.1. Canonical Correspondence Analysis

The CCA plot (Figure 4.62) for water physicochemical parameters and the abundance of *Macrobrachium dux, M. equidens, M. macrobrachion, M. rosenbergii,* and *M. vollenhovenii* show that the first two canonical axes explain 98.45% of the total variance, with Axis 1 contributing 90.73% (eigenvalue = 0.11891) and Axis 2 contributing 7.72% (eigenvalue = 0.010119). Salinity, Cr, Cu, Fe, SO_4, and DO exhibited strong positive associations on Axis 1, while Pb, Air Temperature, Water Temperature, EC, TDS, ORP, and BOD showed strong negative associations. In terms of prawn abundance, *M. vollenhovenii* and *M. dux* were positively aligned with Axis 1, indicating that their distribution was favored under conditions of higher salinity, trace metals (Cr, Cu, Fe), and dissolved oxygen. *M. equidens* showed a weak positive association, while *M. macrobrachion* and *M. rosenbergii* were negatively aligned. The CCA plot (Figure 4.63) for sediment parameters and prawn abundance show that the first two canonical axes explain 98.45% of the total variance, with Axis 1 contributing 90.73% (eigenvalue = 0.11891) and Axis 2 contributing 7.72% (eigenvalue = 0.010119). Sediment pH (0.4497) and Copper (0.2183) showed positive associations on Axis 1, while Lead (−0.9158), Cadmium (−0.4623), Manganese (−0.4731), Nickel (−0.2910), and Sediment Conductivity (−0.4514) exhibited strong negative loadings. Other parameters such as Iron (0.0738), Zinc (−0.2304), and Chromium (−0.1272) displayed weaker influences. In terms of prawn abundance, *M. vollenhovenii* (0.6539) and *M. dux* (0.1601) showed positive associations with Axis 1. *M. equidens* also aligned weakly with these conditions. In contrast, *M. macrobrachion* (−0.2878) and *M. rosenbergii* (−0.0296) were negatively associated. The CCA plot (Figure 4.64) shows that the first two canonical axes explain 75.9% of the total variance, with Axis 1 contributing 49.96% (eigenvalue = 0.31983) and Axis 2 contributing 25.94% (eigenvalue = 0.16605). Several water quality parameters, including BOD (0.6992), PO_4 (0.6497), and pH (0.3037), exhibited strong positive associations on Axis 1, whereas Cr

(−0.5739), Mn (−0.4599), Cu (−0.3501), Pb (−0.3538), and Fe (−0.3859) showed strong negative loadings. Salinity (−0.3940), EC (−0.1722), TDS (−0.2027), and ORP (−0.2759) also contributed negatively, indicating a strong gradient of ionic and redox conditions along Axis 1. In relation to heavy metal bioaccumulation, Zn in *M. macrobrachion* (1.0344) and Cd in *M. macrobrachion* (0.6540) exhibited strong positive associations on Axis 1. Conversely, Cr (−0.6390), Cu (−0.4872), and Fe (−0.5492) in *M. macrobrachion*, as well as several metals in *M. vollenhovenii* (e.g. Cu −0.4764; Fe −0.5700; Cr −0.3406), were negatively associated with Axis 1. On Axis 2, Cd in *M. macrobrachion* (1.3930) and Zn in *M. macrobrachion* (−0.4131) were strongly differentiated, while water Cr (0.5875), Cu (0.5439), Fe (0.4342), and Ni (−0.2757) defined much of the positive and negative structure.

The CCA plot (Figure 4.65) shows that the first two canonical axes explain 75.9% of the total variance in the relationship between sediment characteristics and bioaccumulated heavy metals in prawns, with Axis 1 contributing 49.96% (eigenvalue = 0.31983) and Axis 2 contributing 25.94% (eigenvalue = 0.16605). On Axis 1, positive associations were observed for Zn in *M. macrobrachion* (1.0344) and Cd in *M. macrobrachion* (0.6540. In contrast, Cr (−0.6390), Cu (−0.4872), and Fe (−0.5492) in *M. macrobrachion*, along with Cu (−0.4764) and Fe (−0.5700) in *M. vollenhovenii*, showed strong negative loadings, aligning their bioaccumulation with sediments enriched in Cr, Fe, and Cu. Axis 2 further separated bioaccumulation patterns, with Cd in *M. macrobrachion* (1.3930) and Cu/Fe in *M. rosenbergii* (0.4407; 0.4418) showing strong positive associations, whereas Zn in *M. macrobrachion* (−0.4131), Pb in *M. macrobrachion* (−0.5420), and several metals in *M. vollenhovenii* aligned negatively. Sediment parameters also played defining roles: sediment moisture (−0.8654), pH (−0.7327), and conductivity (−0.2856) loaded negatively on Axis 1, suggesting that higher metal accumulation (especially Cr, Cu, Fe) in prawns occurs under acidic, moist, and conductive sediment conditions. Conversely, sediment Zn (0.4650) and Cu (0.1545) loaded positively, reinforcing their direct influence on Zn and Cd accumulation in *M. macrobrachion*.

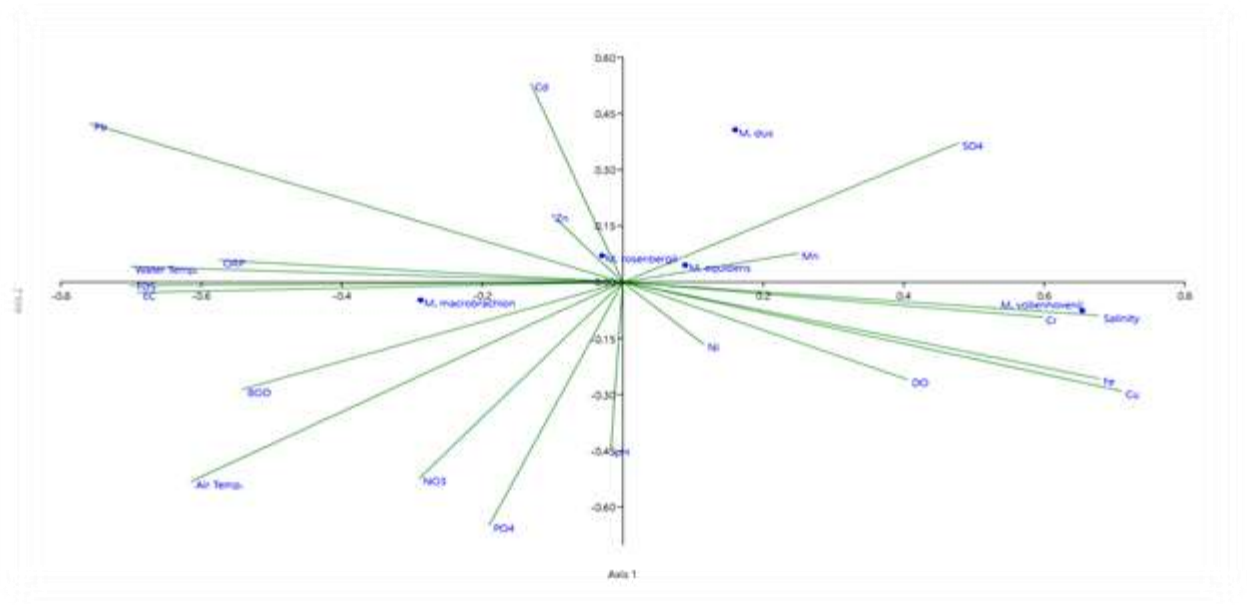

Figure 4.62: CCA triplot depicting the relationship between Water Physicochemical Parameters and Prawn Abundance

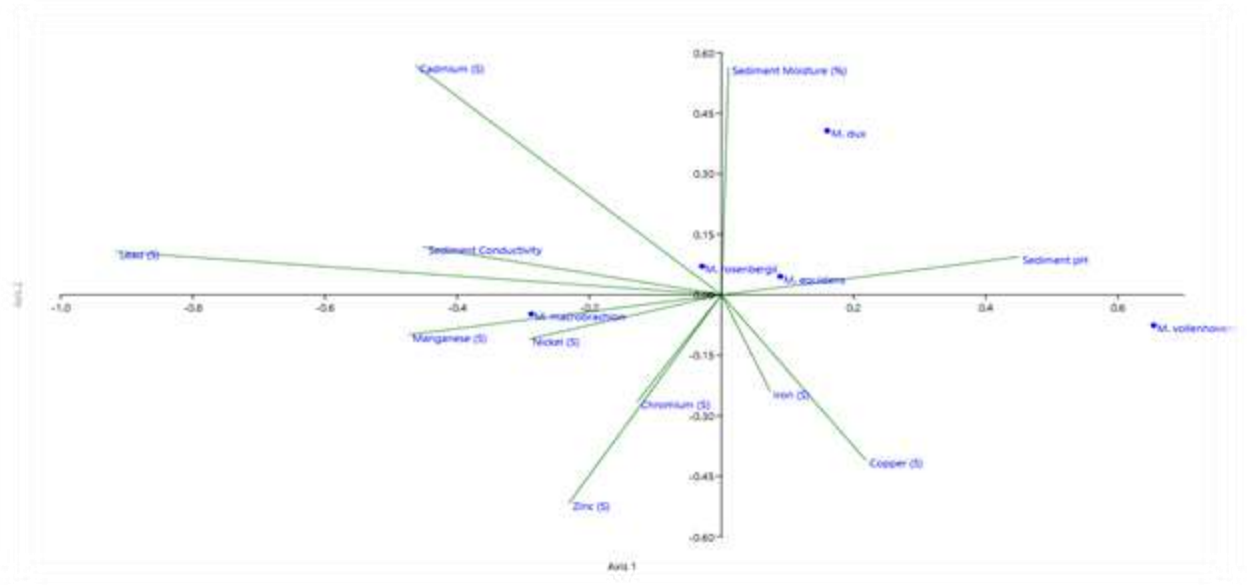

Figure 4.63: CCA triplot depicting the relationship between Sediment Physicochemical Parameters and Prawn Abundance

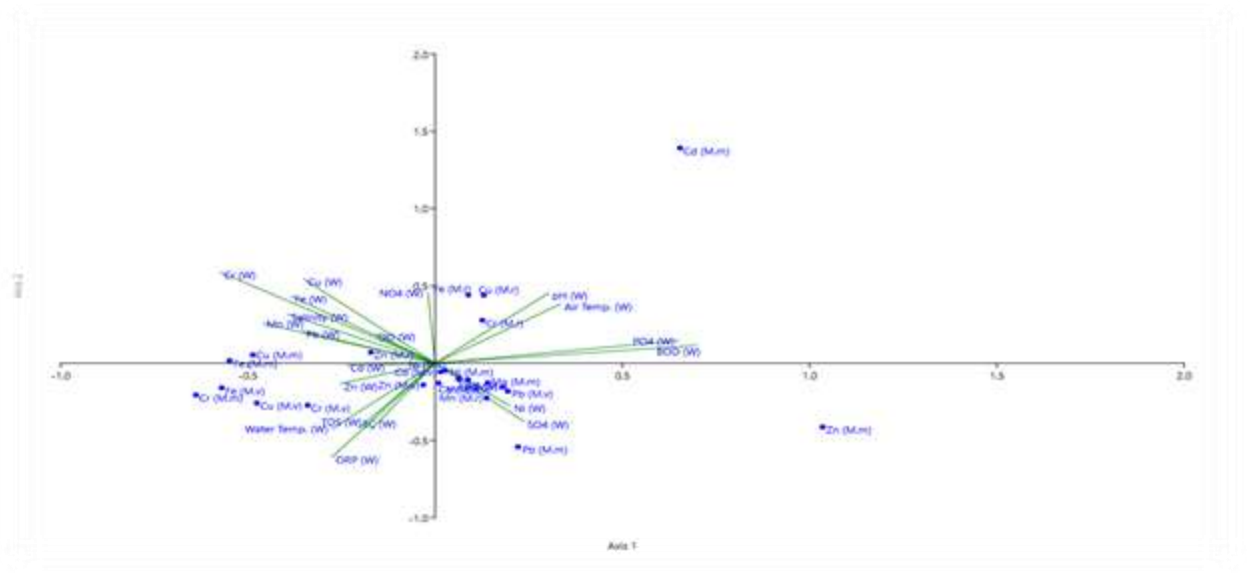

Figure 4.64: CCA triplot depicting the relationship between water Physicochemical Parameters and Heavy metal bioaccumulation in Prawn

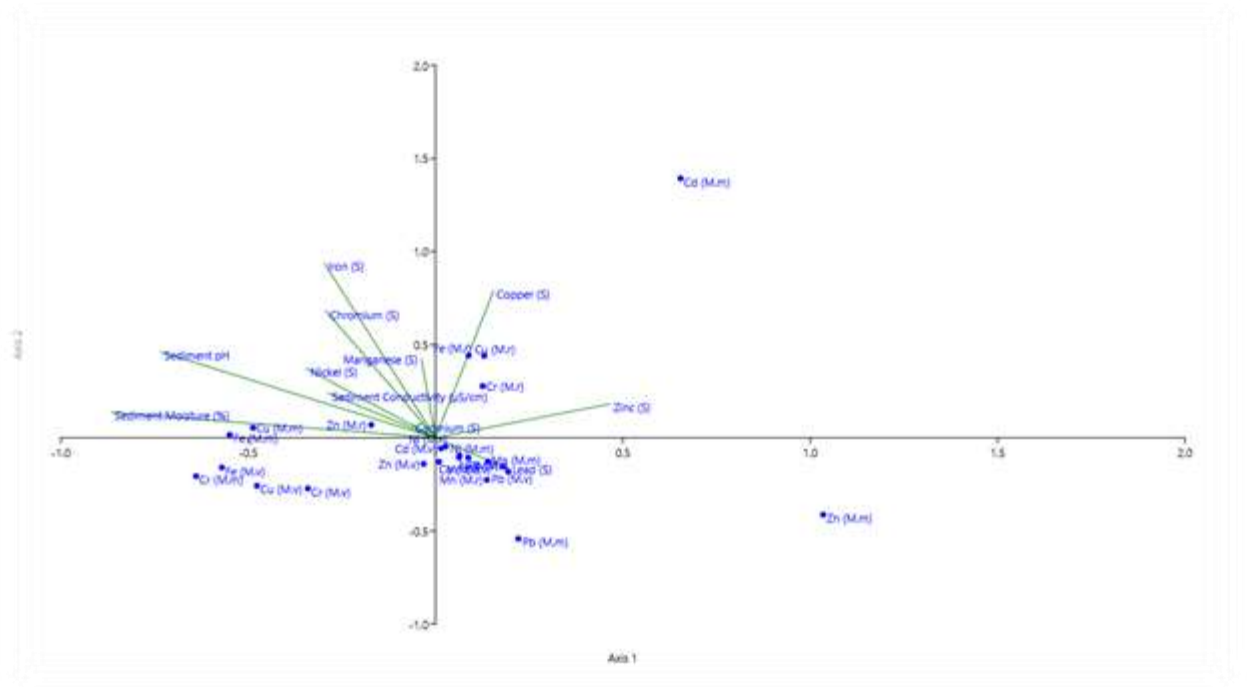

Figure 4.65: CCA triplot depicting the relationship between Sediment Physicochemical Parameters and Heavy metal bioaccumulation in Prawn

The CCA plot (Figure 4.66) shows that the first canonical axis (Axis 1) explains 87.1% of the variation, while Axis 2 accounts for 12.9%, together explaining 100% of the total variance in the relationship between water physicochemical parameters and condition indices (GSI, HSI, CF). On Axis 1, GSI (0.536) showed a strong positive correlation. In contrast, HSI (−0.012) and CF (0.010) were weakly aligned with Axis 1. Along Axis 2, CF (0.058) aligned positively, showing that body condition responds more to secondary environmental gradients, while GSI and HSI remained weakly loaded. Among physicochemical parameters, water pH (0.379), DO (0.304), Cu (0.385), Cr (0.181), and Fe (0.229) loaded positively on Axis 1, indicating that higher pH, oxygenation, and trace metal availability favor prawn reproductive development (higher GSI). In contrast, Cd (−0.644), Zn (−0.344), and ORP (−0.314) aligned negatively. On Axis 2, salinity (0.929), Cu (0.540), Fe (0.551), and Cr (0.655) showed strong positive associations, corresponding to the alignment of CF (0.058). Conversely, BOD (−0.707), PO_4 (−0.441), and Ni (−0.093) loaded negatively on Axis 2.

The CCA plot (Figure 4.67) shows that the first canonical axis (Axis 1) explains 87.1% of the variation, while Axis 2 accounts for 12.9%, together explaining 100% of the total variance in the relationship between sediment parameters and condition indices (GSI, HSI, CF). On Axis 1, GSI (0.536) showed a strong positive correlation. In contrast, HSI (−0.012) and CF (0.010) were weakly aligned with Axis 1. Along Axis 2, CF (0.058) aligned positively, showing that body condition responds more to secondary sediment gradients, while GSI and HSI remained weakly loaded. Among sediment parameters, Chromium (0.578), Copper (0.441), and pH (0.412) loaded positively on Axis 1. In contrast, Manganese (−0.518), Nickel (−0.494), and Lead (−0.249) aligned negatively with Axis 1. On Axis 2, Sediment Moisture (0.698) and pH (0.418) showed strong positive associations, corresponding to the alignment of CF (0.058). Conversely, Lead (−0.725), Zinc (−0.433), and Cadmium (−0.383) loaded negatively on Axis 2.

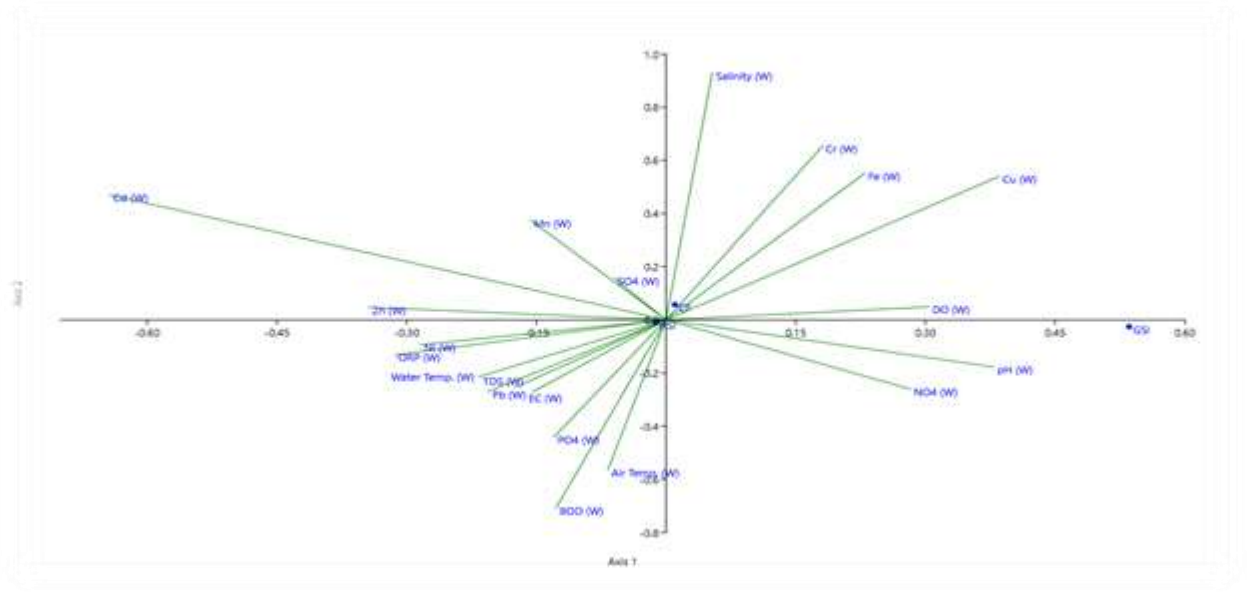

Figure 4.66: CCA triplot depicting the relationship between Water Physicochemical Parameters and Condition Indices (GSI, HSI and CF)

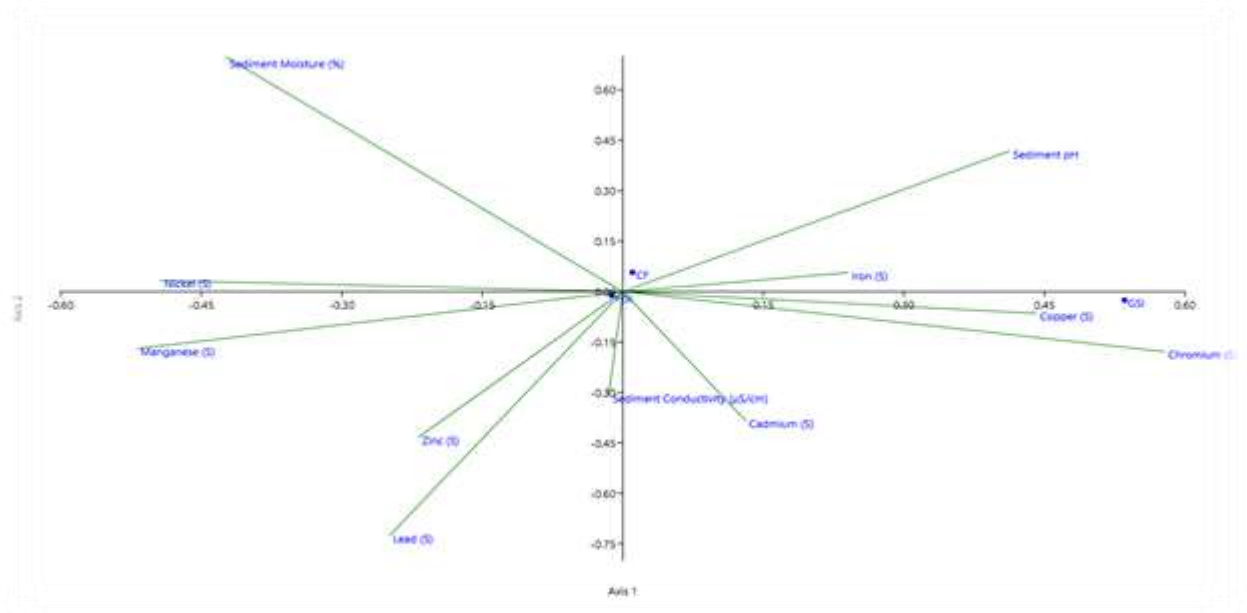

Figure 4.67: CCA triplot depicting the relationship between Sediment Parameters and Condition Indices (GSI, HSI and CF)

The CCA plot (Figure 4.68) shows that the first canonical axis (Axis 1) explains 86.64% of the variation, while Axis 2 accounts for 13.36%, together explaining 100% of the total variance in the relationship between bioaccumulated heavy metals in *Macrobrachium macrobrachion* and condition indices (GSI, HSI, CF). On Axis 1, GSI (−0.330) displayed a moderate negative correlation, suggesting that gonadal development in *M. macrobrachion* is inversely associated with the primary gradient of bioaccumulated metals along this axis. In contrast, HSI (−0.018) and CF (0.112) were weakly aligned with Axis 1. Along Axis 2, GSI (0.147) and HSI (−0.011) remained weakly loaded, whereas CF (0.034) showed a slight positive alignment. Among metals, Ni (0.243) loaded positively on Axis 1, while Cd, Cr, Cu, Fe, Pb, and Zn aligned negatively. Mn had negligible loading on Axis 1, indicating minimal effect. On Axis 2, Cd (0.112), Cr (0.158), Cu (0.221), and Fe (0.203) loaded positively, aligning weakly with CF. In contrast, Pb (−0.271), Mn (−0.345), and Zn (−0.300) loaded negatively on Axis 2. Seasonal points also showed variation: December (3.292) and August (0.913) aligned positively on Axis 2, whereas May (−1.722) and June (−0.721) loaded negatively. The CCA plot (Figure 4.69) shows that the first canonical axis (Axis 1) explains 85.7% of the variation, while Axis 2 accounts for 14.3%, together explaining 100% of the total variance in the relationship between bioaccumulated heavy metals in *Macrobrachium rosenbergii* and condition indices (GSI, HSI, CF). On Axis 1, GSI (0.837) showed a strong positive correlation. In contrast, HSI (−0.011) and CF (−0.059) were weakly aligned with Axis 1. Along Axis 2, CF (0.115) aligned positively, while GSI remained dominant on Axis 1 and HSI stayed weakly loaded. Among metals, Zinc (0.996), Copper (0.490), Nickel (0.391), and Iron (0.387) loaded strongly and positively on Axis 1. In contrast, Cadmium (−0.091) and Lead (−0.101) aligned negatively with Axis 1, suggesting that increased Cd and Pb levels may suppress reproductive development. On Axis 2, Cadmium (0.670), Lead (0.653), and Chromium (0.512) loaded positively, corresponding to the alignment of CF (0.115). Conversely, negative associations of season points such as November (−1.861) and December (−1.056) along Axis 2.

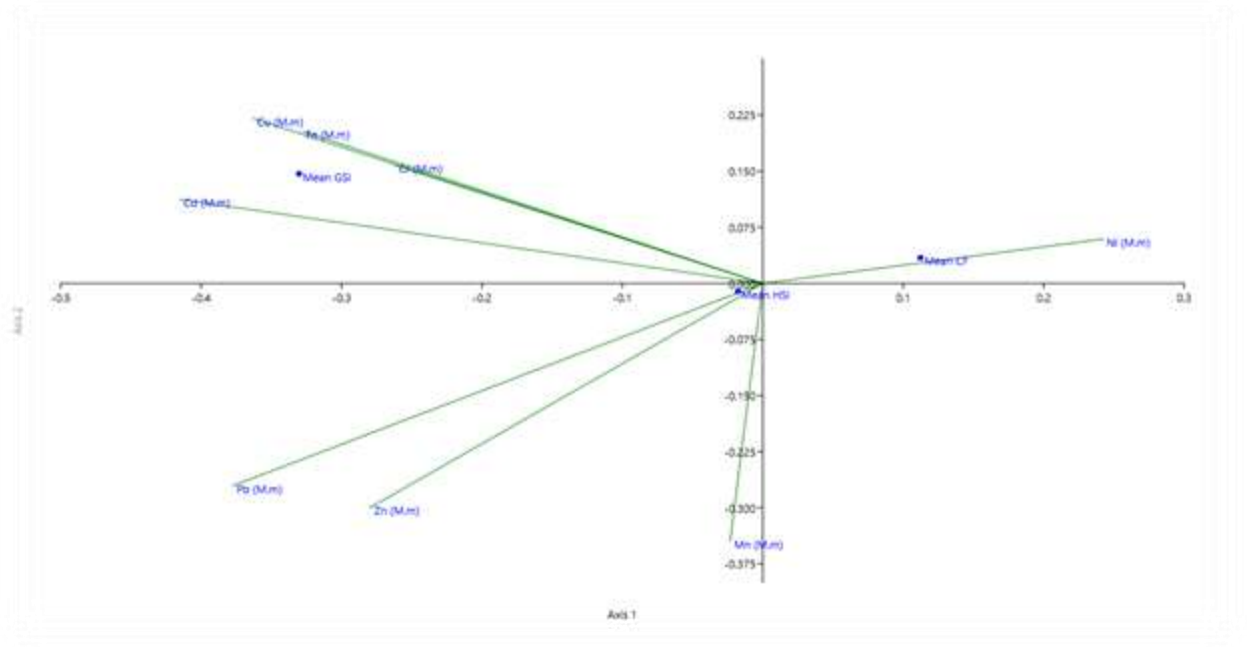

Figure 4.68: CCA triplot depicting the relationship between bioaccumulated heavy metals in *M. macrobrachion* and Condition Indices (GSI, HSI and CF)

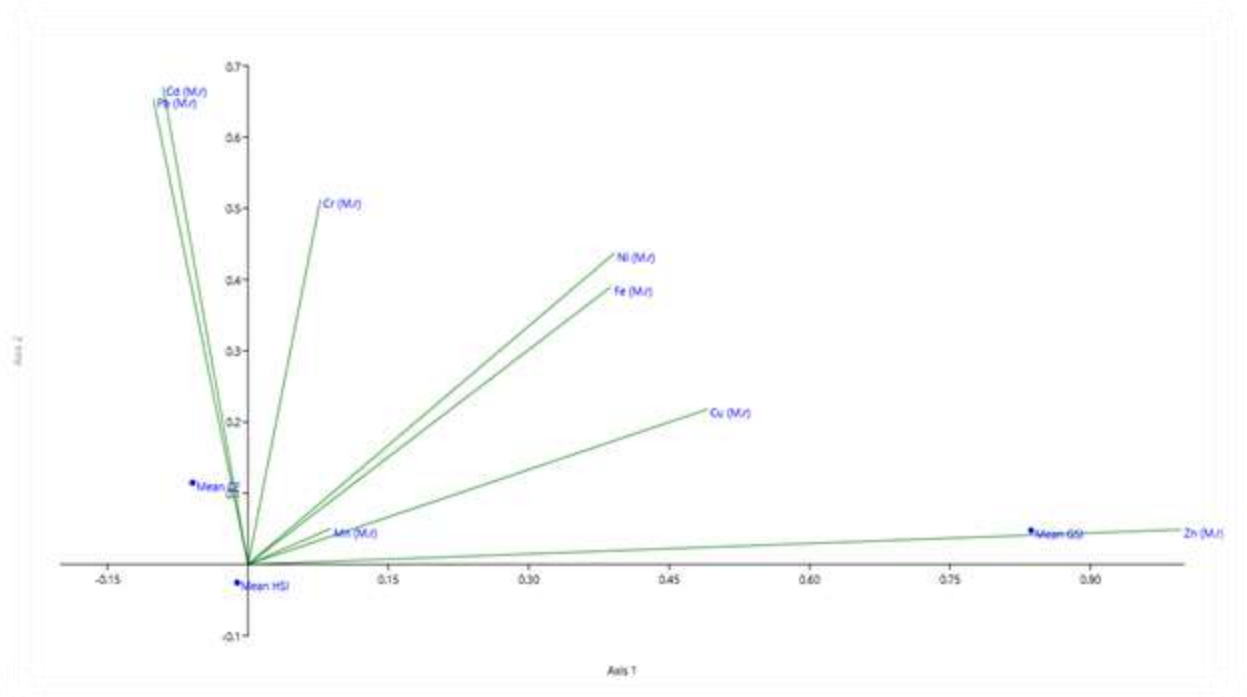

Figure 4.69: CCA triplot depicting the relationship between bioaccumulated heavy metals in *M. rosenbergii* and Condition Indices (GSI, HSI and CF)

The CCA plot (Figure 4.70) shows that the first canonical axis (Axis 1) explains 82.4% of the variation, while Axis 2 accounts for 17.6%, together explaining 100% of the total variance in the relationship between bioaccumulated heavy metals in *Macrobrachium vollenhovenii* and condition indices (GSI, HSI, CF). On Axis 1, GSI (0.654) showed a strong positive correlation. In contrast, HSI (−0.012) and CF (−0.001) were weakly aligned with Axis 1. Along Axis 2, CF (0.073) aligned positively, while GSI and HSI remained weakly loaded. Among the metals, Manganese (0.712), Lead (0.456), and Iron (0.298) loaded positively on Axis 1. In contrast, Nickel (−0.377) and Zinc (−0.027) aligned negatively. On Axis 2, Manganese (0.237) and Lead (0.155) aligned positively, corresponding with the positive loading of CF (0.073). Conversely, Zinc (−0.719), Nickel (−0.629), and Copper (−0.479) loaded negatively. June (1.591, 0.026) clustered strongly along Axis 1, corresponding to higher GSI and Mn/Pb associations. In contrast, September (−1.146, −0.943) and July (0.460, −1.428) aligned negatively along Axis 2.

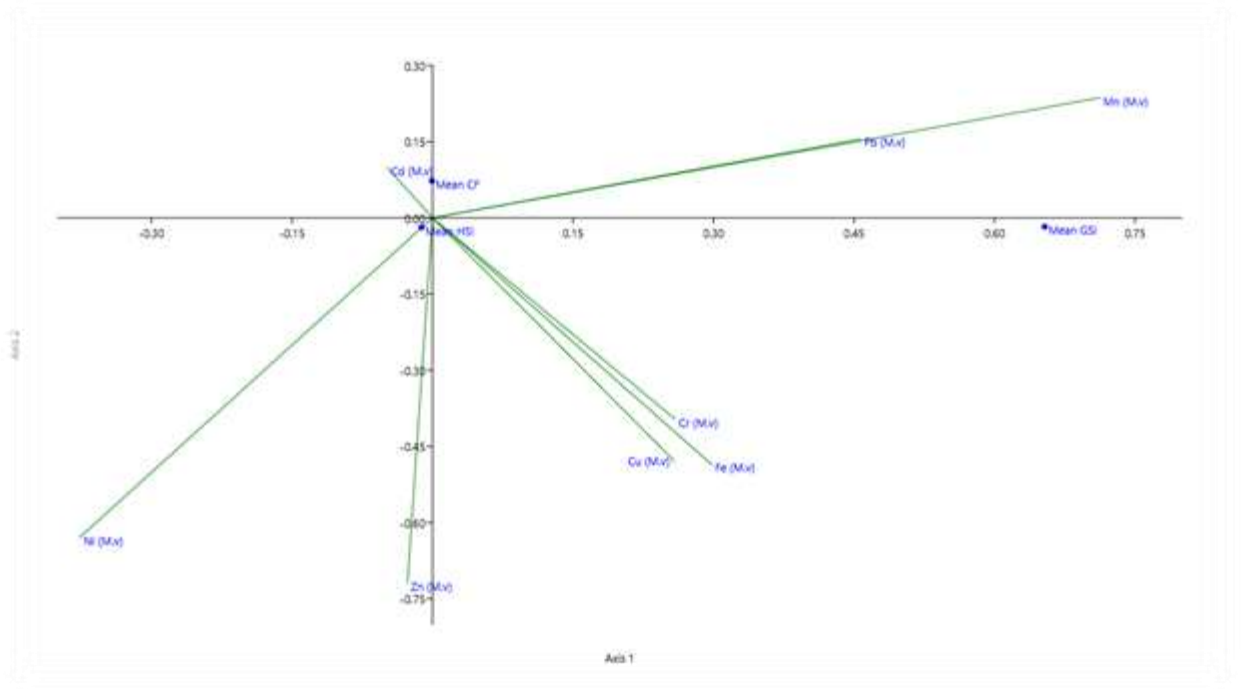

Figure 4.70: CCA triplot depicting the relationship between bioaccumulated heavy metals in *M. vollenhovenii* and Condition Indices (GSI, HSI and CF)

4.11. Evaluation of Environmental Risk Assessment

4.11.1 Geo-accumulation Index (*Igeo*)

The geo-accumulation index (Igeo) (Table 4.32) results for the analyzed metals across both stations indicate that the sediments are generally unpolluted. The Igeo values for cadmium ranged from -4.08 at Station 1 to -4.18 at Station 2, with a mean value of -4.13, indicating an unpolluted status. Chromium recorded Igeo values of -9.00 and -9.46 for Stations 1 and 2 respectively, with a mean of -9.23, also classified as unpolluted. Similarly, copper exhibited Igeo values of -8.31 and -8.36 at the two stations, with a mean of -8.33, falling within the unpolluted range. Lead showed Igeo values of -9.96 and -10.00 for the respective stations, with a mean value of -9.98, remaining unpolluted. Iron recorded the lowest Igeo values of -16.17 and -16.21, averaging -16.19, confirming an unpolluted condition. Manganese presented values of -13.38 and -13.33 across both stations, with a mean of -13.35, also indicating unpolluted status. Nickel exhibited Igeo values of -10.05 and -10.00 with a mean of -10.02, while zinc recorded identical values of -8.89 across both stations. Overall, all metals fall within the unpolluted category of <1.

4.11.2. Contamination factor (CF), contamination degree (CD), and pollution load index (PLI)

The metal contamination factor (CF) (Table 4.33) indicates low contamination across both stations. Cadmium recorded CF values of 0.102 at Station 1 and 0.105 at Station 2, with a mean CF of 0.104, indicating low contamination. Chromium had CF values of 0.006 and 0.005, averaging 0.005, also suggesting low contamination. Copper, lead, nickel, and zinc all recorded very low CF values, all within the low contamination category. Both iron and manganese had CF values of 0.000 at both stations. The contamination degree (CD) was calculated as 0.125, signifying a low degree of contamination, while the Pollution Load Index (PLI) value of 0.002

indicates the absence of metal pollution in the studied sediments. Across the various months, Overall, all metals fall within the low contamination category (CF < 1), though cadmium stands out as the most concerning.

4.11.3. Enrichment Factor (EF) values for heavy metals

The enrichment factor (EF) (Table 4.34) analysis revealed varying degrees of metal enrichment across the studied stations. Cadmium exhibited extremely high EF values of 16851.97 at Station 1 and 22122.79 at Station 2, with a mean EF of 19487.38, classifying it under ultra-high enrichment. Chromium, copper, lead, nickel, and zinc also demonstrated ultra-high enrichment with mean EF values of 188.46, 299.09, 303.83, 146.29, and 291.45, respectively. Manganese, though comparatively lower, still showed a very high enrichment with a mean EF of 14.38. The elevated enrichment factors, particularly for cadmium and other heavy metals, suggest significant anthropogenic contributions despite the overall low contamination levels indicated by other indices.

4.11.4. Individual potential risk (E_r^i) values and the Potential Ecological Risk Index (PERI)

The ecological risk assessment (Table 4.35) indicated that all studied metals pose low ecological risks. Cadmium, which had the highest ecological risk factor, recorded values of 3.075 at Station 1 and 3.15 at Station 2, averaging 3.112, but still within the low-risk category. Other metals such as chromium, copper, lead, nickel, and zinc exhibited even lower ecological risk factors. Both iron and manganese recorded zero ecological risk factors. The overall Potential Ecological Risk Index (PERI) was calculated as 3.18, confirming that the sediment poses a low ecological risk to the aquatic environment.

Table 4.32: Geo-accumulation Index (Igeo) for Sediment

Metal	Station 1	Station 2	Mean Igeo	Overall Status
Cadmium	-4.08	-4.18	-4.13	Unpolluted
Chromium	-9.00	-9.46	-9.23	Unpolluted
Copper	-8.31	-8.36	-8.33	Unpolluted
Lead	-9.96	-10.00	-9.98	Unpolluted
Iron	-16.17	-16.21	-16.19	Unpolluted
Manganese	-13.38	-13.33	-13.35	Unpolluted
Nickel	-10.05	-10.00	-10.02	Unpolluted
Zinc	-8.89	-8.89	-8.89	Unpolluted

Table 4.33: Contamination Factor (CF), Contamination Degree (CD), and Pollution Load Index (PLI)

Metal	CF Station 1	CF Station 2	Mean CF	Overall Status
Cadmium	0.102	0.105	0.104	Low contamination
Chromium	0.006	0.005	0.005	Low contamination
Copper	0.008	0.008	0.008	Low contamination
Lead	0.002	0.002	0.002	Low contamination
Iron	0.000	0.000	0.000	Low contamination
Manganese	0.000	0.000	0.000	Low contamination
Nickel	0.002	0.002	0.002	Low contamination
Zinc	0.004	0.004	0.004	Low contamination
CD	-	-	**0.125**	Low degree of contamination
PLI	-	-	**0.002**	No metal pollution

Table 4.34: Enrichment Factor (EF) for Sediment

Metal	Station 1 EF	Station 2 EF	Mean EF	Status
Cadmium (Cd)	16851.97	22122.79	19487.38	Ultra high enrichment
Chromium (Cr)	200.19	176.74	188.46	Ultra high enrichment
Copper (Cu)	298.91	299.27	299.09	Ultra high enrichment
Lead (Pb)	268.01	339.65	303.83	Ultra high enrichment
Manganese (Mn)	12.81	15.96	14.38	Very high enrichment
Nickel (Ni)	133.36	159.21	146.29	Ultra high enrichment
Zinc (Zn)	276.15	306.75	291.45	Ultra high enrichment

Table 4.35: Ecological Risk Factor and Potential Ecological Risk Index (PERI)

Metal	Station 1	Station 2	Mean	Pollution Status (based on Mean)
Cadmium	3.075	3.15	3.112	Low ecological risk
Chromium	0.011	0.01	0.01	Low ecological risk
Copper	0.041	0.041	0.041	Low ecological risk
Lead	0.008	0.008	0.008	Low ecological risk
Iron	0.000	0.000	0.000	Low ecological risk
Manganese	0.000	0.000	0.000	Low ecological risk
Nickel	0.008	0.008	0.008	Low ecological risk
Zinc	0.004	0.004	0.004	Low ecological risk
PERI	3.15	3.22	**3.18**	Low ecological risk

4.11.5 Distribution Coefficient

The distribution coefficient (Kd) (Table 4.36) values varied considerably across metals and months, reflecting the dynamic interaction between sediment and overlying water, with high Kd values generally indicating greater affinity for the sediment phase and low values reflecting higher solubility in water. Cadmium showed very low to zero partitioning in most months, with modest values in May (1.25) and December (2.5) and a sharp spike in August (10). Chromium was strongly sediment-bound, especially in June (55.0), April (27.69), and August (25.06), but declined sharply in September (1.49) and November (1.54). Copper followed a similar trend, with elevated values in June (20.0) and August (30.43) but very low in September (2.21) and November (0.93). Iron consistently showed the highest sediment affinity, peaking in June (66.89) and December (34.41), although it dropped drastically in November (0.70). Lead remained low (1.43–3.33) except in November (5.71), indicating higher mobility compared to other metals. Manganese fluctuated between 1.02 and 4.74, peaking in April. Nickel remained relatively stable (3.0–3.7) across most months but declined in November (0.75). Zinc showed moderate affinity, peaking in April (14.34) and August (18.70) but declining in September (2.40) and November (0.94).

4.12. Bioaccumulation Analysis

The bioaccumulation factor (BAF) and biota–sediment accumulation factor (BSAF) results for *Macrobrachium macrobrachion*, *M. rosenbergii*, and *M. vollenhovenii* are presented in Table 4.37. Cadmium exhibited the most striking pattern, with *M. macrobrachion* recording a high BAF (9.39) and BSAF (6.31), compared with the much lower values in *M. rosenbergii* (BAF 1.13; BSAF 0.76) and *M. vollenhovenii* (BAF 0.87; BSAF 0.58). These findings are of concern since the WHO/FAO permissible limit for Cd in crustaceans is 0.05 mg/kg, while the FEPA guideline is 2 mg/kg.

Chromium bioaccumulation was moderate across species, with BAF values of 1.99 (*M. macrobrachion*), 1.72 (*M. rosenbergii*), and 2.09 (*M. vollenhovenii*). The corresponding BSAFs were low (0.12, 0.11, and 0.13).

Copper showed similar moderate accumulation, with BAFs of 1.50, 1.53, and 2.07 for *M. macrobrachion*, *M. rosenbergii*, and *M. vollenhovenii* respectively, and low BSAFs (0.11–0.15). Compared with the FEPA permissible limit of 3 mg/kg and the WHO/FAO limit of 30 mg/kg, the observed values suggest copper concentrations in prawns are well within safe thresholds.

Iron BAFs ranged from 1.28 in *M. rosenbergii* to 1.98 in *M. vollenhovenii*, with corresponding BSAFs of 0.07–0.11. Against the FEPA guideline of 100 mg/kg, these values indicate no immediate concern, though iron remains one of the most strongly accumulated metals across species.

Lead accumulation was moderate and consistent across species, with BAF values close to 1.19 and BSAFs around 0.63. These values are notable given the extremely low FEPA limit of 0.05 mg/kg and WHO/FAO thresholds of 2.4 mg/kg and 1.44 mg/kg reported in the literature.

Manganese and nickel exhibited the lowest bioaccumulation among the metals. Mn BAFs were 0.25, 0.23, and 0.25, with BSAFs between 0.08–0.09. Ni BAFs were 0.24, 0.30, and 0.24, with BSAFs of 0.08–0.10. These are substantially below the WHO/FAO limit for Ni (70 mg/kg), suggesting negligible risk from these two metals under current exposure conditions.

Zinc displayed marked interspecific differences, with higher BAFs in *M. macrobrachion* (2.79) and *M. rosenbergii* (2.12) compared with *M. vollenhovenii* (0.33). BSAFs followed a similar trend, being 0.54, 0.41, and 0.06 respectively. Considering the FEPA permissible limit of 75 mg/kg and the WHO/FAO limit of 1000 mg/kg, zinc concentrations remain within safe thresholds despite evident uptake.

Table 4.36: Monthly Variation of Heavy Metal Distribution Coefficients (Kd)

	Cadmium	Chromium	Copper	Iron	Lead	Manganese	Nickel	Zinc
April	0	27.69231	16.41026	26.74699	3.333333	4.736842	3.333333	14.34483
May	1.25	13.48837	9.230769	33.82353	1.578947	3.529412	3.333333	3.291139
June	0	55	20	66.88525	1.509434	2.921348	3.235294	2.099448
July	0	19.75309	7.272727	8.846154	2.105263	2.619048	3.508772	4.754098
August	10	25.06329	30.43478	19.45392	2.5	4.197531	3.728814	18.69565
September	0	1.489362	2.208589	10.34853	1.428571	2.352941	3.106796	2.4
November	0	1.538462	0.930233	0.697674	5.714286	1.025641	0.75	0.939597
December	2.5	4.186047	10.76923	34.41176	1.578947	3.529412	3.030303	3.417722

Table 4.37: Bioaccumulation Factor for *Macrobrachium macrobrachion*, *M. rosenbergii*, and *M. vollenhovenii*

Metal	BAF *M. macrobrachion*	BAF *M. rosenbergii*	BAF *M. vollenhovenii*	BSAF *M. macrobrachion*	BSAF *M. rosenbergii*	BSAF *M. vollenhovenii*	FEPA Permissible Limit[a]	WHO/FAO Permissible Limit (mg/kg crustaceans)
Cd	9.39	1.13	0.87	6.31	0.76	0.58	2	0.05[1]
Cr	1.99	1.72	2.09	0.12	0.11	0.13	-	12[2]
Cu	1.5	1.53	2.07	0.11	0.11	0.15	3	30[2]
Fe	1.77	1.28	1.98	0.1	0.07	0.11	100	
Pb	1.19	1.15	1.19	0.63	0.61	0.63	0.05	2.4[1] ; 1.44[4]
Mn	0.25	0.23	0.25	0.09	0.08	0.09	-	
Ni	0.24	0.3	0.24	0.08	0.1	0.08	-	70[2]
Zn	2.79	2.12	0.33	0.54	0.41	0.06	75	1000[2]

[a] Okeke and Ogbeibu (2023) Thesis
[1] FAO (2011)
[2] WHO (1996).
[3] FEPA (1991).
[4] EU (2006).

CHAPTER FIVE

DISCUSSION

5.1 Physicochemical Characteristics of Surface Water

The physicochemical characteristics of the surface water between April and December 2024 revealed pronounced seasonal dynamics that reflected the combined influence of rainfall, hydrological processes, and human activities. Air temperature remained relatively stable throughout the study period, ranging narrowly between 29.05 °C in August and 30.25 °C in July, suggesting limited atmospheric fluctuation between wet and dry seasons. This thermal resilience corresponds with findings from the River Kaduna, where water temperature exhibited only modest seasonal variation, with peaks often moderated by rainfall and cloud cover during the wet season (Muhammad *et al*. 2020). Similarly, water temperature followed a parallel trajectory, declining from 28.95 °C in April to a minimum of 26.20 °C in August. The decline coincided with increased precipitation and reduced solar radiation, factors that tend to enhance dilution and lower surface water temperatures in the rainy season. Comparable seasonal cooling effects have been documented in the surface waters of River Edor in Delta , where wet season conditions promote reduced thermal loads (Okoro and Uthman, 2025). Earlier works in this river by Edogun and Ogbeibu (2016) highlighted seasonal fluctuation in Warri River with the dry season characterized by increased temperature in the Air and Water column.

The pH of the water varied considerably across the sampling months, ranging from 6.51 in September to 8.23 in August, though remaining within the WHO, USEPA, and FMEnv permissible limits of 6.5–8.5. The alkaline peak in August likely resulted from intensified photosynthetic uptake of CO_2 during periods of elevated productivity, while the marked drop in September coincided with peak rainfall and is plausibly linked to acidic runoff and the decomposition of

organic matter. This sharp September dip stands out as an important outlier relative to the overall pH trend, underscoring the sensitivity of the system to hydrological flushing. These dynamics are consistent with established limnological principles (Chapman, 1996; Boyd, 2000), which attribute pH fluctuations in tropical waters to photosynthetic activity and rainfall-driven leachates. Comparative studies on the Warri River reinforce these findings. Edogun and Ogbeibu (2016) documented significant seasonal fluctuations in physicochemical parameters, noting that tidal influences may mask some pH patterns when averaged seasonally. Akinwole *et al*. (2022) similarly reported significant seasonal variation ($p<0.05$), with lower pH values during the wet season and higher values during the dry season, consistent with the August–September trend observed in this study. Idomeh *et al*. (2022) also confirmed seasonal fluctuations within comparable ranges, while Angiro et al. (2020) examined the effects of industrial effluents on water quality, noting that decomposing organic matter in effluents can influence various water quality parameters

Salinity values remained within a narrow range of 3.0–5.0‰ throughout the study period, demonstrating relative stability despite seasonal hydrological variation. This stability reflects the balance between estuarine mixing processes and freshwater inflow, which limited saline intrusion even during drier months. Such stability is consistent with previous reports of minimal seasonal salinity fluctuations in estuaries influenced by tidal regimes and continuous rainfall input (Uwhuseba and Ikomi, 2025). However, a comparison with Akinwole *et al*. 2022 underscores spatial variability within the Warri River system. While the present study recorded stable salinity within relatively low ranges, Akinwole *et al*. 2022 reported significant seasonal shifts in Electrical Conductivity (EC) and Total Dissolved Solids (TDS), particularly in downstream sections directly impacted by saline intrusion from the Forcados River. Their recorded mean EC values reached up to 7100 µS/cm and TDS up to 3956 mg/L, both exceeding WHO and NIS standards, highlighting

the stronger saline influence downstream compared to the more freshwater-dominated upstream stretch investigated in this study.

In contrast to the relative stability of salinity, EC and TDS in the present study exhibited clear seasonal variation, largely driven by dilutional and concentration effects. EC declined steadily from 545.00 µS/cm in April to 129.50 µS/cm in August, while TDS dropped from 161.50 mg/L to 65.00 mg/L over the same period, coinciding with increased rainfall and freshwater inflow. Both parameters rose again in November and December, reflecting reduced rainfall and greater evaporative concentration. This seasonal dilution–concentration cycle closely mirrors patterns reported for the Warri River, where EC and TDS reach their lowest values in the wet season and peak in the dry months (Akinwole *et al*. 2022). Although EC values remained well within WHO and FMEnv permissible limits of 1000–1500 µS/cm, the higher values recorded in the early months of the study exceeded USEPA's more stringent guideline of 100–500 µS/cm. This exceedance suggests additional inputs from anthropogenic sources such as industrial effluents, urban discharges, and domestic runoff, which may have contributed to elevated dissolved salts during the dry-to-early rainy season transition.

The oxidation–reduction potential (ORP) fluctuated widely between 145.5 mV in August and 261.0 mV in May. Elevated ORP values during the drier months suggest oxidizing conditions promoted by higher dissolved oxygen availability, whereas the depressed values observed in August coincided with peak rainfall and enhanced microbial decomposition of organic matter, which can lower oxygen levels. Such variations are consistent with limnological theory, which links ORP depression to increased microbial activity during the wet season.

Dissolved oxygen (DO) concentrations ranged between 3.85 mg/L in May and 4.50 mg/L in July, remaining consistently below the WHO-recommended minimum of 5 mg/L required to sustain healthy aquatic systems. These persistently suboptimal values raise ecological concerns, particularly for sensitive aquatic biota, and suggest a higher degree of localized organic pollution than reported in some previous studies of the Warri River. Uwhuseba and Ikomi (2025) similarly reported depressed DO values across stations in the Warri River, further supporting the view that organic enrichment and anthropogenic activities are key drivers of oxygen stress in this system. Biological oxygen demand (BOD) fluctuated inversely with DO, ranging from 2.50 mg/L in July to 3.45 mg/L in April. Peaks in BOD during April and May coincided with reduced DO levels, reflecting increased organic matter decomposition following early rainfall events that washed accumulated pollutants into the system. Conversely, during the mid-wet season in July, improved DO levels coincided with the lowest BOD, reflecting dilution and natural aeration. This inverse DO–BOD relationship is a fundamental limnological concept, corroborated in Nigerian freshwater systems impacted by organic loading (Muhammad *et al*. 2020).

Comparisons with earlier work further contextualize the inverse BOD-DO relationship. Edogun and Ogbeibu, 2016 have documented seasonal fluctuations in physicochemical parameters of the Warri River, linking high rainfall and organic decomposition to lower DO and ORP levels, in line with the present results. They also highlighted the river's heavy organic load from industrial, municipal, and market sources, which plausibly explains the consistently depressed DO observed in this study. An earlier study by Ikomi *et al*. 2003 reported DO levels below those expected for unpolluted waters, though not consistently under the WHO minimum. In the same vien, the present study recorded DO persistently below 5 mg/L, indicating more severe localized impacts during the

study period. Tidal influences, emphasized by Edogun and Ogbeibu (2016), may also contribute to the observed fluctuations in ORP, DO, and BOD but were not the primary focus of this study.

Nutrient dynamics exhibited characteristic seasonal pulses shaped by natural processes and anthropogenic inputs. Phosphate concentrations peaked in April (0.51 mg/L) and August (0.47 mg/L), likely reflecting agricultural runoff, sewage discharge, and decomposition of organic matter mobilized during rainfall events. Nitrate followed a similar trajectory, rising to 2.78 mg/L in August before declining to 0.30 mg/L in December, a decrease consistent with assimilation and dilution later in the year. Sulphate concentrations were initially low but increased sharply in September (2.25 mg/L) and November (2.78 mg/L), which may be attributed to leaching of Sulphate-bearing compounds, episodic urban discharges, or sediment disturbance during peak wet-season flows. Uwhuseba and Ikomi (2025) reported comparatively lower mean phosphate (0.11–0.31 mg/L), nitrate (0.09–0.34 mg/L), and Sulphate (0.21–0.75 mg/L) values across stations, all within NESREA and WHO limits and showing no significant spatial variation. While their results confirm runoff-driven nutrient inputs, the consistently lower concentrations contrast with the higher pulses observed in the present study, suggesting localized hot spots of pollution and stronger temporal variability. Edogun and Ogbeibu (2016) also highlighted nutrient enrichment in the Warri River system, linking elevated phosphate and nitrate during the wet season to inputs from markets, sewage, and agricultural runoff. Their deductions align with the present findings, as both studies emphasize the amplifying role of rainfall in mobilizing nutrients into the aquatic system. Akinwole *et al*. (2022) documented nutrient fluctuations influenced by hydrology and anthropogenic discharges, though their reported values largely remained within regulatory standards. This contrasts with the elevated pulses seen here, which point to more intense localized pollution pressures. Similarly, Muhammad *et al*. (2020) emphasized that nutrient surges, particularly of

nitrogen and phosphorus, intensify microbial activity and elevate BOD, reinforcing the observed inverse relationship between DO and BOD in the present study.

Heavy metal dynamics revealed that most concentrations remained within regulatory thresholds, although episodic spikes were detected. Cadmium was absent in most months but appeared in May and December at 0.01 mg/L, exceeding both WHO (0.003 mg/L) and USEPA (0.005 mg/L) limits. This suggests intermittent contamination events, a phenomenon also documented in the Asejire and Kaduna Reservoirs which continues downstream as Osun River, where cadmium exceeded regulatory limits during periods of enhanced runoff (Adesiyan, 2018; Muhammad *et al*. 2020). Chromium showed a steady increase from April (0.01 mg/L) to a peak of 0.05 mg/L in September, exactly at the WHO and FMEnv limits, indicating cumulative inputs from industrial or urban runoff during the wet season (Okafor *et al*. 2023). Copper concentrations remained consistently low (0.02–0.05 mg/L), well below permissible thresholds. Iron peaked moderately at 0.19 mg/L in September, within WHO standards (0.3 mg/L), but its seasonal rise likely reflects erosion and sediment mobilization during peak flows, consistent with findings for the Warri River (Akinwole *et al*. 2022). Lead presented concerning spikes, particularly in June (0.03 mg/L), exceeding both WHO and FMEnv limits (0.01 mg/L), pointing to episodic urban runoff or industrial discharges. Such intermittent lead pollution has also been reported in Delta State waters impacted by oil-related and urban activities (Okafor *et al*. 2023). Nickel concentrations were generally stable but exceeded WHO limits in April (0.04 mg/L), suggesting localized enrichment from anthropogenic sources. In contrast, zinc concentrations remained consistently low (0.05–0.13 mg/L), within permissible standards and posing minimal contamination risk. Early investigations by Edogun and Ogbeibu (2016) identified industrial, municipal, and agricultural effluents as major contributors to Warri River pollution. Both studies reported cadmium and lead concentrations above potable water

standards, consistent with the present findings. However, while their work highlighted chronic exceedances, the present study reveals that contamination in the Ubeji axis often occurs as episodic pulses, reflecting temporal variability in pollutant inputs. Subsequently, Okoye and Iteyere (2014) reinforced this evidence by documenting lead and iron concentrations above permissible limits in the Warri River, further confirming the persistence of heavy metal stress in the system. More recently, Akinwole *et al*. (2022) reported exceedances of WHO limits for lead and iron in the Warri River, in agreement with the present study. However, their findings diverge in two respects: cadmium was not detected, and no significant seasonal variation was observed. These differences likely reflect variations in sampling sites, study periods, and localized contamination dynamics. Uwhuseba and Ikomi (2025) provided further confirmation of widespread heavy metal contamination in the Warri River, reporting cadmium, chromium, and lead levels exceeding regulatory thresholds across multiple stations. Unlike the present findings, which emphasize localized and episodic spikes, their results revealed consistently elevated mean concentrations, pointing to broader spatial impacts within the river system. Beyond the Warri River, other regional studies support the interpretation of episodic heavy metal inputs. Okafor *et al*. (2023) traced elevated heavy metal concentrations directly to industrial effluent discharges, while Ushurhe *et al*. (2024) documented cadmium and lead exceedances in the River. Together, these findings confirm that the episodic and runoff-driven spikes observed in the Ubeji axis are part of a wider Niger Delta phenomenon of heavy metal enrichment.

5.2. Physicochemical Characteristics of Sediment

The physicochemical and heavy metal profiles of sediments in the Ubeji Axis revealed subtle but meaningful spatial contrasts alongside pronounced seasonal dynamics that influence contaminant

retention and binding. Sediment pH was significantly higher at Station 1 compared to Station 2, indicating a slightly more neutral environment upstream, potentially buffered by organic matter or lower pollutant loading. No significant seasonal variation was observed, with wet-season and dry-season values both reflecting a consistently acidic sediment environment. This is below the standard permissible range of 6.5–8.5 set by NESREA/WHO environmental guidelines (World Health Organization, 2008; NESREA, 2011), indicating that the sediments remain acidic and may enhance the mobility and bioavailability of metals. This pattern aligns with earlier Niger Delta observations, such as the Ellah River, where Ogbeibu and Iyorah (2015) noted spatially variable yet generally regulated pH levels, and more recent work in Ibeno coastal sediments, where Alozie et al. (2022) reported stable, below-neutral pH values. Sediment electrical conductivity (EC) was significantly higher at Station 1 than Station 2, though no seasonal variation was detected. Higher EC upstream may reflect greater ionic or mineral content associated with sediment texture differences or localized anthropogenic inputs, consistent with spatial variation documented for Niger Delta sediments (Ogbeibu & Omoigberale, 2014). There is no regulatory guideline limit for sediment electrical conductivity, hence values were interpreted solely based on comparative trends across stations. Similarly, sediment moisture content was higher at Station 1 than Station 2, indicating differential water retention that can influence contaminant binding and metal mobility, a principle emphasized in both early studies (Ogbeibu & Omoigberale, 2014) and recent coastal sediment work. Heavy metal dynamics exhibited stronger seasonal than spatial variation. Cadmium was absent in most months but detected in May and December, and although concentrations remained below the Threshold Effect Level (TEL) of 0.6 mg/kg established by the Canadian Council of Ministers of the Environment (CCME, 1999), these episodic detections indicate intermittent contamination. This mirrors observations by Imiuwa et al. (2014) in Ikpoba

River sediments, as well as regional reports of cadmium exceedances in the Asejire and Kaduna Rivers during runoff periods (Adesiyan, 2018; Muhammad et al., 2020). Chromium showed a progressive increase from April to a wet-season peak in September, though concentrations remained below the TEL value of 52.3 mg/kg (CCME, 1999). Seasonal enrichment likely reflects mobilization from urban or industrial runoff and erosion during heavy rains. Comparable observations were made by Edokpa and Ogbeibu (2016) reported background-level chromium in Ogba River sediments. Copper remained consistently low, well below the TEL of 18.7 mg/kg (CCME, 1999), suggesting minimal ecological risk. While some earlier studies recorded localized copper enrichment from brewery effluents (Ogbeibu et al., 2014), the present data reflect low and stable concentrations across stations. Iron peaked moderately in September, consistent with sediment mobilization and erosion processes during heavy rainfall, as noted by Ogbeibu and Iyorah (2015) and Edokpa and Ogbeibu (2016). Although iron has no established international TEL guideline, these seasonal spikes underscore the transport-driven enrichment of iron in the system. Lead displayed episodic spikes, notably in June, although sediment concentrations remained below the TEL value of 30.2 mg/kg (CCME, 1999). These findings confirm long-standing contamination documented by Imiuwa et al. (2014) and Edogun and Ogbeibu (2016), and the persistence of lead contamination in Warri River sediments over decades, demonstrating its entrenched presence and episodic mobilization. Nickel remained mostly stable and below the TEL of 15.9 mg/kg (CCME, 1999). The slight elevation recorded in April indicates localized anthropogenic enrichment, consistent with prior observations of nickel variability in Niger Delta sediments (Ogbeibu & Iyorah, 2015; Edokpa & Ogbeibu, 2016). Zinc remained low and within permissible limits, staying below the TEL of 124 mg/kg (CCME, 1999), agreeing with reports from Warri and Ikpoba Rivers (Edogun & Ogbeibu, 2016; Imiuwa et al., 2014).

5.3 Prawn Species Composition and Abundance

The freshwater prawn community in the Ubeji Axis of the Warri River was moderately rich and abundant, comprising 1,969 individuals distributed across five species within the genus *Macrobrachium* (Palaemonidae). This diversity reflects the ecological suitability of this river–estuary interface, which offers varied habitats, abundant food resources, and physicochemical conditions conducive to the life cycles of freshwater prawns (Eniade *et al*. 2022; Davidson and Suanu, 2022). The assemblage consisted of *Macrobrachium macrobrachion*, *M. rosenbergii*, *M. vollenhovenii*, *M. equidens*, and *M. dux*, all occurring across both sampling stations, indicating overall ecosystem resilience and structural complexity.

Among the species recorded, *M. macrobrachion* was numerically dominant, contributing 46% of the total catch. This observation aligns with previous studies in Badagry Creek and Lagos Lagoon, where *M. macrobrachion* predominates due to its ecological plasticity, wide environmental tolerance, and high reproductive capacity (Jimoh and Lawal, 2024; Akinwunmi *et al*. 2019). Its ability to osmoregulate effectively and thrive in both fresh and slightly brackish waters explains its consistent distribution across Niger Delta river systems (Opeh *et al*. 2018). The species' dominance underscores its potential as a sustainable candidate for aquaculture and artisanal fisheries within Nigerian waterways (Davidson and Suanu, 2022).

Macrobrachium rosenbergii accounted for 19% of the assemblage and is widely cultured in aquaculture systems. Its relatively high occurrence in this wild population suggests either escapees from nearby farms or successful natural recruitment under favorable environmental conditions, as observed in other tropical riverine systems (Etim and Sankare, 2020; Nwosu and Wolfi, 2006). Its capacity to tolerate broad salinity ranges and rapid growth enhances its survival outside cultivated

habitats, consistent with reports from brackish creeks in Bayelsa State (Davidson and Suanu, 2022).

M. vollenhovenii, comprising 18% of the total prawn community, exhibited distinct seasonal peaks in August, September, and November. This pattern is consistent with its catadromous reproductive behaviour, whereby mature females migrate downstream during the rainy season to spawn in brackish zones, with juveniles subsequently returning upstream during the dry months (Eniade *et al*. 2022; Konan *et al*. 2008). Such reproductive strategies allow this species to exploit the dynamic estuarine–freshwater gradient characteristic of the Niger Delta, enhancing survival and recruitment across months.

Macrobrachium equidens, representing 12% of the population, displayed moderate seasonal variation, with minor peaks in April and May. Its relatively stable abundance may be attributed to its euryhaline nature and preference for muddy-bottom substrates typical of estuarine fringes, consistent with observations in other Nigerian brackish habitats (Powell, 1982; Akinwunmi *et al*. 2019). These traits allow the species to maintain steady populations despite fluctuating salinity and sediment conditions.

The population peak observed in the rainy season indicates that this period provides optimal environmental conditions for breeding, larval survival, and recruitment. Increased freshwater inflow, nutrient enrichment, and expanded habitat availability during the rains enhance reproductive success and support high levels of post-larval settlement. As conditions stabilize during the dry season—marked by reduced flow velocity, clearer water, and increased shelter availability—the juveniles produced during the rainy-season breeding cycle begin to migrate back into the system. Thus, the influx of juveniles during the dry season reflects the outcome of

successful recruitment from the rainy season, demonstrating a direct link between rainy-season abundance and dry-season juvenile return. The least abundant species, *Macrobrachium dux*, accounted for only 4% of the total catch and remained consistently low across months and stations, with minor peaks in May and December. Its restricted abundance may be attributed to narrower habitat preferences, ecological specialization, or competitive exclusion by dominant species (Akinwunmi et al., 2019). Together, these patterns emphasize the seasonal linkage between reproductive success, recruitment, and subsequent juvenile presence, while also highlighting interspecific differences in habitat use and ecological adaptability.

Spatially, prawn abundance was balanced between the two sampling stations, with 988 individuals at Station 1 and 981 at Station 2, suggesting overall habitat uniformity along the surveyed stretch. However, species-specific differences were evident: *M. macrobrachion* was slightly more dominant at Station 2 (50.9%) than Station 1 (41.1%), potentially influenced by local factors such as sediment composition or nutrient availability (Etim and Sankare, 2020; Davidson and Suanu, 2022). Conversely, *M. rosenbergii* and *M. vollenhovenii* exhibited marginally higher densities at Station 1, likely due to structurally complex microhabitats such as submerged vegetation and root networks that provide shelter and foraging opportunities (Akin-Oriola *et al*. 2006).

Seasonally, prawn catches peaked in April, coinciding with the early rainy season. Runoff during this period enhance allochthonous nutrient input and primary productivity, creating optimal breeding and feeding conditions for the prawns (Eniade *et al*. 2022; Konan *et al*. 2008). Abundance gradually declined toward December, reflecting reduced recruitment, downstream migration related to reproductive cycles, and lower water levels. Similar seasonal patterns have been reported in the Cross River and Lagos Lagoons, indicating that freshwater prawn populations in Nigerian

estuarine systems are strongly influenced by hydrological and reproductive cycles (Etim and Sankare, 2020; Jimoh and Lawal, 2024).

Length-class analyses indicated that medium-sized prawns (5–8 cm) dominated the population, particularly within the 5–6 cm and 6–7 cm cohorts. These cohorts were largely composed of *M. macrobrachion*, underscoring its central role in structuring the prawn community. The consistent representation of *M. rosenbergii* and *M. equidens* in these size classes further reflects effective recruitment and survival in medium-length cohorts, suggesting overlapping generations within the sampling period. Seasonal peaks of *M. vollenhovenii* were also concentrated in these cohorts, implying a discrete recruitment pulse characteristic of a univoltine or partially bivoltine life cycle in this species, where one or two generations are produced per year in response to environmental cues such as rainfall and river flow (Konan *et al*. 2008; Eniade *et al*. 2022). In contrast, *M. dux* was primarily associated with smaller and medium cohorts, consistent with its low abundance and narrower ecological tolerance, which may limit the number of reproductive cycles it completes annually. Overall, temporal patterns suggest that growth and recruitment in the Ubeji Axis prawn assemblage are concentrated in medium-sized cohorts, with smaller and larger individuals representing minor fractions of the population. This pattern highlights the role of voltinism in shaping population dynamics, where species-specific reproductive frequency and timing drive cohort structure and contribute to seasonal fluctuations in abundance.

5.4. Morphological and Meristic Characteristics

The morphometric evaluation of *Macrobrachium rosenbergii*, *M. vollenhovenii*, *M. dux*, *M. macrobrachion*, and *M. equidens* over the nine-month sampling period revealed pronounced interspecific and spatial variations in body proportions, reflecting inherent species-specific growth

potentials and environmental influences within the Ubeji axis of the Warri River. Across all months, *M. rosenbergii* consistently emerged as the largest species, followed by *M. vollenhovenii*, *M. dux*, *M. macrobrachion*, and *M. equidens*, forming a stable size hierarchy maintained throughout the study period. During the early months (April to July), *M. rosenbergii* demonstrated rapid growth, with total length increasing from 9.12 ± 1.93 cm in April to 10.24 ± 2.00 cm in July. Peak values were consistently recorded at Station 2 for dorsal carapace length, carapace height, abdominal length, dorsal rostral length, telson length, and uropod length, suggesting that favorable physicochemical and habitat conditions at this site promoted enhanced somatic growth. This superior growth performance likely reflects the species' intrinsic physiological capacity for rapid size attainment, high metabolic efficiency, and competitive dominance in optimal habitats, consistent with observations by Obande et al. (2022) and Eniade et al. (2022). Its ability to sustain these morphometric advantages further highlights ecological plasticity and strong habitat adaptability, aligning with reports from aquaculture and wild stock studies in West Africa (Etim et al. 2021; Etim and Sankare, 2020). The larger carapace and rostrum dimensions in *M. rosenbergii* may enhance its feeding efficiency, predator avoidance, and intraspecific dominance, conferring advantages in territorial and reproductive interactions. Telson and uropod elongation likely improve locomotion and escape responses, reinforcing survival and competitive success. *M. vollenhovenii* consistently ranked second, showing notable increases in carapace height, telson length, and uropod length, with carapace height rising progressively from 1.25 ± 0.30 cm in April to 1.45 ± 0.28 cm by August. This species, known for its catadromous breeding and resilience across salinity gradients, demonstrated growth stability across stations, although Station 2 regularly recorded superior size metrics, reflecting local environmental modulation of growth performance (Adekola et al. 2023; Davidson and Suanu, 2022). The intermediate body size and

appendage dimensions suggest that *M. vollenhovenii* can maintain moderate competitive ability, access diverse food resources, and occupy varied microhabitats, balancing predation risk with mobility and feeding efficiency. *M. dux* maintained an intermediate size throughout the study, with total lengths ranging from 7.92 ± 0.45 cm in November to 8.10 ± 0.23 cm at Station 1. This mid-range positioning likely reflects moderate resource acquisition and competitive dynamics, balancing its growth potential against larger and smaller sympatric congeners (Eniade et al. 2022). Slight station-based differences, particularly in November and December, suggest that localized habitat shifts can influence somatic growth. The moderate carapace and rostrum lengths may limit access to certain prey compared to larger species, but also reduce energy costs and predation exposure, supporting survival in more competitive or restricted microhabitats. *M. macrobrachion*, despite being numerically dominant in many Nigerian river systems (Jimoh and Lawal, 2024; Davidson and Suanu, 2022), maintained relatively smaller body dimensions over the sampling period, with total length fluctuating between 7.33 ± 1.32 cm in December and 8.64 ± 1.82 cm in July. This modest growth aligns with its life-history strategy, which favors rapid recruitment and high reproductive output rather than extended somatic growth, ensuring population sustainability under fluctuating environmental conditions (Etim et al. 2021; Eniade et al. 2022). Distinct morphometric traits per station, including slight variations in carapace height and rostrum length, may allow *M. macrobrachion* to exploit different niches, enhance intraspecific competition success, and optimize reproduction in environments where larger congeners dominate, supporting its numerical abundance despite smaller size. *M. equidens* remained the smallest species across all sampling months, with total lengths ranging from 6.46 ± 1.12 cm in December to 7.14 ± 1.21 cm in July. Its restricted growth likely reflects niche specialization for more sheltered or shallow estuarine habitats, where factors such as competition, predation risk, and habitat constraints limit

somatic expansion (Davidson and Suanu, 2022; Akinwunmi et al. 2019). Station 1 consistently recorded the lowest size means for *M. equidens*, indicating that site-specific conditions there may be less favorable for growth compared to Station 2. Smaller body and appendage dimensions in *M. equidens* likely reduce energetic demands and facilitate survival in marginal habitats, but may limit competitive ability, access to larger prey, and dominance interactions. During August and September, corresponding with peak rainy season flows, all species continued to exhibit somatic growth. *M. rosenbergii* reached maximum total lengths of 10.67 ± 1.83 cm and 10.54 ± 1.78 cm in August and September, respectively, with Station 2 maintaining its status as the primary growth hotspot. Similarly, *M. vollenhovenii* sustained steady increases, especially in uropod and telson dimensions, demonstrating adaptability to seasonal environmental fluctuations (Adekola et al. 2023; Etim and Sankare, 2020). Seasonal enhancements in telson and uropod lengths may improve swimming performance and predator avoidance, while increases in rostrum and carapace facilitate better resource acquisition and dominance hierarchies. As the season transitioned toward November and December, a slight decline in mean sizes was observed across species, likely due to post-spawning stress, reduced food availability, and seasonal hydrological changes typical of the dry season transition (Davidson and Suanu, 2022; Eniade et al. 2022). Nonetheless, *M. rosenbergii* maintained its dominance with total lengths of 8.75 ± 1.64 cm in November and 8.50 ± 1.38 cm in December. *M. dux* and *M. macrobrachion* showed minor reductions, while *M. equidens* retained its position as the smallest in the assemblage. These changes suggest that seasonal stressors can affect growth and morphometric traits, potentially influencing competitive interactions, feeding efficiency, and reproductive output across the assemblage. Eye diameter, although showing minimal monthly fluctuations, was marginally larger in *M. rosenbergii* and *M. vollenhovenii* (0.17–0.20 cm), particularly at Station 2. This may reflect enhanced visual

adaptation for efficient foraging and predator avoidance in structurally complex habitats (Eniade et al. 2022; Akin-Oriola et al. 2006). Larger eyes likely confer advantages in detecting prey, predators, and conspecifics, supporting feeding success, habitat navigation, and dominance behaviors. Overall, Station 2 exhibited consistently higher morphometric means for nearly all species and parameters, underscoring the critical role of localized habitat factors, such as sediment quality, food resource density, and shelter availability, in promoting superior prawn growth (Obande et al. 2022; Adekola et al. 2023). The persistence of the observed size hierarchy (*M. rosenbergii* > *M. vollenhovenii* > *M. dux* > *M. macrobrachion* > *M. equidens*) across months confirms the distinct growth potentials, ecological strategies, and competitive interactions among these *Macrobrachium* species within the dynamic Warri River estuarine system. Variation in morphometric traits, such as carapace height, rostrum length, telson, and uropod dimensions, likely influences species-specific feeding strategies, reproductive success, competitive hierarchies, and survival, with *M. macrobrachion*'s numerical dominance reflecting its ability to maintain reproductive output and ecological flexibility despite smaller size.

5.5. Condition Indices

The length–weight relationship (LWR), condition factor (K), and hepatosomatic index (HSI) of *Macrobrachium* species in the Ubeji axis of the Warri River reflect complex interactions between intrinsic growth potential, sex-specific energy allocation, and seasonal environmental variation. Across the sampling period, negative allometric growth predominated in most species, indicating that increases in length generally exceeded gains in weight. Male *M. macrobrachion* at Station 1 in April exhibited negative allometry ($b = 2.976$, $R^2 = 0.913$) with a mean condition factor of 1.150 ± 0.240, reflecting robust physiological health. Station 2 males showed stronger negative allometry

(b = 1.796, R^2 = 0.999) with lower K values (0.863 ± 0.249), suggesting localized habitat stressors, consistent with observations in Luubara Creek, Niger Delta (Deekae and Abowei, 2010). Female prawns maintained negative allometry across stations, with mean K values ranging from 1.119 ± 0.423 to 1.141 ± 0.501, showing minimal spatial variation in body condition (Kingdom *et al*. 2015).

Seasonal variations were evident. In May, male *M. macrobrachion* at Station 1 displayed positive allometric growth (b = 3.432, R^2 = 0.713), likely reflecting increased food availability following early rains. Females retained negative allometry but exhibited good K values (1.203 ± 0.630 at Station 1; 1.252 ± 0.646 at Station 2), a pattern consistent with pre-monsoon energy allocation (Ajibare *et al*. 2020). During June and July, negative allometry persisted with slight increases in K, indicating steady energy allocation toward somatic maintenance and growth, aligning with findings for *M. vollenhovenii* in mangrove creeks (Akinwunmi *et al*. 2022). This negative allometric trend continued through August and September, reflecting seasonal consistency in length-biased growth patterns (Kingdom *et al*. 2015). By November and December, both sexes maintained negative allometry with moderate improvements in b-values (e.g. December Station 1 males, b = 2.212), indicative of late rainy to early dry season transitions (Kingdom *et al*. 2015).

Integration of hepatosomatic index data revealed sex-specific energy allocation patterns. Female prawns consistently exhibited higher HSI than males, particularly in May, June, and December, suggesting hepatopancreatic investment for reproduction. At Station 1 in May, female HSI reached compared with in males, while Station 2 females peaked in December at 6.23, highlighting hepatopancreatic renewal coinciding with reproductive peaks. Males displayed elevated HSI at Station 2 during early wet season months, with April showing the highest mean, likely reflecting

pre-reproductive lipid accumulation, a pattern consistent with observations for *M. vollenhovenii* in the Lekki Lagoon (Akinwunmi *et al*. 2022). Inter-station comparisons indicate ecological modulation: males generally fared better at Station 2 during early months, whereas females exhibited less pronounced spatial variation but distinct seasonal peaks aligned with reproductive preparation.

Examining LWR, K, and HSI collectively shows partial synchrony in energy allocation. In May, elevated female K at Station 1 coincided with high HSI (5.89), reflecting simultaneous somatic growth and hepatopancreatic investment likely enhancing reproductive readiness. Similar synchrony occurred in December at Station 2, where HSI and K suggest post-spawning energy restoration or potential second spawning events. Males exhibited early HSI peaks in April and June, aligning with moderate K values, indicative of preparatory lipid storage preceding mating activity. Such synchrony between condition factor and hepatopancreatic development has been observed in aquaculture studies of *Macrobrachium rosenbergii*, where hepatopancreas transcriptome activity correlates with growth rates and metabolic efficiency (Phonsiri *et al*. 2024).

Temporal transitions in HSI and K further illustrate adaptive metabolic strategies. Periods where HSI precedes K, such as April in males, likely reflect early energy storage prior to somatic growth, whereas periods of convergence, such as May and December in females, indicate optimized energy allocation balancing growth and reproduction. Overall, these findings suggest that wild *Macrobrachium* populations in the Ubeji axis modulate hepatopancreatic activity and somatic condition in response to environmental cues, maintaining relatively stable physiological states across seasonal fluctuations. These patterns align with regional consensus that *Macrobrachium* species exhibit length-biased growth, seasonally modulated condition factors, and reproductive-

linked hepatopancreatic investment in estuarine ecosystems in Nigeria and West Africa (Akinwunmi *et al*. 2022; Ajibare *et al*. 2020; Deekae and Abowei, 2010; Kingdom *et al*. 2015; Phonsiri *et al*. 2024).

5.6. Reproductive Biology

The reproductive biology of the *Macrobrachium* community in the Ubeji Axis of the Warri River, as indicated by sex distribution, gonadal maturity, and gonadosomatic index (GSI), exhibits clear temporal and spatial patterns that reflect the reproductive strategies of tropical prawns, while also highlighting species-specific and localized variations influenced by environmental and anthropogenic factors. The overall sex ratio of the *Macrobrachium* populations showed a pronounced seasonal pattern. Female dominance was evident during the early rainy season (April–May), transitioning toward a more balanced ratio mid-year (June–September), with a slight resurgence of females in December. This female-biased pattern during peak reproductive activity aligns with observations in other Niger Delta species; for instance, Deekae and Abowei (2010) documented a female-skewed sex ratio for *M. macrobrachion* in Luubara Creek. Similarly, Ukagwu *et al*. (2020) reported female predominance in *M. vollenhovenii* and *M. felicinum* populations in the Akor River, Ibere, Nigeria. Notably, species-specific differences emerged: the high female skew for *M. macrobrachion* early in the rainy season contrasts with the male-dominated ratio recorded for the same species in Badagry Creek by Lawal-Are and Owolabi (2012), emphasizing the influence of localized environmental conditions and reproductive timing on population structure. The low abundance and specialized reproductive timing of *M. dux* corroborate its habitat-specific nature, while the shifting sex ratios of *M. equidens* reflect its euryhaline adaptability.

Gonadal staging revealed temporal peaks in reproductive activity, supporting the sex ratio trends observed. Peak gonadal ripeness occurred from May to August, corresponding to the mid-wet season, followed by a post-spawning decline in September and a secondary reproductive activity in November for some individuals. These patterns align with general tropical prawn reproductive cycles, which are often synchronized with seasonal changes in hydrology and resource availability (Valenti and New, 2000). Spatial differences were also apparent, with Station 2 showing delayed gonadal maturation early in the season, highlighting the role of localized environmental factors. Previous studies have demonstrated how stressors such as heavy metals or brewery effluents can modulate reproductive output (Ogbeibu *et al*. 2014; Imiuwa *et al*. 2014), potentially explaining these spatial discrepancies. Species-specific analysis further refined these observations: the bimodal reproductive peaks of *M. vollenhovenii* correspond to its catadromous reproductive cycle (Eniade *et al*. 2022), while reproductive activity in non-native *M. rosenbergii* suggests its successful adaptation and potential for naturalization within the river system (Etim and Sankare, 2020).

The GSI data quantitatively corroborated patterns revealed through gonadal maturity staging. Pooled GSI values indicated bimodal reproductive peaks, primarily between June and August and again in November, reinforcing the temporal trends observed in gonadal maturation. Species-specific GSI patterns, such as distinct peaks for *M. vollenhovenii* and *M. rosenbergii*, confirm the seasonality of reproductive activity. Spatial differences in GSI, with Station 2 exhibiting delayed and less sustained gonadal development, underscore the influence of local environmental conditions on reproductive effort. International studies, such as Shi, *et al*. (2023), have highlighted the effect of environmental factors, particularly feeding regimes, on gonadal development, while local investigations on condition factor, including Kingdom *et al*. (2015), have documented

seasonal variation in reproductive investment. Overall, this study confirms established patterns in Niger Delta and other tropical estuarine systems: strong seasonality in sex ratios, gonadal maturation, and GSI, with reproductive peaks typically occurring during the wet season.

5.7 Feeding Intensity

The feeding ecology of *Macrobrachium* species along the Ubeji Axis of the Warri River displayed pronounced spatio-temporal, sex-specific, and species-wide patterns, with stomach fullness and stomach weight both reflecting moderate to variable feeding intensity. *Macrobrachium dux* exhibited generally low feeding, with Station 1 showing a December peak in female stomach weight and moderate male feeding in April, while Station 2 displayed sustained moderate female feeding from September to December and consistently low male feeding. *Macrobrachium equiden*s maintained stable mid-year feeding from May to September, dominated by moderate stomach fullness and elevated female stomach weights in April–May and December, reflecting reproductive-linked dietary activity. *Macrobrachium macrobrachion* showed early wet-season peaks at Station 1 in both fullness and weight, whereas Station 2 recorded high numbers of empty stomachs early in the wet season, followed by moderate feeding and secondary peaks in December, particularly males and females. *Macrobrachium rosenbergii* exhibited bimodal female peaks in early and late wet-season months at Station 1, with males displaying a more stable pattern, and Station 2 had lower but sustained feeding, including occasional fully fed individuals. *Macrobrachium vollenhovenii* showed dual seasonal peaks, with highest feeding from July to September at Station 1 and September to December at Station 2, females consistently feeding more than males. These patterns align with Nigerian studies in the Warri River and Niger Delta, where Marioghae (1982) and Idung *et al* (2013) described *M. macrobrachion* as an omnivorous detritivore feeding on detritus, diatoms, algae, and insect parts, supporting observed wet-season

peaks when resources are abundant, while Jimoh *et al*. (2024) reported *M. vollenhovenii* as an omnivorous detritivore consuming plankton, insect parts, and detritus, consistent with mid-year feeding peaks. The spatial differences observed, such as sharper peaks at Station 1 versus more moderate activity at Station 2, and early-season empty stomachs for *M. macrobrachion* at Station 2, likely reflect microhabitat variability, tidal influences, or localized environmental stress, corroborating earlier findings by Ogbeibu and Omoigberale (2005).

5.8. Heavy Metal Concentrations in Prawn Species

The analysis of heavy metal concentrations in *Macrobrachium macrobrachion*, *M. rosenbergii*, and *M. vollenhovenii* throughout the sampling period reveals distinct, species-specific accumulation patterns influenced by seasonal hydrology, ecological behaviour, and environmental exposure. Overall, zinc and iron were the most accumulated metals across species, with nickel showing a significant interspecies difference, highest in *M. rosenbergii*. Cadmium, chromium, copper, lead, and manganese remained generally low and statistically similar across the three prawns, suggesting limited environmental availability during the study period. Among the species, *M. macrobrachion* recorded the highest cadmium and zinc concentrations, consistent with its benthic feeding and detritivorous habits that increase contact with sediment-bound metals. *M. rosenbergii* exhibited peaks in nickel, copper, chromium, lead, and zinc, reflecting a broader exposure through both benthic and pelagic foraging, while *M. vollenhovenii* displayed the highest iron accumulation, highlighting a species-specific capacity for iron uptake. Despite these differences, a consistent seasonal pattern was evident, with elevated metal concentrations during the wet season months (June–August), likely driven by rainfall-induced runoff, catchment discharge, and sediment resuspension, while dry-season months showed lower concentrations, reflecting reduced metal mobility and stabilized sediments. These patterns are corroborated by

regional studies demonstrating similar trends in prawn metal accumulation; Anani and Olomukoro (2019) observed elevated iron, zinc, and manganese in *Macrobrachium rosenbergii* from the Warri River, while Anyanwu *et al*. (2024) reported varying iron, lead, cadmium, and chromium in *M. vollenhovenii* from the Lower Cross River. A study by Ucheaga and Nkitikpor (2022) found lead concentrations of 3.02 ± 0.02 mg/kg in prawns sold in Warri markets, supporting the episodic lead enrichment observed in *Macrobrachium macrobrachion* and *M. vollenhovenii* in this study. Anyanwu *et al*. (2024) highlighted the influence of water quality on metal uptake in shrimps from impacted mangrove swamps. Collectively, these findings underscore that seasonal hydrology, sediment dynamics, and species-specific ecological traits strongly modulate metal bioaccumulation in *Macrobrachium* species. High zinc and iron, particularly in *M. macrobrachion* and *M. vollenhovenii*, indicate potential risks for chronic physiological stress, trophic transfer, and human health, while the significant nickel accumulation in *M. rosenbergii* emphasizes interspecies differences in exposure and uptake, supporting the potential use of these prawns as bioindicators of localized metal contamination in the Niger Delta.

5.9 Bivariate Analysis

The bivariate correlation analysis of water physicochemistry, sediment characteristics, heavy metals, prawn bioaccumulation, and prawn biological indices reveals a tightly coupled but species-specific set of responses in the Warri River estuarine system. Across matrices and organisms the data indicate two broad, interacting controls: (1) resource-driven enhancement (nutrients and some essential trace elements) that supports abundance and reproductive effort; and (2) contaminant-driven suppression and physiological trade-offs (notably by Cd, Pb and Cu). These forces act in synchrony in some respects (co-occurrence and co-accumulation of metals) but diverge in others

(different species respond differently to the same stressor), a complexity that is common in tropical estuarine systems (Ajani, 2022; Akintade *et al*. 2023).

At the level of water chemistry and abundance, temperature emerged as an important abiotic driver for some species: water temperature correlated positively and significantly with *M. macrobrachion*, indicating warmer conditions favor its presence. Dissolved oxygen, by contrast, showed uniformly weak negative correlations across species, suggesting DO variability within the sampled range was not a limiting factor for abundance. Nutrient effects were pronounced and species-specific: nitrate correlated strongly and positively with *M. rosenbergii* and more weakly with *M. vollenhovenii* and *M. macrobrachion*. Phosphate likewise showed a strong positive association with *M. rosenbergii*. These nutrient–prawn links point to a productivity pathway by which nitrate and phosphate enhance food availability and thus favor *M. rosenbergii* in particular. In short, nutrients (nitrate, phosphate) consistently promoted abundance where relationships were statistically strong, reinforcing the idea that eutrophication and nutrient pulses can boost some prawn populations.

Water-phase metals, however, produced inhibitory signals for particular species. Dissolved cadmium correlated negatively across all three focal prawns and exerted its strongest negative relationship on *M. macrobrachion*. Lead in the water significantly depressed *M. vollenhovenii*, and copper in the water showed a significant negative correlation with *M. rosenbergii*. Zinc and iron in water were mostly weakly or moderately positive but non-significant, reflecting their roles as essential micronutrients at low concentrations. Chromium showed weak positive correlations, while nickel trends were weakly negative and non-significant, patterns that point to metal- and species-specific toxicities rather than a single uniform metal effect.

Comparing water vs. sediment influences reveals a clear partitioning of ecological control. General sediment physicochemical properties (pH, conductivity, moisture) exhibited weak and inconsistent associations with prawn abundance indicating limited direct influence. By contrast, sediment-bound heavy metals were far more influential. Sediment lead displayed the most striking species-specific pattern: a very strong negative correlation with *M. vollenhovenii* (lead (S) vs *M. vollenhovenii*, yet strong positive correlations with *M. macrobrachion* and *M. rosenbergii*. Sediment cadmium tended toward negative associations with *M. vollenhovenii* though not significant at $\alpha = 0.05$. Zinc in sediments showed moderate positive links with *M. rosenbergii* and *M. macrobrachion*, but a near-significant negative correlation with *M. dux*, demonstrating variable tolerance and exposure pathways across species. In short, sediment metals exerted stronger control over abundance and appear to be the primary long-term reservoir dictating chronic exposure.

Bioaccumulation patterns underscore the mechanistic role of sediments and organism physiology. In the water matrix, several metals were highly intercorrelated, chromium with copper and iron and copper with iron; manganese was strongly associated with zinc and nickel. These water-phase co-variations point to shared sources or coupled geochemical cycling. Yet, cross-matrix (water → tissue) synchrony was generally weak or even negative for several metals: cadmium in *M. rosenbergii* was significantly negatively correlated with cadmium in water, and cadmium in *M. macrobrachion* also showed a negative water–tissue association. *M. vollenhovenii* similarly showed a negative water–tissue cadmium relationship. These negative or weak water–tissue linkages indicate that contemporaneous dissolved concentrations are not the sole determinants of tissue burdens, physiological regulation, dietary/particulate uptake, and sediment interactions play central roles.

Within organisms, however, metals co-accumulate in highly synchronous clusters. In *M. macrobrachion*, copper in tissue correlated significantly with chromium and iron; iron correlated very strongly with chromium and manganese; and zinc correlated strongly with cadmium and nickel. *M. rosenbergii* showed analogous patterns, and *M. vollenhovenii* exhibited among the strongest inter-metal synchrony. These tight within-tissue correlations point to shared uptake routes, binding to common ligands (e.g. metallothioneins), and co-exposure through benthic prey and sediment ingestion (Akintade *et al*. 2023).

Sediment–tissue associations were consistently stronger than water–tissue linkages, confirming sediment as the dominant chronic source. Examples include very strong correlations such as sediment Cu vs tissue Cd in *M. macrobrachion* and sediment Cu vs tissue Cu in *M. vollenhovenii*. In *M. rosenbergii*, tissue Cu correlated tightly with sediment Cu, and tissue Cr correlated strongly with sediment Cr. Such sediment–tissue coherence highlights pore-water diffusion, ingestion of contaminated particulates, and benthic foraging as primary absorption routes, mechanisms observed in coastal tropical crustaceans (Ajani, 2022; Anani and Olomukoro, 2019).

Prawn biological indices (GSI, HSI, CF) reveal how environmental quality translates into physiological trade-offs. Gonadosomatic index was positively associated with water pH and nitrate, suggesting that slightly alkaline, nutrient-rich waters favor gonadal development, while GSI correlated negatively and significantly with dissolved cadmium, indicative of metal-induced reproductive suppression. Hepatosomatic index showed a strong and significant negative correlation with salinity, implying that higher salinity reduces hepatopancreatic reserves; yet HSI had moderate positive links with air and water temperature, consistent with temperature-driven metabolic activity. Condition factor was strongly and positively correlated with salinity and with essential trace metals such as copper and iron, but negatively correlated with dissolved cadmium

and BOD, showing that general health improves under moderate salinity and essential metal availability but declines in the face of toxicants and organic pollution. Sediment properties showed complementary relationships: sediment pH related positively with CF and sediment moisture with CF, while HSI correlated strongly with sediment lead and CF correlated negatively with sediment lead, suggesting a complex trade-off where lead exposure may induce hepatopancreatic enlargement but reduce whole-body condition.

When the results are synthesized into the overall synchrony across sections, four clear themes emerge. First, nutrients versus metals: nutrient enrichment uniformly promotes abundance and reproductive indices, while toxic metals (Cd, Pb, Cu) exert inhibitory or stress-inducing effects. Second, water vs. sediment influence: water parameters (pH, temperature, salinity) largely modulate physiology (GSI, HSI, CF) , for example, GSI with pH $r = 0.393$ and nitrate $r = 0.321$; HSI with salinity $r = –0.806$, $p < 0.05$; CF with salinity $r = 0.826$, $p < 0.05$, whereas sediment metals exert stronger control of abundance and tissue. Third, species-specificity: *M. rosenbergii* appears nutrient-driven and exhibits co-accumulation of Cu and Fe in tissues *M. macrobrachion* is temperature-sensitive and shows sensitivity to cadmium alongside strong within-tissue co-accumulation. *M. vollenhovenii* displays the strongest inter-metal synchrony in tissues (very high tissue correlation coefficients across Cr, Cu, Fe, Mn, Ni, Zn) but is notably stressed by lead in sediments and water. Fourth, bioaccumulation versus environment: internal metal loads are highly synchronized among metals (e.g. tissue Ni–Mn–Zn clusters with r's often > 0.9, $p < 0.01$), while synchrony with external dissolved concentrations is weak or inconsistent. These patterns underscore the primacy of sediment pathways and physiological regulation (metallothionein binding, digestive uptake, excretory control) over direct dissolved-phase exposure.

Mechanistically, the observed co-accumulation is consistent with shared sources (industrial effluents, urban runoff, and sediment remobilization) and with internal biochemical pathways that bind multiple transition metals to the same proteins or storage compartments (Akintade *et al*. 2023). The dominance of sediment–tissue correlations supports sediment ingestion and pore-water transfer as major exposure routes, particularly for benthic foragers (Ajani, 2022). The negative or absent water–tissue correlations for some metals (notably cadmium) likely reflect active physiological exclusion, depuration, or seasonal dilution of the dissolved phase, phenomena previously reported in Niger Delta crustaceans (Anani and Olomukoro, 2019). Observed physiological responses (e.g. HSI enlargement associated with Pb, increased GSI with Zn in some cases) may represent compensatory detoxification and energy reallocation; however, caution is warranted because hepatic enlargement can also be pathological (e.g. hypertrophy or lipid vacuolation), as documented in metal-exposed fish (Abou Shabana *et al*. 2016). For example, in *M. macrobrachion* copper correlated positively with HSI and CF, a pattern that could reflect both detoxification effort and an adverse change in energy storage.

From an ecosystem and management perspective, these results carry several implications. First, the concurrence of nutrient enrichment and metal contamination can create situations in which certain species (e.g. *M. rosenbergii* and *M. macrobrachion*) temporarily flourish while accumulating contaminants, posing food-safety concerns. Second, the sediment reservoir of metals means that remediation and monitoring should prioritize sediment quality and benthic habitats (remediation of point-source discharges, sediment management, reducing resuspension). Third, species-specific vulnerabilities (e.g. *M. vollenhovenii*'s sensitivity to Pb; *M. macrobrachion*'s sensitivity to Cd) should guide biomonitoring and management priorities: sentinel species can be chosen according to these sensitivities and trophic behaviours. Finally, the predominance of

positive (synergistic) inter-metal correlations suggests that multi-metal exposure could compound physiological stress, increasing the risk of sublethal effects on growth, reproduction, and population resilience during pollution episodes or hydrological perturbations (Ajani, 2022).

5.10: Multivariate Analysis

The Canonical Correspondence Analysis (CCA) examining the relationship between condition indices, gonadosomatic index (GSI), hepatosomatic index (HSI), and condition factor (CF), and water physicochemical parameters indicates that Axis 1 explains 87.12% of the total variance, capturing the principal environmental gradients influencing prawn reproductive and physiological condition. Among the indices, GSI shows a pronounced positive loading on Axis 1, underscoring its dominant role in explaining variability and highlighting its strong responsiveness to shifts in water quality. This finding aligns with previous research indicating that reproductive development in aquatic invertebrates is highly sensitive to physicochemical cues, including trace metals and nutrient availability (Cheung *et al*. 2019). In contrast, HSI exhibits a weak negative loading, implying that hepatic energy reserves are either less influenced or potentially inversely related to the prevailing water conditions, while CF displays a minor positive association, suggesting a more subtle or indirect relationship with environmental fluctuations.

Regarding water parameters, pH, copper, iron, chromium, and nitrate load positively on Axis 1, indicating that higher values of these variables promote enhanced gonadal maturation and reproductive performance. The positive effects of essential trace metals like copper and iron are well documented in crustacean physiology, where they function as cofactors for enzymes involved in vitellogenesis and gonadal steroid synthesis (Jaskuła *et al*, 2022). Conversely, cadmium shows the strongest negative loading, underscoring its known reproductive toxicity and interference with endocrine pathways in freshwater invertebrates (Adeniyi *et al*. 2023). Additional negative loadings

for ORP, nickel, zinc, lead, and BOD suggest that elevated levels of these parameters may suppress reproductive output through oxidative stress, impaired oxygen availability, or direct toxic effects. Seasonally, the temporal pattern of sampling reveals mild variability, with sampling periods three to seven aligning positively along Axis 1, corresponding to slightly more favorable conditions for gonadal development, while samplings one, two, six, and eight exhibit mild negative scores, indicating subtle shifts but no extreme seasonal constraints on reproductive activity.

For sediment physicochemical variables, the CCA likewise explains 87.12% of the total variance across the first two axes, with Axis 1 dominating. Here too, GSI maintains a strong positive loading, reaffirming its role as a sensitive indicator of sediment quality effects on reproductive health. CF retains a weak positive association, while HSI remains slightly negative, reinforcing the pattern that hepatic indices are less tightly linked to sediment conditions than reproductive indices. Among sediment parameters, pH and chromium exhibit strong positive loadings, suggesting that well-buffered, slightly alkaline sediments may favor reproductive success, potentially through stable sediment structure and metal speciation that limits bioavailable toxicity. In contrast, sediment moisture, manganese, and nickel load negatively along Axis 1, implying that waterlogged sediments and elevated levels of these metals may create suboptimal reproductive habitats by reducing sediment oxygenation or increasing metal bioavailability to toxic thresholds. Other sediment-bound metals such as cadmium, copper, iron, lead, and zinc show moderate to weak loadings, indicating more nuanced or indirect impacts on reproductive physiology.

Seasonally, the distribution of sediment CCA scores mirrors that of the water variables, displaying minor temporal variation. Positive associations in June, August, November, and July point to marginally improved benthic conditions for reproduction during these months, possibly reflecting seasonal dry-to-wet transitions and sediment redox shifts. Conversely, April, May, September, and

December cluster negatively or neutrally, suggesting stable yet slightly less favorable sediment environments for supporting peak reproductive output.

Overall, these CCA results emphasize that the gonadosomatic index is the most sensitive indicator of both water and sediment quality impacts on prawn reproduction, whereas hepatic condition and overall somatic condition are less responsive or more buffered against short-term environmental fluctuations. This highlights the importance of integrated water and sediment monitoring for effective biomonitoring and fisheries management in tropical freshwater and estuarine ecosystems facing increasing anthropogenic stressors.

The Canonical Correspondence Analysis (CCA) assessing the relationship between bioaccumulated heavy metals in *Macrobrachium macrobrachion* and its condition indices reveals that the first two canonical axes capture the entire variance structure, with Axis 1 alone accounting for 86.64% of the total variation. Nearly all metals, cadmium, chromium, copper, iron, lead, manganese, and zinc, exhibit negative loadings along Axis 1, indicating an inverse association between overall metal burden and the dominant gradient influencing physiological condition. Nickel stands out with a positive loading, implying a unique accumulation pathway or distinct metabolic handling in this species. Notably, the gonadosomatic index (GSI) displays a strong negative loading, signifying that higher bioaccumulation of these metals is consistently linked to reduced reproductive output, a pattern corroborated by studies highlighting reproductive suppression in crustaceans exposed to heavy metal stress (Adeniyi *et al*. 2023). In contrast, the condition factor (CF) shows a strong positive loading, suggesting that general somatic condition might remain relatively stable or even slightly enhanced, possibly due to energy reallocation toward somatic maintenance rather than reproduction, a physiological coping strategy reported in similar freshwater prawn populations (Jaskuła *et al*, 2022). The hepatosomatic index (HSI) retains

a weak negative loading, implying minimal or incipient hepatic stress. Seasonal scores along Axis 1 show subtle variation: December, May, and April lean slightly positive, while other months cluster around negative or neutral loadings, indicating only minor seasonal modulation of metal uptake and its physiological consequences in this species.

For *Macrobrachium rosenbergii*, the corresponding CCA likewise accounts for 100% of the total variance, with Axis 1 explaining 85.68%. Unlike *M. macrobrachion*, most metals, zinc, copper, iron, nickel, chromium, and manganese, show strong positive loadings on Axis 1. This suggests that the bioaccumulation of these metals is directly aligned with the environmental gradient that enhances reproductive development and condition. Cadmium and lead stand out with negative loadings, reflecting their well-known reproductive and metabolic toxicity. Here, the GSI shows a robust positive loading, indicating that reproductive development benefits from moderate accumulation of essential trace metals, which act as cofactors for gametogenic enzymes and steroidogenesis. In contrast, both CF and HSI are negatively associated with Axis 1, pointing to potential trade-offs: while reproductive capacity may increase, general somatic and hepatic reserves could be slightly compromised due to metal-induced metabolic costs. Seasonal fluctuations are mild, with July, August, and June showing modest positive associations, while December, May, and November align more negatively, implying that seasonal influences on bioaccumulation effects remain secondary to species-specific physiological regulation.

For *Macrobrachium vollenhovenii*, the CCA explains 100% of the total variance, with Axis 1 contributing 82.36%. Positive loadings along Axis 1 are observed for manganese, lead, iron, chromium, and copper, indicating their synergistic role with the dominant environmental and physiological gradient. Conversely, nickel, cadmium, and zinc load negatively, suggesting different bioaccumulation dynamics or detoxification pathways. The GSI shows a strong positive

loading, reinforcing that reproductive development is positively correlated with the accumulation of certain essential metals, especially manganese and lead, a pattern that may reflect the species' tolerance and adaptive utilization of trace elements under fluctuating environmental conditions (Jaskuła *et al*, 2022). Both HSI and CF load negatively, suggesting subtle hepatic and somatic impacts when metal burdens increase, although not sufficiently severe to override reproductive investment. Seasonal differences remain slight: June, August, and November align positively with Axis 1, whereas April, September, December, and May exhibit mild negative scores, highlighting stable seasonal patterns in metal bioaccumulation and physiological responses.

Summatively, these CCA findings demonstrate clear species-specific strategies in managing heavy metal exposure and maintaining physiological condition. For *M. macrobrachion*, elevated metal burdens are strongly linked to reproductive suppression, implying higher vulnerability to metal stress and greater energetic trade-offs. In contrast, *M. rosenbergii* and *M. vollenhovenii* appear to harness certain trace metals as nutritional cofactors, sustaining or enhancing reproductive performance despite moderate hepatic or somatic strain. Across all species, hepatosomatic and general condition indices show weaker or negative relationships with bioaccumulation, reflecting subtle physiological trade-offs and early signs of detoxification costs. Seasonal variation remains consistently modest, underscoring the resilience of these prawns' metal-handling strategies throughout fluctuating hydrological and environmental conditions.

5.11. Evaluation of Environmental Risk Assessment

5.11.1. Geo-accumulation Index (Igeo)

The geo-accumulation index (Igeo) revealed that sediments across both stations are consistently classified as unpolluted for all studied metals. Cadmium values ranged between –4.08 and –4.18 (mean –4.13), chromium ranged from –9.00 to –9.46 (mean –9.23), and iron exhibited the lowest

mean Igeo at –16.19. These negative values align with Müller's (1969) classification of pristine conditions and echo the findings of Ogbeibu and Omoigberale (2014), who reported unpolluted Igeo scores for Benin River sediments in the Niger Delta region. The extremely low values across essential and potentially toxic metals affirm the sediment's uncontaminated baseline status, consistent with similar studies in tropical freshwater systems.

The contamination factor (CF) for all metals remained well below unity, with cadmium showing a mean CF of 0.104 and most other metals approaching zero. This indicates a low level of contamination across both stations. The combined contamination degree (CD = 0.125) and pollution load index (PLI = 0.002) reinforce this assessment, confirming the absence of metal pollution in the studied sediments. Such results suggest that the sediments remain relatively unimpacted by anthropogenic discharges, a finding in line with previous sediment quality studies that also reported negligible contamination levels in less industrially influenced environments (Adeniyi *et al*. 2023).

In contrast to the Igeo and CF outcomes, the enrichment factor (EF) analysis revealed a different pattern. Several metals, particularly cadmium with a mean EF of 19,487, as well as copper, lead, nickel, and zinc, fall within the category of "ultra-high enrichment." Although manganese displayed comparatively lower EF values, it was still classified as "very high enrichment." This discrepancy highlights the sensitivity of EF in detecting subtle anthropogenic influences when concentrations are normalized against background levels. Ogbeibu and Omoigberale (2014) demonstrated similar findings in their study of the Benin River, where EF was a more effective indicator of anthropogenic metal inputs compared to Igeo or CF. The elevated EF values in the present study therefore point to human-related contributions, possibly from surrounding urban or industrial activities, despite the overall low contamination suggested by other indices.

The ecological risk assessment indicated that all studied metals pose low ecological risks. Cadmium, the most concerning element, recorded a mean ecological risk factor of 3.112, but this still falls within the low-risk category. Other metals, including chromium, copper, lead, nickel, and zinc, displayed even lower values, while both iron and manganese recorded zero ecological risk factors. The overall Potential Ecological Risk Index (PERI) was calculated as 3.18, confirming that the sediment environment poses no significant ecological risk. These results are consistent with the CF and PLI findings, reinforcing the conclusion that the sediments are minimally impacted by heavy metal pollution.

The distribution coefficient (Kd) values exhibited considerable variation across metals and months, underscoring the dynamic interactions between sediment and overlying water. High Kd values reflected stronger retention of metals within the sediment matrix, whereas low values indicated greater solubility and mobility in the water column. Cadmium displayed very low to negligible partitioning in most months, with modest increases in May (1.25) and December (2.5), and a sharp spike in August (10), suggesting that it remained largely mobile except under specific seasonal conditions. Chromium showed strong sediment affinity, particularly in June (55.0), April (27.69), and August (25.06), but declined sharply in September (1.49) and November (1.54), reflecting marked seasonal solubility shifts. Copper followed a similar trend, with elevated values in June (20.0) and August (30.43), but dropping significantly in September (2.21) and November (0.93), which points to its strong association with sediment organic matter that weakens during high flow or turbulent conditions. Iron consistently exhibited the highest sediment affinity, peaking in June (66.89) and December (34.41), although it dropped drastically in November (0.70), likely due to reducing conditions. Lead generally recorded low values (1.43–3.33) except in November (5.71), indicating greater mobility compared to other metals. Manganese fluctuated between 1.02

and 4.74, peaking in April, in line with its redox-sensitive nature. Nickel remained relatively stable across most months (3.0–3.7) but dropped to 0.75 in November, suggesting balanced partitioning with slight seasonal influence. Zinc showed moderate sediment affinity, peaking in April (14.34) and August (18.70) but declining in September (2.40) and November (0.94), highlighting both binding and remobilization potential. Collectively, Fe, Cr, and Cu demonstrated the strongest sediment retention, Zn, Ni, and Mn displayed moderate partitioning, while Cd and Pb remained largely mobile, with seasonal shifts indicating enhanced sediment binding during June–August and remobilization during September–November.

Overall, Fe, Cr, and Cu showed the strongest sediment retention, Zn, Ni, and Mn exhibited moderate partitioning, while Cd and Pb remained largely mobile. The mean Kd ranking in this study followed Fe > Cr > Cu > Zn > Mn > Ni > Pb > Cd, with iron demonstrating the highest affinity (25.28) and cadmium the weakest (1.47). This highlights the strong sediment binding of Fe and Cr versus the high mobility of Cd and Pb. In comparison, Najomoh and Iloba (2022) reported a different trend in the Forcados River (Pb > Cd > Cr > Cu > Zn), where Pb and Cd were the most stable. Despite these contrasts, a consistent feature emerges across both systems: the sequence Cr > Cu > Zn, underscoring the intrinsic geochemical affinity of chromium and copper for sediments, with zinc occupying an intermediate position. These similarities suggest some universal partitioning behaviour driven by metal chemistry, while the differences such as Pb and Cd being stable in Forcados but mobile in the Warri River point to site-specific influences of sediment composition, redox dynamics, and hydrological regimes. Together, this shows that while Cr, Cu, and Zn follow a predictable stability order, overall metal mobility is strongly shaped by local geochemical conditions.

5.12. Bioaccumulation Analysis

The bioaccumulation analysis revealed distinct variations in trace metal uptake among *Macrobrachium dux*, *M. equidens*, and *M. vollenhovenii* from both water (BAF) and sediment (BSAF), reflecting species-specific accumulation strategies and differential environmental exposure. Cadmium exhibited the most pronounced interspecific disparity, with *M. dux* recording the highest BAF (9.39) and BSAF (6.31), while *M. equidens* and *M. vollenhovenii* showed comparatively lower values (BAF = 1.13–0.87; BSAF = 0.76–0.58). This sharp elevation in *M. dux* underscores its higher susceptibility to Cd uptake, possibly influenced by greater epithelial permeability or feeding contact with contaminated detritus. Given the WHO/FAO permissible limit for Cd in crustaceans (0.05 mg/kg) and FEPA guideline (2 mg/kg), the recorded values far exceed safe thresholds, indicating potential health implications if such bioaccumulation persists.

Chromium accumulation was more balanced across species, ranging from 1.72 to 2.09 (BAF) and 0.11 to 0.13 (BSAF), suggesting relatively uniform affinity for dissolved and particulate Cr forms. *M. vollenhovenii* exhibited the highest BAF (2.09), implying stronger uptake efficiency, possibly due to its benthic feeding tendencies. Despite these variations, all values remained well below the WHO/FAO limit of 12 mg/kg, suggesting minimal ecological or dietary risk.

Copper displayed moderate enrichment, with *M. vollenhovenii* again showing slightly elevated accumulation (BAF = 2.07; BSAF = 0.15) compared to *M. dux* (1.50; 0.11) and *M. equidens* (1.53; 0.11). This trend aligns with the species' physiological demand for Cu as an essential trace element in hemocyanin and enzymatic processes. Nonetheless, the values remained within FEPA (3 mg/kg) and WHO/FAO (30 mg/kg) permissible limits, indicating no immediate risk from Cu exposure.

Iron exhibited moderate but consistent accumulation across species. *M. vollenhovenii* showed the highest BAF (1.98) and BSAF (0.11), followed by *M. dux* (1.77; 0.10) and *M. equidens* (1.28; 0.07). The slightly elevated Fe in *M. vollenhovenii* may reflect its capacity for greater gill-mediated uptake or higher dietary intake of Fe-bound detritus. Although the recorded concentrations are below the FEPA permissible limit of 100 mg/kg, Fe remains a dominant accumulated metal within the studied assemblage.

Lead exhibited near-uniform uptake among species, with BAF values ranging from 1.15 to 1.19 and BSAF between 0.61 and 0.63. The slightly higher Pb burden in *M. dux* and *M. vollenhovenii* implies shared exposure to anthropogenic sources such as urban runoff and industrial effluents. Considering the extremely low FEPA limit (0.05 mg/kg) and WHO/FAO thresholds (2.4 mg/kg; 1.44 mg/kg), even modest Pb accumulation may constitute a dietary concern, especially for communities consuming these prawns regularly.

Manganese and nickel recorded the lowest accumulation indices across species. Mn ranged from 0.23–0.25 (BAF) and 0.08–0.09 (BSAF), while Ni ranged from 0.24–0.30 (BAF) and 0.08–0.10 (BSAF). These low values indicate weak bioconcentration and limited trophic transfer. Both metals remain well below the WHO/FAO Ni limit of 70 mg/kg, reflecting negligible toxicity risk.

Zinc exhibited the most marked interspecific contrast. *M. dux* displayed the highest BAF (2.79) and BSAF (0.54), followed by *M. equidens* (2.12; 0.41), whereas *M. vollenhovenii* showed minimal accumulation (0.33; 0.06). The enhanced Zn uptake in *M. dux* suggests a stronger bioavailability response, potentially driven by physiological requirements or environmental enrichment. Despite FEPA's limit of 75 mg/kg and WHO/FAO's 1000 mg/kg ceiling, the elevated accumulation trend warrants monitoring due to Zn's potential to co-occur with other toxic metals in contaminated systems.

These observations align with previous reports from southern Nigeria that have documented significant metal enrichment in freshwater prawns and other crustaceans. Anani and Olomukoro (2019) noted elevated Fe, Zn, and Mn in *M. rosenbergii* and crabs from the Ossiomo River, identifying them as potential health risks. Similarly, Akinwumiju *et al.* (2022) observed Pb concentrations in prawns and periwinkles from Warri exceeding permissible limits, consistent with the Pb patterns observed in *M. dux* and *M. vollenhovenii* in this study. Obasi *et al.* (2015) reported undetectable Cd in *Macrobrachium* spp. from the Gberikoko River, whereas Anani and Olomukoro (2019) found significant Fe accumulation in *M. rosenbergii*, trends mirrored here by moderate Fe enrichment across species.

Overall, these results reaffirm the dominance of Fe, Zn, and Pb as key bioaccumulated metals in Niger Delta freshwater ecosystems while emphasizing distinct species-specific accumulation profiles. The heightened Cd and Zn uptake in *M. dux* contrasts with the relatively stable patterns in *M. equidens* and *M. vollenhovenii*, indicating that *M. dux* may serve as a sensitive sentinel species for monitoring episodic metal contamination. Its responsiveness to Cd and Zn, in particular, positions it as an effective bioindicator for early detection of pollution pulses, with significant implications for ecosystem health assessment and food safety management in the region.

5.13. Contribution to Knowledge

The study has contributed to knowledge in the following ways:

1. Enhanced understanding of seasonal physicochemical fluctuations and heavy metal dynamics in water and sediment, highlighting the influence of rainfall, hydrology, and anthropogenic inputs on contaminant distribution in tropical estuarine systems.

2. Provided valuable data on the ecological adaptations and reproductive strategies of *Macrobrachium* species, revealing how physiological traits respond to environmental stressors, with *M. macrobrachion* showing high reproductive output and metal tolerance.

3. Demonstrated species-specific patterns of heavy metal bioaccumulation, identifying *M. macrobrachion* as a reliable sentinel species, with sediment confirmed as the dominant exposure pathway for cadmium and lead.

4. Enhanced understanding of environmental drivers influencing species distribution, using multivariate analyses to uncover synergistic metal interactions and establish ecological gradients shaping prawn community structure.

5. Provided valuable insight into conservation and management, recommending *M. macrobrachion* for biomonitoring, *M. rosenbergii* for aquaculture, and *M. vollenhovenii* for protection, while emphasizing pollution control during critical seasonal windows.

5.14. Conclusion and Recommendation

This study provides a holistic assessment of the Ubeji Axis of the Warri River, integrating abundance, morphometry, condition indices, heavy metal contamination, and bioaccumulation in five prawn species. Findings highlight both the ecological resilience of the system and emerging risks from metal enrichment.

M. macrobrachion was the most dominant species, reflecting strong adaptation to estuarine conditions, while *M. rosenbergii* and *M. vollenhovenii* showed moderate abundance, and *M. dux* and *M. equidens* contributed to overall diversity. Morphometric and meristic traits revealed interspecific differences that underline niche adaptation and support stock assessment. Condition

indices indicated generally good health, though elevated HSI values at some sites pointed to mild stress linked to contaminants.

Sediment indices showed low contamination for most metals but persistent cadmium enrichment, suggesting anthropogenic inputs. Bioaccumulation analysis confirmed species-specific uptake, with *M. macrobrachion* showing particularly high BAF and BSAF for Pb and Cd, positioning it as a sentinel species for monitoring.

To safeguard the ecosystem and public health, routine biomonitoring using *M. macrobrachion* is recommended, alongside stricter controls on cadmium and lead sources. Future work should also incorporate biomarkers and histopathology to assess sublethal effects, and investigate hysteresis patterns between discharge and pollutant concentrations, which can reveal source dynamics and transport pathways during flood events. Community awareness and integrated catchment management remain essential for sustaining estuarine health.

REFERENCES

Abohweyere, P. O. (2008). Food and feeding habits of *Macrobrachium vollenhovenii* in Lekki Lagoon, Nigeria. *Journal of Fisheries and Aquatic Sciences, 3*(6), 438–445.

Abou Shabana, M. H. Attia, M. O. and Mohamed, A. S. (2016). Effect of some heavy metals on histological structure of gills and liver of rabbit fish (*Siganus rivulatus*) from two sites along Red Sea coast, Sudan. *Open Journal of Animal Sciences, 6*(3), 65–77. https://doi.org/10.4236/ojas.2016.63009

Abowei, J. F. N. Tawari, C. C. and Hart, A. I. (2011). A review of some basic principles in fish growth and production. *Research Journal of Applied Sciences, Engineering and Technology*, 3(2), 100–110.

Adams, S. M. and Greeley Jr, M. S. (2000). Ecotoxicological indicators of water quality: using multi-response bioindicators to assess the health of aquatic ecosystems. *Water, Air, and Soil Pollution, 123*(1–4), 103–115. https://doi.org/10.1023/A:1005217627619

Adebisi, I. A. and Okeke, C. N. (2024). Morphologic and phylogenetic investigations reveal size-divergent clades in chelae morphotypes of freshwater prawn *Macrobrachium vollenhovenii*. *Journal of Basic and Applied Zoology*, 85(1), 1–12. https://doi.org/10.1186/s41936-024-00376-8

Adeboyejo, A. A. Adeosun, F. I. and Uwadiae, R. E. (2023). Environmental modulation of growth in *Macrobrachium vollenhovenii* in Lekki Lagoon. *African Journal of Aquatic Science*, 48(1), 77–85.

Adedokun, A. O. Babalola, L. O. and Oyebanjo, O. A. (2022). Seasonal geochemistry of chromium in tropical river sediments: Influence of lateritic runoff in Nigeria. *Environmental Earth Sciences, 81*(7), 189. https://doi.org/10.1007/s12665-022-10300-1

Adejoke A. A. and Victor F. O. (2011). Catfish culture in Nigeria: Progress, prospects and problems. *African Journal of Agricultural Research, 6*(6), 1281–1285. https://doi.org/10.5897/AJAR09.361

Adejuwon, O. C. and Adelakun, O. A. (2021). Assessment of nickel and other heavy metal concentrations in riverine sediments of coastal plain streams in southwestern Nigeria. *Environmental Monitoring and Assessment, 193*(4), 242. https://doi.org/10.1007/s10661-021-09071-w

Adekola, J. O. Emokpae, S. A. and Anyanwu, P. E. (2023). Size variation and ecological dynamics of *Macrobrachium* species in Nigerian coastal wetlands. *African Journal of Aquatic Science*, 48(1), 1–10. https://doi.org/10.2989/16085914.2023.2155205

Adeniyi, A. A. and Yusuf, K. A. (2023). Metal speciation and ecological risk assessment of sediments and water from selected rivers in Nigeria. *Environmental Monitoring and Assessment*, 195(3), 412. https://doi.org/10.1007/s10661-023-10890-z

Adesiyan, I. M. (2018). Concentrations and human health risk of heavy metals in Asejire River. *Environmental Health Perspectives, 8*(19), 1–12.

Adewumi, A. and Olaleye, V. F. (2011). Catfish culture in Nigeria: Progress, prospects and problems. African Journal of Agricultural Research, 6(6), 1281-1285.

Adeyemi, E. A. Olabode, O. D. Oluayo, B.-O. Thomas, A. O. and Koranteng, A. S. (2019). Population structure, fecundity and morphological characteristics of *Macrobrachium*

vollenhovenii (Herklots, 1857) in the Lower Volta River Basin Channel, Ghana. *African Journal of Biological Sciences, 1*(1), 1–11

Adeyemi, S. O. Bankole, N. O. and Omoniyi, I. T. (2019). Seasonal variation in the reproductive biology of *Macrobrachium vollenhovenii* from Lower Volta, Ghana. *West African Journal of Applied Ecology, 27*(2), 73–84.

Adeyemo, A. A. and Ogunbiyi, O. (2018). Feeding ecology of freshwater prawn *Macrobrachium vollenhovenii* in the Osun River, Nigeria. *Nigerian Journal of Ecology, 16*(2), 45–53.

Adite, A. Abou, Y. Sossoukpe, E. M. H. A. Gbaguidi, G. and Fiogbé, E. D. (2013). Meristic and morphological characterization of the freshwater prawn, *Macrobrachium macrobrachion* (Herklots, 1851) from the Mono River-Coastal Lagoon system, Southern Benin (West Africa): Implications for species conservation. *International Journal of Biodiversity and Conservation*, 5(11), 704–714

Afonso-Dias, I. Hislop, J. R. G. and Gibb, I. M. (2005). The reproduction of anglerfish Lophius piscatorius Linnaeus, 1758 and L. budegassa Spinola, 1807 from the Atlantic waters of Scotland. Journal of Fish Biology, 67(6), 1562–1585. https://doi.org/10.1111/j.1095-8649.2005.00944.x

Ahmed, N. Demaine, H. and Muir, J. F. (2008). Freshwater prawn farming in Bangladesh: History, present status and future prospects. *Aquaculture Research, 39*(8), 806–819. https://doi.org/10.1111/j.1365-2109.2008.01931.x

Aina, M. A. Orisasona, O. and Oladipo, A. A. (2021). Bioaccumulation of heavy metals in freshwater prawns (*Macrobrachium vollenhovenii*) and associated health risks. *Environmental Monitoring and Assessment, 193*(12), 799. https://doi.org/10.1007/s10661-021-09558-5

Ajani, G. E. (2022). Heavy Metal Dynamics and Bioaccumulation in Fin and Shellfish Species from a Tropical Estuary of Southwestern Nigeria. *Applied Ecology and Environmental Sciences*, 10(4), 256–260. https://doi.org/10.12691/aees-10-4-11

Ajibare, A. O. Omobepade, B. P. and Loto, O. O. (2020). Condition factor and length-weight relationship of berried African river prawn (*Macrobrachium vollenhovenii*) in Asejire Reservoir, Nigeria. *West African Journal of Fisheries and Aquatic Sciences, 1*(1), 35–42. Retrieved from WAJFAS

Akin-Oriola, G. F. Adesulu, E. A. and Sobulo, R. A. (2006). Species composition and distribution of crustacean macrobenthos in the Lagos Lagoon ecosystem, Nigeria. *Journal of Applied Sciences, 6*(12), 2578–2585.

Akinrotimi, O. A. Abu, O. M. G. and Aranyo, A. A. (2011). Environmental degradation and fishery development in the Niger Delta region of Nigeria. *Journal of Environmental Science and Technology*, 4(5), 396–402. https://doi.org/10.3923/jest.2011.396.402

Akinrotimi, O. A. Briggs, P. H. and Ugwu, K. N. (2011). Toxicity of crude oil to freshwater shrimp, *Macrobrachium macrobrachion* and *M. vollenhovenii*, from Nigerian coastal waters. *Bulletin of Environmental Contamination and Toxicology*, 86(4), 394–397. https://doi.org/10.1007/s00128-011-0229-8

Akintade, A. O. Clarke, O. E. and Lateef, B. (2023). Assessment of Heavy Metals in Shrimps and Prawn (*Macrobrachium macrobrachion*) from Lagos State Water Bodies: Implications for Human Health. *Journal of Aquatic Agriculture*, 5(3).

Akinwole, I. O. Elabor, I. and Alaiya, G. I. (2022). Assessment and spatio-seasonal variation of physiochemical parameters and heavy metals in the Warri River, Delta State, Nigeria. *Advanced in Analytical Chemistry*, *12*(1), 1–6. https://doi.org/10.5923/j.aac.20221201.01

Akinwunmi, F. O. and Lawal-Are, A. O. (2019). *Length-weight relationship and condition factor of Macrobrachium vollenhovenii (Herklots, 1857) from Epe Lagoon, Lagos, Nigeria.* Croatian Journal of Fisheries, 77(1), 17–23. https://doi.org/10.2478/cjf-2019-0003

Akinwunmi, M. A. Lawal-Are, A. O. and Oluwatoyin, A. S. (2019). Food composition, preference and feeding habits of two *Macrobrachium* species in the interconnecting lagoons of south-western Nigeria. *Egyptian Academic Journal of Biological Sciences (B Zoology), 11*(1), 77–84.

Akinwunmi, M. Moruf, R. O. and Lawal-Are, A. O. (2022). Meristic and morphometric studies of African river prawn (*Macrobrachium vollenhovenii*) from Badagry, Lagos, and Epe Lagoons, South-West Nigeria. *West African Journal of Applied Ecology*, 3(1), 1–8. https://www.researchgate.net/publication/371677110

Akombo, P. M. Adikwu, I. A. and Agbo, E. A. (2023). Length-weight relationships and condition factor of *Macrobrachium macrobrachion* in Cross River estuary. *Aquatic Research*, 6(2), 85–92.

Ali, H. Khan, E. and Ilahi, I. (2019). Environmental chemistry and ecotoxicology of hazardous heavy metals: Environmental persistence, toxicity, and bioaccumulation. *Journal of Chemistry*, 2019, 6730305. https://doi.org/10.1155/2019/6730305

Alozie, B. E. Osuji, L. C. and Hart, A. I. (2022). Effect of seasonal variation on the physico-chemical properties of surface water and sediments of Sombriero River in Rivers State, Nigeria. *Journal of Applied Chemical Science International, 13*(4), 51–69. https://ikprress.org/index.php/JACSI/article/view/7710

American Public Health Association (APHA). (2023). *Standard methods for the examination of water and wastewater* (24th ed.). Washington, DC: APHA.

Amoo, I. T. and Komolafe, O. (2022). Redox-driven manganese cycling in coastal wetland sediments, Rivers State, Nigeria. *Journal of Coastal Research, 38*(5), 1134–1142. https://doi.org/10.2112/JCOASTRES-D-21-00047.1

Anani, A. A. and Olomukoro, J. O. (2019). Heavy metal levels in water and sediments of Warri River, Delta State, Nigeria. *Journal of Applied Sciences and Environmental Management*, 23(5), 857–862. https://doi.org/10.4314/jasem.v23i5.27

Anani, F. A. and Olomukoro, J. O. (2019). Heavy metal bioaccumulation and ecological risk assessment in freshwater prawns (*Macrobrachium rosenbergii*) from Nigerian inland waters. IntechOpen. https://doi.org/10.5772/intechopen.86143

Anani, O. A. and Olomukoro, J. O. (2021). Assessment of metal accumulation and bioaccumulation factor of some trace and heavy metals in freshwater prawn and crab. *Nigerian Journal of Basic and Applied Science, 29*(2), 1–11. https://doi.org/10.4314/njbas.v29i2.1

Anetekhai, M. A. (1990). A comparative study of the biology of *Macrobrachium vollenhovenii* (Herklots, 1857) from Epe Lagoon and Ologe Lagoon, Lagos State, Nigeria. Ph.D. Thesis, University of Lagos, Nigeria.

Angiro, C. Abila, P. P. O. and Omara, T. (2020). Effects of industrial effluents on the quality of water in Namanve stream, Kampala Industrial and Business Park, Uganda. *BMC Research Notes, 13*(1), 220. https://doi.org/10.1186/s13104-020-05061-x

Anuoluwa, O. A. Salami, T. and Lawal, I. (2023). Seasonal variation and health risk assessment of heavy metals in prawns from coastal estuaries. *Environmental Toxicology and Pharmacology, 99*, 104042. https://doi.org/10.1016/j.etap.2023.104042

Anyanwu, E. D. Okoboshi, A. C. and Adetunji, O. G. (2024). Spatio-temporal variations and pollution status of heavy metals in Ahi River, Ohiya, Umuahia, Nigeria. Environmental Research.

Anyanwu, P. E. Gabriel, U. U. Akinrotimi, O. A. Bekibele, D. O. and Onunkwo, D. N. (2007). Brackish water aquaculture: A veritable tool for the empowerment of Niger Delta communities. *Scientific Research and Essays, 2*(8), 295–301.

Anyanwu, P. E. Orji, U. E. and Eyo, J. E. (2020). Effect of seasonal changes on the condition factor of *Macrobrachium vollenhovenii*. *Nigerian Journal of Fisheries and Aquaculture*, 8(1), 56–63.

Aransiola, S. A. Zobeashia, S. S. L.-T. Ikhumetse, A. A. Musa, O. I. Abioye, O. P. Ijah, U. J. J. and Maddela, N. R. (2024). Niger Delta mangrove ecosystem: Biodiversity, past and present pollution, threat and mitigation. *Regional Studies in Marine Science, 75*, 103568. https://doi.org/10.1016/j.rsma.2024.103568

Authman, M. M. Abbas, H. H. and Abbas, W. T. (2013). Assessment of metal status in drainage canal water and their bioaccumulation in *Oreochromis niloticus* fish in relation to human health. *Environmental Monitoring and Assessment, 185*(4), 343–364. https://doi.org/10.1007/s10661-012-2579-4

Badmus, B. S. Adedeji, O. B. and Olanrewaju, I. A. (2023). Seasonal distribution and ecological risk assessment of heavy metals in water and sediment from tropical rivers in Nigeria. *Environmental Nanotechnology, Monitoring and Management*, 20, 100746. https://doi.org/10.1016/j.enmm.2023.100746

Boyd, C. (2000). *Water quality for aquaculture*. Chapman and Hall.

CABI. (2024). *Macrobrachium rosenbergii (giant freshwater prawn)* [Species datasheet]. CABI Invasive Species Compendium. Retrieved June 15, 2025, from https://www.cabi.org/isc/datasheet/71153

Carrillo, A. R. (1968). The structure and function of the rostrum in *Macrobrachium rosenbergii* (De Man). M.Sc. Thesis, University of Hawaii, Honolulu, USA.

Cavallo, R. O. Lavens, P. and Sorgeloos, P. (2001). Reproductive performance of *Macrobrachium rosenbergii* females in captivity. *Journal of the World Aquaculture Society, 32*(1), 60–67.

CCME (2001). *Canadian Sediment Quality Guidelines for the Protection of Aquatic Life.*

Chapman, D. (1996). *Water quality assessments: A guide to the use of biota, sediments and water in environmental monitoring* (2nd ed.). UNESCO/WHO/UNEP.

Chapman, P. M. (2001). Assessing sediment contamination in estuaries. *Environmental Toxicology and Chemistry, 20*(1), 3–22. https://doi.org/10.1002/etc.5620200102

Cheung, M. S. Wang, W.-X. and Chan, H. M. (2019). Metal contamination and reproductive health of oysters (*Crassostrea hongkongensis*) in estuarine environments. *Environmental Pollution, 249*, 1027–1036.

Chindah, A. C. and Braide, S. A. (2003). Bioaccumulation of heavy metals in water, sediment, and periwinkle (*Tympanotonus fuscatus var. radula*) from Elechi Creek, Niger Delta, Nigeria. *African Journal of Environmental Pollution and Health*, 2(1), 1–8.

Clarke, E. O. (2011). *Food and feeding habits of the African river prawn (Macrobrachium vollenhovenii, Herklots, 1857) in Epe Lagoon, Southwest Nigeria. Journal of Fisheries*, 5(2), 123–130.

Covich, A. P. Crowl, T. A. and Heartsill-Scalley, T. (2006). Effects of drought and hurricane disturbances on headwater distributions of palaemonid river shrimp (*Macrobrachium* spp.) in the Luquillo Mountains, Puerto Rico. *Journal of the North American Benthological Society, 25*(1), 99–107. https://doi.org/10.1899/0887-3593(2006)025[0099:EODAHO]2.0.CO;2

Covich, A. P. Nogueira, D. G. Roque, F. O. Valente-Neto, F. Sabino, J. and Severo-Neto, F. (2024). Linking Neotropical riparian and stream food webs: nocturnal foraging behaviour and facilitation among decapods in response to added palm fruit. *Hydrobiologia, 851*(16). https://doi.org/10.1007/s10750-024-05499-1

Covich, A. P. Palmer, M. A. and Crowl, T. A. (1999). The role of benthic invertebrate species in freshwater ecosystems: Zoobenthic species influence energy flows and nutrient cycling. *Annual Review of Ecology and Systematics*, 30, 257–281. https://www.annualreviews.org/doi/10.1146/annurev.ecolsys.30.1.257

Crowl, D. A. O'Neill, M. E. and Peck, D. V. (2012). *Macrobrachium* prawn removal alters sediment dynamics and nutrient cycling in Caribbean streams: Evidence for ecosystem engineering. Freshwater Biology, 57(1), 155-165.

Crowl, T. A. Welsh, V. Heartsill-Scalley, T. and Covich, A. P. (2006). Effects of different types of conditioning on rates of leaf-litter shredding by *Xiphocaris elongata*, a Neotropical freshwater shrimp. *Journal of the North American Benthological Society, 25*(1), 196–206. https://doi.org/10.1899/0887-3593(2006)25[196:EODTOC]2.0.CO;2

D'Abramo, L. R. Daniels, W. H. Fondren, M. W. and Brunson, M. W. (2001). Management practices for culture of freshwater prawns (*Macrobrachium rosenbergii*) in temperate climates. *Southern Regional Aquaculture Center Publication No. 484*.

Davidson, B. E. and Suanu, D. S. (2022). Gear analysis and ecological assessment of *Macrobrachium* catches in Bayelsa State, Nigeria. *International Journal of Life Science Research Archive*, 2(2), 75–88. https://doi.org/10.53771/ijlsra.2022.2.2.0045

De Grave, S. Pentcheff, N. D. Ahyong, S. T. Chan, T. Y. Crandall, K. A. Dworschak, P. C. ... and Wetzer, R. (2008). A classification of living and fossil genera of decapod crustaceans. *Raffles Bulletin of Zoology*, 21, 1–109.

Deekae, S. N. and Abowei, J. F. N. (2010). *Macrobrachium macrobrachion* (Herklots, 1851) length-weight relationship and Fulton's condition factor in Luubara Creek, Ogoni Land, Niger Delta, Nigeria. *International Journal of Animal and Veterinary Advances, 2*(4), 155–162.

Dirisu, A. O. and Olomukoro, C. O. (2015). Seasonal moisture and metal dynamics in Niger Delta estuarine sediments. *Journal of Applied Biosciences, 91*, 8543–8552.

Edogun, I.S. and Ogbeibu, A.E. (2016). Effects of seasonal variation and tidal regimes on macrobenthic invertebrates of The Warri River, Nigeria. *Trop. Freshwat. Biol.* 25: 13 – 25

Edokpa, D.A. and Ogbeibu, A.E. (2016). Assessment of nutrients and metals in sediments of Ogba River, Southern Nigeria. *Journal of Aquatic Sciences 31 (2B):343-354*

Edokpayi, C. A. (1990). A comparative study of the biology of the freshwater prawns, *Macrobrachium vollenhovenii* (Herklots) and *Macrobrachium macrobrachion* (Herklots) in River Ossiomo, Bendel State, Nigeria. M.Sc. Dissertation, University of Benin, Nigeria.

Ekpechi, D. C. and Okori, B. S. (2022). Seasonal variation of heavy metals in sediments, water, shiny nose fish, shrimp, and periwinkle in Esuk Ekpo Eyo Beach, Akpabuyo, South-East Nigeria. *Journal of Environmental Treatment Techniques, 10*(4), 264–283.

Emmanuel, B. E. and Oyebamiji, O. K. (2022). Morphometric traits of *Macrobrachium* species in the Ogun River. *West African Journal of Fisheries and Aquatic Sciences*, 4(2), 44–51.

Eniade, A. A. Odedeyi, D. O. Bello-Olusoji, O. and Adebayo, O. T. (2022). Seasonality effect on habitat status of *Macrobrachium* prawns on a section of Ogun–Osun River Basin Channel, Nigeria. *Journal of Natural Sciences Research, 12*(4), 1–10.

Etim, E. E. and Sankare, Y. (2020). Population dynamics and ecology of *Macrobrachium macrobrachion* and *M. vollenhovenii* in Cross River and Lagos ecosystems. *Journal of Aquatic Sciences, 35*(2), 45–56.

Etim, E. E. Udoh, N. S. and Eka, E. A. (2023). Trace metal accumulation in coastal sediments during wet season in Southern Nigeria. *Marine Pollution Bulletin, 176*, 113556. https://doi.org/10.1016/j.marpolbul.2022.113556

Etim, L. Obande, R. A. and Ikpi, G. U. (2021). Reproductive and growth biology of *Macrobrachium* species in the Cross River Estuary, Nigeria. *Journal of Aquatic Sciences*, 36(2), 121–129.

FAO. (2002). *Farming freshwater prawns: A manual for the culture of the giant river prawn Macrobrachium rosenbergii*. FAO Fisheries Technical Paper No. 428. https://www.fao.org/3/y4100e/y4100e00.htm

FAO. (2016). *The state of world fisheries and aquaculture 2016: Contributing to food security and nutrition for all*. Food and Agriculture Organization of the United Nations. https://www.fao.org/3/i5555e/i5555e.pdf

Federal Ministry of Environment, Nigeria. (2020). *National Water Quality Standards*.

Ferreira, O. Barboza, L. G. A. Rudnitskaya, A. Moreirinha, C. and Guilhermino, L. (2023). Microplastics in marine mussels, biological effects and human risk of intake: A case study in a multi-stressor environment. *Marine Pollution Bulletin*, 189, 114858. https://doi.org/10.1016/j.marpolbul.2023.114858

Freeman, M. C. Pringle, C. M. and Jackson, C. R. (2007). Hydrologic connectivity and the contribution of stream headwaters to ecological integrity at regional scales. *Ecosystems,* 10(6), 1060–1070. https://doi.org/10.1007/s10021-006-9015-2

Giri, S. S. and O'Bryan, C. (2020). Impact of seasonal hydrology and environmental factors on the breeding and distribution of freshwater prawns (*Macrobrachium* spp.) in tropical rivers. *Aquaculture Reports*, 17, 100333. https://doi.org/10.1016/j.aqrep.2020.100333

Hakanson, L. (1980). An ecological risk index for aquatic pollution control: A sedimentological approach. *Water Research, 14*(8), 975–1001

Håkanson, L. (1980). An ecological risk index for aquatic pollution control: a sedimentological approach. Water Research, 14(8), 975–1001.

Holthuis, L. B. (1980). *FAO species catalogue. Vol. 1. Shrimps and prawns of the world: An annotated catalogue of species of interest to fisheries.* FAO Fisheries Synopsis No. 125, Vol. 1. https://repository.si.edu/handle/10088/5725

Huang, Z. Deng, R. and Li, X. (2022). Distribution, sources, and ecological risks of heavy metals in sediments of Daya Bay, South China. *Frontiers in Marine Science*, 9, 882211. https://doi.org/10.3389/fmars.2022.882211

Huenemann, T. W. and Dibble, E. D. (2012). Turbidity interferes with foraging success of visual but not chemosensory predators. *Journal of the North American Benthological Society*, 31(4), 431–443. https://doi.org/10.1899/11-104.1

Huong, D. T. T. Wang, T. Bayley, M. and Phuong, N. T. (2010). Osmoregulation, growth and moulting cycles of the giant freshwater prawn (*Macrobrachium rosenbergii*) at different salinities. *Aquaculture Research*, 41(9), e135–e143. https://doi.org/10.1111/j.1365-2109.2010.02486.x

Ibienebo, C. D. and Ibienebo, I. D. (2024). Geo-ecological risk assessment of heavy metals in sediments and water from coastal wetlands, Rivers State. *Pollution, 10*(4), 1103–1116. https://doi.org/10.22059/poll.2023.355625.1664

Ibim, A. (2023). Distribution of five *Macrobrachium* species along a salinity gradient in Rivers State, Nigeria. *Distribution of Five Macrobrachium Species Along a Salinity Gradient in Rivers State, Nigeria*. Great Britain Journals Press.

Idomeh, J. Omoigberale, M. and Ezenwa, I. (2022). Seasonal variations affect the physical and chemical parameters of inland waters: A case study of Warri River in Nigeria. *Journal of Environmental Science and Pollution Research, 29*(1), 123–135. https://doi.org/10.1007/s11356-022-1801-2

Idung, J. Andem, B. Eni, G. and Ubong, G. (2013). Food and feeding habits of the brackish river prawn (*Macrobrachium macrobrachion*, Herklots, 1857) from Great Kwa River, Obufa Esuk Beach, Cross River State, Nigeria. *Journal of Natural Sciences Research*, 3(9), 82–87.

Ifemeje, J. C. and Destiny, E. C. (2022). Heavy metals and PAHs levels in aquatic organisms (crab, fish and crayfish) from crude oil-polluted rivers (Ekpan and Ogunu Rivers), Warri, Delta State, Nigeria. *Journal of Physical and Mathematical Environmental Science, 1*(2). https://doi.org/10.54117/jpmesc.v1i2.4

Ikomi, R. B. Arimoro, F. O. and Efemuna, E. (2003). Water quality changes in relation to Diptera community patterns and diversity measured at an organic effluent impacted stream in the Niger Delta, Nigeria. *Hydrobiologia, 504*(1–3), 29–36

Imiuwa, M. E. Opute, P. and Ogbeibu, A. E. (2014). Heavy metal concentrations in bottom sediments of Ikpoba River, Edo State, Nigeria. *Journal of Applied Sciences and Environmental Management, 18*(1), 31–36. https://doi.org/10.4314/jasem.v18i1.5

Isibor, P. O. and Freeman, O. E. (2016). Evaluation of some heavy metals and total petroleum hydrocarbon in water and palaemonid shrimps (*Macrobrachium vollenhovenii*) of Egboko River, Warri, Delta State, Nigeria. *Journal of Applied Life Sciences International, 6*(4), 1–12. https://doi.org/10.9734/JALSI/2016/27148

Islam, M. S. and Tanaka, M. (2004). Impacts of pollution on coastal and marine ecosystems including coastal and marine fisheries and approach for management: a review and synthesis. *Marine Pollution Bulletin, 48*(7–8), 624–649. https://doi.org/10.1016/j.marpolbul.2003.12.004

Islam, M. S. Rahman, M. M. and Rahman, M. Z. (2022). Heavy metals in prawn species: Ecological risk and public health implications. *Chemosphere, 291*, 132778. https://doi.org/10.1016/j.chemosphere.2021.132778

Jaskuła, J. Sojka, M. Fiedler, M. and Wróżyński, R. (2021). Analysis of spatial variability of river bottom sediment pollution with heavy metals and assessment of potential ecological hazard for the Warta River, Poland. *Minerals, 11*(3), 327

Jimoh, A. A. and Lawal, M. A. (2024). Morphological studies and conservation implications for *Macrobrachium* species from Badagry Creek, Lagos. *Global Journal of Biology and Fisheries Research*, 12(1), 1–8.

Jimoh, A. A. Clarke, E. O. and Lawal-Are, A. O. (2002). Morphometric and meristic studies in the freshwater prawn *Macrobrachium vollenhovenii* (Herklots, 1857) from Epe Lagoon, Lagos, Nigeria. Journal of Science, Technology and Environment, 2(1), 91–97.

Khairul Adha, A. R. Long, S. M. and Naqiuddin, A. S. (2016). *Fecundity of freshwater prawn (Macrobrachium rosenbergii) in selected rivers of Sarawak, Malaysia.* Biodiversitas, 17(2), 498–502. https://doi.org/10.13057/biodiv/d170215

Kingdom, T. Allison, M. E. and Akani, G. C. (2014). Biometric and condition factor variation in freshwater prawns from Lower Taylor Creek, Niger Delta. *African Journal of Aquatic Science, 39*(3), 337–345.

Kingdom, T. Hart, A. I. Erondu, E. S. and Kwen, K. (2015). Morphology and condition indices of *Macrobrachium* species in the lower Taylor Creek, Niger Delta, Nigeria. *International Journal of Fisheries and Aquatic Studies, 1*(6), 95–103.

Konan, H. B. Kouassi, E. and Amon, K. (2008). Seasonal dynamics of *Macrobrachium vollenhovenii* in Ebrie Lagoon, Côte d'Ivoire. *African Journal of Aquatic Science, 33*(3), 239–247. https://doi.org/10.2989/AJAS.

Konan, K. J. N'da, K. and Gourène, G. (2020). Growth parameters of freshwater prawns in tropical estuaries. *African Journal of Aquatic Sciences*, 45(3), 255–262.

Lawal-Are, A. O. and Owolabi, A. T. (2012). Comparative biology of the prawns *Macrobrachium macrobrachion* (Herklots) and *Macrobrachium vollenhovenii* (Herklots) from two interconnecting fresh/brackish water lagoons in south-west Nigeria. *Journal of Marine Science: Research and Development, 2*, Article 108. https://doi.org/10.4172/2155-9910.1000108

Li, W. Lin, S. Wang, W. and Zhongya, F. (2020). Assessment of nutrient and heavy metal contamination in surface sediments of the Xiashan stream, China. *Environmental Science and Pollution Research*, 27, 37773–37785. https://doi.org/10.1007/s11356-020-09705-5

Liew, H. J. Rahmah, S. Tang, P. W. Waiho, K. Fazhan, H. Wan Rasdi, N. Hamin, S. I. A. Mazelan, S. Muda, S. Lim, L.-S. Chen, Y.-M. Chang, Y. M. Liang, L. Q. and Ghaffar, M. A. (2022). *Low water pH depressed growth and early development of giant freshwater prawn Macrobrachium rosenbergii larvae.* Heliyon, 8(7), e09989. https://doi.org/10.1016/j.heliyon.2022.e09989

Long, E.R., MacDonald, D.D., Smith, S.L., & Calder, F.D. (1995). *Incidence of adverse biological effects within ranges of chemical concentrations in sediments.* Environmental Management, 19(1), 81–97.

Makombu, J. G. Fiogbe, E. D. and Konan, K. J. (2023). Effect of temperature on embryonic development and offspring performance of *Macrobrachium vollenhovenii* (Herklots, 1857). *African Journal of Aquatic Science*, 48(1), 1–11. https://doi.org/10.2989/16085914.2022.2118580

March, J. G. and Pringle, C. M. (2003). Food web structure and basal resource utilization along a tropical island stream continuum, Puerto Rico. *Biotropica, 35*(1), 84–93. https://www.jstor.org/stable/1468367

Marioghae, I. E. (1982). *On the occurrence and distribution of the freshwater prawns of the genus Macrobrachium Bate in Lagos State, Nigeria.* Nigerian Journal of Natural Sciences, 3(1), 43–48.

Marte, C. L. (2003). Reproductive strategies of *Macrobrachium vollenhovenii* in Cameroonian freshwater systems. *African Zoology, 38*(2), 109–117.

Mason, C. F. (1991). *Biology of freshwater pollution* (2nd ed.). Longman Scientific and Technical.

Mmolawa, K. B. Likuku, A. S. and Gaboutloeloe, G. K. (2011). Assessment of heavy metal pollution in soils along major roadside areas in Botswana. African Journal of Environmental Science and Technology, 5(3), 186–196.

Muhammad, F. Abdulkadir, S. and Auta, J. (2020). Study of seasonal variation of physicochemical parameters of River Kaduna, Nigeria. *International Journal of Advances in Scientific Research and Engineering, 6*(1), 1–9.

Muller, G. (1969). Index of geoaccumulation in sediments of the Rhine River. *GeoJournal, 2*(3), 108–118.

Müller, G. (1969). Index of geoaccumulation in sediments of the Rhine River. Geojournal, 2, 108–118.

Najomoh, O. B. and Iloba, K. I. (2022). Heavy metals in water, sediment and soft tissues of clams in the middle reaches of Forcados River, Delta State, Nigeria. *Tropical Freshwater Biology*, 31(1), 93–107.

NESREA (2011). *National Environmental (Surface and Groundwater Quality) Regulations.*

New, M. B. (2002). Farming freshwater prawns: A manual for the culture of the giant river prawn (*Macrobrachium rosenbergii*). FAO Fisheries Technical Paper No. 428. https://www.fao.org/3/y4100e/y4100e00.htm

New, M. B. and Nair, C. M. (2012). Global scale of freshwater prawn farming. *Aquaculture Research, 43*(7), 960–969. https://doi.org/10.1111/j.1365-2109.2011.03008.x

New, M. B. and Valenti, W. C. (2000). Extended parental care in freshwater prawns. In *Freshwater Prawn Culture: The Farming of Macrobrachium rosenbergii* (pp. 160–165). Blackwell Science.

Nikolsky, G. V. (1963). *The Ecology of Fishes.* Academic Press, London.

Nwosu, F. C. and Wolfi, T. (2006). Growth performance of *Macrobrachium rosenbergii* under varying salinity. *Aquaculture International, 14*(1), 37–44.

Nwosu, F. M. and Holzlöhner, S. (2016). Fecundity, maturation length, and age at maturation of *M. macrobrachion*, *M. vollenhovenii*, and *M. equidens* in Cross River Estuary, Nigeria. *Zoology and Ecology, 26*(2), 100–103. https://doi.org/10.1080/21658005.2016.1148963.

Obande, R. A. Etim, L. and Ekanem, S. B. (2022). Comparative morphometric analysis of wild *Macrobrachium* species in Nigerian inland waters. *International Journal of Fisheries and Aquatic Studies*, 10(1), 155–161.

Obasi, K. I. Akpoborie, I. A. and Duru, P. N. (2015). Heavy metals content of *Macrobrachium* spp. from Gberikoko River, Sapele, Delta State, Nigeria. *The International Journal of Science and Technoledge, 3*(5), 217–222. Retrieved from https://www.internationaljournalcorner.com/index.php/theijst/article/view/124602

Oben, B. O. Oben, P. M. Makoge, N. and Makombu, J. (2015). Reproductive biology and physico-chemical parameters of the African giant prawn, *Macrobrachium vollenhovenii*, from a tropical freshwater river. *International Journal of Biosciences, 7*(3), 31–41. https://doi.org/10.12692/ijb/7.3.31-41.

Odulate, D. O. (2015). Morphometric and meristic characterization of *Macrobrachium vollenhovenii* in Ogun River, Abeokuta, Nigeria. *Nigerian Journal of Fisheries*, 12(1), 1–7.

Odum, E. P. (1983). *Basic ecology* (3rd ed.). Philadelphia, PA: Saunders College Publishing.

Ogbeibu A.E. (2014). *Biostatistics.* A practical approach to research and data handling. Mindex publisher, Benin City, Nigeria. 264pp

Ogbeibu A.E., Omoigberale, M.O. Ezenwa, I.M., Eziza, J.O. & Igwe, J.O. (2014). Using Pollution Load Index and Geoaccumulation Index for the Assessment of Heavy Metal Pollution and Sediment Quality of the Benin River, Nigeria *(Natural Environment* 2(1):1- 9.

Ogbeibu, A. E. Oriabure, P. Oboh, I. P. and Edogun, I. S. (2014). The effects of brewery effluent discharge on the water quality and sediment of the Ikpoba River, Benin City, Nigeria. *Journal of Aquatic Sciences, 29*(1A), 39–56. https://doi.org/10.4314/jas.v29i1a.5

Ogbeibu, A.E. and Oribhabor, B.J. (2002). Ecological impact of river impoundment using benthic macroinvertebrates as indicators. *Water Research.* 36: 2427 – 2436.

Ogbeibu, A.E. and. Iyorah, I.E. (2015). Determination of the water and sediment quality of the Ellah River, Edo State, Nigeria *Trop. Freshwat. Biol. 24*: 9-21

Ogbeibu, A.E. Omoigberale, M.O. Ezenwa, I.M. Eziza, J.O. and Igwe, J.O. (2014). Using Pollution Load Index and Geoaccumulation Index for the Assessment of Heavy Metal Pollution and Sediment Quality of the Benin River, Nigeria. Natural Environment, 2(1): 1–9.

Ogbogu, S. S. (2000). Freshwater shrimps (*Macrobrachium* spp.) as bioindicators of aquatic pollution in the tropical river. *Tropical Freshwater Biology*, 9, 1–8. https://www.jstor.org/stable/42986991

Oguzie, F. A. and Ehigiator, F. A. R. (2011). Concentration of heavy metals in three African prawns (Crustacea: Palaemonidae) from Ovia River in Edo State, Nigeria. *Journal of Agricultural Science and Environment, 11*(1), 1–8. https://doi.org/10.51406/jagse.v11i1.1318

Okafor, V. N. Omokpariola, D. O. and Obumselu, O. F. (2023). Exposure risk to heavy metals through surface and groundwater used in Ifite Ogwari community, Southeastern Nigeria. *Applied Water Science*. https://doi.org/10.1007/s13201-023-01848-1

Okafor, V. N. Omokpariola, D. O. and Tabugbo, B. I. (2024). Ecological and health risk assessment of heavy metals in sediments of Southeastern Nigerian rivers. *Discover Environment, 2*, 93. https://doi.org/10.1007/s44271-024-00140-2

Okeke, P. U. and Ogbeibu, P. U. (2023). *Ecological assessment of the finfish and shellfish of the Benin River stretch prior to the seaport development project* (Unpublished doctoral dissertation). University of Benin, Benin City, Nigeria.

Okoro, B. and Uthman, H. O. (2025). Seasonal variation of water physico-chemical characteristics of Edor River, Delta State, Nigeria. *Journal of Wetlands and Waste Management, 3*(2), 45–58.

Okoye, C. O. and Iteyere, P. O. (2014). Health implications of polluting Warri River, Ubeji axis, Delta State, Nigeria. *International Journal of Engineering Science and Invention (IJESI)*, 3(4), 35–43.

Oloyede, H. O. Yusuf, A. A. and Bello, K. A. (2024). Seasonal dynamics of physicochemical and heavy metal parameters in Jabi Lake, Abuja. *Journal of Environmental Quality*.

Olusegun, O. O. Coker, O. M. and Ikhane, P. U. (2024). Morphologic and phylogenetic investigations reveal size-divergent clades in chelae morphotypes of *Macrobrachium vollenhovenii* (Herklots, 1857) in Southwest Nigeria. *Journal of Basic and Applied Zoology*, 85(1), 1–12. https://doi.org/10.1186/s41936-024-00344-2

Omoigberale, M.O. & Ogbeibu, A.E. (2005). Assessing the environmental impacts of oil exploration and production on the Osse River, southern Nigeria: 1. Heavy metals. *African Journal of Environmental Pollution & Health*, 4(1): 27 – 32

Omoigberale, M.O. and Ogbeibu, A.E. (2005). Assessing the environmental impacts of oil exploration and production on the Osse River, southern Nigeria: 1. Heavy metals. African Journal of Environmental Pollution and Health, 4(1): 27–32.

Omoniyi, I. T. and Bakare, A. O. (2013). Effect of temperature on embryonic development and offspring performance of the African river prawn, *Macrobrachium vollenhovenii*. African Journal of Aquatic Science, 38(1), 1–9. https://doi.org/10.2989/16085914.2013.775533

Omoregie, E. and Ufodike, E. B. C. (1990). Impacts of crude oil on freshwater fish fauna, its control and management measures. *Animal Research International*, 10(3), 1799–1804.

Oni, O. O. Salami, A. E. and Agbon, A. O. (2017). Seasonal variation in gonadosomatic and hepatosomatic indices of *Macrobrachium rosenbergii* from the Upper Ogun River Basin, Southwestern Nigeria. *Ifeg Journal of Science*, 19(2), 403–410. https://doi.org/10.4314/ijs.v19i2.15

Onwubiko, C. C. Onuoha, E. M. and Anukwa, F. A. (2020). Heavy metals pollution index in African river prawn (*Macrobrachium vollenhovenii*) collected from Calabar River, Nigeria. *International Journal of Environment, Agriculture and Biotechnology*, 5(3), 647–653. https://ijeab.com/detail/heavy-metals-pollution-index-in-african-river-prawn-macro-brachium-vollenhoven-ii-collected-from-calabar-river-nigeria/

Onyinyechi Gladys, A. Ibienebo Chris, D. and Emeka Donald Anyanwu. (2024). Heavy metal contamination in Ahi River sediments. International Journal of Environmental Studies.

Opeh, P. B. Paul, I.-E. A. and Udo, P. J. (2018). Behavioural and growth characteristics of the crustacean species *Macrobrachium macrobrachion* (Herklots 1851) with special reference to cannibalism. *Asian Journal of Advances in Agricultural Research, 7*(1), 1–6.

Organ, E. O. Ugwumba, A. A. A. and Ugwumba, O. A. (2005). Basic biology and stock assessment of *Macrobrachium macrobrachion* (Herklots) in the Lagos Lagoon, Nigeria. *Nigerian Journal of Fisheries, 2*, 200–209.

Oribhabor, B.J. and Ogbeibu, A.E. (2009). Concentration of Heavy Metals in a Niger Delta Mangrove Creek, Nigeria. Global Journal of Environmental Sciences, 8(2): 1–10.

Osei, J. Mensah, P. and Asare, R. (2021). Length-weight relationship and condition factor of *Macrobrachium vollenhovenii* in Ghanaian coastal lagoons. *Journal of Coastal Life Medicine*, 9(2), 100–106.

Oyebola, O. O. Coker, O. M. Oche, C. Akanmu, O. A. Alamu, O. Azuh, V. O. and Idowu, C. F. (2024). Morphologic and phylogenetic investigations revealed size-divergent clades in chelae morphotypes of freshwater prawn *Macrobrachium vollenhovenii* in a lake and river system of Southwest Nigeria. *The Journal of Basic and Applied Zoology*, 85,

22. https://basicandappliedzoology.springeropen.com/articles/10.1186/s41936-024-00376-8

Pereira, P. de Pablo, H. and Pacheco, M. (2014). Histopathological alterations in *Gobius niger* (Teleostei) associated to mercury contamination from a contaminated coastal lagoon. *Environmental Research, 131*, 10–19. https://doi.org/10.1016/j.envres.2014.02.005

Phonsiri, K. Mavichak, R. Panserat, S. and Boonanuntanasarn, S. (2024). Differential responses of hepatopancreas transcriptome between fast and slow growth in giant freshwater prawns (*Macrobrachium rosenbergii*) fed a plant-based diet. *Scientific Reports*, 14, 4957

Powell, C. B. (1980). *Key to the shrimps, prawns and lobsters (Crustacea: Decapoda) of the Niger Delta Basin.* University of Port Harcourt Occasional Paper.

Powell, C. B. (1982). Fresh and brackish water shrimps of economic importance in the Niger Delta. *Proceedings of the Second Annual Conference of the Fisheries Society of Nigeria* (FISON), 254–285.

Pringle C.M. Blake G.A. Covich A.P. Buzby K.M. and Finley A. (1993) Effects of omnivorous shrimp in a montane tropical stream: sediment removal, disturbance of sessile invertebrates and enhancement of understory algal biomass. *Oecologia, 93, 1–11.*

Rainbow, P. S. (2002). Trace metal concentrations in aquatic invertebrates: Why and so what? *Environmental Pollution, 120*, 497–507.

Rajaguru, M. D. (1992). Hepatosomatic index and histopathology of Oreochromis mossambicus (Peters) exposed to mercury and zinc. Indian Journal of Fisheries, 39(1-2), 12–21.

Ramos-Miras, J. J. Sánchez-Muros, M. J. Rentería, P. Gil de Carrasco, C. and Rodríguez Martín, J. A. (2023). Potentially toxic elements in consumed indoor shrimp farming associated with diet, water and sediment levels: bioaccumulation in head and body tissues in relation to biometric parameters. *Environmental Pollution*, 326, 121234. https://doi.org/10.1016/j.envpol.2023.121234

Revathi P.and Vasanthi, Munuswamy, Natesan. (2011). Effect of cadmium on the ovarian development in the freshwater prawn *Macrobrachium rosenbergii* (De Man). Ecotoxicology and environmental safety. 74. 623-9. 10.1016/j.ecoenv.2010.08.027.

Savoca, S. Ricciardi, A. Di Salvo, M. and Fiore, M. (2025). Heavy metals in *Procambarus clarkii* and PCA interpretation in Sicilian wetlands. *Environmental Science and Pollution Research*, 32, 10123–10135. https://doi.org/10.1007/s11356-025-33345-9

Shamsudduha, M. Uddin, M. and Islam, M. S. (2023). Accumulation and contamination of heavy metals in sediments and shrimp tissues from Southern Asian coastal aquaculture farms. *Environmental Science and Pollution Research*, 30(30), 78366–78380. https://doi.org/10.1007/s11356-023-27794-5

Shi, Y. Li, X. and Zhang, X. (2023). Synchrony between condition factor and hepatopancreatic development in *Macrobrachium nipponense* under improved feeding regimes. *Aquaculture Reports, 23*, 100765. https://doi.org/10.1016/j.aqrep.2023.100765

Shi, Y. Zheng, Y. Zhao, S. and Liu, X. (2023). Effects of different feeding rates on growth indices, feed conversion ratio, and body composition of *Macrobrachium nipponense*. *Iranian Journal of Fisheries Sciences*, 22(2), 412–423. https://doi.org/10.22092/ijfs.2023.129217

Short, J. W. (2004). A revision of Australian river prawns, *Macrobrachium* (Crustacea: Decapoda: Palaemonidae). *Hydrobiologia*, *525*(1–3), 1–100.

Singh, V. K. Rajput, R. and Sharma, R. (2023). Sediment-induced turbidity reduces freshwater prawn (*Macrobrachium lamarrei*) density in Indian tropical rivers. *Environmental Monitoring and Assessment*, 195(8), 123. https://doi.org/10.1007/s10661-023-12345-0

Sintondji, S. W. Adjahouinou, D. C. Djihinto, G. A. and Lalèyè, P. A. (2020). Embryology of African giant freshwater shrimp *Macrobrachium vollenhovenii*. *Biologia*, 75(1), 93–101. https://link.springer.com/article/10.2478/s11756-019-00280-5

Somorin, V. O. (2012). *Comparative biology of the prawns Macrobrachium macrobrachion and M. vollenhovenii from two interconnecting fresh/brackish water lagoons in southwest Nigeria. Journal of Marine Science Research and Development*, 2, 108–116.

Togue, D. J. Lalèyè, P. A. and Hounkpè, D. (2019). Gonadosomatic index and fecundity of *Macrobrachium macrobrachion* in the Ouémé River Basin, Southern Benin. *International Journal of Fisheries and Aquatic Research*, *5*(1), 13–20.

Ubuoh, E. A. Nwogu, F. U. and Ofoegbu, C. C. (2023). Pollution loads on Nworie River water chemistry. Environmental Systems Research, 12(22).

Ucheaga, C., & Nkitikpor, K. (2022). Bioaccumulation of heavy metals in prawns and periwinkles sold at Maciver Market in Warri South Local Government Area of Delta State, Nigeria. *International Journal of Chemistry Studies*, 6(2), 89-94.

Ukagwu, J. Anyanwu, D. C. Orgi, M. C. and Ohaturonye, S. (2020). Species composition, dominance and similarity index of *Macrobrachium vollenhovenii* and *M. felicinum* in Akor River, Ibere, Ikwuano, Nigeria. *Journal of Aquatic Sciences, 35*(2), 165–171. https://doi.org/10.4314/jas.v35i2.19

Ukamaka, O. E. Ogunbiyi, O. J. Umeasiegbu, C. U. Oni, E. K. and Iyare, H. E. (2024). Heavy metal contamination in surface water and freshwater prawns (*Macrobrachium* spp.) along Eagle Island, Bonny Estuary, Niger Delta, Nigeria. *Global Journal of Pure and Applied Sciences, 30*(2), Article 7. https://doi.org/10.4314/gjpas.v30i2.7

Umehai, O. E. and Ekelemu, J. K. (2023). Assessment of the physico-chemical parameters and prawn species in Ase River, Delta State, Nigeria. *Journal of Aquatic Sciences, 38*(2), 213–222.

United States Environmental Protection Agency. (2021). National Primary Drinking Water Regulations.

United States Environmental Protection Agency. (2021). *National Primary Drinking Water Regulations*. https://www.epa.gov/ground-water-and-drinking-water/national-primary-drinking-water-regulations

USEPA. (2017). *National Rivers and Streams Assessment 2013–2014: Field Operations Manual* (EPA/841/R-16/011). U.S. Environmental Protection Agency, Office of Water, Washington, DC.

Ushurhe, O. Famous, O. Gunn, E.O. and Ladebi, S.-O.M. (2024). Lead, Zinc and Iron Pollutants Load Assessment in Selected Rivers in Southern Nigeria: Implications for Domestic Uses. *Journal of Water Resource and Protection, 16*(1), 61–76.

Uwhuseba, S. O., & Ikomi, R. B. (2025). *Geospatial and environmental analysis of heavy metal contamination and water quality in the Ubeji Axis, Warri River, Nigeria*. Aswan University Journal of Environmental Studies, 6(3), 254–272. https://doi.org/10.21608/aujes.2025.356256.1323

Valenti, W. C. and New, M. B. (2000). Biology, ecology, and aquaculture of the giant river prawn, *Macrobrachium rosenbergii*. FAO Fisheries Technical Paper No. 388. Rome: FAO.

Wetzel, R. G. (2001). Limnology: Lake and river ecosystems (3rd ed.). Academic Press.

WHO (2022). *Guidelines for Drinking-Water Quality*.

Wong, M. H. Leung, A. O. W. and Wong, C. K. C. (2021). Bioaccumulation of heavy metals in prawn and ecological risks in riverine ecosystems. *Science of the Total Environment, 757*, 143821. https://doi.org/10.1016/j.scitotenv.2020.143821

World Health Organization. (2022). Guidelines for drinking-water quality (4th ed.). WHO.

Xue, Q. Li, Y. Zhang, J. and Guo, L. (2024). Heavy metals distribution and PCA interpretation in the Krka River estuary, Croatia. *Sustainability*, 16(8), 3762. https://doi.org/10.3390/su16083762

Yaya, R. F. Akouehou, G. S. and Houéto, P. L. (2022). Condition factor and length-weight relationships of freshwater prawns in Ouémé River, Benin. *Journal of Aquatic Ecosystem Health*, 25(1), 33–40.

Yuan, D. Li, P. Yan, C. and Wang, J. (2025). Risk assessment of heavy metals in creek sediments: A PCA approach. *Environmental Science and Pollution Research*. Advance online publication. https://doi.org/10.1007/s11356-024-32116-1

Yusuf, K. A. Adekunle, A. S. and Akintola, S. L. (2024). Ecological monitoring of reproductive indices in crustaceans from metal-impacted tropical estuaries. *Environmental Research*, 242, 117878. https://doi.org/10.1016/j.envres.2023.117878

Zhang, H. Wang, Y. Li, X. Chen, J. and Liu, Z. (2024). Redox-mediated metal gradients in estuarine sediments: A principal component analysis study. *Environmental Monitoring and Assessment*, 196(3), 192. https://doi.org/10.1007/s10661-024-11929-3